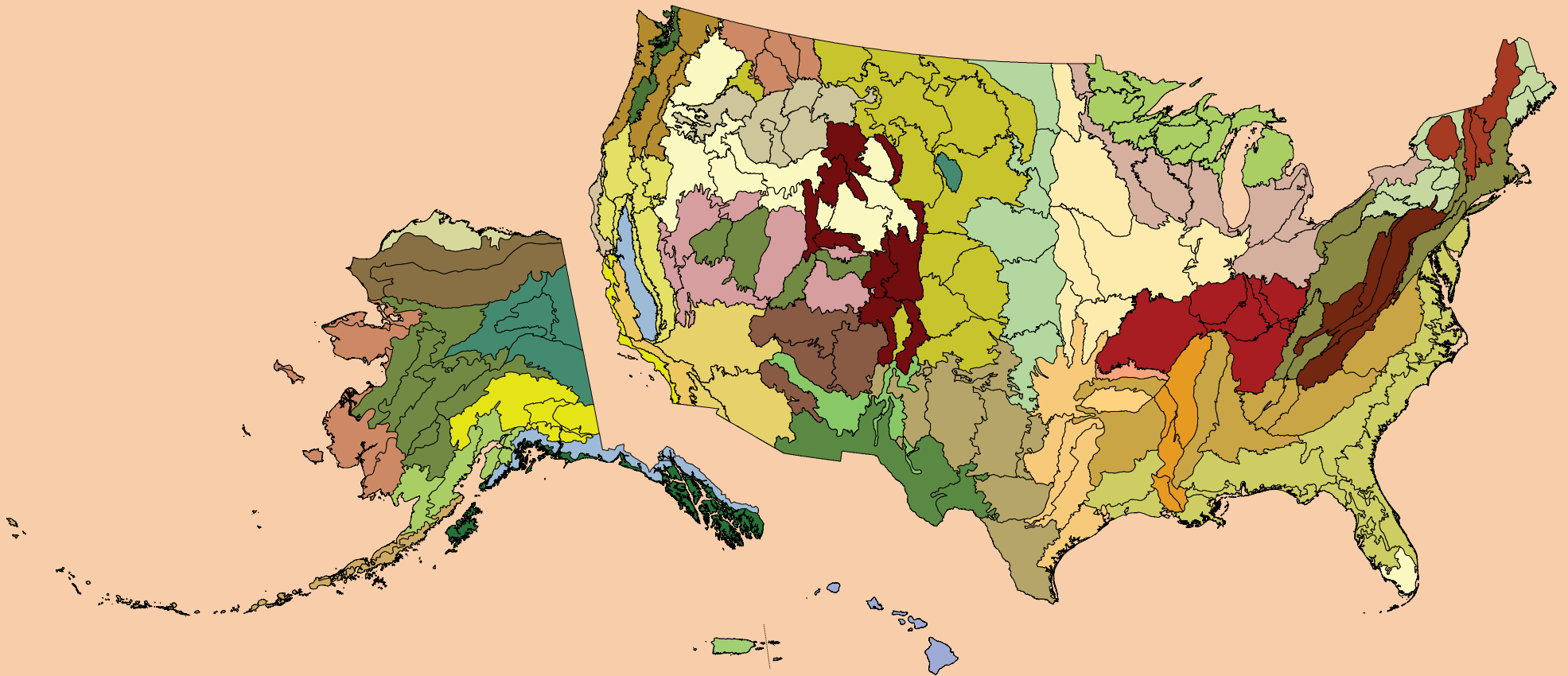




United States Department of Agriculture

Forest Health Monitoring: National Status, Trends, and Analysis 2018

Editors Kevin M. Potter Barbara L. Conkling



Forest Service
Research & Development
Southern Research Station
General Technical Report SRS-239
June 2019

Front cover map:

Ecoregion provinces and ecoregion sections for the conterminous United States (Cleland and others 2007) and for Alaska (Nowacki and Brock 1995), along with the islands of Hawaii, Puerto Rico, and the U.S. Virgin Islands, for which no corresponding ecoregion treatments exist.

Back cover maps:

Tree canopy cover (green) for the conterminous 48 States based on data from a cooperative project between the Multi-Resolution Land Characteristics Consortium and the U.S. Department of Agriculture Forest Service Geospatial Technology and Applications Center (GTAC) using the 2011 National Land Cover Database. Forest cover for Alaska derived from MODIS imagery by the Forest Service Remote Sensing Applications Center (RSAC). Forest cover for Hawaii from the LANDFIRE program. Forest cover for Puerto Rico and the U.S. Virgin Islands from the Forest Service International Institute of Tropical Forestry (IITF), derived from a cloud-free Landsat image mosaic and developed in cooperation with RSAC.

June 2019

Southern Research Station

200 W.T. Weaver Blvd.
Asheville, NC 28804



www.srs.fs.usda.gov

Forest Health Monitoring: National Status, Trends, and Analysis 2018

Editors

Kevin M. Potter, Research Associate Professor, North Carolina State University, Department of Forestry and Environmental Resources, Raleigh, NC 27695

Barbara L. Conkling, Research Assistant Professor, North Carolina State University, Department of Forestry and Environmental Resources, Raleigh, NC 27695

ABSTRACT

The annual national report of the Forest Health Monitoring (FHM) program of the Forest Service, U.S. Department of Agriculture, presents forest health status and trends from a national or multi-State regional perspective using a variety of sources, introduces new techniques for analyzing forest health data, and summarizes results of recently completed Evaluation Monitoring projects funded through the FHM national program. In this 18th edition in a series of annual reports, national survey data are used to identify geographic patterns of insect and disease activity. Satellite data are employed to detect geographic patterns of forest fire occurrence. Recent drought and moisture surplus conditions are compared across the conterminous United States. Data collected by the Forest Inventory and Analysis (FIA) Program are employed to detect regional differences in

tree mortality. Forest Inventory and Analysis data also were used to identify forest types in the Eastern United States with relatively high or low rates of invasion by invasive plants. Methods are explored for more accurately reporting insect and disease damage across multiple regions and nationally using the new Digital Mobile Sketch Mapper (DMSM) platform. National Land Cover Database (NLCD) tree canopy cover data are applied to adjust Forest Health Protection (FHP) Insect and Disease Survey data to better represent acres of forest damage. Three recently completed Evaluation Monitoring projects are summarized, addressing forest health concerns at smaller scales.

Keywords—Change detection, drought, fire, forest health, forest insects and disease, invasive species, tree canopy, tree mortality.

CONTENTS

LIST OF FIGURES	vi
LIST OF TABLES	xiv
EXECUTIVE SUMMARY	1
LITERATURE CITED	4
CHAPTER 1.	
Introduction	5
KEVIN M. POTTER	
THE FOREST HEALTH	
MONITORING PROGRAM	7
DATA SOURCES.	11
FHM REPORT PRODUCTION.	13
LITERATURE CITED	13

SECTION 1.

Analyses of Short-Term Forest Health Data	19
---	----

CHAPTER 2.

Large-Scale Patterns of Insect and Disease Activity in the Conterminous United States, Alaska, and Hawaii from the National Insect and Disease Survey, 2017	21
---	----

KEVIN M. POTTER, JEANINE L. PASCHKE,
FRANK H. KOCH, AND MARK O. ZWEIFLER

INTRODUCTION	21
METHODS	21
RESULTS AND DISCUSSION.	28
CONCLUSION	44
LITERATURE CITED	47

CHAPTER 3.

Large-Scale Patterns of Forest Fire Occurrence across the 50 United States and the Caribbean Territories, 2017	51
--	----

KEVIN M. POTTER

INTRODUCTION	51
METHODS	52
RESULTS AND DISCUSSION.	57
CONCLUSIONS AND FUTURE WORK.	72
LITERATURE CITED	73

Contents, cont.

CHAPTER 4.

Drought and Moisture Surplus Patterns
in the Conterminous United States: 2017,
2015–2017, and 2013–2017. 77

FRANK H. KOCH AND JOHN W. COULSTON

INTRODUCTION 77
METHODS. 78
RESULTS AND DISCUSSION. 83
LITERATURE CITED 92

CHAPTER 5.

Tree Mortality 97

MARK J. AMBROSE

INTRODUCTION 97
DATA. 97
METHODS. 98
RESULTS AND DISCUSSION. 100
SUMMARY 107
LITERATURE CITED 109

SECTION 2.

Analyses of Long-Term Forest Health Trends and
Presentations of New Techniques 113

CHAPTER 6.

The Invasibility and Invadedness of Eastern
U.S. Forest Types 115

KURT H. RIITERS AND KEVIN M. POTTER

INTRODUCTION 115
METHODS. 115
RESULTS AND DISCUSSION 117
CONCLUSIONS 122
ACKNOWLEDGMENTS 123
LITERATURE CITED 124

CHAPTER 7.

Using Tree Canopy Cover Data to Help Estimate
Acres of Damage. 125

ERIN BERRYMAN AND ANDREW McMAHAN

INTRODUCTION 125
METHODS. 127
RESULTS 130
DISCUSSION 137
LITERATURE CITED 141

SECTION 3.

Evaluation Monitoring Project Summaries . . . 143

LITERATURE CITED 143

CHAPTER 8.

Investigating Causes of Bishop Pine Decline on California's North Coast (Project WC-B-16-02) 145

CHRISTOPHER A. LEE, STEVE VOELKER,
AND PETER A. ANGWIN

INTRODUCTION 145

METHODS 145

RESULTS 147

DISCUSSION AND CONCLUSIONS 150

LITERATURE CITED 152

CHAPTER 9.

Monitoring *Myoporum* thrips, *Klambothrips myopori* (Thysanoptera: Phlaeothripidae), in Hawaii (Project WC-EM-B-10-02) 155

LEYLA V. KAUFMAN, ELLIOTT PARSONS,
DOMINIQUE ZARDERS, CYNTHIA KING, AND
ROBERT HAUFF

INTRODUCTION 155

METHODS 155

RESULTS 156

DISCUSSION 157

CONCLUSIONS 159

ACKNOWLEDGMENTS 160

LITERATURE CITED 160

CHAPTER 10.

Monitoring the Impact of Climate Change on the Frequency and Severity of Fires and Distribution of Great Basin Bristlecone Pine Sky Island Ecosystems 161

MICHAEL J. JENKINS AND CURTIS A. GRAY

INTRODUCTION 161

METHODS 161

RESULTS AND DISCUSSION 163

CONCLUSIONS 164

LITERATURE CITED 164

ACKNOWLEDGMENTS 166

AUTHOR INFORMATION 167

Contents, cont.

LIST OF FIGURES

<i>Figure 1.1</i> —Ecoregion provinces and sections for the conterminous United States (Cleland and others 2007) and Alaska (Nowacki and Brock 1995). Ecoregion sections within each ecoregion province are shown in the same color. Note that no equivalent ecoregion treatments exist for Hawaii, Puerto Rico, and the U.S. Virgin Islands	8
<i>Figure 1.2</i> —The design of the Forest Health Monitoring program.	10
<i>Figure 1.3</i> —The Forest Inventory and Analysis mapped plot design. Subplot 1 is the center of the cluster with subplots 2, 3, and 4 located 120 feet away at azimuths of 360°, 120°, and 240°, respectively (Woudenberg and others 2010)	12
<i>Figure 2.1</i> —The extent of surveys for insect and disease activity conducted in the conterminous United States, Alaska, and Hawaii in 2017. Gray areas were surveyed using the new Digital Mobile Sketch Mapping (DMSM) platform, rather than the older Digital Aerial Sketch Mapping (DASM) approach, which is portrayed in green. The blue lines delineate Forest Health Monitoring regions. Note: Alaska and Hawaii are not shown to scale with map of the conterminous United States. For West Virginia, the survey was ground survey-based with assistance from remote sensing. (Data source: U.S. Department of Agriculture Forest Service, Forest Health Protection).	23
<i>Figure 2.2</i> —The percent of surveyed forest exposed to mortality agents, by ecoregion section within the conterminous 48 States, for 2017. The gray lines delineate ecoregion sections (Cleland and others 2007). The 240-m tree canopy cover is based on data from a cooperative project between the Multi-Resolution Land Characteristics Consortium (Coulston and others 2012) and the Forest Service Remote Sensing Applications Center using the 2011 National Land Cover Database. (Data source: U.S. Department of Agriculture Forest Service, Forest Health Protection)	31
<i>Figure 2.3</i> —Hot spots of the density of occurrences of mortality-causing insects and diseases in 2017 for (A) the conterminous 48 States and (B) for separate Forest Health Monitoring regions, by hexagons containing >5 percent tree canopy cover. Values are Getis-Ord G_i^* scores, with values >2 representing significant clustering of high mortality occurrence densities and <-2 representing significant clustering of low mortality occurrence densities. The gray lines delineate ecoregion sections (Cleland and others 2007), and blue lines delineate Forest Health Monitoring regions. Tree canopy cover is based on data from a cooperative project between the Multi-Resolution Land Characteristics Consortium (Coulston and others 2012) and the Forest Service Remote Sensing Applications Center using the 2011 National Land Cover Database. (Data source: U.S. Department of Agriculture Forest Service, Forest Health Protection)	33

Box Figure 2.1—The Southern Pine Beetle story map provides interactive maps and background information on southern pine beetle, its hosts, and its management. 36

Figure 2.4—The percent of surveyed forest exposed to defoliating agents, by ecoregion section within the conterminous 48 States, for 2017. The gray lines delineate ecoregion sections (Cleland and others 2007). The 240-m tree canopy cover is based on data from a cooperative project between the Multi-Resolution Land Characteristics Consortium (Coulston and others 2012) and the Forest Service Remote Sensing Applications Center using the 2011 National Land Cover Database. (Data source: U.S. Department of Agriculture Forest Service, Forest Health Protection) 39

Figure 2.5—Hot spots of the density of occurrences of defoliation-causing insects and diseases in 2017 for (A) the conterminous 48 States and (B) for separate Forest Health Monitoring regions, by hexagons containing >5 percent tree canopy cover. Values are Getis-Ord G_i^* scores, with values >2 representing significant clustering of high defoliation occurrence densities. (No areas of significant clustering of low densities, <-2, were detected.) The gray lines delineate ecoregion sections (Cleland and others 2007), and blue lines delineate Forest Health Monitoring regions. Tree canopy cover is based on data from a cooperative project between the Multi-Resolution Land Characteristics Consortium (Coulston and others 2012) and the Forest Service Remote Sensing Applications Center using the 2011

National Land Cover Database. (Data source: U.S. Department of Agriculture Forest Service, Forest Health Protection) 41

Figure 2.6—Percentage of surveyed forest in Alaska ecoregion sections exposed to mortality-causing insects and diseases in 2017. The gray lines delineate ecoregion sections (Nowacki and Brock 1995). Background forest cover is derived from MODIS imagery by the Forest Service Remote Sensing Applications Center. (Data source: U.S. Department of Agriculture Forest Service, Forest Health Protection) 43

Figure 2.7—Percentage of surveyed forest in Alaska ecoregion sections exposed to defoliation-causing insects and diseases in 2017. The gray lines delineate ecoregion sections (Nowacki and Brock 1995). Background forest cover is derived from MODIS imagery by the Forest Service Remote Sensing Applications Center. (Data source: U.S. Department of Agriculture Forest Service, Forest Health Protection) 45

Figure 2.8—Percentage of surveyed forest on Hawaii islands (and by county council district on the Big Island of Hawai'i) exposed to mortality-causing insects and diseases in 2017. Background forest cover is derived from the LANDFIRE program (LANDFIRE 2014). (Data source: U.S. Department of Agriculture Forest Service, Forest Health Protection) 46

Figures, cont.

Figures, cont.

Figure 3.1—Forest fire occurrences detected by MODIS from 2001 to 2017 for the conterminous United States, Alaska, and Hawaii, and for the entire nation combined. (Data source: U.S. Department of Agriculture Forest Service, Remote Sensing Applications Center, in conjunction with the NASA MODIS Rapid Response group) 57

Figure 3.2—The number of forest fire occurrences, per 100 km² (10 000 ha) of forested area, by ecoregion section within the conterminous 48 States, for 2017. The gray lines delineate ecoregion sections (Cleland and others 2007). Forest cover is derived from MODIS imagery by the Forest Service Remote Sensing Applications Center. (Source of fire data: U.S. Department of Agriculture Forest Service, Remote Sensing Applications Center, in conjunction with the NASA MODIS Rapid Response group) 59

Figure 3.3—The number of forest fire occurrences, per 100 km² (10 000 ha) of forested area, by ecoregion section within Alaska, for 2017. The gray lines delineate ecoregion sections (Nowacki and Brock 1995). Forest cover is derived from MODIS imagery by the Forest Service Remote Sensing Applications Center. (Source of fire data: U.S. Department of Agriculture Forest Service, Remote Sensing Applications Center, in conjunction with the NASA MODIS Rapid Response group). 61

Figure 3.4—The number of forest fire occurrences, per 100 km² (10 000 ha) of forested area, by island in Hawaii, for 2017.

Background forest cover is derived from the LANDFIRE program (LANDFIRE 2014). (Source of fire data: U.S. Department of Agriculture Forest Service, Remote Sensing Applications Center, in conjunction with the NASA MODIS Rapid Response group) 63

Figure 3.5—The number of forest fire occurrences, per 100 km² (10 000 ha) of forested area, by island in Puerto Rico and the U.S. Virgin Islands, for 2017. Forest cover is from the Forest Service International Institute of Tropical Forestry, derived from a cloud-free Landsat image mosaic developed in cooperation with Forest Service Remote Sensing Applications Center (Kennaway and Helmer 2007, Kennaway and others 2008) 64

Figure 3.6—(A) Mean number and (B) standard deviation of forest fire occurrences per 100 km² (10 000 ha) of forested area from 2001 through 2016, by ecoregion section within the conterminous 48 States. (C) Degree of 2017 fire occurrence density excess or deficiency by ecoregion relative to 2001–2016 and accounting for variation over that time period. The gray lines delineate ecoregion sections (Cleland and others 2007). Forest cover is derived from MODIS imagery by the Forest Service Remote Sensing Applications Center. (Source of fire data: U.S. Department of Agriculture Forest Service, Remote Sensing Applications Center, in conjunction with the NASA MODIS Rapid Response group) 65

Figure 3.7—(A) Mean number and (B) standard deviation of forest fire occurrences per 100 km² (10 000 ha) of forested area from 2001 through 2016, by ecoregion section in Alaska. (C) Degree of 2017 fire occurrence density excess or deficiency by ecoregion relative to 2001–2016 and accounting for variation over that time period. The gray lines delineate ecoregion sections (Nowacki and Brock 1995). Forest cover is derived from MODIS imagery by the Forest Service Remote Sensing Applications Center. (Source of fire data: U.S. Department of Agriculture Forest Service, Remote Sensing Applications Center, in conjunction with the NASA MODIS Rapid Response group). 68

Figure 3.8—(A) Mean number and (B) standard deviation of forest fire occurrences per 100 km² (10 000 ha) of forested area from 2001 through 2016, by island in Hawaii. (C) Degree of 2017 fire occurrence density excess or deficiency by ecoregion relative to 2001–2016 and accounting for variation over that time period. Background forest cover is derived from the LANDFIRE program (LANDFIRE 2014). (Source of fire data: U.S. Department of Agriculture Forest Service, Remote Sensing Applications Center, in conjunction with the NASA MODIS Rapid Response group) 69

Figure 3.9—(A) Mean number and (B) standard deviation of forest fire occurrences per 100 km² (10 000 ha) of forested area from 2001 through 2016, by island in Puerto Rico and the U.S. Virgin Islands. (C) Degree of 2017 fire occurrence density excess or deficiency by ecoregion

relative to 2001–2016 and accounting for variation over that time period. Forest cover is from the Forest Service International Institute of Tropical Forestry (IITF), derived from a cloud-free Landsat image mosaic developed in cooperation with Forest Service Remote Sensing Applications Center (Kennaway and Helmer 2007, Kennaway and others 2008). 70

Figure 3.10—Hot spots of fire occurrence across the conterminous United States for 2017. Values are Getis-Ord G_i^* scores, with values >2 representing significant clustering of high fire occurrence densities. (No areas of significant clustering of lower fire occurrence densities, <-2, were detected.) The gray lines delineate ecoregion sections (Cleland and others 2007). Background forest cover is derived from MODIS imagery by the Forest Service Remote Sensing Applications Center. (Source of fire data: U.S. Department of Agriculture Forest Service, Remote Sensing Applications Center, in conjunction with the NASA MODIS Rapid Response group) 71

Figure 4.1—The 100-year (1918–2017) mean annual moisture index, or $MI'_{100norm}$, for the conterminous United States. Ecoregion section (Cleland and others 2007) boundaries and labels are included for reference. Forest cover data (overlaid green hatching) derived from Moderate Resolution Imaging Spectroradiometer (MODIS) imagery by the Forest Service Remote Sensing Applications Center. (Data source: PRISM Climate Group, Oregon State University) 82

Figures, cont.

Figures, cont.

Figure 4.2—The 2017 annual (i.e., 1-year) moisture difference z-score, or *MDZ*, for the conterminous United States. Ecoregion section (Cleland and others 2007) boundaries and labels are included for reference. Forest cover data (overlaid green hatching) derived from MODIS imagery by the Forest Service Remote Sensing Applications Center. (Data source: PRISM Climate Group, Oregon State University) . . . 85

Figure 4.3—The 2016 annual (i.e., 1-year) moisture difference z-score, or *MDZ*, for the conterminous United States. Ecoregion section (Cleland and others 2007) boundaries and labels are included for reference. Forest cover data (overlaid green hatching) derived from MODIS imagery by the Forest Service Remote Sensing Applications Center. (Data source: PRISM Climate Group, Oregon State University) . . . 86

Figure 4.4—The 2015–2017 (i.e., 3-year) moisture difference z-score (*MDZ*) for the conterminous United States. Ecoregion section (Cleland and others 2007) boundaries are included for reference. Forest cover data (overlaid green hatching) derived from MODIS imagery by the Forest Service Remote Sensing Applications Center. (Data source: PRISM Climate Group, Oregon State University). 89

Figure 4.5—The 2013–2017 (i.e., 5-year) moisture difference z-score (*MDZ*) for the conterminous United States. Ecoregion section (Cleland and others 2007) boundaries are included for reference. Forest cover data (overlaid green hatching) derived from MODIS imagery by the Forest Service

Remote Sensing Applications Center. (Data source: PRISM Climate Group, Oregon State University). 90

Figure 5.1—Forest cover in the States where mortality was analyzed by ecoregion section (Cleland and others 2007). Mortality in Eastern and Central States was analyzed using a complete remeasurement cycle; in Western States, mortality was analyzed using a partial cycle of remeasurements, and results there should be considered preliminary. Forest cover was derived from MODIS satellite imagery (USDA Forest Service 2008) 99

Figure 5.2—Tree mortality expressed as the ratio of annual mortality volume to gross annual volume growth (*MRATIO*) by ecoregion section (Cleland and others 2007). (Data source: U.S. Department of Agriculture Forest Service, Forest Inventory and Analysis program) 101

Figure 5.3—Annual tree mortality expressed as a percentage of live tree volume by ecoregion section (Cleland and others 2007) for the Western United States. (Data source: U.S. Department of Agriculture, Forest Service Forest Inventory and Analysis program). Mortality was analyzed using a partial cycle of remeasurements, and results there should be considered preliminary. . . . 108

Figure 6.1—The study area encompassed most of the temperate and boreal forest in the Eastern United States. (Data source: Cleland and others 2007) 116

Figure 6.2—Summary of invaded and uninvaded forest area by forest type and ownership. The four panels (A, B, C, D) group forest types with similar total area; note the change in the horizontal axis scale between panels. Within each panel, forest types are sorted by decreasing total area. The invaded area is indicated by negative numbers (left of zero); the uninvaded area is indicated by positive numbers (right of zero). Colors indicate ownership, with lighter shades used for the invaded area. (Data sources: Forest Service Forest Inventory and Analysis; Riitters and others 2017) 120

Figure 6.3—Share of public ownership in relation to percent of area invaded for 74 forest types. The forest types with less than one-third of total area invaded are labeled. Public ownership includes Federal, State, and local government ownership. The estimated linear regression line is shown for information only. 123

Figure 7.1—Kappa statistic (TCC versus FNF) for each Level 3 Ecoregion plotted against the canopy cover threshold, grouped into western U.S. ecoregions and eastern U.S. ecoregions. Boxplots approximate the distribution of the kappa values within each category, showing the median kappa as the horizontal line, bracketed by the first and third quantiles as the extent of the boxes. Outliers are outside 1.5 times the range indicated by

the box height. This illustrates that (1) the best performing TCC threshold is higher for eastern ecoregions compared to western ecoregions; (2) western ecoregions overall show a poorer fit of TCC with FNF. 131

Figure 7.2—Kappa statistic (TCC at 30-percent threshold versus FNF) for each Level 3 Ecoregion plotted against the mean annual precipitation class (MAPclass) of the ecoregion. Boxplots approximate the distribution of the kappa values within each category, showing the median kappa as the horizontal line, bracketed by the first and third quantiles as the extent of the boxes. Outliers are outside 1.5 times the range indicated by the box height. This illustrates TCC forested cover compares better to FNF forested cover in wetter ecoregions than in drier ecoregions. Therefore, caution should be used when using TCC to delineate forested cover in dry forests. 131

Figure 7.3—Histogram of (A) 2008 and (B) 2015 IDS polygon treed proportion (according to FNF) only including polygons >50 acres. . 132

Figure 7.4—Mean treed area by Level 1 Ecoregion within 480-m superpixels centered inside large, round 2015 IDS polygons using five different treed cover or canopy cover layers: FNF (FHA AST native); NLCD 2011 with a 10-, 20-, and 30-percent canopy cover threshold; and NLCD TCC. Error bars represent +/- standard error. 133

Figures, cont.

Figures, cont.

Figure 7.5—2015 IDS polygons where there was at least a 30-percent difference in treed area between using a 10-percent TCC threshold for NLCD and a 30-percent threshold for NLCD. This represents 2 percent of the total damage acreage mapped via polygons in 2015. Note that, because not all land was surveyed in 2015, this figure only indicates presence of damage and not absence of damage and may include false negatives 134

Figure 7.6—NAIP imagery from selected 480-m superpixels randomly sampled from large, round IDS polygons in 2008 and 2015 and different estimates of the percentage of treed area within the superpixel. (A) An area containing standing dead trees from a wildfire, which are read as “untreed” by NLCD. (B) An area where complex terrain results in spatial heterogeneity of forest density and widely varying assessments of treed cover depending on canopy cover threshold and expert. The red text indicates the layer that came closest to the expert assessment of treed cover. NLCD10 = treed cover from NLCD using a 10-percent canopy cover threshold; NLCD20 = treed cover from NLCD using a 20-percent canopy cover threshold; NLCD30 = treed cover from NLCD using a 30-percent canopy cover threshold; FNF = FHAASST native treed layer (Ellenwood and others 2015); O1 = observer 1’s visual assessment from NAIP imagery; O2 = observer 2’s visual assessment from NAIP imagery 136

Figure 7.7—IDS data from 2015 showing 1920-m grid cells used to map emerald ash borer mortality in Michigan. Grid cell A has higher tree cover than grid cell B, and both cells were mapped at the same mortality severity (Light). 139

Figure 8.1—Study site locations 145

Figure 8.2—Bishop pine decline in northern Sonoma County. (A) Wide-scale, synchronous mortality; (B) gradual decline in crown conditions. (Photos by Christopher Lee, California Department of Forestry and Fire Protection) 147

Figure 8.3—Bishop pine crown health metrics (mean percent crown density and mean percent crown dieback) across study sites with multiple plots containing Bishop pine. . 148

Figure 8.4—Basal area increment (BAI) averaged across all cored bishop pines at all study sites. 148

Figure 8.5—Dates of bishop pine establishment across study sites. 148

Figure 9.1—Monitoring sites on Hawai’i Island 156

Figure 9.2—Infestation scale: (A) 0 = no galls; (B) 1 = <33 percent tissue galled; (C) 2 = 33–66 percent of tissue galled; (D) 3 = >66 percent of tissue galled. (Photos by Leyla Kaufman, The Pacific Cooperative Studies Unit (PCSU), University of Hawai’i) 157

Figure 9.3—Dieback scale: (A) 0 = no dieback;
(B) 1 = <33 percent tissue with dieback;
(C) 2 = 33–66 percent of tissue with dieback;
(D) 3 = >66 percent of tissue with dieback.
(Photos by Leyla Kaufman, The Pacific
Cooperative Studies Unit (PCSU), University
of Hawai'i)157

Figure 9.4—Naio thrips infestation levels
by year (selected sites), on a 0–3 scale as
described under Methods158

Figure 9.5—Plant dieback levels by year
(selected sites), attributed to naio thrips159

Figure 9.6—Naio mortality by elevation
attributable to naio thrips damage160

Figures, cont.

LIST OF TABLES

<i>Table 2.1</i> —Mortality agents and complexes affecting more than 5000 ha in the conterminous United States during 2017 . . .	29	<i>Table 5.2</i> —Ecoregion sections in the Eastern and Central United States having the highest mortality relative to growth (MRATIO), annual growth and mortality rates, and associated causes of mortality	102
<i>Table 2.2</i> —Beetle taxa included in the “western bark beetle” group.	29	<i>Table 6.1</i> —Total area and invadedness of 10 FIA forest type groups in the Eastern United States, by percent area invaded	117
<i>Table 2.3</i> —The top five mortality agents or complexes for each Forest Health Monitoring region, and for Alaska and Hawaii, in 2017 . . .	30	<i>Table 6.2</i> —Invadedness and area by forest type	118
<i>Table 2.4</i> —Defoliation agents and complexes affecting more than 5000 ha in the conterminous United States in 2017	37	<i>Table 6.3</i> —Area and invadedness by ownership	120
<i>Table 2.5</i> —The top five defoliation agents or complexes for each Forest Health Monitoring region and for Alaska in 2017.	38	<i>Table 7.1</i> —Summaries of analyses for this report	130
<i>Table 3.1</i> —The 15 ecoregion sections in the conterminous United States with the highest fire occurrence densities in 2017	60	<i>Table 7.2</i> —Root mean squared error (RMSE) between treed cover estimates from expert assessment and from canopy cover layers derived from NLCD for 480-m superpixels randomly selected from large, round polygons located west of the Great Plains (“West”) and east of the Great Plains (“East”) in 2008 and 2015	135
<i>Table 3.2</i> —The 14 ecoregion sections in the conterminous United States with the highest annual mean fire occurrence densities from 2001 through 2016	66	<i>Table 8.1</i> —Pests observed on bishop pine, arranged by plant part affected	149
<i>Table 4.1</i> —Moisture difference z-score (MDZ) value ranges for nine wetness and drought categories, along with each category’s approximate theoretical frequency of occurrence.	83		
<i>Table 5.1</i> —Western States from which repeated Forest Inventory and Analysis Phase 2 measurements were available, the time period spanned by the data, and the effective sample intensity (on the proportion of plots that had been remeasured) in the available datasets	98		

EXECUTIVE SUMMARY

Healthy ecosystems are those that are stable and sustainable, able to maintain their organization and autonomy over time while remaining resilient to stress (Costanza 1992). Healthy forests are vital to our future (Edmonds and others 2011), and consistent, large-scale, and long-term monitoring of key indicators of forest health status, change, and trends is necessary to identify forest resources deteriorating across large regions (Riitters and Tkacz 2004). The Forest Health Monitoring (FHM) program of the Forest Service, U.S. Department of Agriculture, with cooperating researchers within and outside the Forest Service and with State partners, quantifies status and trends in the health of U.S. forests (ch. 1). The analyses and results outlined in sections 1 and 2 of this FHM annual national report offer a snapshot of the current condition of U.S. forests from a national or multi-State regional perspective, incorporating baseline investigations of forest ecosystem health, examinations of change over time in forest health metrics, and assessments of developing threats to forest stability and sustainability. For datasets collected on an annual basis, analyses are presented from 2017 data. For datasets collected over several years, analyses are presented at a longer temporal scale. Finally, section 3 of this report presents summaries of results from recently completed Evaluation Monitoring (EM) projects that have been funded through the FHM national program to determine the extent, severity, and/or causes of specific forest health problems (FHM 2018).

Monitoring the occurrence of forest pest and pathogen outbreaks is important at regional scales because of the significant impact insects and diseases can have on forest health across landscapes (ch. 2). National Insect and Disease Survey data collected in 2017 by the Forest Health Protection program of the Forest Service and partners in State agencies identified 63 different mortality-causing agents and complexes on 3.27 million ha in the conterminous United States, and 50 defoliating agents and complexes on approximately 2.34 million ha. Geographic hot spots of forest mortality were associated with bark beetle infestations (mostly fir engraver, western pine beetle, mountain pine beetle, and spruce beetle) in the West, and with emerald ash borer and southern pine beetle in the East. Hot spots of defoliation were associated with gypsy moth, forest tent caterpillar, spruce budworm, baldcypress leafroller, jumping oak gall wasp, white pine needle damage, and browntail moth in the East, and with western spruce budworm in the West. Extensive spruce beetle mortality was detected in Alaska. The most important defoliation agents in Alaska were aspen leafminer, willow leaf blotchminer, and speckled green fruitworm. In Hawaii, approximately 37 000 ha of mortality were attributed to rapid ‘ōhi‘a death.

Forest fire occurrence outside the historic range of frequency and intensity can result in extensive economic and ecological impacts. The detection of regional patterns of fire occurrence density can allow for the identification of areas

at greatest risk of significant impact and for the selection of locations for more intensive analysis (ch. 3). In 2017, the number of satellite-detected forest fire occurrences recorded for the conterminous States was the fifth most in 17 full years of data collection and the most since 2014. Ecoregion sections in the Pacific Northwest, the northern Rocky Mountains, and California had the highest forest fire occurrence density per 100 km² of forested area. Geographic hot spots of high fire occurrence density were detected in these same areas, as well as in the Southeast and southern Arizona. Ecoregion sections in southern, central, and northern California; the Cascade Mountains of Oregon and Washington; and northern Idaho and northwestern Montana experienced greater fire occurrence density than normal compared to the previous 15-year mean and accounting for variability over time. Alaska experienced low fire occurrence densities except in one northeastern ecoregion section. The Big Island of Hawai'i experienced a lower fire occurrence density than in recent years as a result of an ongoing volcanic eruption.

Most U.S. forests experience droughts, with varying degrees of intensity and duration between and within forest ecosystems. Arguably, the duration of a drought event is more critical than its intensity. A standardized drought and moisture surplus indexing approach was applied to monthly climate data from 2017 to map drought conditions and surplus moisture availability across the conterminous United States at a fine scale (ch. 4). Much of the

Southwest and parts of southern California had extreme drought conditions in 2017, while portions of the central Midwest, northern Great Plains, and the Southeast had moderate to severe drought. Areas near the Great Lakes, west of the Appalachian Mountains, and in the interior Northwest had moderate to extreme moisture surplus conditions. Analyses of longer term (3-year and 5-year) conditions show that much of the West had undergone long-term drought conditions, as had coastal New England and a swath of the South extending from western North Carolina through Georgia and Florida. The remainder of the country generally experienced at least mild moisture surplus conditions for these longer periods, with severe or extreme moisture surplus in Texas, the northern Midwest, and along the coasts of North and South Carolina.

Mortality is a natural process in all forested ecosystems, but high levels of mortality at large scales may indicate that the health of forests is declining. Phase 2 data collected by the Forest Inventory and Analysis (FIA) program of the Forest Service offer tree mortality information on a relatively spatially intense basis of approximately one plot per 6,000 acres (ch. 5). An analysis of FIA plots from all the Central and Eastern States found that in most areas, tree mortality is low relative to tree growth, while the areas of highest mortality occur mostly in riparian forests of the Great Plains. Specifically, the highest ratios of annual mortality to gross growth occurred in ecoregion sections located

in South Dakota, North Dakota, Nebraska, northwestern Ohio and eastern Michigan, north-central Arkansas, eastern Oklahoma, southeastern Kansas, and east Texas. Similar analyses were conducted for the Pacific Coast States, where the FIA remeasurement cycle is 10 years. Throughout much of this area, mortality relative to growth was low, but in parts of southern California, mortality exceeded growth. Areas of highest annual mortality as a percentage of total live tree volume were in southern California, northeastern Utah, and southeastern Montana. Results for the western U.S. should be considered preliminary, however.

Invasive plant species can cause a variety of undesirable changes in forest health simply by altering forest species composition, and a large proportion of rural forest in the Eastern United States already contains harmful invasive plant species. The statistical power of the FIA forest inventory system was combined with the predictive power of a plot-level plant invasion model to compare forest types in the Eastern United States with respect to the likelihood that they contain invasive forest plants, and to evaluate the relative roles of public versus private forest ownership for conserving the uninvaded forest area (ch. 6). Half of the total area of 74 forest types was found to be invaded, with invasions almost twice as likely on privately owned land than on publicly owned land. Individual forest types varied widely in terms of historical invasions, but ownership alone was the deciding factor for the most-invaded forest

types. There were no forest types for which a remediation focus on public land would be efficient, i.e., consideration of privately owned lands is probably necessary for controlling invasive plants. For the least-invaded forest types, there were several instances for which the efficiency of a conservation focus on either public or private land would depend on the forest type.

The Digital Mobile Sketch Mapper (DMSM) platform is replacing the Digital Aerial Sketch Mapper (DASM) platform as the primary way that data are collected, stored, accessed, and processed for the national Insect and Disease Survey, coordinated by the Forest Health Assessment and Applied Sciences Team (FHAASST) of the Forest Health Protection (FHP) program (ch. 7). One goal of this change is to better allow for accurate reporting of total damage across multiple regions and nationally, despite the variability in canopy density across and even within regions. This concept of “acres of” damage, rather than “acres with” damage, can be helpful when comparing damage summaries across different regions, hosts, or agents. The use of mortality and defoliation severity classes in DMSM will allow for an initial estimate of “acres of” damage by multiplying polygon or grid “acres with” damage by the midpoint of the assigned mortality or defoliation class. Further adjustments for treed cover will have less of an impact on “acres of” damage but may be necessary for large, general polygons and grid cells. The National Land

Cover Database produces a Tree Canopy Cover (TCC) raster that can be used with a threshold to delineate treed and untreed area for the purposes of “acres of” damage calculations. Important considerations include region and forest type of interest, with arid western areas requiring a lower TCC threshold than wetter eastern forests. Crosswalking legacy measures of damage severity with DMSM will be challenging. Further analysis and testing are recommended to determine the appropriate methodology for representing cumulative “acres of” damage in an outbreak that spans both DASM and DMSM.

Finally, three recently completed Evaluation Monitoring (EM) projects address a wide variety of forest health concerns at a scale smaller than the national or multi-State regional analyses included in the first sections of the report. These EM projects (funded by the FHM program):

- Investigated the causes of a dramatic decline of bishop pine (*Pinus muricata*) stands in California’s northern coastal areas using dendroecological methods and an inventory of pathogen and insect problems present in these stands (ch. 8);
- Documented the infestation of myoporum thrips (*Klambothrips myopori*) and resulting dieback rates of the native naio (*Myoporum sandwicense*) on the Big Island of Hawai‘i, where this native tree species has high cultural and ecological importance (ch. 9); and

- Compared the relationship between forest structure and environmental gradients to predict changes in surface and canopy fuels of Great Basin bristlecone pine (*Pinus longaeva*) communities with increasing temperatures in Nevada and western Utah (ch. 10).

The FHM program, in cooperation with forest health specialists and researchers inside and outside the Forest Service, continues to investigate a broad range of issues relating to forest health using a wide variety of data and techniques. This report presents some of the latest results from ongoing national-scale detection monitoring and smaller scale environmental monitoring efforts by FHM and its cooperators. For more information about efforts to determine the status, changes, and trends in indicators of the condition of U.S. forests, please visit the FHM Web site at www.fs.fed.us/foresthealth/fhm.

LITERATURE CITED

- Costanza, R. 1992. Toward an operational definition of ecosystem health. In: Costanza, R.; Norton, B.G.; Haskell, B.D., eds. Ecosystem health: new goals for environmental management. Washington, DC: Island Press: 239–256.
- Edmonds, R.L.; Agee, J.K.; Gara, R.I. 2011. Forest health and protection. Long Grove, IL: Waveland Press, Inc. 667 p.
- Forest Health Monitoring (FHM). 2018. Program description. Forest Health Monitoring fact sheet series. <https://www.fhm.fs.fed.us/fact/>. [Date accessed: September 20, 2018].
- Riitters, K.H.; Tkacz, B. 2004. The U.S. Forest Health Monitoring program. In: Wiersma, G.B., ed. Environmental monitoring. Boca Raton, FL: CRC Press: 669–683.

Forests cover a vast area of the United States, 304 million ha or approximately one-third of the Nation's land area (Smith and others 2009). These forests possess the capacity to provide a broad range of goods and services to current and future generations, to safeguard biological diversity, and to contribute to the resilience of ecosystems, societies, and economies (USDA Forest Service 2011). Their ecological roles include supplying large and consistent quantities of clean water, preventing soil erosion, and providing habitat for a broad diversity of plant and animal species. Their socioeconomic benefits include wood products, nontimber goods, recreational opportunities, and pleasing natural beauty. Both the ecological integrity and the continued capacity of these forests to provide ecological and economic goods and services are of concern, however, in the face of a long list of threats, including insect and disease infestation, fragmentation and conversion to other land uses, catastrophic fire, invasive species, and the effects of climate change.

Natural and anthropogenic stresses vary among biophysical regions and local environments; they also change over time and interact with each other. These and other factors make it challenging to establish baselines of forest health and to detect important departures from normal forest ecosystem functioning (Riitters and Tkacz 2004). Monitoring the health of forests is a critically important task, however, reflected within the Criteria and Indicators for the Conservation and Sustainable Management of Temperate and Boreal Forests (Montréal

Process Working Group 1995), which the Forest Service, U.S. Department of Agriculture (USDA), uses as a forest sustainability assessment framework (USDA Forest Service 2004, 2011). The primary objective of such monitoring is to identify ecological resources whose condition is deteriorating in subtle ways over large regions in response to cumulative stresses, a goal that requires consistent, large-scale, and long-term monitoring of key indicators of forest health status, change, and trends (Riitters and Tkacz 2004). This is best accomplished through the participation of multiple Federal, State, academic, and private partners.

Although the concept of a healthy forest has universal appeal, forest ecologists and managers have struggled with how exactly to define forest health (Teale and Castello 2011), and there is no universally accepted definition. Most definitions of forest health can be categorized as representing an ecological or a utilitarian perspective (Kolb and others 1994). From an ecological perspective, the current understanding of ecosystem dynamics suggests that healthy ecosystems are those that are able to maintain their organization and autonomy over time while remaining resilient to stress (Costanza 1992), and that evaluations of forest health should emphasize factors that affect the inherent processes and resilience of forests (Edmonds and others 2011, Kolb and others 1994, Raffa and others 2009). On the other hand, the utilitarian perspective holds that a forest is healthy if management objectives are met, and that a forest is unhealthy if these objectives are not met (Kolb and others 1994). Although this definition

CHAPTER 1.

Introduction

KEVIN M. POTTER

may be appropriate when a single, unambiguous management objective exists, such as the production of wood fiber or the maintenance of wilderness attributes, it is too narrow when multiple management objectives are required (Edmonds and others 2011, Teale and Castello 2011). Teale and Castello (2011) incorporate both ecological and utilitarian perspectives into their two-component definition of forest health: first, a healthy forest must be sustainable with respect to its size structure, including a correspondence between baseline and observed mortality; second, a healthy forest must meet the landowner's objectives, provided that these objectives do not conflict with sustainability.

This national report, the 18th in an annual series sponsored by the Forest Health Monitoring (FHM) program of the Forest Service, attempts to quantify the status of, changes to, and trends in a wide variety of broadly defined indicators of forest health. The indicators described in this report encompass forest insect and disease activity, wildland fire occurrence, drought, tree mortality, and invasive species, among others. The previous reports in this series are Ambrose and Conkling (2007, 2009), Conkling (2011), Conkling and others (2005), Coulston and others (2005a, 2005b, 2005c), and Potter and Conkling (2012a, 2012b, 2013a, 2013b, 2014, 2015a, 2015b, 2016, 2017, 2018).

This report has three specific objectives. The first is to present information about forest health from a national perspective, or from a multi-State regional perspective when appropriate, using data collected by the Forest

Health Protection (FHP) and Forest Inventory and Analysis (FIA) programs of the Forest Service, as well as from other sources available at a wide extent. The chapters that present analyses at a national scale, or multi-State regional scale, are divided between section 1 and section 2 of the report. Section 1 presents results from the analyses of forest health data that are available on an annual basis. Such repeated analyses of regularly collected indicator measurements allow for the detection of trends over time and help establish a baseline for future comparisons (Riitters and Tkacz 2004). Section 2 presents longer term forest health trends, in addition to describing new techniques for analyzing forest health data at national or regional scales (the second objective of the report). While in-depth interpretation and analysis of specific geographic or ecological regions are beyond the scope of these parts of the report, the chapters in sections 1 and 2 present information that can be used to identify areas that may require investigation at a finer scale.

The second objective of the report is to present new techniques for analyzing forest health data as well as new applications of established techniques, often applied to longer timescales, presented in selected chapters of section 2. Examples in this report are chapters 6 and 7, which, respectively, identify forest types in the Eastern United States with relatively high or low probabilities of invasion by invasive plants, and explore approaches for more accurately reporting insect and disease

damage across multiple regions and nationally using the new Digital Mobile Sketch Mapper (DMSM) platform.

The third objective of the report is to present results of recently completed Evaluation Monitoring (EM) projects funded through the FHM national program. These project summaries, presented in section 3, determine the extent, severity, and/or cause of forest health problems (FHM 2016), generally at a finer scale than that addressed by the analyses in sections 1 and 2. Each of the three chapters in section 3 contains an overview of an EM project, key results, and contacts for more information.

When appropriate throughout this report, authors use the Forest Service revised ecoregions for the conterminous United States and Alaska (Cleland and others 2007, Nowacki and Brock 1995) as a common ecologically based spatial framework for their forest health assessments (fig. 1.1). (No corresponding ecoregion data exist for Hawaii and the U.S. Caribbean territories.) Specifically, when the spatial scale of the data and the expectation of an identifiable pattern in the data are appropriate, authors use ecoregion sections or provinces as assessment units for their analyses. Bailey's hierarchical system bases the two broadest ecoregion scales, domains and divisions, on large ecological climate zones, while each division is broken into provinces based on vegetation macro features (Bailey 1995). Provinces are further divided into sections, which may be thousands of km² in area and are expected to encompass regions similar

in their geology, climate, soils, potential natural vegetation, and potential natural communities (Cleland and others 1997).

THE FOREST HEALTH MONITORING PROGRAM

The national FHM program is designed to determine the status, changes, and trends in indicators of forest condition on an annual basis and covers all forested lands through a partnership encompassing the Forest Service, State foresters, and other State and Federal agencies and academic groups (FHM 2016). The FHM program utilizes data from a wide variety of data sources, both inside and outside the Forest Service, and develops analytical approaches for addressing forest health issues that affect the sustainability of forest ecosystems. The FHM program has four major components (fig. 1.2):

- Detection Monitoring—nationally standardized aerial and ground surveys to evaluate status and change in condition of forest ecosystems (sections 1 and 2 of this report).
- Evaluation Monitoring—projects to determine the extent, severity, and causes of undesirable changes in forest health identified through Detection Monitoring (section 3 of this report).
- Research on Monitoring Techniques—work to develop or improve indicators, monitoring systems, and analytical techniques, such as urban and riparian forest health monitoring, early detection of invasive species, multivariate analyses of forest health indicators, and spatial scan statistics (section 2 of this report).

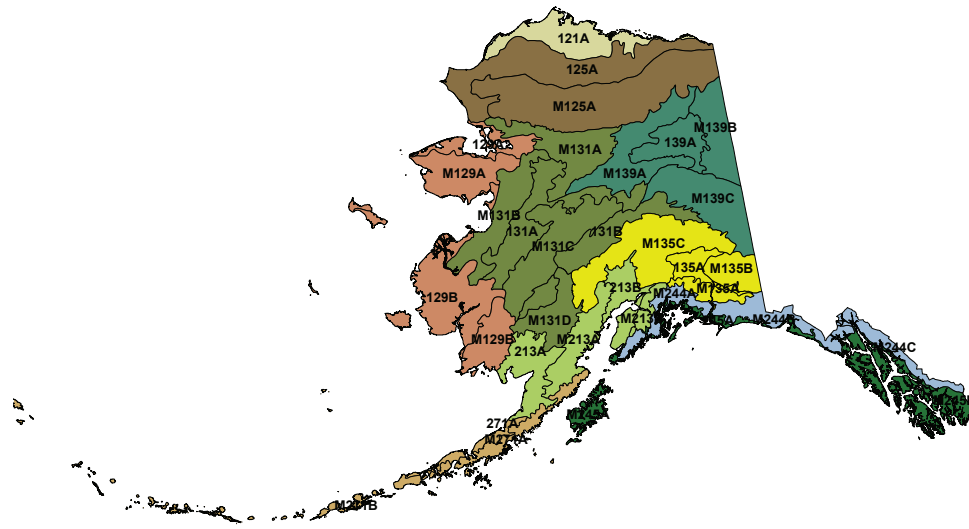
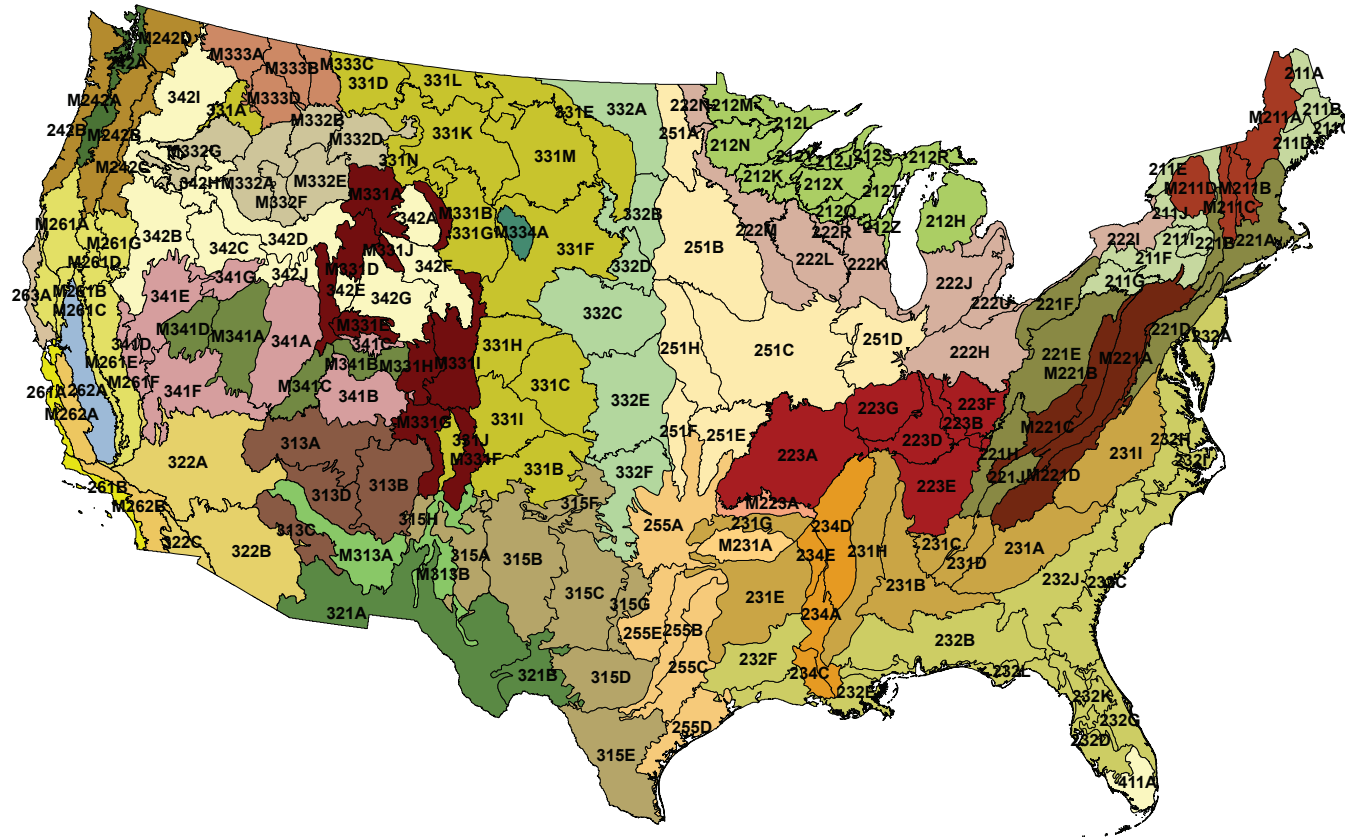


























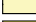

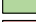
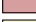


















Figure 1.1—Ecoregion provinces and sections for the conterminous United States (Cleland and others 2007) and Alaska (Nowacki and Brock 1995). Ecoregion sections within each ecoregion province are shown in the same color. Note that no equivalent ecoregion treatments exist for Hawaii, Puerto Rico, and the U.S. Virgin Islands.



Alaska ecoregion provinces

-  Alaska Mixed Forest (213)
-  Alaska Range Taiga (135)
-  Aleutian Meadow (271)
-  Arctic Tundra (121)
-  Bering Sea Tundra (129)
-  Brooks Range Tundra (125)
-  Pacific Coastal Icefields (244)
-  Pacific Gulf Coast Forest (245)
-  Upper Yukon Taiga (139)
-  Yukon Intermontaine Taiga (131)

Conterminous States ecoregion provinces

-  Adirondack-New England Mixed Forest - Coniferous Forest - Alpine Meadow (M211)
-  American Semi-Desert and Desert (322)
-  Arizona-New Mexico Mountains Semi-Desert - Open Woodland - Coniferous Forest - Alpine Meadow (M313)
-  Black Hills Coniferous Forest (M334)
-  California Coastal Chaparral Forest and Shrub (261)
-  California Coastal Range Open Woodland - Shrub - Coniferous Forest - Meadow (M262)
-  California Coastal Steppe - Mixed Forest - Redwood Forest (263)
-  California Dry Steppe (262)
-  Cascade Mixed Forest - Coniferous Forest - Alpine Meadow (M242)
-  Central Appalachian Broadleaf Forest - Coniferous Forest - Meadow (M221)
-  Central Interior Broadleaf Forest (223)
-  Chihuahuan Semi-Desert (321)
-  Colorado Plateau Semi-Desert (313)
-  Eastern Broadleaf Forest (221)
-  Everglades (411)
-  Great Plains - Palouse Dry Steppe (331)
-  Great Plains Steppe (332)
-  Intermountain Semi-Desert and Desert (341)
-  Intermountain Semi-Desert (342)
-  Laurentian Mixed Forest (212)
-  Lower Mississippi Riverine Forest (234)
-  Middle Rocky Mountain Steppe - Coniferous Forest - Alpine Meadow (M332)
-  Midwest Broadleaf Forest (222)
-  Nevada-Utah Mountains Semi-Desert - Coniferous Forest - Alpine Meadow (M341)
-  Northeastern Mixed Forest (211)
-  Northern Rocky Mountain Forest-Steppe - Coniferous Forest - Alpine Meadow (M333)
-  Ouachita Mixed Forest-Meadow (M231)
-  Outer Coastal Plain Mixed Forest (232)
-  Ozark Broadleaf Forest (M223)
-  Pacific Lowland Mixed Forest (242)
-  Prairie Parkland (Subtropical) (255)
-  Prairie Parkland (Temperate) (251)
-  Sierran Steppe - Mixed Forest - Coniferous Forest - Alpine Meadow (M261)
-  Southeastern Mixed Forest (231)
-  Southern Rocky Mountain Steppe - Open Woodland - Coniferous Forest - Alpine Meadow (M331)
-  Southwest Plateau and Plains Dry Steppe and Shrub (315)

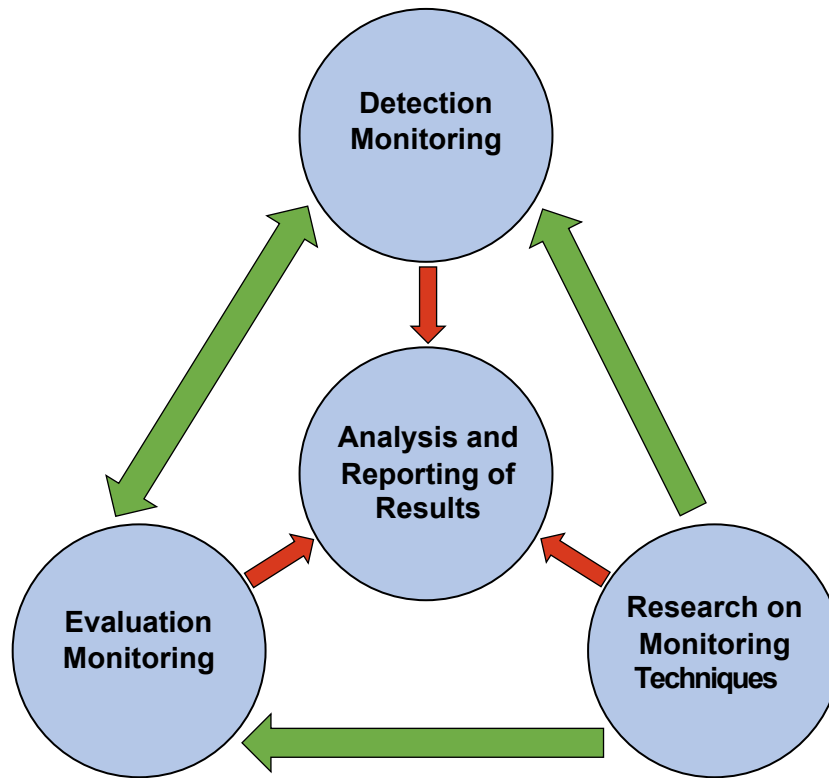


Figure 1.2—The design of the Forest Health Monitoring (FHM) program.

- **Analysis and Reporting**—synthesis of information from various data sources within and external to the Forest Service to produce issue-driven reports on status and change in forest health at national, regional, and State levels (sections 1, 2, and 3 of this report).

The FHM program, in addition to national reporting, generates regional and State reports, often in cooperation with FHM partners, both within the Forest Service and in State forestry

and agricultural departments. For example, the FHM regions cooperate with their respective State partners to produce the annual Forest Health Highlights report series, available on the FHM Web site at www.fs.fed.us/foresthealth/fhm. Other examples include Steinman (2004) and Harris and others (2011).

The FHM program and its partners also produce reports and journal articles on monitoring techniques and analytical methods,

including forest health data (Potter and others 2016, Siry and others 2018, Smith and Conkling 2004); soils as an indicator of forest health (O'Neill and others 2005); urban forest health monitoring (Bigsby and others 2014; Cumming and others 2006, 2007; Lake and others 2006); remote sensing of forest disturbances (Chastain and others 2015, Rebbeck and others 2015); health conditions in national forests (Morin and others 2006); crown conditions (Morin and others 2015; Randolph 2010a, 2010b, 2013; Randolph and Moser 2009; Schomaker and others 2007); indicators of regeneration (McWilliams and others 2015); vegetation diversity and structure (Schulz and Gray 2013, Schulz and others 2009, Simkin and others 2016); forest lichen communities (Jovan and others 2012, Root and others 2014); downed woody materials in forests (Woodall and others 2012, 2013); drought (Vose and others 2016); ozone monitoring (Rose and Coulston 2009); patterns of nonnative invasive plant occurrence (Guo and others 2015, 2017; Iannone and others 2015, 2016a, 2016b; Jo and others 2018; Oswalt and others 2015; Riitters and others 2018); assessments of alien-invasive forest insect and disease risk (Koch and others 2011, 2014; Krist and others 2014; Vogt and Koch 2016; Yemshanov and others 2014); spatial patterns of landcover (Riitters 2011; Riitters and Costanza 2019; Riitters and others 2012, 2016, 2017; Riitters and Wickham 2012); impacts of deer browse on forest structure (Russell and others 2017); broad-scale assessments of forest biodiversity (Potter 2018; Potter and Koch 2014; Potter and Woodall 2012, 2014); predictions and

indicators of climate change effects on forests and forest tree species (Fei and others 2017, Heath and others 2015, Potter and Hargrove 2013); and the overall forest health indicator program (Woodall and others 2010).

For more information about the FHM program, visit the FHM Web site at www.fs.fed.us/foresthealth/fhm. Among other resources, this Web site includes links to all past national forest health reports (www.fs.fed.us/foresthealth/fhm/pubs), information about funded Evaluation Monitoring projects (www.fs.fed.us/foresthealth/fhm/em), and annual State forest health highlight reports (www.fs.fed.us/foresthealth/fhm/fhh/fhmusamap.shtml).

DATA SOURCES

Forest Service data sources in this edition of the FHM national report include FIA annualized Phase 2 and Phase 3 survey data (Bechtold and Patterson 2005, Woodall and others 2010, Woudenberg and others 2010); FHP national Insect and Disease Survey forest mortality and defoliation data for 2017 (FHP 2018); Moderate Resolution Imaging Spectroradiometer (MODIS) Active Fire Detections for the United States data for 2017 (USDA Forest Service 2017); forest cover data developed from MODIS satellite imagery by the Forest Service Geospatial Technology and Applications Center (GTAC); and FIA's publicly available Environmental Monitoring and Assessment Program (EMAP) hexagons (Brand and others 2000). Other sources of data include Parameter-elevation Regression on Independent Slopes Model

(PRISM) climate mapping system data (PRISM Climate Group 2018) and tree canopy cover data generated from the 2011 National Land Cover Database (Homer and others 2015) through a cooperative project between the Multi-Resolution Land Characteristics Consortium and GTAC (Coulston and others 2012).

As a major source of data for several FHM analyses, the FIA program merits detailed description. The FIA program collects forest inventory information across all forest land ownerships in the United States and maintains a network of more than 130,000 permanent forested ground plots across the conterminous United States and southeastern Alaska, with a sampling intensity of approximately one plot/2428 ha. Forest Inventory and Analysis Phase 2 encompasses the annualized inventory measured on plots at regular intervals, with each plot surveyed every 5 to 7 years in most Eastern States, but with plots in the Rocky Mountain and Pacific Northwest regions surveyed once every 10 years (Reams and others 2005). The standard 0.067-ha plot (fig. 1.3) consists of four 7.315-m (24-foot) radius subplots (approximately 168.6 m² or 1/24th acre), on which field crews measure trees at least 12.7 cm (5 inches) in diameter. Within each of these subplots is nested a 2.073-m (6.8-foot) radius microplot (approximately 13.48 m² or 1/300th acre), on which crews measure trees smaller than 12.7 cm (5 inches) in diameter. A core-optional variant of the standard design includes four “macroplots,” each with a radius of 17.953 m

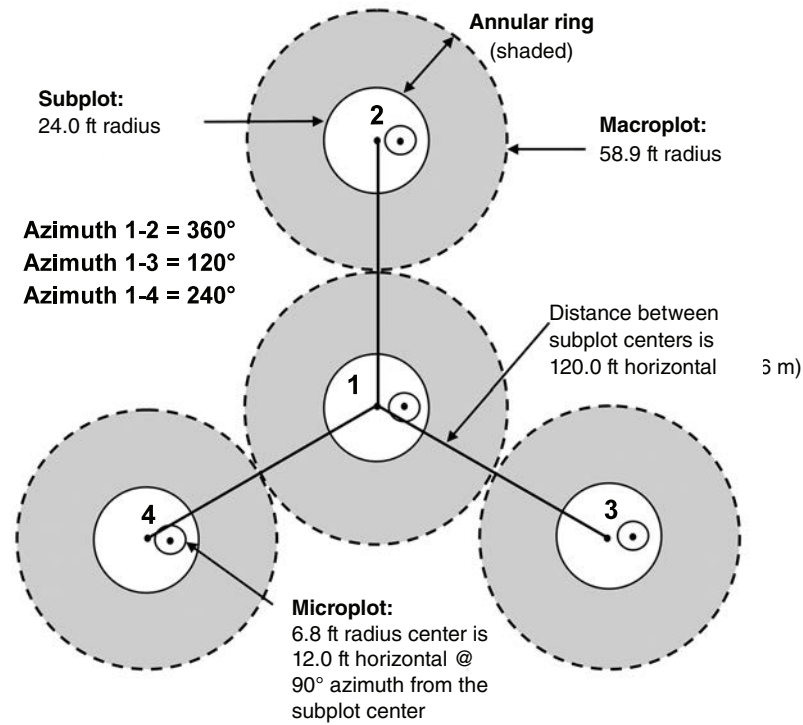


Figure 1.3—The Forest Inventory and Analysis mapped plot design. Subplot 1 is the center of the cluster with subplots 2, 3, and 4 located 120 feet away at azimuths of 360°, 120°, and 240°, respectively (Woudenberg and others 2010).

(or approximately 0.1012 ha) that originates at the center of each subplot (Woudenberg and others 2010).

Forest Inventory and Analysis Phase 3 plots have represented a subset of these Phase 2 plots, with one Phase 3 plot for every 16 standard FIA Phase 2 plots. In addition to traditional forest inventory measurements, data for a variety of important ecological indicators have been collected from Phase 3 plots, including tree crown condition, lichen communities, downed

woody material, soil condition, and vegetation structure and diversity, whereas data on ozone bioindicator plants are collected on a separate grid of plots (Woodall and others 2010, 2011). Most of these additional forest health indicators were measured as part of the FHM Detection Monitoring ground plot system prior to 2000¹ (Palmer and others 1991).

FHM REPORT PRODUCTION

This FHM national report, the 18th in a series of such annual documents, is produced by forest health monitoring researchers at the Eastern Forest Environmental Threat Assessment Center (EFETAC) in collaboration with North Carolina State University cooperators. A unit of the Southern Research Station of the Forest Service, EFETAC was established under the Healthy Forests Restoration Act of 2003 to generate the knowledge and tools needed to anticipate and respond to environmental threats. For more information about the research team and about threats to U.S. forests, please visit www.forestthreats.org/about.

LITERATURE CITED

Ambrose, M.J.; Conkling, B.L., eds. 2007. Forest Health Monitoring 2005 national technical report. Gen. Tech. Rep. SRS-104. Asheville, NC: U.S. Department of Agriculture Forest Service, Southern Research Station. 76 p.

¹ USDA Forest Service. 1998. Forest Health Monitoring 1998 field methods guide. Research Triangle Park, NC: U.S. Department of Agriculture Forest Service, Forest Health Monitoring program. 473 p. On file with Forest Health Monitoring program, 3041 Cornwallis Rd., Research Triangle Park, NC 27709.

- Ambrose, M.J.; Conkling, B.L., eds. 2009. Forest Health Monitoring 2006 national technical report. Gen. Tech. Rep. SRS-117. Asheville, NC: U.S. Department of Agriculture Forest Service, Southern Research Station. 118 p.
- Bailey, R.G. 1995. Descriptions of the ecoregions of the United States. 2d ed. Miscellaneous Publication No. 1391. Washington, DC: U.S. Department of Agriculture Forest Service. 108 p. Map; presentation scale 1:7,500,000.
- Bechtold, W.A.; Patterson, P.L., eds. 2005. The enhanced Forest Inventory and Analysis program—national sampling design and estimation procedures. Gen. Tech. Rep. SRS-80. Asheville, NC: U.S. Department of Agriculture Forest Service, Southern Research Station. 85 p.
- Bigsby, K.M.; Ambrose, M.J.; Tobin, P.C.; Sills, E.O. 2014. The cost of gypsy moth sex in the city. *Urban Forestry & Urban Greening*. 13(3): 459–468.
- Brand, G.J.; Nelson, M.D.; Wendt, D.G.; Nimerfro, K.K. 2000. The hexagon/panel system for selecting FIA plots under an annual inventory. In: McRoberts, R.E.; Reams, G.A.; Van Deusen, P.C., eds. Proceedings of the first annual Forest Inventory and Analysis symposium. Gen. Tech. Rep. NC-213. St. Paul, MN: U.S. Department of Agriculture Forest Service, North Central Research Station: 8–13.
- Chastain, R.A.; Fisk, H.; Ellenwood, J.R. [and others]. 2015. Near-real time delivery of MODIS-based information on forest disturbances. In: Lippitt, C.D.; Stow, D.A.; Coulter, L.L., eds. Time sensitive remote sensing. New York, NY: Springer: 147–164.
- Cleland, D.T.; Avers, P.E.; McNab, W.H. [and others]. 1997. National hierarchical framework of ecological units. In: Boyce, M.S.; Haney, A., eds. Ecosystem management applications for sustainable forest and wildlife resources. New Haven, CT: Yale University Press: 181–200.
- Cleland, D.T.; Freeouf, J.A.; Keys, J.E. [and others]. 2007. Ecological subregions: sections and subsections for the conterminous United States. Gen. Tech. Rep. WO-76D. Washington, DC: U.S. Department of Agriculture Forest Service. Map; Sloan, A.M., cartographer; presentation scale 1:3,500,000; colored. Also on CD-ROM as a GIS coverage in ArcINFO format or at <http://data.fs.usda.gov/geodata/edw/datasets.php>. [Date accessed: July 20, 2015].

- Conkling, B.L., ed. 2011. Forest Health Monitoring 2007 national technical report. Gen. Tech. Rep. SRS-147. Asheville, NC: U.S. Department of Agriculture Forest Service, Southern Research Station. 159 p.
- Conkling, B.L.; Coulston, J.W.; Ambrose, M.J., eds. 2005. Forest Health Monitoring 2001 national technical report. Gen. Tech. Rep. SRS-81. Asheville, NC: U.S. Department of Agriculture Forest Service, Southern Research Station. 204 p.
- Costanza, R. 1992. Toward an operational definition of ecosystem health. In: Costanza, R.; Norton, B.G.; Haskell, B.D., eds. Ecosystem health: new goals for environmental management. Washington, DC: Island Press: 239–256.
- Coulston, J.W.; Riitters, K.H.; Conkling, B.L., eds. 2005a. Forest Health Monitoring 2002 national technical report. Gen. Tech. Rep. SRS-84. Asheville, NC: U.S. Department of Agriculture Forest Service, Southern Research Station. 97 p.
- Coulston, J.W.; Ambrose, M.J.; Riitters, K.H. [and others], eds. 2005b. Forest Health Monitoring 2003 national technical report. Gen. Tech. Rep. SRS-85. Asheville, NC: U.S. Department of Agriculture Forest Service, Southern Research Station. 97 p.
- Coulston, J.W.; Ambrose, M.J.; Riitters, K.H.; Conkling, B.L., eds. 2005c. Forest Health Monitoring 2004 national technical report. Gen. Tech. Rep. SRS-90. Asheville, NC: U.S. Department of Agriculture Forest Service, Southern Research Station. 81 p.
- Coulston, J.W.; Moisen, G.G.; Wilson, B.T. [and others]. 2012. Modeling percent tree canopy cover: a pilot study. Photogrammetric Engineering and Remote Sensing. 78(7): 715–727.
- Cumming, A.B.; Nowak, D.J.; Twardus, D.B. [and others]. 2007. Urban forests of Wisconsin: pilot monitoring project 2002. NA-FR-05-07. Newtown Square, PA: U.S. Department of Agriculture Forest Service, Northeastern Area State and Private Forestry. 33 p. Low resolution: http://www.na.fs.fed.us/pubs/fhm/pilot/pilot_study_wisconsin_02_lr.pdf. High resolution: http://www.na.fs.fed.us/pubs/fhm/pilot/pilot_study_wisconsin2_02_hr.pdf. [Date accessed: October 19, 2007].
- Cumming, A.B.; Twardus, D.B.; Smith, W.D. 2006. National Forest Health Monitoring program, Maryland and Massachusetts street tree monitoring pilot projects. NA-FR-01-06. Newtown Square, PA: U.S. Department of Agriculture Forest Service, Northeastern Area, State and Private Forestry. 23 p.
- Edmonds, R.L.; Agee, J.K.; Gara, R.I. 2011. Forest health and protection. Long Grove, IL: Waveland Press, Inc. 667 p.
- Fei, S.; Desprez, J.M.; Potter, K.M. [and others]. 2017. Divergence of species responses to climate change. *Science Advances*. 3(5):e1603055. DOI: 10.1126/sciadv.1603055.
- Forest Health Monitoring (FHM). 2016. Program description. Forest Health Monitoring fact sheet series. <http://www.fhm.fs.fed.us/fact/>. [Date accessed: September 8, 2016].
- Forest Health Protection (FHP). 2018. Insect and Disease Detection Survey Database (IDS). [Online database]. Fort Collins, CO: U.S. Department of Agriculture Forest Service, Forest Health Technology Enterprise Team. <https://www.fs.fed.us/foresthealth/applied-sciences/mapping-reporting/gis-spatial-analysis/detection-surveys.shtml#idsdownloads>. [Date accessed: October 24, 2018].
- Guo, G.; Fei, S.; Dukes, J.S. [and others]. 2015. A unified approach to quantify invasibility and degree of invasion. *Ecology*. 95(10): 2613–2621.
- Guo, G.; Iannone, B.V.; Nunez-Mir, G.C. [and others]. 2017. Species pool, human population, and global vs. regional invasion patterns. *Landscape Ecology*. 32(2): 229–238.
- Harris, J.L., comp.; Region 2 Forest Health Protection staff. 2011. Forest health conditions, 2009–2010: Rocky Mountain Region (R2). R2-11-RO-31. Golden, CO: U.S. Department of Agriculture Forest Service, Renewable Resources, Forest Health Protection, Rocky Mountain Region. 108 p.
- Heath, L.S.; Anderson, S.; Emery, M.R. [and others]. 2015. Indicators for climate change impacts for forests: National Climate Assessment indicators. Gen. Tech. Rep. NRS-155. Newtown Square, PA: U.S. Department of Agriculture Forest Service, Northern Research Station. 143 p.
- Homer, C.G.; Dewitz, J.A.; Yang, L. [and others]. 2015. Completion of the 2011 National Land Cover Database for the conterminous United States: representing a decade of land cover change information. *Photogrammetric Engineering and Remote Sensing*. 81(5): 345–354.

- Iannone, B.V.; Oswalt, C.M.; Liebhold, A.M. [and others]. 2015. Region-specific patterns and drivers of macroscale forest plant invasions. *Diversity and Distributions*. 21: 1181–1192.
- Iannone, B.V.; Potter, K.M.; Guo, Q. [and others]. 2016a. Biological invasion hotspots: a trait-based perspective reveals new sub-continental patterns. *Ecography*. 39: 961–969.
- Iannone, B.V.; Potter, K.M.; Hamil, K.-A.D. [and others]. 2016b. Evidence of biotic resistance to invasions in forests of the Eastern USA. *Landscape Ecology*. 31: 85–99.
- Jo, I.; Potter, K.M.; Domke, G.; Fei, S. 2018. Dominant forest tree mycorrhizal type mediates understory plant invasions. *Ecology Letters*. 21: 217–224.
- Jovan, S.; Riddell, J.; Padgett, P.E.; Nash, T.H., III. 2012. Eutrophic lichens respond to multiple forms of N: implications for critical levels and critical loads research. *Ecological Applications*. 22(7): 1910–1922.
- Koch, F.H.; Yemshanov, D.; Colunga-Garcia, M. [and others]. 2011. Potential establishment of alien-invasive forest insect species in the United States: where and how many? *Biological Invasions*. 13: 969–985.
- Koch, F.H.; Yemshanov, D.; Haack, R.A.; Magarey, R.D. 2014. Using a network model to assess risk of forest pest spread via recreational travel. *PLOS ONE*. 9(7): e102105.
- Kolb, T.E.; Wagner, M.R.; Covington, W.W. 1994. Concepts of forest health: utilitarian and ecosystem perspectives. *Journal of Forestry*. 92: 10–15.
- Krist, F.J., Jr.; Ellenwood, J.R.; Woods, M.E. [and others]. 2014. 2012–2027 national insect and disease forest risk assessment. FHTET-14-01. U.S. Department of Agriculture Forest Service, Forest Health Technology Enterprise Team. 199 p. http://www.fs.fed.us/foresthealth/technology/pdfs/2012_RiskMap_Report_web.pdf. [Date accessed: July 24, 2014].
- Lake, M.; Marshall, P.; Mielke, M. [and others]. 2006. National Forest Health Monitoring program monitoring urban forests in Indiana: pilot study 2002, part 1. Analysis of field methods and data collection. Gen. Tech Rep. NA-FR-06-06. Newtown Square, PA: U.S. Department of Agriculture Forest Service, Northeastern Area. <http://www.fhm.fs.fed.us/pubs/ufhm/indianaforests02/indianaforests02.html>. [Date accessed: November 6, 2007].
- McWilliams, W.H.; Westfall, J.A.; Brose, P.H. [and others]. 2015. A regeneration indicator for Forest Inventory and Analysis: history, sampling, estimation, analytics, and potential use in the Midwest and Northeast United States. Gen. Tech. Rep. NRS-148. Newtown Square, PA: U.S. Department of Agriculture Forest Service, Northern Research Station. 74 p.
- Montréal Process Working Group. 1995. Criteria and indicators for the conservation and sustainable management of temperate and boreal forests. <http://www.montrealprocess.org/>. [Date accessed: March 4, 2015].
- Morin, R.S.; Liebhold, A.M.; Gottschalk, K.W. [and others]. 2006. Analysis of Forest Health Monitoring surveys on the Allegheny National Forest (1998–2001). Gen. Tech. Rep. NE-339. Newtown Square, PA: U.S. Department of Agriculture Forest Service, Northeastern Research Station. 102 p. http://www.fs.fed.us/ne/newtown_square/publications. [Date accessed: November 6, 2007].
- Morin, R.S.; Randolph, K.C.; Steinman, J. 2015. Mortality rates associated with crown health for eastern forest tree species. *Environmental Monitoring and Assessment*. 187(3): 87.
- Nowacki, G.; Brock, T. 1995. Ecoregions and subregions of Alaska [EcoMap]. Version 2.0. Juneau, AK: U.S. Department of Agriculture Forest Service, Alaska Region. Map; presentation scale 1:5,000,000; colored.
- O'Neill, K.P.; Amacher, M.C.; Perry, C.H. 2005. Soils as an indicator of forest health: a guide to the collection, analysis, and interpretation of soil indicator data in the Forest Inventory and Analysis program. Gen. Tech. Rep. NC-258. St. Paul, MN: U.S. Department of Agriculture Forest Service, North Central Research Station. 53 p.
- Oswalt, C.M.; Fei, S.; Guo, G. [and others]. 2015. A subcontinental view of forest plant invasions. *NeoBiota*. 24: 49–54.
- Palmer, C.J.; Riitters, K.H.; Strickland, T. [and others]. 1991. Monitoring and research strategy for forests—Environmental Monitoring and Assessment Program (EMAP). EPA/600/4-91/012. Washington, DC: U.S. Environmental Protection Agency. 189 p.
- Potter, K.M. 2018. Do United States protected areas effectively conserve forest tree rarity and evolutionary distinctiveness? *Biological Conservation*. 224: 34–46.

- Potter, K.M.; Conkling, B.L., eds. 2012a. Forest Health Monitoring 2008 national technical report. Gen. Tech. Rep. SRS-158. Asheville, NC: U.S. Department of Agriculture Forest Service, Southern Research Station. 179 p.
- Potter, K.M.; Conkling, B.L., eds. 2012b. Forest Health Monitoring 2009 national technical report. Gen. Tech. Rep. SRS-167. Asheville, NC: U.S. Department of Agriculture Forest Service, Southern Research Station. 252 p.
- Potter, K.M.; Conkling, B.L., eds. 2013a. Forest Health Monitoring: national status, trends, and analysis, 2010. Gen. Tech. Rep. SRS-176. Asheville, NC: U.S. Department of Agriculture Forest Service, Southern Research Station. 162 p.
- Potter, K.M.; Conkling, B.L., eds. 2013b. Forest Health Monitoring: national status, trends, and analysis 2011. Gen. Tech. Rep. SRS-185. Asheville, NC: U.S. Department of Agriculture Forest Service, Southern Research Station. 149 p.
- Potter, K.M.; Conkling, B.L., eds. 2014. Forest Health Monitoring: national status, trends, and analysis 2012. Gen. Tech. Rep. SRS-198. Asheville, NC: U.S. Department of Agriculture Forest Service, Southern Research Station. 192 p.
- Potter, K.M.; Conkling, B.L., eds. 2015a. Forest Health Monitoring: national status, trends, and analysis, 2013. Gen. Tech. Rep. SRS-207. Asheville, NC: U.S. Department of Agriculture Forest Service, Southern Research Station. 199 p.
- Potter, K.M.; Conkling, B.L., eds. 2015b. Forest Health Monitoring: national status, trends, and analysis, 2014. Gen. Tech. Rep. SRS-209. Asheville, NC: U.S. Department of Agriculture Forest Service, Southern Research Station. 190 p.
- Potter, K.M.; Conkling, B.L., eds. 2016. Forest Health Monitoring: national status, trends, and analysis, 2015. Gen. Tech. Rep. SRS-213. Asheville, NC: U.S. Department of Agriculture Forest Service, Southern Research Station. 199 p.
- Potter, K.M.; Conkling, B.L., eds. 2017. Forest Health Monitoring: national status, trends, and analysis, 2016. Gen. Tech. Rep. SRS-222. Asheville, NC: U.S. Department of Agriculture Forest Service, Southern Research Station. 195 p.
- Potter, K.M.; Conkling, B.L., eds. 2018. Forest Health Monitoring: national status, trends, and analysis, 2017. Gen. Tech. Rep. SRS-233. Asheville, NC: U.S. Department of Agriculture Forest Service, Southern Research Station. 190 p.
- Potter, K.M.; Hargrove, W.W. 2013. Quantitative metrics for assessing predicted climate change pressure on North American tree species. *Mathematical and Computational Forestry and Natural Resources Sciences*. 5(2): 151–169.
- Potter, K.M.; Koch, F.H. 2014. Phylogenetic community structure of forests across the conterminous United States: regional ecological patterns and forest health implications. *Forest Science*. 60(5): 851–861.
- Potter, K.M.; Koch, F.H.; Oswalt, C.M.; Iannone, B.V. 2016. Data, data everywhere: detecting spatial patterns in fine-scale ecological information collected across a continent. *Landscape Ecology*. 31: 67–84.
- Potter, K.M.; Woodall, C.W. 2012. Trends over time in tree and seedling phylogenetic diversity indicate regional differences in forest biodiversity change. *Ecological Applications*. 22(2): 517–531.
- Potter, K.M.; Woodall, C.W. 2014. Does biodiversity make a difference? Relationships between species richness, evolutionary diversity, and aboveground live tree biomass across U.S. forests. *Forest Ecology and Management*. 321: 117–129.
- PRISM Climate Group. 2018. 2.5-arcmin (4 km) gridded monthly climate data. <http://www.prism.oregonstate.edu>. [Date accessed: June 14, 2018].
- Raffa, K.F.; Aukema, B.; Bentz, B.J. [and others]. 2009. A literal use of “forest health” safeguards against misuse and misapplication. *Journal of Forestry*. 107: 276–277.
- Randolph, K.C. 2010a. Equations relating compacted and uncompacted live crown ratio for common tree species in the South. *Southern Journal of Applied Forestry*. 34(3): 118–123.

- Randolph, K.C. 2010b. Comparison of the arithmetic and geometric means in estimating crown diameter and crown cross-sectional area. *Southern Journal of Applied Forestry*. 34(4): 186–189.
- Randolph, K.C. 2013. Development history and bibliography of the U.S. Forest Service crown-condition indicator for forest health monitoring. *Environmental Monitoring and Assessment*. 185(6): 4977–4993.
- Randolph, K.C.; Moser, W.K. 2009. Tree crown condition in Missouri, 2000–2003. Gen. Tech. Rep. SRS-113. Asheville, NC: U.S. Department of Agriculture Forest Service, Southern Research Station. 11 p.
- Reams, G.A.; Smith, W.D.; Hansen, M.H. [and others]. 2005. The Forest Inventory and Analysis sampling frame. In: Bechtold, W.A.; Patterson, P.L., eds. *The enhanced Forest Inventory and Analysis program—national sampling design and estimation procedures*. Asheville, NC: U.S. Department of Agriculture Forest Service, Southern Research Station: 11–26.
- Rebbeck, J.; Kloss, A.; Bowden, M. [and others]. 2015. Aerial detection of seed-bearing female *Ailanthus altissima*: a cost-effective method to map an invasive tree in forested landscapes. *Forest Science*. 61: 1068–1078.
- Riitters, K.H. 2011. Spatial patterns of land cover in the United States: a technical document supporting the Forest Service 2010 RPA assessment. Gen. Tech. Rep. SRS-136. Asheville, NC: U.S. Department of Agriculture Forest Service, Southern Research Station. 64 p.
- Riitters, K.; Costanza, J. 2019. The landscape context of family forests in the United States: anthropogenic interfaces and forest fragmentation from 2001 to 2011. *Landscape and Urban Planning*. 188: 64–71.
- Riitters, K.H.; Costanza, J.K.; Buma, B. 2017. Interpreting multiscale domains of tree cover disturbance patterns in North America. *Ecological Indicators*. 80: 147–152.
- Riitters, K.H.; Coulston, J.W.; Wickham, J.D. 2012. Fragmentation of forest communities in the Eastern United States. *Forest Ecology and Management*. 263: 85–93.
- Riitters, K.; Potter, K.M.; Iannone, B.V.; [and others]. 2018. Landscape correlates of forest plant invasions: a high-resolution analysis across the Eastern United States. *Diversity and Distributions*. 24: 274–284.
- Riitters, K.H.; Tkacz, B. 2004. The U.S. Forest Health Monitoring program. In: Wiersma, G.B., ed. *Environmental monitoring*. Boca Raton, FL: CRC Press: 669–683.
- Riitters, K.H.; Wickham, J.D. 2012. Decline of forest interior conditions in the conterminous United States. *Scientific Reports*. 2: 653. 4 p. DOI: 10.1038.srep00653. [Published online: September 13, 2012].
- Riitters, K.H.; Wickham, J.D.; Costanza, J.K.; Vogt, P. 2016. A global evaluation of forest interior area dynamics using tree cover data from 2000 to 2012. *Landscape Ecology*. 31: 137–148.
- Root, H.T.; McCune, B.; Jovan, S. 2014. Lichen communities and species indicate climate thresholds in southeast and south-central Alaska, USA. *The Bryologist*. 117(3): 241–252.
- Rose, A.K.; Coulston, J.W. 2009. Ozone injury across the Southern United States, 2002–06. Gen. Tech. Rep. SRS-118. Asheville, NC: U.S. Department of Agriculture Forest Service, Southern Research Station. 25 p.
- Russell, M.B.; Woodall, C.W.; Potter, K.M. [and others]. 2017. Interactions between white-tailed deer density and the composition of forest understories in the northern United States. *Forest Ecology and Management*. 384: 26–33.
- Schomaker, M.E.; Zarnoch, S.J.; Bechtold, W.A. [and others]. 2007. *Crown-condition classification: a guide to data collection and analysis*. Gen. Tech. Rep. SRS-102. Asheville, NC: U.S. Department of Agriculture, Forest Service, Southern Research Station. 78 p.
- Schulz, B.K.; Bechtold, W.A.; Zarnoch, S.J. 2009. Sampling and estimation procedures for the vegetation diversity and structure indicator. Gen. Tech. Rep. PNW-781. Portland, OR: U.S. Department of Agriculture, Forest Service, Pacific Northwest Research Station. 53 p.
- Schulz, B.K.; Gray, A.N. 2013. The new flora of northeastern USA: quantifying introduced plant species occupancy in forest ecosystems. *Environmental Monitoring and Assessment*. 185: 3931–3957.
- Simkin, S.M.; Allen, E.B.; Bowman, W.D. [and others]. 2016. Conditional vulnerability of plant diversity to atmospheric nitrogen deposition across the United States. *Proceedings of the National Academy of Sciences of the United States of America*. 113: 4086–4091.

- Siry, J.; Cabbage, F.W.; Potter, K.M.; McGinley, K. 2018. Current perspectives on sustainable forest management: North America. *Current Forestry Reports*. 4(3): 138–149.
- Smith, W.D.; Conkling, B.L. 2004. Analyzing forest health data. Gen. Tech. Rep. SRS-077. Asheville, NC: U.S. Department of Agriculture Forest Service, Southern Research Station. 33 p. http://www.srs.fs.usda.gov/pubs/gtr/gtr_srs077.pdf. [Date accessed: November 6, 2007].
- Smith, W.B.; Miles, P.D.; Perry, C.H.; Pugh, S.A. 2009. Forest resources of the United States, 2007. Gen. Tech. Rep. WO-78. St. Paul, MN: U.S. Department of Agriculture Forest Service, Washington Office. 336 p.
- Steinman, J. 2004. Forest Health Monitoring in the Northeastern United States: disturbances and conditions during 1993–2002. NA-Technical Paper 01-04. Newtown Square, PA: U.S. Department of Agriculture Forest Service, Northeastern Area State and Private Forestry. 46 p. http://fhm.fs.fed.us/pubs/tp/dist_cond/dc.shtml. [Date accessed: December 8, 2009].
- Teale, S.A.; Castello, J.D. 2011. The past as key to the future: a new perspective on forest health. In: Castello, J.D.; Teale, S.A., eds. *Forest health: an integrated perspective*. New York: Cambridge University Press: 3–16.
- U.S. Department of Agriculture (USDA) Forest Service. 2004. National report on sustainable forests—2003. FS-766. Washington, DC: U.S. Department of Agriculture Forest Service. 139 p.
- U.S. Department of Agriculture (USDA) Forest Service. 2011. National report on sustainable forests—2010. Report FS-979. Washington, DC: U.S. Department of Agriculture Forest Service. 134 p.
- U.S. Department of Agriculture (USDA) Forest Service. 2018. MODIS active fire mapping program: fire detection GIS data. <https://fsapps.nwcg.gov/afm/gisdata.php>. [Date accessed: January 12, 2018].
- Vogt, J.T.; Koch, F.H. 2016. The evolving role of Forest Inventory and Analysis data in invasive insect research. *American Entomologist*. 62(1): 46–58.
- Vose, J.M.; Clark, J.S.; Luce, C.H.; Patel-Weynand, T., eds. 2016. Effects of drought on forests and rangelands in the United States: a comprehensive science synthesis. Gen. Tech. Rep. WO-93b. Washington, DC: U.S. Department of Agriculture Forest Service, Washington Office. 289 p.
- Woodall, C.W.; Amacher, M.C.; Bechtold, W.A. [and others]. 2011. Status and future of the forest health indicators program of the USA. *Environmental Monitoring and Assessment*. 177: 419–436.
- Woodall, C.W.; Conkling, B.L.; Amacher, M.C. [and others]. 2010. The Forest Inventory and Analysis database version 4.0: database description and users manual for Phase 3. Gen. Tech. Rep. NRS-61. Newtown Square, PA: U.S. Department of Agriculture Forest Service, Northern Research Station. 180 p.
- Woodall, C.W.; Walters, B.F.; Oswalt, S.N. [and others]. 2013. Biomass and carbon attributes of downed woody materials in forests of the United States. *Forest Ecology and Management*. 305: 48–59.
- Woodall, C.W.; Walters, B.F.; Westfall, J.A. 2012. Tracking downed dead wood in forests over time: development of a piece matching algorithm for line intercept sampling. *Forest Ecology and Management*. 277: 196–204.
- Woudenberg, S.W.; Conkling, B.L.; O’Connell, B.M. [and others]. 2010. The Forest Inventory and Analysis database: database description and users manual version 4.0 for Phase 2. Gen. Tech. Rep. RMRS-245. Fort Collins, CO: United States Department of Agriculture Forest Service, Rocky Mountain Research Station. 336 p.
- Yemshanov, D.; Koch, F.H.; Lu, B. [and others]. 2014. There is no silver bullet: the value of diversification in planning invasive species surveillance. *Ecological Economics*. 104: 61–72.

SECTION 1.

Analyses of Short-Term Forest Health Data

INTRODUCTION

Insects and diseases cause changes in forest structure and function, species succession, and biodiversity, which may be considered negative or positive depending on management objectives (Edmonds and others 2011). An important task for forest managers, pathologists, and entomologists is recognizing and distinguishing between natural and excessive mortality, a task that relates to ecologically based or commodity-based management objectives (Teale and Castello 2011). The impacts of insects and diseases on forests vary from natural thinning to extraordinary levels of tree mortality, but insects and diseases are not necessarily enemies of the forest because they kill trees (Teale and Castello 2011). If disturbances, including insects and diseases, are viewed in their full ecological context, then some amount can be considered “healthy” to sustain the structure of the forest (Manion 2003, Zhang and others 2011) by causing tree mortality that culls weak competitors and releases resources that are needed to support the growth of surviving trees (Teale and Castello 2011).

Analyzing patterns of forest insect infestations, disease occurrences, forest declines, and related biotic stress factors is necessary to monitor the health of forested ecosystems and their potential impacts on forest structure, composition, biodiversity, and species distributions (Castello and others 1995). Introduced nonnative insects and diseases, in particular, can extensively damage the biodiversity, ecology, and economy of affected

areas (Brockhoff and others 2006, Mack and others 2000). Few forests remain unaffected by invasive species, and their devastating impacts in forests are undeniable, including, in some cases, wholesale changes to the structure and function of an ecosystem (Parry and Teale 2011).

Examining insect pest occurrences and related stress factors from a landscape-scale perspective is useful, given the regional extent of many infestations and the large-scale complexity of interactions between host distribution, stress factors, and the development of insect pest outbreaks (Holdenrieder and others 2004, Liebhold and others 2013). One such landscape-scale approach is detecting geographic patterns of disturbance, which allows for the identification of areas at greater risk of significant ecological and economic impacts and for the selection of locations for more intensive monitoring and analysis.

METHODS

Data

Forest Health Protection (FHP) national Insect and Disease Survey (IDS) data (FHP 2018) consist of information from low-altitude aerial survey and ground survey efforts by FHP and partners in State agencies. These data can be used to identify forest landscape-scale patterns associated with geographic hot spots of forest insect and disease activity in the conterminous 48 States and to summarize insect and disease activity by ecoregion in Alaska (Potter 2012, 2013; Potter and Koch 2012; Potter and Paschke 2013, 2014, 2015a, 2015b, 2016, 2017;

CHAPTER 2.

Large-Scale Patterns of Insect and Disease Activity in the Conterminous United States, Alaska, and Hawaii from the National Insect and Disease Survey, 2017

KEVIN M. POTTER

JEANINE L. PASCHKE

FRANK H. KOCH

MARK O. ZWEIFLER

Potter and others 2018) and by island in Hawaii (Potter and Paschke 2015b, 2017).

The IDS data identify areas of mortality and defoliation caused by insect and disease activity, although some important forest insects [such as emerald ash borer (*Agrilus planipennis*) and hemlock woolly adelgid (*Adelges tsugae*)], diseases [such as laurel wilt (*Raffaelea lauricola*), Dutch elm disease (*Ophiostoma novo-ulmi*), white pine blister rust (*Cronartium ribicola*), and thousand cankers disease (*Geosmithia morbida*)], and mortality complexes (such as oak decline) are not easily detected or thoroughly quantified through aerial detection surveys. Such pests may attack hosts that are widely dispersed throughout forests with high tree species diversity or may cause mortality or defoliation that is otherwise difficult to detect. A pathogen or insect might be considered a mortality-causing agent in one location and a defoliation-causing agent in another, depending on the level of damage to the forest in a given area and the convergence of other stress factors such as drought. In some cases, the identified agents of mortality or defoliation are actually complexes of multiple agents summarized under an impact label related to a specific host tree species (e.g., “beech bark disease complex” or “yellow-cedar decline”). Additionally, differences in data collection, attribute recognition, and coding procedures among States and regions can complicate data analysis and interpretation of the results.

In 2017, IDS surveys of the conterminous United States covered about 202.17 million ha,

of which approximately 140.36 million ha were forested (about 55.1 percent of the total forested area of the conterminous States). A total of 161.87 million ha were surveyed using the new Digital Mobile Sketch Mapping (DMSM) approach (fig. 2.1), while an additional 52.29 million ha were surveyed in 2017 using the legacy Digital Aerial Sketch Mapping (DASM) approach. (These numbers exceed the total area surveyed because of overlaps in locations covered by the two methodologies.) In Alaska, roughly 5.94 million ha were surveyed in 2017, using the DMSM approach, of which 3.76 million ha were forested, about 7.3 percent of the total forested area of the State. For Hawaii, slightly >1 million ha were surveyed in 2017, with 530 500 ha forested, approximately 80.1 percent of the State’s total forested area.

Digital Mobile Sketch Mapping includes tablet hardware, software, and data support processes that allow trained aerial surveyors in light aircraft, as well as ground observers, to record forest disturbances and their causal agents. Digital Mobile Sketch Mapping is replacing the legacy DASM approach and will greatly enhance the quality and quantity of forest health data while improving safety by integrating with programs such as operational remote sensing (ORS), which uses satellite imagery to monitor disturbances in areas of higher aviation risk (FHP 2016). Geospatial data collected with DMSM and DASM are stored in the national Insect and Disease Survey (IDS) database. Digital Mobile Sketch Mapping includes both polygon geometry, used for damage areas where boundaries are discrete and obvious from the air,

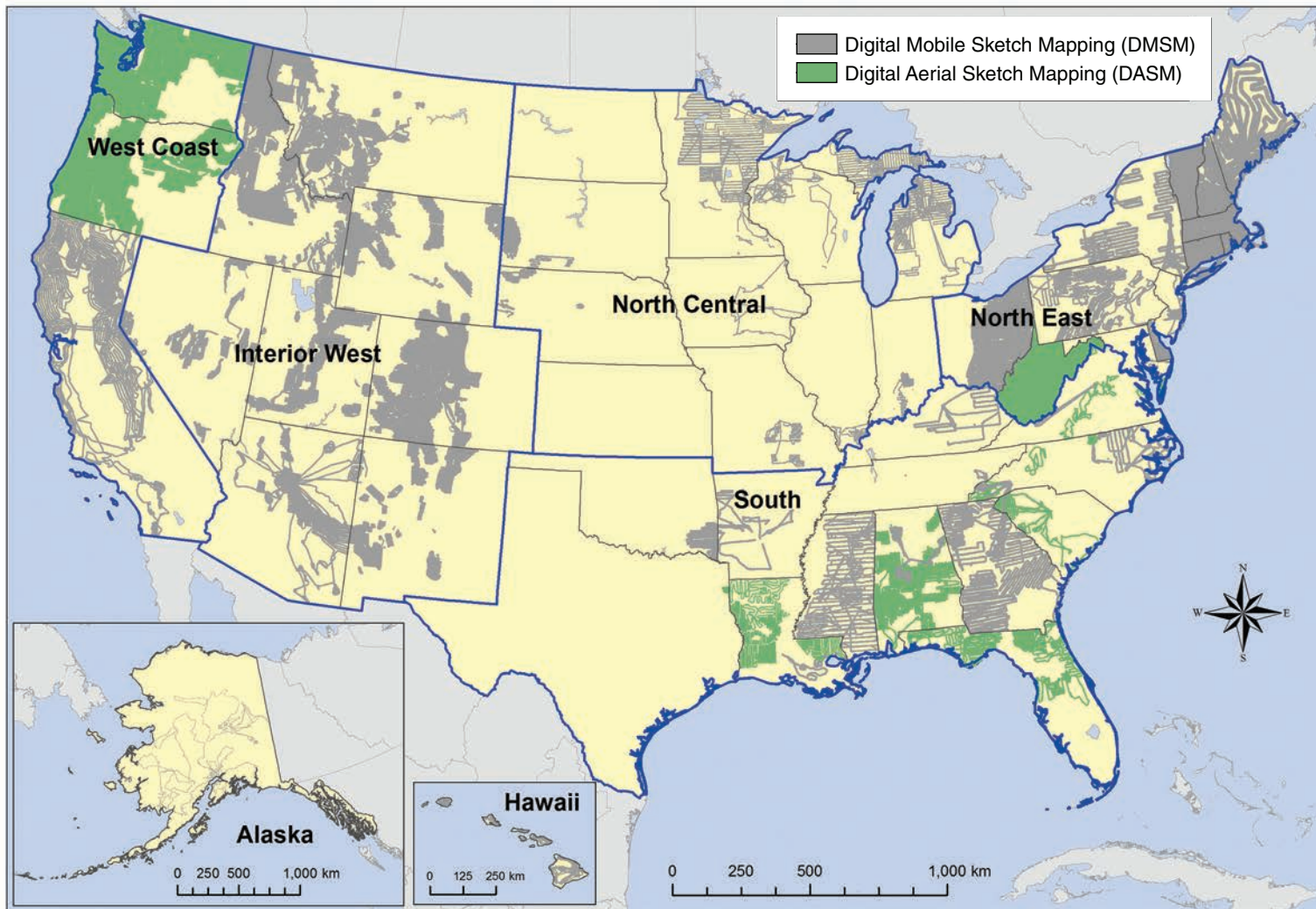


Figure 2.1—The extent of surveys for insect and disease activity conducted in the conterminous United States, Alaska, and Hawaii in 2017. Gray areas were surveyed using the new Digital Mobile Sketch Mapping (DMSM) platform, rather than the older Digital Aerial Sketch Mapping (DASM) approach, which is portrayed in green. The blue lines delineate Forest Health Monitoring regions. Note: Alaska and Hawaii are not shown to scale with map of the conterminous United States. For West Virginia, the survey was ground survey-based with assistance from remote sensing. (Data source: U.S. Department of Agriculture Forest Service, Forest Health Protection)

and point geometry, used for small clusters of damage where the size and shape of the damage are less important than recording the location of damage, such as for sudden oak death, southern pine beetle (*Dendroctonus frontalis*), and some types of bark beetle damage in the West. For the 2017 data, most of the points that did not overlap with a damage polygon of the same type were assigned an area of 0.8 ha (about 2 acres). Additionally, DMSM allows for the use of grid cells (240-, 480-, 960-, or 1920-m resolution) to estimate the percent of trees affected by damages that may be widespread and diffuse, such as those associated with European gypsy moth (*Lymantria dispar dispar*) and emerald ash borer. For our analyses, the entire areas of these grid cells were used in summing damage areas (e.g., 240-m cell = 5.76 ha).

The 2017 mortality and defoliation polygons were used to identify the select mortality and defoliation agents and complexes causing damage on >5000 ha of forest in the conterminous United States in that year, and to identify and list the most widely detected mortality and defoliation agents for Alaska and mortality agents for Hawaii. Because of the insect and disease aerial sketch-mapping process (i.e., digitization of polygons by a human interpreter aboard the aircraft), all quantities are approximate “footprint” areas for each agent or complex, delineating areas of visible damage within which the agent or complex is present. Unaffected trees may exist within the footprint, and the amount of damage within the footprint is not reflected in the estimates of forest area affected. The sum of areas affected by all agents

and complexes is not equal to the total affected area as a result of reporting multiple agents per polygon in some situations.

Analyses

As an indicator of the extent of damaging insect and disease agents, we summarized the percent of surveyed area with tree canopy cover exposed to mortality and defoliation separately for ecoregions within the conterminous 48 States and Alaska, and for islands in Hawaii. This required first separately dissolving the mortality and defoliation polygon boundaries to generate an overall footprint of each general type of disturbance, and then masking the dissolved polygons using a forest cover map (1-km resolution) derived from Moderate Resolution Imaging Spectroradiometer (MODIS) satellite imagery by the U.S. Department of Agriculture Forest Service, Geospatial Technology and Applications Center (USDA Forest Service 2008). The same process was undertaken with the polygons of the surveyed area. For the conterminous States, percent of surveyed area with tree canopy cover exposed to mortality and defoliation was calculated within each of 190 ecoregion sections (Cleland and others 2007). Similarly, the mortality and defoliation data were summarized by ecoregion section in Alaska (Nowacki and Brock 1995). In Hawaii, the percent of surveyed forest affected by mortality or defoliation agents was calculated by island with the exception of the Big Island, where this information was summarized for each of eight county council districts to better assess the prevalence of rapid ‘ōhi‘a death. Statistics were not calculated for analysis regions in the

conterminous United States or Hawaii with <5 percent of the forest surveyed, nor in Alaska with <2.5 percent surveyed.

Additionally, we used the Spatial Association of Scalable Hexagons (SASH) analytical approach to identify surveyed forest areas in the conterminous 48 States with the greatest exposure to the detected mortality-causing and defoliation-causing agents and complexes (from data collected using both DMSM and DASM). This method identifies locations where ecological phenomena occur at greater or lower frequency than expected by random chance and is based on a sampling frame optimized for spatial neighborhood analysis, adjustable to the appropriate spatial resolution, and applicable to multiple data types (Potter and others 2016). Specifically, it consists of dividing an analysis area into scalable equal-area hexagonal cells within which data are aggregated, followed by identifying statistically significant geographic clusters of hexagonal cells within which mean values are greater or less than those expected by chance. To identify these clusters, we employed a Getis-Ord (G_i^*) hot spot analysis (Getis and Ord 1992) in ArcMap[®] 10.3 (ESRI 2015). We conducted two sets of hot spot analyses for both mortality-causing and defoliation-causing agents: one nationally, and one for each of the five Forest Health Monitoring (FHM) regions within the continental United States (West Coast, Interior West, North Central, North East, and South).

The units of analysis were 9,810 hexagonal cells, each approximately 834 km² in area,

generated in a lattice across the conterminous United States using intensification of the Environmental Monitoring and Assessment Program (EMAP) North American hexagon coordinates (White and others 1992). These coordinates are the foundation of a sampling frame in which a hexagonal lattice was projected onto the conterminous United States by centering a large base hexagon over the region (Reams and others 2005, White and others 1992). This base hexagon can be subdivided into many smaller hexagons, depending on sampling needs, and serves as the basis of the plot sampling frame for the Forest Inventory and Analysis (FIA) program (Reams and others 2005). Importantly, the hexagons maintain equal areas across the study region regardless of the degree of intensification of the EMAP hexagon coordinates. In addition, the hexagons are compact and uniform in their distance to the centroids of neighboring hexagons, meaning that a hexagonal lattice has a higher degree of isotropy (uniformity in all directions) than does a square grid (Shima and others 2010). These are convenient and highly useful attributes for spatial neighborhood analyses. These scalable hexagons also are independent of geopolitical and ecological boundaries, avoiding the possibility of different sample units (such as counties, States, or watersheds) encompassing vastly different areas (Potter and others 2016). We selected hexagons 834 km² in area because this is a manageable size for making monitoring and management decisions in analyses that are national in extent (Potter and others 2016).

We used a different variable for this set of hot spot analyses than in previous reports, when we focused on the percentage of area with tree canopy cover in each hexagon exposed to either mortality-causing or defoliation-causing agents, based on the footprints of these disturbances. With the transition from the DASM to the DMSM data collection approach, the hot spot analyses need to account for the existence of three types of data: point geometry, polygon geometry, and grid cells (see above). We therefore used a point sampling approach that estimates the number of mortality or defoliation point occurrences per 100 km² of tree canopy coverage area within each hexagon. For this estimation, point detections remained as point occurrences. Polygons (including grid cells) were clipped by 240-m tree canopy cover data and converted from multipart to singlepart geometry. We derived the tree canopy cover data from a 30-m raster dataset that provides an estimate of the percent tree canopy cover (from 0 to 100 percent) for each grid cell and was generated from the 2011 National Land Cover Database (Homer and others 2015) through a cooperative project between the Multi-Resolution Land Characteristics Consortium and the Forest Service Geospatial Technology and Applications Center (Coulston and others 2012). For our purposes, we treated any cell with >0 percent tree canopy cover as forest. The mortality and defoliation polygons, after clipping by the tree canopy data, were then separated into two groups: small polygons <5.76 ha in area (the size of the smallest resolution [240-m] DMSM grid cells), and large polygons ≥5.76 ha in area. For

the small polygons, we extracted the centroid points for each. For the large polygons, we employed a zonal statistics analysis to determine the number of 240-m tree canopy grid cells (i.e., center points) contained within each polygon, after we intersected them with the 834-km² hexagons. The zonal statistics approach has the additional advantage of accounting for overlapping polygons; that is, it can iteratively calculate the number of tree canopy grid center points contained within each of any number of stacked mortality or defoliation polygons. The three types of resulting point occurrence data (from the original point detections, from the centroids of the small polygons, and from the 240-m tree canopy grid center points from the large polygons) were added together for each hexagon, with the sum of mortality and defoliation point occurrences divided by the total tree canopy coverage area present in the hexagon.

The Getis-Ord G_i^* statistic was then used to identify clusters of hexagonal cells in which the density of occurrences of mortality- or defoliation-causing insects and diseases was higher than expected by chance. This statistic allows for the decomposition of a global measure of spatial association into its contributing factors, by location, and is therefore particularly suitable for detecting instances of nonstationarity in a dataset, such as when spatial clustering is concentrated in one subregion of the data (Anselin 1992).

The Getis-Ord G_i^* statistic for each hexagon summed the differences between the mean

values in a local sample, determined by a moving window consisting of the hexagon and its 18 first- and second-order neighbors (the 6 adjacent hexagons and the 12 additional hexagons contiguous to those 6) and a global mean. Our first analysis encompassed a global mean of all the forested hexagonal cells in the conterminous 48 States, while we conducted another set of analyses separately within each of the five FHM regions. The G_i^* statistic was standardized as a z -score with a mean of 0 and a standard deviation of 1, with values >1.96 representing significant ($p < 0.025$) local clustering of high values and values <-1.96 representing significant clustering of low values ($p < 0.025$), since 95 percent of the observations under a normal distribution should be within approximately two (exactly 1.96) standard deviations of the mean (Laffan 2006). In other words, a G_i^* value of 1.96 indicates that the local mean of the percentage of forest exposed to mortality-causing or defoliation-causing agents for a hexagon and its 18 neighbors is approximately two standard deviations greater than the mean expected in the absence of spatial clustering, while a G_i^* value of -1.96 indicates that the local mortality or defoliation mean for a hexagon and its 18 neighbors is approximately two standard deviations less than the mean expected in the absence of spatial clustering. Values between -1.96 and 1.96 have no statistically significant concentration of high or low values. In other words, when a hexagon has a G_i^* value between -1.96 and 1.96, mortality or defoliation damage within it and its 18 neighbors is not statistically different from

a normal expectation. As described in Laffan (2006), it is calculated as

$$G_i^* (d) = \frac{\sum_j w_{ij}(d) x_j - W_i^* \bar{x}^*}{s^* \sqrt{\frac{(ns_{1i}^*) - W_i^{*2}}{n-1}}}$$

where

G_i^* = the local clustering statistic (in this case, for the target hexagon)

i = the center of local neighborhood (the target hexagon)

d = the width of local sample window (the target hexagon and its first- and second-order neighbors)

x_j = the value of neighbor j

w_{ij} = the weight of neighbor j from location i (all the neighboring hexagons in the moving window were given an equal weight of 1)

n = number of samples in the dataset (the 9,810 hexagons)

W_i^* = the sum of the weights

s_{1i}^* = the number of samples within d of the central location (19: the focal hexagon and its 18 first- and second-order neighbors)

\bar{x}^* = mean of whole dataset (in this case, for all 9,810 hexagons)

s^* = the standard deviation of whole dataset (for all 9,810 hexagons)

It is worth noting that the -1.96 and 1.96 threshold values are not exact because the correlation of spatial data violates the assumption of independence required for statistical significance (Laffan 2006). The Getis-Ord approach does not require that the input data be normally distributed because the local G_i^* values are computed under a randomization assumption, with G_i^* equating to a standardized z-score that asymptotically tends to a normal distribution (Anselin 1992). The z-scores are reliable, even with skewed data, as long as the distance band used to define the local sample around the target observation is large enough to include several neighbors for each feature (ESRI 2015).

The low density of survey data in 2017 from Alaska and the small spatial extent of Hawaii (fig. 2.1) precluded the use of Getis-Ord G_i^* hot spot analyses for these States.

RESULTS AND DISCUSSION

Conterminous United States Mortality

The national IDS survey data identified 63 different mortality-causing agents and complexes on approximately 3.27 million ha across the conterminous United States in 2017, similar to the combined land area of Massachusetts and Connecticut. By way of comparison, forests are estimated to cover approximately 252 million ha of the conterminous 48 States (Smith and others 2009). Twenty-three of the agents were detected on >5000 ha.

Emerald ash borer was the most widespread mortality agent in 2017, identified on 1.42 million ha (table 2.1). Four other mortality agents and complexes were detected on >100 000 ha: fir engraver (*Scolytus ventralis*) on 959 000 ha, western pine beetle (*D. brevicomis*) on 185 000 ha, mountain pine beetle (*D. ponderosae*) on 165 000 ha, and spruce beetle (*D. rufipennis*) on 157 000 ha. Mortality from the western bark beetle group, which encompasses 19 different agents in the IDS data (table 2.2), was detected on approximately 1.61 million ha in 2017, representing about half the total area on which mortality was recorded across the conterminous States.

The FHM North Central region had the largest area on which mortality agents and complexes were detected, about 1.54 million ha (table 2.3). Almost all of this area (1.41 million ha, or 91 percent of the total) was exposed to emerald ash borer mortality. Eighteen other mortality-causing agents and complexes were recorded, with the most widespread being eastern larch beetle (*D. simplex*) (5.6 percent of the mortality area), oak decline (1.3 percent), and beech bark disease complex (0.7 percent). As a result of emerald ash borer infestation, 24.1 percent of the surveyed forest in the 222K–Southwestern Great Lakes Morainal ecoregion section (along the western shore of Lake Michigan in Wisconsin and Illinois), and 14.2 percent of the neighboring 222L–North Central U.S. Driftless and Escarpment, were exposed to mortality (fig. 2.2). A geographic hot spot of extremely

Table 2.1—Mortality agents and complexes affecting more than 5000 ha in the conterminous United States during 2017

Agents/complexes causing mortality, 2017	Area <i>ha</i>
Emerald ash borer	1 424 453
Fir engraver	959 223
Western pine beetle	185 153
Mountain pine beetle	165 459
Spruce beetle	156 911
Eastern larch beetle	86 504
Douglas-fir beetle	85 637
Jeffrey pine beetle	55 337
Western balsam bark beetle	34 774
Unknown	27 722
Unknown bark beetle	24 284
Oak decline	21 186
Root disease and beetle complex	21 163
Balsam woolly adelgid	20 758
Southern pine beetle	13 788
Beech bark disease complex	12 222
Ips engraver beetles	10 760
Oak wilt	9573
Flatheaded fir borer	9240
Pinyon ips	8905
Flatheaded borer	7394
California fivespined ips	7020
Sudden oak death	6335
Other (40)	24 888
Total, all mortality agents	3 266 598

Note: All values are “footprint” areas for each agent or complex. The sum of the individual agents is not equal to the total for all agents due to the reporting of multiple agents per polygon.

Table 2.2—Beetle taxa included in the “western bark beetle” group

Western bark beetle mortality agents	
Common name	Scientific name
California fivespined ips	<i>Ips paraconfusus</i>
Cedar and cypress bark beetles	<i>Phloeosinus</i> spp.
Douglas-fir beetle	<i>Dendroctonus pseudotsugae</i>
Douglas-fir engraver	<i>Scolytus unispinosus</i>
Fir engraver	<i>Scolytus ventralis</i>
Flatheaded borer	Family Buprestidae
Ips engraver beetles	<i>Ips</i> spp.
Jeffrey pine beetle	<i>Dendroctonus jeffreyi</i>
Mountain pine beetle	<i>Dendroctonus ponderosae</i>
Pine engraver	<i>Ips pini</i>
Pinyon ips	<i>Ips confuses</i>
Root disease and beetle complex	N/A
Roundheaded pine beetle	<i>Dendroctonus adjunctus</i>
Silver fir beetle	<i>Pseudohylesinus sericeus</i>
Spruce beetle	<i>Dendroctonus rufipennis</i>
Unknown bark beetle	N/A
Western balsam bark beetle	<i>Dryocoetes confuses</i>
Western cedar bark beetle	<i>Phloeosinus punctatus</i>
Western pine beetle	<i>Dendroctonus brevicomis</i>

Table 2.3—The top five mortality agents or complexes for each Forest Health Monitoring region, and for Alaska and Hawaii, in 2017

Mortality agents and complexes, 2017	Area	Mortality agents and complexes, 2017	Area
	<i>ha</i>		<i>ha</i>
Interior West		South	
Spruce beetle	152 625	Southern pine beetle	10 558
Douglas-fir beetle	42 360	Ips engraver beetles	7 487
Fir engraver	42 055	Emerald ash borer	5 341
Western balsam bark beetle	24 387	Unknown	1 700
Unknown bark beetle	22 954	Unknown bark beetle	139
Other mortality agents (15)	59 732	Other mortality agents (4)	85
Total, all mortality agents and complexes	338 820	Total, all mortality agents and complexes	25 309
North Central		West Coast	
Emerald ash borer	1 408 766	Fir engraver	917 168
Eastern larch beetle	86 504	Western pine beetle	182 265
Oak decline	20 556	Mountain pine beetle	146 312
Beech bark disease complex	11 490	Jeffrey pine beetle	55 269
Oak wilt	9 561	Douglas-fir beetle	43 277
Other mortality agents (14)	8 327	Other mortality agents (23)	88 219
Total, all mortality agents and complexes	1 542 611	Total, all mortality agents and complexes	1 328 361
North East		Alaska	
Emerald ash borer	10 346	Spruce beetle	164 281
Unknown	6 053	Yellow-cedar decline	19 188
Gypsy moth	4 954	Northern spruce engraver	2 428
Southern pine beetle	3 230	Unknown	39
Balsam woolly adelgid	2 680	Western balsam bark beetle	16
Other mortality agents (13)	4 290	Total, all mortality agents and complexes	185 951
Total, all mortality agents and complexes	31 497		
		Hawaii	
		Unknown	30 320
		Total, all mortality agents and complexes	30 320

Note: The total area affected by other agents is listed at the end of each section. All values are “footprint” areas for each agent or complex. The sum of the individual agents is not equal to the total for all agents due to the reporting of multiple agents per polygon.

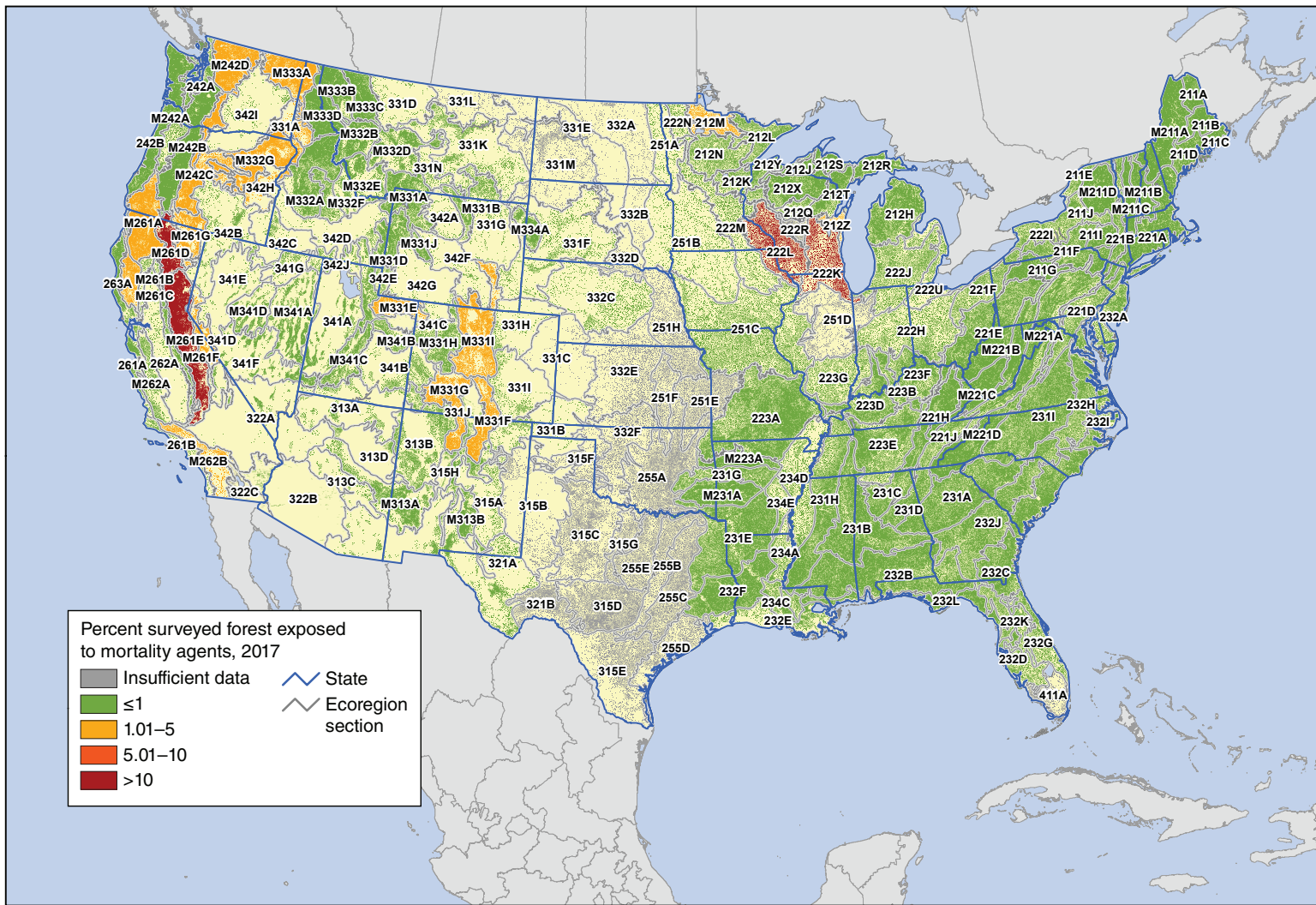


Figure 2.2—The percent of surveyed forest exposed to mortality agents, by ecoregion section within the conterminous 48 States, for 2017. The gray lines delineate ecoregion sections (Cleland and others 2007). The 240-m tree canopy cover is based on data from a cooperative project between the Multi-Resolution Land Characteristics Consortium (Coulston and others 2012) and the Forest Service Remote Sensing Applications Center using the 2011 National Land Cover Database. (Data source: U.S. Department of Agriculture Forest Service, Forest Health Protection)

high density of mortality occurrences was detected in the first of these ecoregion sections in the conterminous United States analysis, and a hot spot of very high density was identified in the second (fig. 2.3A). Similar hot spots were identified in the analysis limited to the North Central FHM region (fig. 2.3B).

All the other North Central ecoregion sections had <1 percent forest exposure to mortality agents, with the exception of 4.5 percent in 212M–Northern Minnesota and Ontario (fig. 2.2), where surveyors found much mortality associated with eastern larch beetle. A national hot spot of moderate mortality occurrence density was detected in this ecoregion section as well (fig. 2.3A). Other national and regional mortality hot spots in the North Central region were associated with emerald ash borer, including in 251C–Central Dissected Till Plains (southeastern Iowa), and in 222M–Minnesota and Northeast Iowa Morainal-Oak Savannah (northeastern Iowa and southern Minnesota) with 212K–Western Superior Uplands.

In the FHM West Coast region, 28 mortality agents and complexes were detected on about 1.33 million ha (table 2.3). Fir engraver was the leading cause of mortality and was identified on about 917 000 ha, approximately 69 percent of the entire affected area. Other bark beetles, including western pine beetle, mountain pine beetle, Jeffrey pine beetle (*D. jeffreyi*), and Douglas-fir beetle (*D. pseudotsugae*), were also widespread causes of mortality in the region. The first two of these were detected on approximately

182 000 ha and 146 000 ha, respectively. As a result of bark beetle infestations, 14.7 percent of the surveyed forest in the M261E–Sierra Nevada ecoregion section and 10.2 percent of the forest in M261D–Southern Cascades were exposed to mortality (fig. 2.2). Several other ecoregion sections in the West Coast region had between 1 and 5 percent of their surveyed forest exposed to mortality agents.

At the same time, a hot spot of high mortality density was centered on the M261E–Sierra Nevada ecoregion section, and extended into several neighboring ecoregion sections, both for the national (fig. 2.3A) and regional (fig. 2.3B) analyses. An additional hot spot of high mortality density was identified in the M332G–Blue Mountains of eastern Oregon (in both the national and regional analyses), associated with mortality caused by fir engraver, mountain pine beetle, and western pine beetle. Similarly, the national analyses identified a high-density mortality hot spot in M333A–Okanogan Highland, caused by western pine beetle and several other bark beetles, including mountain pine beetle, Douglas-fir beetle, fir engraver, and Ips engraver beetles (*Ips* spp.). The same area was a moderate-density hot spot in the regional analysis.

The FHM Interior West region had approximately 339 000 ha on which 20 mortality-causing agents and complexes were detected in 2017 (table 2.3). About 45 percent of this was associated with spruce beetle (153 000 ha). Other bark beetles were also

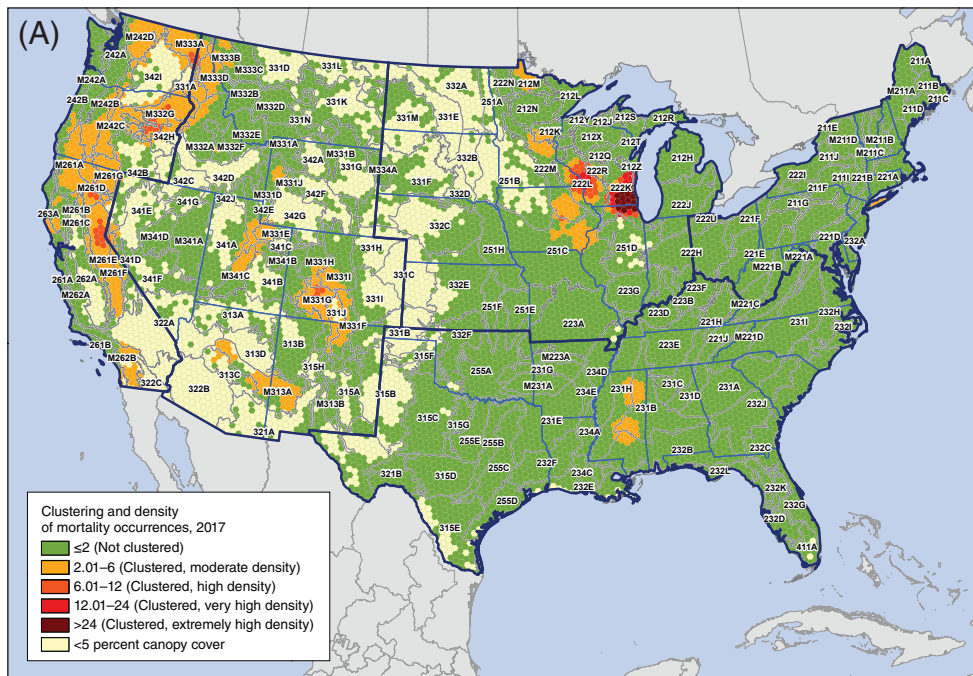
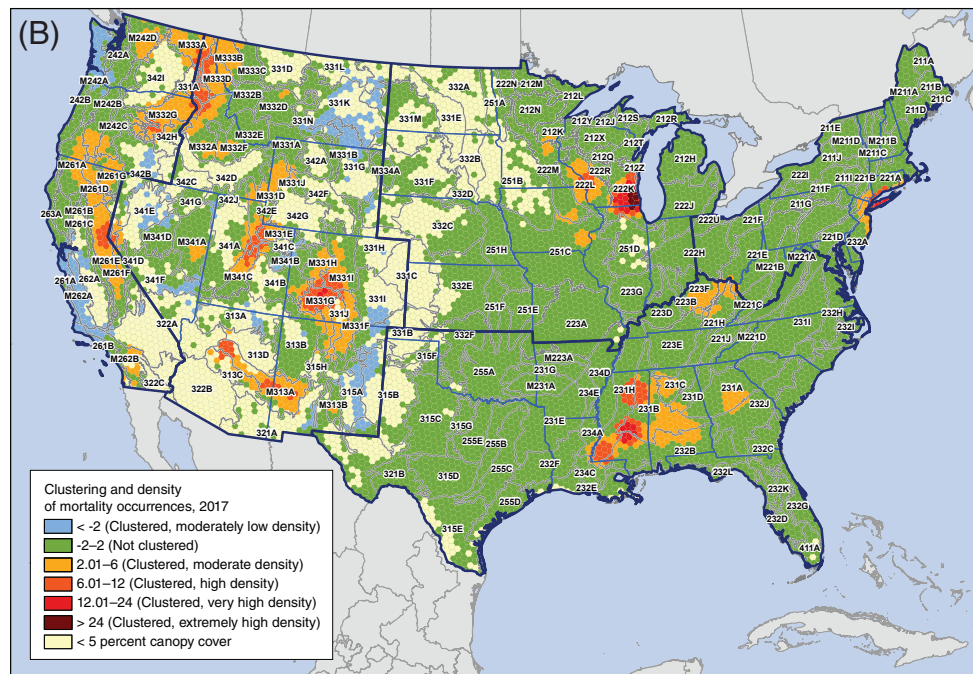


Figure 2.3—Hot spots of the density of occurrences of mortality-causing insects and diseases in 2017 for (A) the conterminous 48 States and (B) for separate Forest Health Monitoring regions, by hexagons containing >5 percent tree canopy cover. Values are Getis-Ord G_i^* scores, with values >2 representing significant clustering of high mortality occurrence densities and <-2 representing significant clustering of low mortality occurrence densities. The gray lines delineate ecoregion sections (Cleland and others 2007), and blue lines delineate Forest Health Monitoring regions. Tree canopy cover is based on data from a cooperative project between the Multi-Resolution Land Characteristics Consortium (Coulston and others 2012) and the Forest Service Remote Sensing Applications Center using the 2011 National Land Cover Database. (Data source: U.S. Department of Agriculture Forest Service, Forest Health Protection)



widely detected, including Douglas-fir beetle and fir engraver (each about 42 000 ha, or 12 percent of the total) and western balsam bark beetle (*Dryocoetes confusus*) (24 000 ha, 7 percent).

As a result of bark beetle infestations, several ecoregion sections in the central Rocky Mountains experienced between 1 and 5 percent mortality in surveyed areas with tree canopy cover, including M331E–Uinta Mountains of northeastern Utah (3.4 percent), M331G–South-Central Highlands (2.5 percent) and M331F–Southern Parks and Rocky Mountain Range (1.4 percent) of southern Colorado and northern New Mexico, and M331I–Northern Parks and Ranges of northern Colorado and southern Wyoming (1.1 percent) (fig. 2.2). Most of the mortality in these areas was attributed to spruce beetle, although Douglas-fir beetle, western balsam bark beetle, and mountain pine beetle were also present.

The national Getis-Ord analysis revealed several geographic hot spots of mortality in the Interior West FHM region, one of which resulted from high mortality occurrence density (fig. 2.3A). This was caused by the spruce beetle outbreak in southern Colorado, and was centered on M331G–South-Central Highlands. The regional analysis (fig. 2.3B), meanwhile, identified four high mortality density hot spots that were classified as moderate density hot spots in the national analysis. These were located in:

- Northern Idaho (M333D–Bitterroot Mountains, 331A–Palouse Prairie, M333A–Okanogan Highland, and M332G–Blue Mountains) associated mainly with fir engraver as well as with mountain pine beetle, Douglas-fir beetle, spruce beetle, and pine engraver (*Ips pini*);
- North-central Utah (M331D–Overthrust Mountains, M331E–Uinta Mountains, M341C–Utah High Plateau, and M341B–Tavaputs Plateau), the result of spruce beetle in Engelmann spruce, Marssonina blight (*Drepanopeziza* spp.) in quaking aspen (*Populus tremuloides*), Douglas-fir beetle in Douglas-fir, root disease and beetle complex in subalpine fir (*Abies lasiocarpa*), and fir engraver in white fir (*A. concolor*); and
- Central Arizona, and southeastern Arizona and southwestern New Mexico, both within M313A–White Mountains-San Francisco Peaks-Mogollon Rim, and both associated with an unknown bark beetle in ponderosa pine (*Pinus ponderosa*).

Additionally, the national and regional analyses found a hot spot of moderate mortality exposure in northwestern Wyoming (M331D–Overthrust Mountains, M331A–Yellowstone Highlands, and M331J–Wind River Mountains) related to spruce beetle and subalpine fir mortality complex.

In the North East FHM region, mortality was recorded on approximately 32 000 ha, caused by 18 mortality agents and complexes. The cause of about a third of this mortality was emerald ash borer (10 000 ha). None of the ecoregion sections in the North East was exposed to >1 percent surveyed forest mortality (fig. 2.2). A hot spot of moderate mortality density in the national analysis (fig. 2.3A), and of very high mortality density in the regional analysis (fig. 2.3B), was identified in areas adjacent to Long Island Sound (in 221A–Lower New England), associated with southern pine beetle in pitch pine (*P. rigida*) stands and with oak decline in northern red oak (*Quercus rubra*) on Long Island, and with emerald ash borer in Connecticut.

In the South FHM region, mortality from nine agents was detected on about 25 000 ha (table 2.3). The most common causal agent was southern pine beetle, constituting 42 percent of the mortality (11 000 ha), followed by Ips engraver beetles (7000 ha, 30 percent) and emerald ash borer (5000 ha, 21 percent). No ecoregion sections in the South were exposed to >1 percent surveyed forest mortality (fig. 2.2). The national hot spot analysis identified two areas of moderately clustered mortality density in Mississippi (fig. 2.3A), both caused by the southern pine beetle outbreak in the region (box 2.1). One was located in the northeastern

part of the State (231H–Coastal Plains-Loess and 231B–Coastal Plains-Middle), and the other in south-central Mississippi (231B–Coastal Plains-Middle and 232B–Gulf Coastal Plains and Flatwoods). In the regional analysis (fig. 2.3B), the second of these exhibited clustering of very high mortality density, while the first was of high mortality density. The regional analysis detected an additional hot spot of high mortality density, also associated with southern pine beetle, in the southwestern corner of Mississippi (231H–Coastal Plains-Loess). Hot spots of moderate southern pine beetle mortality density also appeared in neighboring Alabama and Georgia.

Eastern Kentucky (223F–Interior Low Plateau-Bluegrass, 221E–Southern Unglaciaded Allegheny Plateau, and 221H–Northern Cumberland Plateau) was the location of a moderate mortality exposure hot spot in the regional analysis (fig. 2.3B). This was caused by emerald ash borer.

Conterminous United States Defoliation

In 2017, the national IDS survey identified 50 defoliation agents and complexes affecting approximately 2.34 million ha across the conterminous United States (table 2.4), an area slightly larger than the land area of New Hampshire. The most widespread defoliation agent was gypsy moth, which was detected on approximately 913 000 ha, or 39 percent of the

BOX 2.1**Southern pine beetle story map**

Southern pine beetle (SPB, *Dendroctonus frontalis*) is the most economically significant pest in the Southern United States, where it impacts both southern yellow pine timber production and forest ecology. The host species of SPB, especially loblolly (*Pinus taeda*), shortleaf (*P. echinata*), pitch (*P. rigida*), and Virginia (*P. virginiana*) pines, play significant roles in the functioning of southern forest ecosystems and/or are important timber-producing species.

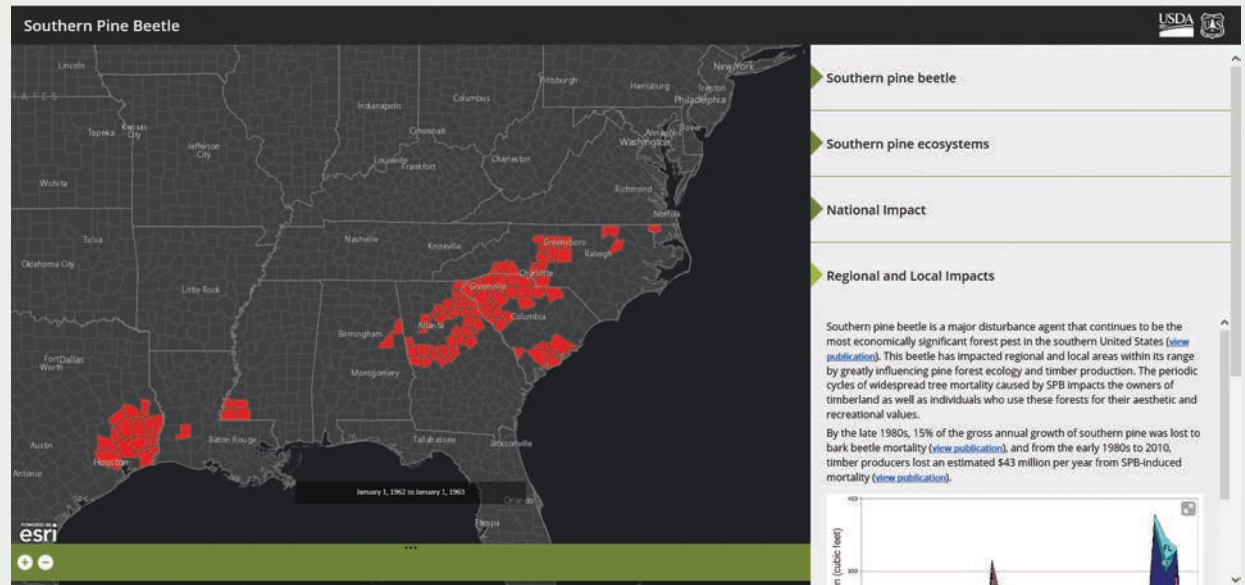
The periodic cycles of widespread tree mortality caused by SPB impact the owners of timberland as well as individuals who use these forests for their aesthetic and recreational values. Despite increases in the amount of intensively managed pine in the South, SPB activity across the South declined significantly since the late 1990s due, in part, to regional improvements in plantation silviculture, most notably stand thinning. In recent years, however, mostly localized

but severe SPB activity has appeared in some areas, particularly across the national forests of Mississippi, Alabama, and Georgia. In these areas, thinning practices have fallen behind growth rates due to depressed markets for pine, resulting in a large concentration of overstocked stands.

A story map (<https://arcgis.com/rD01j>, pictured below) provides an overview of SPB and its hosts. This includes interactive maps of SPB infestations from 1960 to 2017 and of the extent of its pine host species,

background on the life cycle of the insect, discussion of its recent impacts on national forests in the South, and information about the management and monitoring of SPB outbreaks.

The story map was developed by the Forest Health Assessment and Applied Sciences Team of the U.S. Department of Agriculture, Forest Service, in association with the Forest Health Monitoring program and Forest Health Protection.



The Southern Pine Beetle story map provides interactive maps and background information on southern pine beetle, its hosts, and its management.

Table 2.4—Defoliation agents and complexes affecting more than 5000 ha in the conterminous United States in 2017

Agents/complexes causing defoliation, 2017	Area <i>ha</i>
Gypsy moth	912 678
Western spruce budworm	502 398
Forest tent caterpillar	286 962
Unknown gallmaker	183 583
Jumping oak gall wasp	147 456
Spruce budworm	122 257
Baldcypress leafroller	80 752
Unknown defoliator	35 691
White pine needle damage	27 471
Larch casebearer	25 891
Browntail moth	22 194
Winter moth	12 760
Cherry scallop shell moth	11 972
Unknown	9187
Pandora moth	7974
Other (35)	31 271
Total, all defoliation agents	2 344 302

Note: All values are “footprint” areas for each agent or complex. The sum of the individual agents is not equal to the total for all agents due to the reporting of multiple agents per polygon.

total. Five other insects were also detected on >100 000 ha each: western spruce budworm (*Choristoneura freemani*) on 502 000 ha, forest tent caterpillar (*Malacosoma disstria*) on 287 000 ha, an unknown gallmaker on 184 000 ha, jumping oak gall wasp (*Neuroterus saltatorius*) on 147 000 ha, and spruce budworm (*C. fumiferana*) on 122 000 ha (table 2.4).

The North East FHM region had by far the largest area on which defoliating agents and complexes were detected in 2017, slightly >1 million ha (table 2.5). Almost 87 percent of this (869 000 ha) was associated with gypsy moth (table 2.5). Seventeen other agents and complexes constituted the remaining defoliated area. The 221A–Lower New England ecoregion section had the highest percent of surveyed forest exposed to defoliation in the country, 17.9 percent (fig. 2.4), mostly as a result of the gypsy moth infestation, especially in Massachusetts, Connecticut, and Rhode Island. There was also white pine needle damage in southern Maine. Two neighboring ecoregion sections, 211D–Central Maine Coastal Embayment and M211C–Green-Taconic-Berkshire Mountains, had 1.3 percent and 1.1 percent of surveyed forest exposed to defoliators as a result of, respectively, white pine needle damage and browntail moth (*Euproctis chrysorrhoea*), and forest tent caterpillar.

Table 2.5—The top five defoliation agents or complexes for each Forest Health Monitoring region and for Alaska in 2017

Defoliation agents and complexes, 2017	Area	Defoliation agents and complexes, 2017	Area
	<i>ha</i>		<i>ha</i>
Interior West		South	
Western spruce budworm	486 076	Unknown gallmaker	183 583
Unknown defoliator	35 607	Forest tent caterpillar	136 705
Pandora moth	7974	Baldcypress leafroller	80 752
Marssonina blight	4097	Gypsy moth	13 739
Spruce aphid	2276	Unknown	2843
Other defoliation agents (15)	9250	Other defoliation agents (2)	394
Total, all defoliation agents and complexes	544 363	Total, all defoliation agents and complexes	345 593
North Central		West Coast	
Jumping oak gall wasp	147 456	Western spruce budworm	16 321
Spruce budworm	122 257	Larch casebearer	7428
Forest tent caterpillar	96 392	Needlecast	2511
Gypsy moth	30 295	Unknown	570
Larch casebearer	18 463	Swiss needle cast	555
Other defoliation agents (7)	12 118	Other defoliation agents (12)	1308
Total, all defoliation agents and complexes	425 062	Total, all defoliation agents and complexes	28 464
North East		Alaska	
Gypsy moth	868 644	Aspen leafminer	59 713
Forest tent caterpillar	53 663	Unknown defoliator	42 331
White pine needle damage	27 471	Willow leaf blotchminer	29 325
Browntail moth	22 194	Speckled green fruitworm	14 872
Winter moth	12 760	Birch aphid	1318
Other defoliation agents (13)	16 793	Other defoliation agents (6)	805
Total, all defoliation agents and complexes	1 000 820	Total, all defoliation agents and complexes	146 212

Note: The total area affected by other agents is listed at the end of each section. All values are “footprint” areas for each agent or complex. The sum of the individual agents is not equal to the total for all agents due to the reporting of multiple agents per polygon.

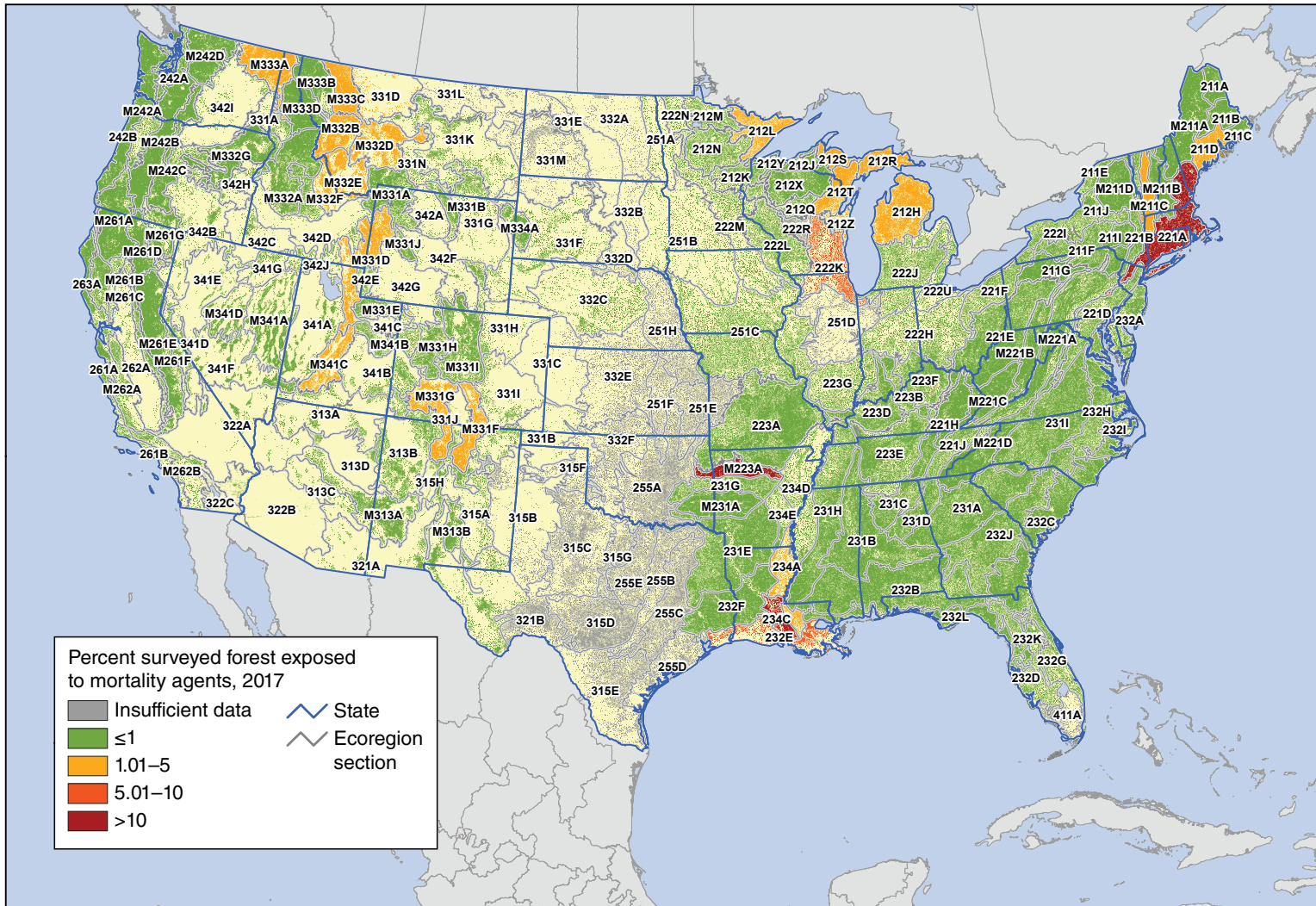


Figure 2.4—The percent of surveyed forest exposed to defoliating agents, by ecoregion section within the conterminous 48 States, for 2017. The gray lines delineate ecoregion sections (Cleland and others 2007). The 240-m tree canopy cover is based on data from a cooperative project between the Multi-Resolution Land Characteristics Consortium (Coulston and others 2012) and the Forest Service Remote Sensing Applications Center using the 2011 National Land Cover Database. (Data source: U.S. Department of Agriculture Forest Service, Forest Health Protection)

Three hot spots of defoliation were detected in the North East region. One, of extremely high defoliation density in the national analysis (fig. 2.5A) and of very high defoliation density in the regional analysis (fig. 2.5B), was associated with the gypsy moth infestation in 221A–Lower New England. A hot spot of high and moderate defoliation density in the national analysis, and of moderate density in the regional analysis, was associated with white pine needle damage and browntail moth in 211D–Central Maine Coastal Embayment and 221A–Lower New England. Finally, the national analysis revealed a hot spot of moderate forest tent caterpillar defoliation density in northern Vermont (M211C–Green-Taconic-Berkshire Mountains, M211B–New England Piedmont, and M211A–White Mountains).

Surveyors in the Interior West FHM region, meanwhile, detected defoliation by 20 agents and complexes on 544 000 ha (table 2.5). Most commonly found, by far, was western spruce budworm (486 000 ha, or 89 percent). Several ecoregion sections in the Interior West experienced between 1 and 5 percent of surveyed area defoliation (fig. 2.4), almost entirely attributed to western spruce budworm:

- M331G–South-Central Highlands (3.8 percent)
- M331F–Southern Parks and Rocky Mountain Range (3.1 percent)
- M331D–Overthrust Mountains (2.4 percent)
- M332E–Beaverhead Mountains (2.3 percent)
- M332B–Northern Rockies and Bitterroot Valley (2.1 percent)

- M332D–Belt Mountains (2.1 percent)
- M341C–Utah High Plateau (1.3 percent)

The 2017 Getis-Ord analysis detected hot spots of defoliation density in many of these same ecoregion sections, both in the national (fig. 2.5A) and regional (fig. 2.5B) analyses.

Meanwhile, 12 agents and complexes were associated with about 425 000 ha with defoliation in the North Central FHM region (table 2.5). Jumping oak gall wasp and spruce budworm were the most commonly detected defoliation agents, identified on 147 000 ha and 122 000 ha, respectively, representing 35 and 29 percent of the total area of defoliation in the region. Other widespread defoliators were forest tent caterpillar (96 000 ha), gypsy moth (30 000 ha), and larch casebearer (*Coleophora laricella*) (18 000 ha).

Several ecoregion sections bordering the Great Lakes had moderately high exposure to defoliation agents. The highest percentage of surveyed forest exposed to defoliators (5.2 percent) was in 222K–Southwestern Great Lakes Morainal in Wisconsin and Illinois, where a high concentration of jumping oak gall wasp was identified (fig. 2.4). The other ecoregion sections with >1 percent defoliation of surveyed forest were:

- 212Z–Green Bay-Manitowoc Upland (5.0 percent): jumping oak gall wasp
- 212R–Eastern Upper Peninsula (4.6 percent): spruce budworm and forest tent caterpillar

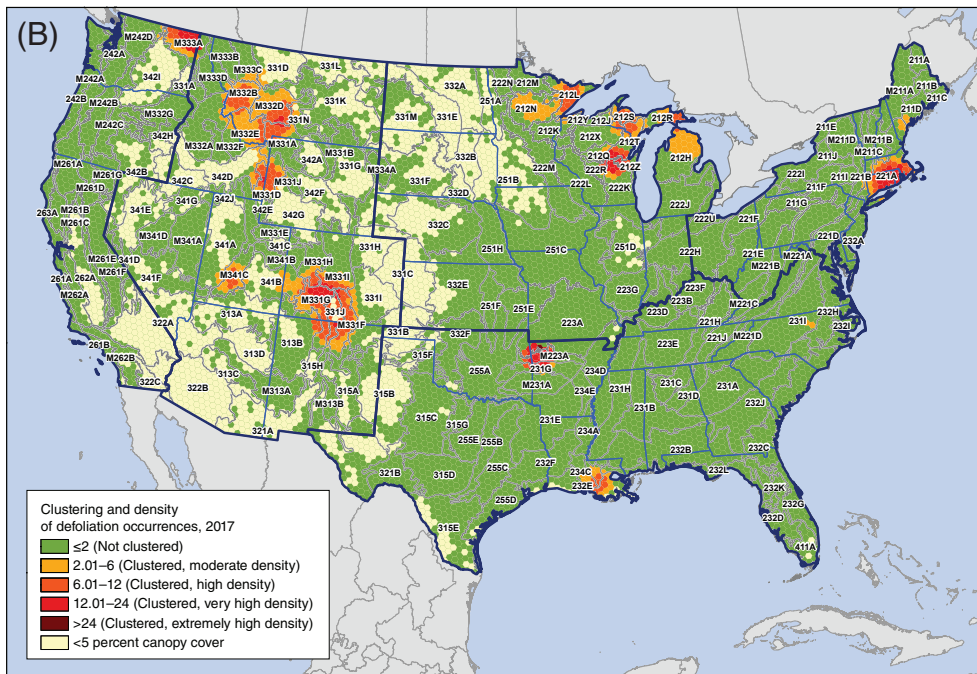
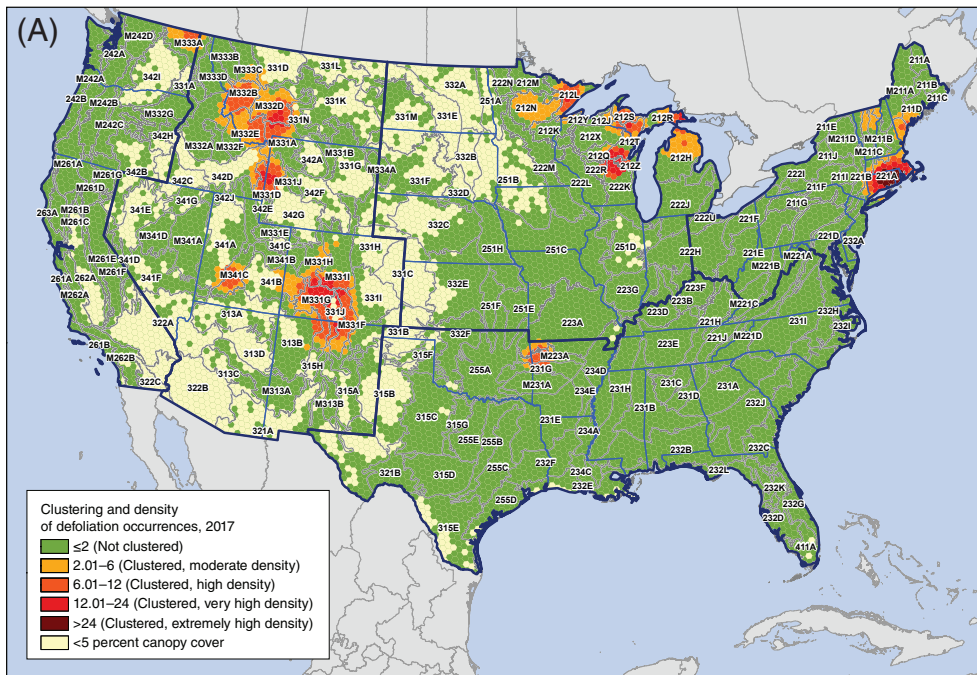


Figure 2.5—Hot spots of the density of occurrences of defoliation-causing insects and diseases in 2017 for (A) the conterminous 48 States and (B) for separate Forest Health Monitoring regions, by hexagons containing >5 percent tree canopy cover. Values are Getis-Ord G_i^* scores, with values >2 representing significant clustering of high defoliation occurrence densities. (No areas of significant clustering of low densities, <-2, were detected.) The gray lines delineate ecoregion sections (Cleland and others 2007), and blue lines delineate Forest Health Monitoring regions. Tree canopy cover is based on data from a cooperative project between the Multi-Resolution Land Characteristics Consortium (Coulston and others 2012) and the Forest Service Remote Sensing Applications Center using the 2011 National Land Cover Database. (Data source: U.S. Department of Agriculture Forest Service, Forest Health Protection)

- 212S–Northern Upper Peninsula (3.1 percent): spruce budworm and forest tent caterpillar
- 212T–Northern Green Bay Lobe (2.4 percent): spruce budworm, large aspen tortrix, and larch casebearer
- 212H–Northern Lower Peninsula (2.1 percent): gypsy moth and forest tent caterpillar
- 212L–Northern Superior Uplands (1.2 percent): spruce budworm and forest tent caterpillar

The national (fig. 2.5A) and regional (2.5B) analyses revealed hot spots of similar extent within these ecoregion sections bordering the Great Lakes.

Approximately 346 000 ha of defoliation were documented in the South FHM region during 2017. Slightly more than half of this (53 percent, 184 000 ha) was attributed to an unknown gallmaker (table 2.5). Forest tent caterpillar was associated with an additional 40 percent (137 000 ha), and baldcypress leafroller (*Archips goyerana*) with about 23 percent (81 000 ha). As a result of an infestation by the unknown gallmaker, 12.7 percent of the surveyed forest in the M223A–Boston Mountains ecoregion section in northwestern Arkansas was exposed to defoliation (fig. 2.4), and this area was the location of a hot spot of high defoliation density nationally (fig. 2.5A) and very high defoliation density regionally (fig. 2.5B). Similarly, baldcypress leafroller and forest tent caterpillar resulted in a regional hot spot of high defoliation density (fig. 2.5B) in ecoregion

sections of southern Louisiana that also had high percentages of surveyed forest exposed to defoliators: 234C–Atchafalaya and Red River Alluvial Plains (12 percent) and 232E–Louisiana Coastal Prairie and Marshes (7.9 percent) (fig. 2.4).

Finally, 17 defoliating agents and complexes were identified in the FHM West Coast region, with western spruce budworm accounting for about 57 percent of the approximately 28 000 ha with defoliation (table 2.5). The only ecoregion section with at least 1 percent of surveyed forest exposed to defoliating agents was M333A–Okanogan Highland (1.0 percent) of northeastern Washington, where outbreaks of western spruce budworm and larch casebearer were detected (fig. 2.4). This ecoregion section was the site of a hot spot of high defoliation density nationally (fig. 2.5A) and of very high defoliation density regionally (fig. 2.5B).

Alaska and Hawaii

In Alaska, mortality was recorded on nearly 186 000 ha in 2017, attributed to five agents and complexes (table 2.3). Spruce beetle was the most widely detected mortality agent, representing 88 percent of the total area with mortality (164 000 ha). Yellow-cedar (*Chamaecyparis nootkatensis*) decline was detected on 19 000 ha, 10 percent of the total. The ecoregion section with the highest percent of surveyed forest exposed to mortality (21 percent) was 213B–Cook Inlet Lowlands in the south-central part of the State (fig. 2.6), where surveyors detected extensive mortality due to spruce beetle. The infestation carried over into

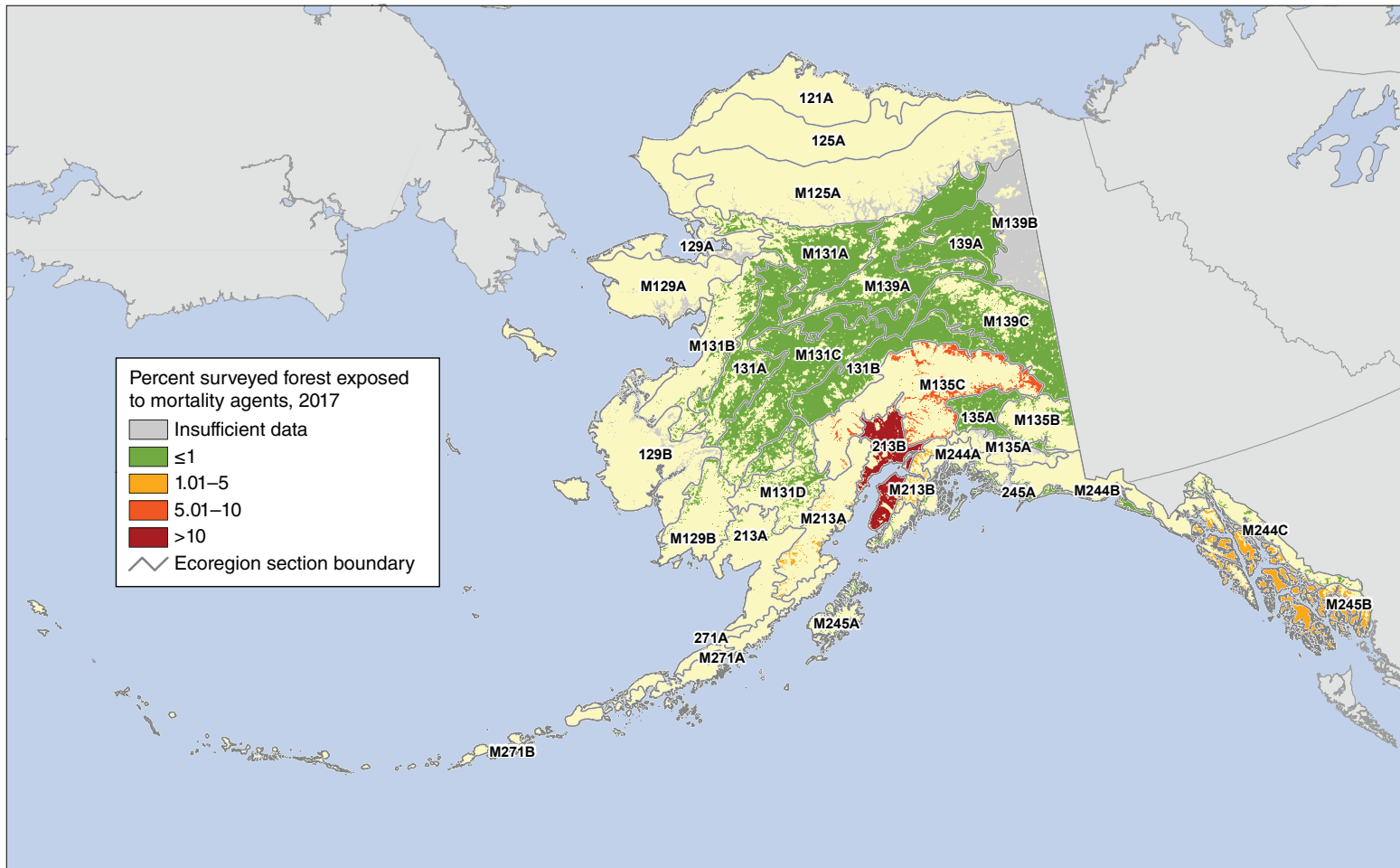


Figure 2.6—Percentage of surveyed forest in Alaska ecoregion sections exposed to mortality-causing insects and diseases in 2017. The gray lines delineate ecoregion sections (Nowacki and Brock 1995). Background forest cover is derived from MODIS imagery by the Forest Service Remote Sensing Applications Center. (Data source: U.S. Department of Agriculture Forest Service, Forest Health Protection)

the neighboring M135C–Alaska Range, where 9.8 percent of surveyed forest was exposed to mortality, as well as M213A–Northern Aleutian Range (3.9 percent) and M213B–Kenai Mountains (2.2 percent). In the panhandle of Alaska, the percent of surveyed forest exposed to mortality was 2.0 in M245B–Alexander Archipelago, location of extensive yellow-cedar decline.

At the same time, 11 defoliators in Alaska were detected on 146 000 ha (table 2.5). Of this area, about 41 percent (60 000 ha) was attributed to aspen leafminer (*Phyllocnistis populiella*). Meanwhile, willow leaf blotchminer (*Micrurapteryx salicifoliella*) was recorded on 29 000 ha (20 percent) and speckled green fruitworm (*Orthosia hibisci*) on about 15 000 ha (10 percent). The Alaska ecoregion section with the highest proportion of surveyed forest area affected by defoliators in 2017 was 139A–Yukon Flats (12.7 percent of surveyed forest) (fig. 2.7), where willow leaf blotchminer and aspen leafminer were commonly reported in willow (*Salix* spp.) and quaking aspen stands. Aspen leafminer was also commonly detected in neighboring M139C–Dawson Range (8.1 percent defoliation in surveyed forest). Several other ecoregion sections in central Alaska had defoliation detected on 1 to 5 percent of their surveyed forest, while surveyors detected defoliation, caused by unknown defoliators, on 12.2 percent of the surveyed forest in 245A–Gulf of Alaska Forelands.

In 2017, approximately 30 000 ha with mortality were recorded in Hawaii (table 2.3),

which are officially labeled as having an unknown cause but may be associated with rapid ‘ōhi‘a death, a wilt disease caused by the fungal pathogens *Ceratocystis lukuohia* and *C. huliolia* (Barnes and others 2018) that affects ‘ōhi‘a lehua (*Metrosideros polymorpha*), a highly ecologically and culturally important tree species in Hawaiian native forests (University of Hawai‘i 2017). All of this mortality was on the Big Island, with higher percentages of surveyed forests affected on the windward (eastern) side of the island, especially in council districts 2, 5, and 3 (12.1, 11.4, and 11 percent, respectively) (fig. 2.8), which encompass much of the Puna and Hilo areas. Mortality did not exceed 1 percent of surveyed forest on any of the other islands in the State. No defoliation was recorded in Hawaii during 2017.

CONCLUSION

Continued monitoring of insect and disease outbreaks across the United States will be necessary for determining appropriate follow-up investigation and management activities. Due to the limitations of survey efforts to detect certain important forest insects and diseases, the pests and pathogens discussed in this chapter do not include all the biotic forest health threats that should be considered when making management decisions and budget allocations. However, large-scale assessments of mortality and defoliation exposure, including geographical hot spot detection analyses, offer a useful approach for identifying geographic areas where the concentration of monitoring and management activities might be most effective.

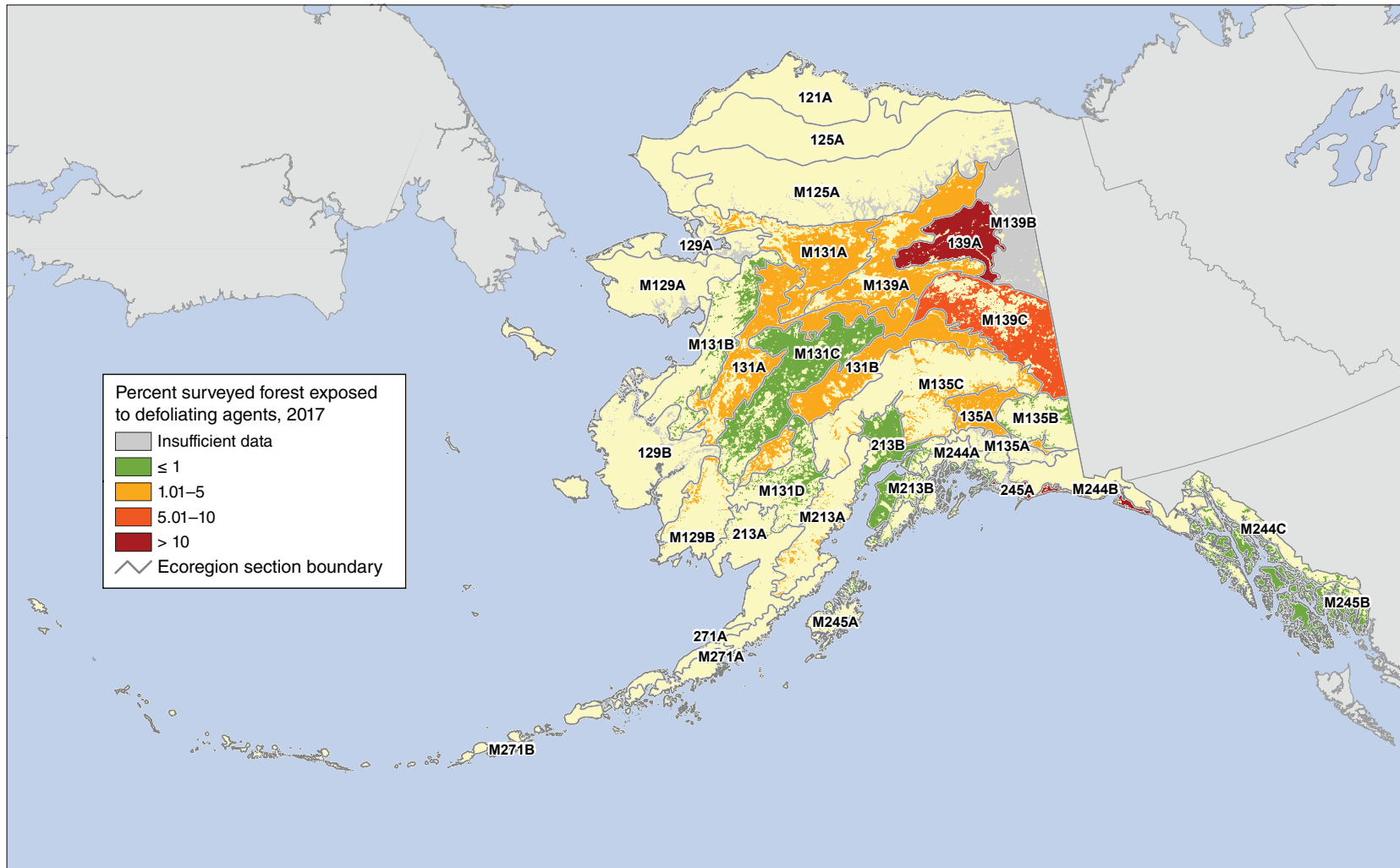


Figure 2.7—Percentage of surveyed forest in Alaska ecoregion sections exposed to defoliation-causing insects and diseases in 2017. The gray lines delineate ecoregion sections (Nowacki and Brock 1995). Background forest cover is derived from MODIS imagery by the Forest Service Remote Sensing Applications Center. (Data source: U.S. Department of Agriculture Forest Service, Forest Health Protection)

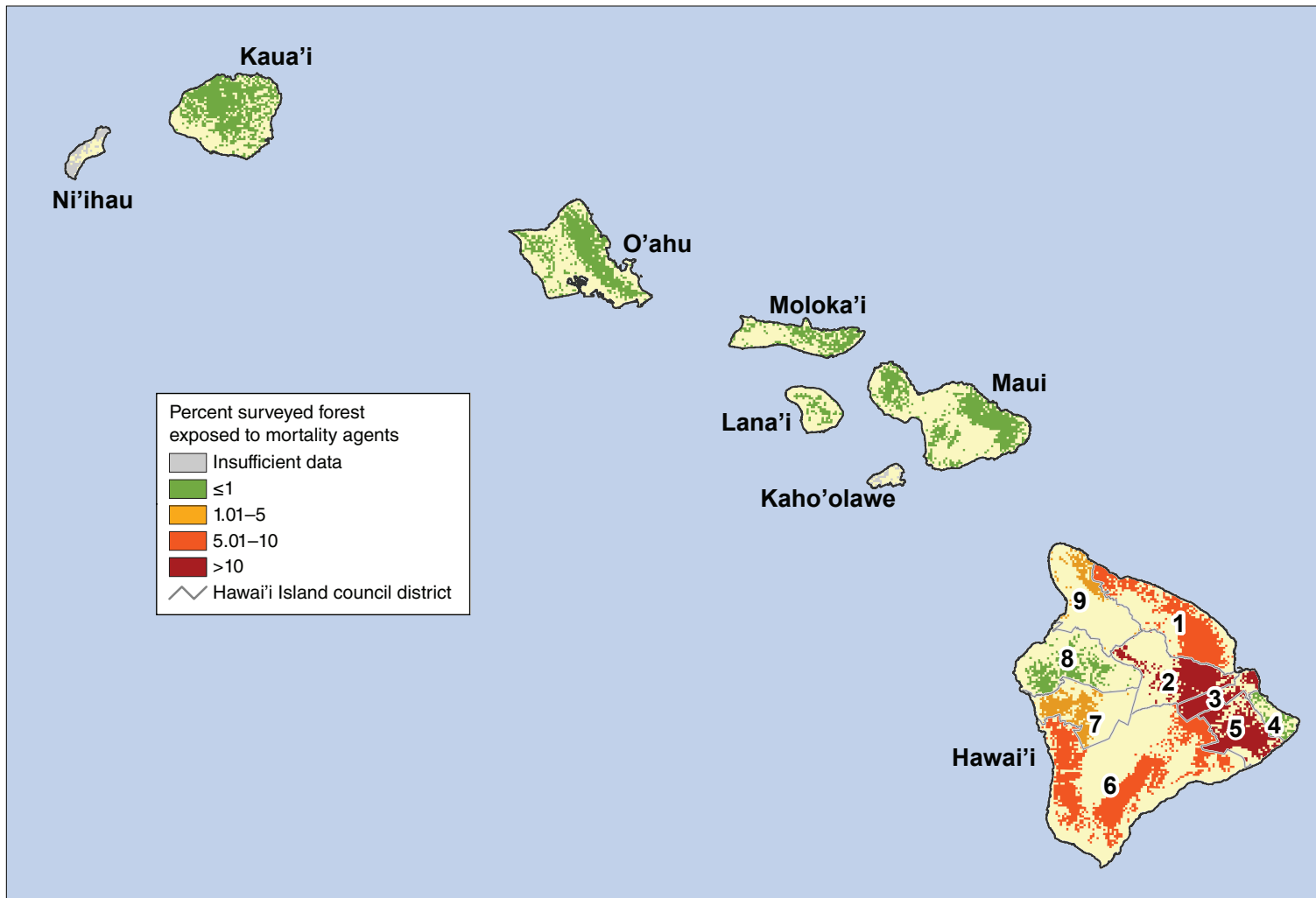


Figure 2.8—Percentage of surveyed forest on Hawaii islands (and by county council district on the Big Island of Hawai'i) exposed to mortality-causing insects and diseases in 2017. Background forest cover is derived from the LANDFIRE program (LANDFIRE 2014). (Data source: U.S. Department of Agriculture Forest Service, Forest Health Protection)

LITERATURE CITED

- Anselin, L. 1992. Spatial data analysis with GIS: an introduction to application in the social sciences. Tech. Rep. 92-10. Santa Barbara, CA: National Center for Geographic Information and Analysis. 53 p.
- Barnes, I.; Fourie, A.; Wingfield, M.J. [and others]. 2018. New *Ceratocystis* species associated with rapid death of *Metrosideros polymorpha* in Hawaii. *Persoonia-Molecular Phylogeny and Evolution of Fungi*. 40(1): 154–181.
- Brockerhoff, E.G.; Liebhold, A.M.; Jactel, H. 2006. The ecology of forest insect invasions and advances in their management. *Canadian Journal of Forest Research*. 36(2): 263–268.
- Castello, J.D.; Leopold, D.J.; Smallidge, P.J. 1995. Pathogens, patterns, and processes in forest ecosystems. *BioScience*. 45(1): 16–24.
- Cleland, D.T.; Freeouf, J.A.; Keys, J.E. [and others]. 2007. Ecological subregions: sections and subsections for the conterminous United States. Gen. Tech. Report WO-76D. Washington, DC: U.S. Department of Agriculture Forest Service. Map; Sloan, A.M., cartographer; presentation scale 1:3,500,000; colored. Also on CD-ROM as a GIS coverage in ArcINFO format or at <http://data.fs.usda.gov/geodata/edw/datasets.php>. [Date accessed: July 20, 2015].
- Coulston, J.W.; Moisen, G.G.; Wilson, B.T. [and others]. 2012. Modeling percent tree canopy cover: a pilot study. *Photogrammetric Engineering and Remote Sensing*. 78(7): 715–727.
- Edmonds, R.L.; Agee, J.K.; Gara, R.I. 2011. Forest health and protection. Long Grove, IL: Waveland Press, Inc. 667 p.
- ESRI. 2015. ArcMap® 10.3. Redlands, CA: Environmental Systems Research Institute, Inc.
- Forest Health Protection (FHP). 2016. Detection surveys. Fort Collins, CO: U.S. Department of Agriculture Forest Service, Forest Health Technology Enterprise Team. http://www.fs.fed.us/foresthealth/technology/detection_surveys.shtml. [Date accessed: July 23, 2016].
- Forest Health Protection (FHP). 2018. Insect and Disease Detection Survey Database (IDS). [Online database]. Fort Collins, CO: U.S. Department of Agriculture Forest Service, Forest Health Technology Enterprise Team. <https://www.fs.fed.us/foresthealth/applied-sciences/mapping-reporting/gis-spatial-analysis/detection-surveys.shtml#idsdownloads>. [Date accessed: October 24, 2018].
- Getis, A.; Ord, J.K. 1992. The analysis of spatial association by use of distance statistics. *Geographical Analysis*. 24(3): 189–206.
- Holdenrieder, O.; Pautasso, M.; Weisberg, P.J.; Lonsdale, D. 2004. Tree diseases and landscape processes: the challenge of landscape pathology. *Trends in Ecology & Evolution*. 19(8): 446–452.
- Homer, C.G.; Dewitz, J.A.; Yang, L. [and others]. 2015. Completion of the 2011 National Land Cover Database for the conterminous United States: representing a decade of land cover change information. *Photogrammetric Engineering and Remote Sensing*. 81(5): 345–354.
- Laffan, S.W. 2006. Assessing regional scale weed distributions, with an Australian example using *Nassella trichotoma*. *Weed Research*. 46(3): 194–206.
- LANDFIRE. 2014. Existing vegetation type layer, LANDFIRE 1.4.0. U.S. Department of the Interior, Geological Survey. <https://www.landfire.gov/evt.php>. [Date accessed: May 2, 2014].
- Liebhold, A.M.; McCullough, D.G.; Blackburn, L.M. [and others]. 2013. A highly aggregated geographical distribution of forest pest invasions in the USA. *Diversity and Distributions*. 19: 1208–1216.
- Mack, R.N.; Simberloff, D.; Lonsdale, W.M. [and others]. 2000. Biotic invasions: causes, epidemiology, global consequences, and control. *Ecological Applications*. 10(3): 689–710.
- Manion, P.D. 2003. Evolution of concepts in forest pathology. *Phytopathology*. 93: 1052–1055.
- Nowacki, G.; Brock, T. 1995. Ecoregions and subregions of Alaska [EcoMap]. Version 2.0. Juneau, AK: U.S. Department of Agriculture Forest Service, Alaska Region. Map; presentation scale 1:5,000,000; colored.

- Parry, D.; Teale, S.A. 2011. Alien invasions: the effects of introduced species on forest structure and function. In: Castello, J.D.; Teale, S.A., eds. *Forest health: an integrated perspective*. New York: Cambridge University Press. 115–162.
- Potter, K.M. 2012. Large-scale patterns of insect and disease activity in the conterminous United States and Alaska from the national insect and disease detection survey database, 2007 and 2008. In: Potter, K.M.; Conkling, B.L., eds. *Forest Health Monitoring 2009 national technical report*. Gen. Tech. Rep. SRS-167. Asheville, NC: U.S. Department of Agriculture Forest Service, Southern Research Station: 63–78.
- Potter, K.M. 2013. Large-scale patterns of insect and disease activity in the conterminous United States and Alaska from the national insect and disease detection survey, 2009. In: Potter, K.M.; Conkling, B.L., eds. *Forest Health Monitoring: national status, trends, and analysis, 2010*. Gen. Tech. Rep. SRS-176. Asheville, NC: U.S. Department of Agriculture Forest Service, Southern Research Station: 15–29.
- Potter, K.M.; Koch, F.H. 2012. Large-scale patterns of insect and disease activity in the conterminous United States and Alaska, 2006. In: Potter, K.M.; Conkling, B.L., eds. *Forest Health Monitoring 2008 national technical report*. Gen. Tech. Rep. SRS-158. Asheville, NC: U.S. Department of Agriculture Forest Service, Southern Research Station: 63–72.
- Potter, K.M.; Koch, F.H.; Oswalt, C.M.; Iannone, B.V. 2016. Data, data everywhere: detecting spatial patterns in fine-scale ecological information collected across a continent. *Landscape Ecology*. 31: 67–84.
- Potter, K.M.; Paschke, J.L. 2013. Large-scale patterns of insect and disease activity in the conterminous United States and Alaska from the national Insect and Disease Detection Survey Database, 2010. In: Potter, K.M.; Conkling, B.L., eds. *Forest Health Monitoring: national status, trends, and analysis, 2011*. Gen. Tech. Rep. SRS-185. Asheville, NC: U.S. Department of Agriculture Forest Service, Southern Research Station: 15–28.
- Potter, K.M.; Paschke, J.L. 2014. Large-scale patterns of insect and disease activity in the conterminous United States and Alaska from the national Insect and Disease Survey Database, 2011. In: Potter, K.M.; Conkling, B.L., eds. *Forest Health Monitoring: national status, trends, and analysis, 2012*. Gen. Tech. Rep. SRS-198. Asheville, NC: U.S. Department of Agriculture Forest Service, Southern Research Station: 19–34.
- Potter, K.M.; Paschke, J.L. 2015a. Large-scale patterns of insect and disease activity in the conterminous United States and Alaska from the national insect and disease survey, 2012. In: Potter, K.M.; Conkling, B.L., eds. *Forest Health Monitoring: national status, trends, and analysis, 2013*. Gen. Tech. Rep. SRS-207. Asheville, NC: U.S. Department of Agriculture Forest Service, Southern Research Station: 19–36.
- Potter, K.M.; Paschke, J.L. 2015b. Large-scale patterns of insect and disease activity in the conterminous United States, Alaska, and Hawaii from the national insect and disease survey, 2013. In: Potter, K.M.; Conkling, B.L., eds. *Forest Health Monitoring: national status, trends, and analysis, 2014*. Gen. Tech. Rep. SRS-209. Asheville, NC: U.S. Department of Agriculture Forest Service, Southern Research Station: 19–38.
- Potter, K.M.; Paschke, J.L. 2016. Large-scale patterns of insect and disease activity in the conterminous United States and Alaska from the national insect and disease survey, 2014. In: Potter, K.M.; Conkling, B.L., eds. *Forest Health Monitoring: national status, trends, and analysis, 2015*. Gen. Tech. Rep. SRS-213. Asheville, NC: U.S. Department of Agriculture Forest Service, Southern Research Station: 21–40.
- Potter, K.M.; Paschke, J.L. 2017. Large-scale patterns of insect and disease activity in the conterminous United States and Alaska from the national insect and disease survey, 2015. In: Potter, K.M.; Conkling, B.L., eds. *Forest Health Monitoring: national status, trends, and analysis, 2016*. Gen. Tech. Rep. SRS-222. Asheville, NC: U.S. Department of Agriculture Forest Service, Southern Research Station: 21–42.

- Potter, K.M.; Paschke, J.L.; Zweifler, M. 2018. Large-scale patterns of insect and disease activity in the conterminous United States, Alaska and Hawai'i from the national insect and disease survey, 2016. In: Potter, K.M.; Conkling, B.L., eds. Forest Health Monitoring: national status, trends, and analysis, 2017. Gen. Tech. Rep. SRS-233. Asheville, NC: U.S. Department of Agriculture Forest Service, Southern Research Station: 23–44.
- Reams, G.A.; Smith, W.D.; Hansen, M.H. [and others]. 2005. The Forest Inventory and Analysis sampling frame. In: Bechtold, W.A.; Patterson, P.L., eds. The enhanced Forest Inventory and Analysis program—national sampling design and estimation procedures. Asheville, NC: U.S. Department of Agriculture Forest Service, Southern Research Station: 11–26.
- Shima T.; Sugimoto S.; Okutomi, M. 2010. Comparison of image alignment on hexagonal and square lattices. 2010 IEEE International Conference on Image Processing: 141–144. DOI: 10.1109/icip.2010.5654351.
- Smith, W.B.; Miles, P.D.; Perry, C.H.; Pugh, S.A. 2009. Forest resources of the United States, 2007. Gen. Tech. Rep. WO-78. Washington, DC: U.S. Department of Agriculture Forest Service. 336 p.
- Teale, S.A.; Castello, J.D. 2011. Regulators and terminators: the importance of biotic factors to a healthy forest. In: Castello, J.D.; Teale, S.A., eds. Forest health: an integrated perspective. New York: Cambridge University Press: 81–114.
- University of Hawai'i, College of Tropical Agriculture and Human Resources. 2017. Rapid 'Ōhi'a Death/*Ceratocystis* Wilt of 'Ōhi'a. <http://rapidohiadeath.org>. [Date accessed: July 17, 2017].
- U.S. Department of Agriculture (USDA) Forest Service. 2008. National forest type data development. http://svinetfc4.fs.fed.us/rastergateway/forest_type/. [Date accessed: May 13, 2008].
- White, D.; Kimerling, A.J.; Overton, W.S. 1992. Cartographic and geometric components of a global sampling design for environmental monitoring. *Cartography and Geographic Information Systems*. 19(1): 5–22.
- Zhang, L.; Rubin, B.D.; Manion, P.D. 2011. Mortality: the essence of a healthy forest. In: Castello, J.D.; Teale, S.A., eds. Forest health: an integrated perspective. New York: Cambridge University Press: 17–49.

INTRODUCTION

As a pervasive disturbance agent operating at many spatial and temporal scales, wildland fire is a key abiotic factor affecting forest health both positively and negatively. In some ecosystems, for example, wildland fires have been essential for regulating processes that maintain forest health (Lundquist and others 2011). Wildland fire is an important ecological mechanism that shapes the distributions of species, maintains the structure and function of fire-prone communities, and acts as a significant evolutionary force (Bond and Keeley 2005). At the same time, wildland fires have created forest health (i.e., sustainability) problems in some ecosystems (Edmonds and others 2011). Specifically, fire outside the historic range of frequency and intensity can impose extensive ecological and socioeconomic impacts. Current fire regimes on more than half of the forested area in the conterminous United States have been moderately or significantly altered from historical regimes, potentially altering key ecosystem components such as species composition, structural stage, stand age, canopy closure, and fuel loadings (Schmidt and others 2002). As a result of intensive fire suppression efforts during most of the 20th century, the forest area burned annually decreased from approximately 16–20 million ha (40–50 million acres) in the early 1930s to about 2 million ha

(5 million acres) in the 1970s (Vinton 2004). Understanding existing fire regimes is essential for properly assessing the impact of fire on forest health because changes to historical fire regimes can alter forest developmental patterns, including the establishment, growth, and mortality of trees (Lundquist and others 2011).

Fire regimes have been dramatically altered by fire suppression (Barbour and others 1999) and by the introduction of nonnative invasive plants, which can change fuel properties and in turn both affect fire behavior and alter fire regime characteristics such as frequency, intensity, type, and seasonality (Brooks and others 2004). Fires in some regions and ecosystems have become larger, more intense, and more damaging because of the accumulation of fuels as a result of prolonged fire suppression (Pyne 2010). Such large wildland fires also can have long-lasting social and economic consequences, which include the loss of human life and property, smoke-related human health impacts, and the economic cost and dangers of fighting the fires themselves (Gill and others 2013, Richardson and others 2012). In some regions, plant communities have experienced or are undergoing rapid compositional and structural changes as a result of fire suppression (Nowacki and Abrams 2008). Additionally, changes in fire intensity and recurrence could result in decreased forest resilience and persistence

CHAPTER 3.

Large-Scale Patterns of Forest Fire Occurrence across the 50 United States and the Caribbean Territories, 2017

KEVIN M. POTTER

(Lundquist and others 2011), and fire regimes altered by global climate change could cause large-scale shifts in vegetation spatial patterns (McKenzie and others 1996). Given the relationships of fires to forest dynamics, it is important to monitor and assess spatiotemporal trends in forest fires across the United States and its territories.

This chapter presents analyses of daily satellite-based fire occurrence data that map and quantify the locations and intensities of fire occurrences spatially across the conterminous United States, Alaska, Hawaii, and the Caribbean territories in 2017. It also compares 2017 fire occurrences, within a geographic context, to all the recent years for which such data are available. Quantifying and monitoring such large-scale patterns of fire occurrence across the United States can help improve our understanding of the ecological and economic impacts of fire as well as the appropriate management and prescribed use of fire. Specifically, large-scale assessments of fire occurrence can help identify areas where specific management activities may be needed, or where research into the ecological and socioeconomic impacts of fires may be required.

METHODS

Data

Annual monitoring and reporting of active wildland fire events using the Moderate Resolution Imaging Spectroradiometer (MODIS)

Active Fire Detections for the United States database (USDA Forest Service 2018) allow analysts to spatially display and summarize fire occurrences across broad geographic regions (Coulston and others 2005; Potter 2012a, 2012b, 2013a, 2013b, 2014, 2015a, 2015b, 2016, 2017, 2018). A fire occurrence is defined as one daily satellite detection of wildland fire in a 1-km pixel, with multiple fire occurrences possible on a pixel across multiple days resulting from a single wildland fire that lasts more than a single day. The data are derived using the MODIS Rapid Response System (Justice and others 2002, 2011) to extract fire location and intensity information from the thermal infrared bands of imagery collected daily by two satellites at a resolution of 1 km, with the center of a pixel recorded as a fire occurrence (USDA Forest Service 2018). The Terra and Aqua satellites' MODIS sensors identify the presence of a fire at the time of image collection, with Terra observations collected in the morning and Aqua observations collected in the afternoon. The resulting fire occurrence data represent only whether a fire was active because the MODIS data bands may not differentiate between a hot fire in a relatively small area (0.01 km², for example) and a cooler fire over a larger area (1 km², for example) if the foreground to background temperature contrast is not sufficiently high. The MODIS Active Fire database does well at capturing large fires during cloud-free conditions but may underrepresent rapidly burning, small, and low-intensity fires,

as well as fires in areas with frequent cloud cover (Hawbaker and others 2008). For large-scale assessments, the dataset represents a good alternative to the use of information on ignition points, which may be preferable but can be difficult to obtain or may not exist (Tonini and others 2009). For more information about the performance of this product, see Justice and others (2011).

It is important to underscore that estimates of burned area and calculations of MODIS-detected fire occurrences are two different metrics for quantifying fire activity within a given year. Most importantly, the MODIS data contain both spatial and temporal components because persistent fire will be detected repeatedly over several days on a given 1-km pixel. In other words, a location can be counted as having a fire occurrence multiple times, once for each day a fire is detected at the location. Analyses of the MODIS-detected fire occurrences, therefore, measure the total number of daily 1-km pixels with fire during a year, as opposed to quantifying only the area on which fire occurred at some point during the course of the year. A fire detected on a single pixel on every day of the year would be equivalent to 365 fire occurrences.

It is worth noting that the Terra and Aqua satellites, which carry the MODIS sensors, were launched in 1999 and 2002, respectively,

and will eventually be decommissioned. An alternative fire occurrence data source is the Visible Infrared Imaging Radiometer Suite (VIIRS) sensor on board the Suomi National Polar-orbiting Partnership (Suomi NPP) weather satellite. The transition to this new data source will require a comparison of fire occurrence detections between it and MODIS.

Analyses

These MODIS products for 2017, and for the 16 preceding full years of data, were processed in ArcMap® (ESRI 2015) to determine the number of fire occurrences per 100 km² (10 000 ha) of forested area for each ecoregion section in the conterminous United States (Cleland and others 2007) and Alaska (Nowacki and Brock 1995), and for each of the major islands of Hawaii and of the Caribbean territories of Puerto Rico and the U.S. Virgin Islands. This forest fire occurrence density measure for the conterminous 48 States and Alaska was calculated after screening out wildland fires on nonforested pixels using a forest cover layer derived from MODIS imagery by the U.S. Department of Agriculture Forest Service, Remote Sensing Applications Center (RSAC) (USDA Forest Service 2008). The same process was repeated for the Hawaiian islands using 30-m vegetation type data from the LANDFIRE program (LANDFIRE 2014), resampled to 1 km, and for Puerto Rico and the U.S. Virgin Islands

using 30-m landcover data (also resampled to 1 km) from the Forest Service International Institute of Tropical Forestry (IITF) that were derived from a cloud-free Landsat image mosaic developed in cooperation with RSAC (Kennaway and Helmer 2007, Kennaway and others 2008). The total numbers of forest fire occurrences were also determined separately for the conterminous States, Alaska, Hawaii, and the Caribbean territories.

The fire occurrence density value for each of the ecoregion sections and the Hawaiian and Caribbean islands in 2017 was then compared with the mean fire density values for the first 16 full years of MODIS Active Fire data collection (2001–2016). Specifically, the difference of the 2017 value and the previous 16-year mean for an ecoregion was divided by the standard deviation across the previous 16-year period, assuming a normal distribution of fire density over time in the ecoregion. The result for each ecoregion was a standardized z-score, which is a dimensionless quantity describing the degree to which the fire occurrence density in the ecoregion in 2017 was higher, lower, or the same relative to all the previous years for which data have been collected, accounting for the variability in the previous years. The z-score is the number of standard deviations between the observation and the mean of the historic observations in the previous years.

Approximately 68 percent of observations would be expected within one standard deviation of the mean, and 95 percent within two standard deviations. Near-normal conditions are classified as those within a single standard deviation of the mean, although such a threshold is somewhat arbitrary. Conditions between about one and two standard deviations of the mean are moderately different from mean conditions, but are not significantly different statistically. Those outside about two standard deviations would be considered statistically greater than or less than the long-term mean (at $p < 0.025$ at each tail of the distribution).

Additionally, we used the Spatial Association of Scalable Hexagons (SASH) analytical approach to identify forested areas in the conterminous United States with higher-than-expected fire occurrence density in 2017. This method identifies locations where ecological phenomena occur at greater or lower occurrences than expected by random chance and is based on a sampling frame optimized for spatial neighborhood analysis, adjustable to the appropriate spatial resolution, and applicable to multiple data types (Potter and others 2016). Specifically, it consists of dividing an analysis area into scalable equal-area hexagonal cells within which data are aggregated, followed by identifying statistically significant geographic clusters of hexagonal cells within which mean

values are greater or less than those expected by chance. To identify these clusters, we employed a Getis-Ord G_i^* hot spot analysis (Getis and Ord 1992) in ArcMap[®] 10.3 (ESRI 2015).

The spatial units of analysis were 9,810 hexagonal cells, each approximately 834 km² in area, generated in a lattice across the conterminous United States using intensification of the Environmental Monitoring and Assessment Program (EMAP) North American hexagon coordinates (White and others 1992). These coordinates are the foundation of a sampling frame in which a hexagonal lattice was projected onto the conterminous United States by centering a large base hexagon over the region (Reams and others 2005, White and others 1992). This base hexagon can be subdivided into many smaller hexagons, depending on sampling needs, and serves as the basis of the plot sampling frame for the Forest Inventory and Analysis (FIA) program (Reams and others 2005). Importantly, the hexagons maintain equal areas across the study region regardless of the degree of intensification of the EMAP hexagon coordinates. In addition, the hexagons are compact and uniform in their distance to the centroids of neighboring hexagons, meaning that a hexagonal lattice has a higher degree of isotropy (uniformity in all directions) than does a square grid (Shima and others 2010). These are convenient and highly useful attributes for spatial neighborhood

analyses. These scalable hexagons also are independent of geopolitical and ecological boundaries, avoiding the possibility of different sample units (such as counties, States, or watersheds) encompassing vastly different areas (Potter and others 2016). We selected hexagons 834 km² in area because this is a manageable size for making monitoring and management decisions in analyses across the conterminous United States (Potter and others 2016).

Fire occurrence density values for each hexagon were quantified as the number of forest fire occurrences per 100 km² of forested area within the hexagon. The Getis-Ord G_i^* statistic was used to identify clusters of hexagonal cells with fire occurrence density values higher than expected by chance. This statistic allows for the decomposition of a global measure of spatial association into its contributing factors, by location, and is therefore particularly suitable for detecting outlier assemblages of similar conditions in a dataset, such as when spatial clustering is concentrated in one subregion of the data (Anselin 1992).

Briefly, G_i^* sums the differences between the mean values in a local sample, determined in this case by a moving window of each hexagon and its 18 first- and second-order neighbors (the 6 adjacent hexagons and the 12 additional hexagons contiguous to those 6) and the global mean of the 7,595 forested hexagonal cells (of

the total 9,810) in the conterminous United States. As described in Laffan (2006), it is calculated as

$$G_i^*(d) = \frac{\sum_j w_{ij}(d)x_j - W_i \bar{x}^*}{s^* \sqrt{\frac{(ns_{1i}^*) - W_i^2}{n-1}}}$$

where

G_i^* = the local clustering statistic (in this case, for the target hexagon)

i = the center of local neighborhood (the target hexagon)

d = the width of local sample window (the target hexagon and its first- and second-order neighbors)

x_j = the value of neighbor j

w_{ij} = the weight of neighbor j from location i (all the neighboring hexagons in the moving window were given an equal weight of 1)

n = number of samples in the dataset (the 7,595 forested hexagons)

W_i^* = the sum of the weights

s_{1i}^* = the number of samples within d of the central location (19: the focal hexagon and its 18 first- and second-order neighbors)

\bar{x}^* = the mean of whole dataset (in this case, for all 7,595 forested hexagons)

s^* = the standard deviation of whole dataset (for all 7,595 forested hexagons)

G_i^* is standardized as a z-score with a mean of 0 and a standard deviation of 1, with values >1.96 representing significant local clustering of higher fire occurrence densities ($p < 0.025$) and values <-1.96 representing significant clustering of lower fire occurrence densities ($p < 0.025$), because 95 percent of the observations under a normal distribution should be within approximately two standard deviations of the mean (Laffan 2006). Values between -1.96 and 1.96 have no statistically significant concentration of high or low values; a hexagon and its 18 neighbors, in other words, have a normal range of both high and low numbers of fire occurrences per 100 km² of forested area. It is worth noting that the threshold values are not exact because the correlation of spatial data violates the assumption of independence required for statistical significance (Laffan 2006). In addition, the Getis-Ord approach does not require that the input data be normally distributed, because the local G_i^* values are computed under a randomization assumption, with G_i^* equating to a standardized z-score that asymptotically tends to a normal distribution (Anselin 1992). The z-scores are considered to be reliable, even with skewed data, as long as the local neighborhood encompasses several observations (ESRI 2015), in this case, via the target hexagon and its 18 first- and second-order neighbors.

RESULTS AND DISCUSSION

Trends in Forest Fire Occurrence Detections for 2017

The MODIS Active Fire database recorded 92,864 forest fire occurrences across the conterminous United States in 2017, the fifth most in 17 full years of data collection and the most since 2014 (fig. 3.1). This was approximately 95 percent more than in 2016 (47,744 total forest fire occurrences), and about 43 percent higher than the annual mean of 64,913 forest fire occurrences across the previous 16 years of data collection. In Alaska, meanwhile, the MODIS database captured 2,043 forest fire occurrences in 2017, about 7 percent less than the preceding year (2,196) and about 82 percent less than the previous 16-year annual

mean of 11,317. Meanwhile, Hawaii had 118 fire occurrences in 2017, a decrease of about 90 percent from the previous year (1,210) and 72 percent below the average of 426 fire occurrences over the previous 16 years. Finally, 10 forest fire occurrences were detected in Puerto Rico, 27 percent fewer than the previous average of 13.7 per year.

The increase in the total number of fire occurrences across the United States is generally consistent with the official wildland fire statistics (National Interagency Coordination Center 2018). In 2017, 71,499 wildland fires were reported across the United States, an increase from 67,743 in 2016. At the same time, the area burned nationally (4 057 413 ha) was 153 percent above the 10-year annual average

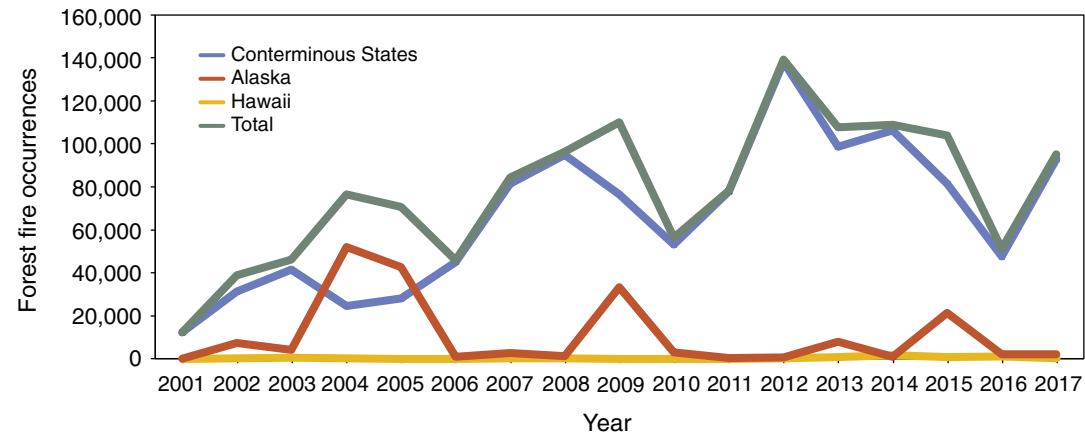


Figure 3.1—Forest fire occurrences detected by MODIS from 2001 to 2017 for the conterminous United States, Alaska, and Hawaii, and for the entire Nation combined. (Data source: U.S. Department of Agriculture Forest Service, Remote Sensing Applications Center, in conjunction with the NASA MODIS Rapid Response group)

and 73 percent greater than the area burned in 2016 (2 339 815 ha) (National Interagency Coordination Center 2017, 2018). Also in 2017, 44 wildland fires and fire complexes exceeded 16 187 ha, compared to 19 in 2016 and 52 in 2015 (National Interagency Coordination Center 2017, 2018). As noted in the Methods section, estimates of burned area are different metrics for quantifying fire activity than calculations of MODIS-detected fire occurrences, though the two may be correlated.

Areas with the highest fire occurrence densities were in the Pacific Northwest region and in California (fig. 3.2). Precipitation was above normal in these areas early in 2017, promoting significant growth of fine fuels; July and August were then very dry in many areas, except in central and southern parts of California, which dried considerably later in the year with the lack of autumn rain combined with strong winds (National Interagency Coordination Center 2018). The ecoregion section with the highest fire occurrence density by far was M332B–Northern Rockies and Bitterroot Valley in western Montana, with 41.8 fire occurrences/100 km² of forest (table 3.1). This was the location of the Rice Ridge Fire, a lightning-ignited fire that burned 64 825 ha between July 24 and October 17 and cost approximately \$49.3 million in damages and containment (National Interagency Coordination Center 2018). Fire occurrence densities were also very high in M261A–Klamath Mountains in northwestern California and southwestern Oregon (27.9 fire occurrences/100 km² of

forest), location of the Chetco Bar Fire, which scorched 77 346 ha from its lightning ignition on July 12 until October 26 and cost approximately \$72 million to contain (National Interagency Coordination Center 2018). Two other ecoregion sections experienced >20 fires/100 km² of forest: M333C–Northern Rockies (22.0) and 261B–Southern California Coast (20.7) (table 3.1). The latter of these was the site of the 109 265-ha Thomas Fire, which burned in Ventura and Santa Barbara Counties from December 4 through the end of the year and cost at least \$123.8 million (National Interagency Coordination Center 2018). This was the largest wildfire in recorded California history (CAL FIRE 2018).

Fire occurrence densities were also comparatively quite high (12.1–24 fire occurrences/100 km² of forest) throughout the Cascade Range of Washington and Oregon (M242D–Northern Cascades and M242B–Western Cascades) and in parts of the northern Rockies in central and northern Idaho and western Montana (M332A–Idaho Batholith and M333D–Bitterroot Mountains) (fig. 3.2).

Other ecoregion sections in the Southeast and scattered throughout the West had moderately high fire occurrence densities (6.1–12 fire occurrences/100 km² of forest) (fig. 3.2). In the Southeast, this included an area from southern Mississippi along the Gulf Coast (232B–Gulf Coastal Plains and Flatwoods) and northeast through Georgia and South Carolina into North Carolina (232J–Southern Atlantic Coastal Plains and Flatwoods). Fire occurrence densities

Table 3.1—The 15 ecoregion sections in the conterminous United States with the highest fire occurrence densities in 2017

Section	Name	Forest area <i>km</i> ²	Fire occurrences	Density
M332B	Northern Rockies and Bitterroot Valley	158.8	6,643	41.8
M261A	Klamath Mountains	343.1	9,566	27.9
M333C	Northern Rockies	172.7	3,807	22.0
261B	Southern California Coast	40.7	843	20.7
M332A	Idaho Batholith	361.0	7,007	19.4
M242D	Northern Cascades	230.7	3,374	14.6
M242B	Western Cascades	417.7	6,041	14.5
M333D	Bitterroot Mountains	222.9	2,850	12.8
M333B	Flathead Valley	160.6	1,575	9.8
263A	Northern California Coast	123.2	1,184	9.6
322C	Colorado Desert	0.4	4	9.1
M261F	Sierra Nevada Foothills	71.2	626	8.8
M261E	Sierra Nevada	438.1	3,708	8.5
232J	Southern Atlantic Coastal Plains and Flatwoods	439.5	3,551	8.1
232B	Gulf Coastal Plains and Flatwoods	732.3	5,664	7.7

were also moderately high in two neighboring ecoregion sections in Arkansas and Oklahoma: 231G–Arkansas Valley and 255A–Cross Timbers and Prairie.

Additionally, moderately high fire occurrence densities were recorded in several Western ecoregion sections, all with 6.1–12 fire occurrences/100 km² of forest: 321A–Basin and Range, in southeastern Arizona, southern New Mexico, and far western Texas; M261E–Sierra Nevada and M261F–Sierra Nevada Foothills, in California; 263A–Northern California

Coast and M261B–Northern California Coast Ranges; and M333B–Flathead Valley, in northwestern Montana.

Meanwhile, Alaska experienced above-average temperatures, but periodic precipitation events minimized the fire impacts of the heat (National Interagency Coordination Center 2018). Fire occurrence densities were low across the State (fig. 3.3), with the exception of M139B–Olgivie Mountains in eastern Alaska (3.6 fires occurrences/100 km² of forest). This was where the 37 846-ha Campbell River Fire

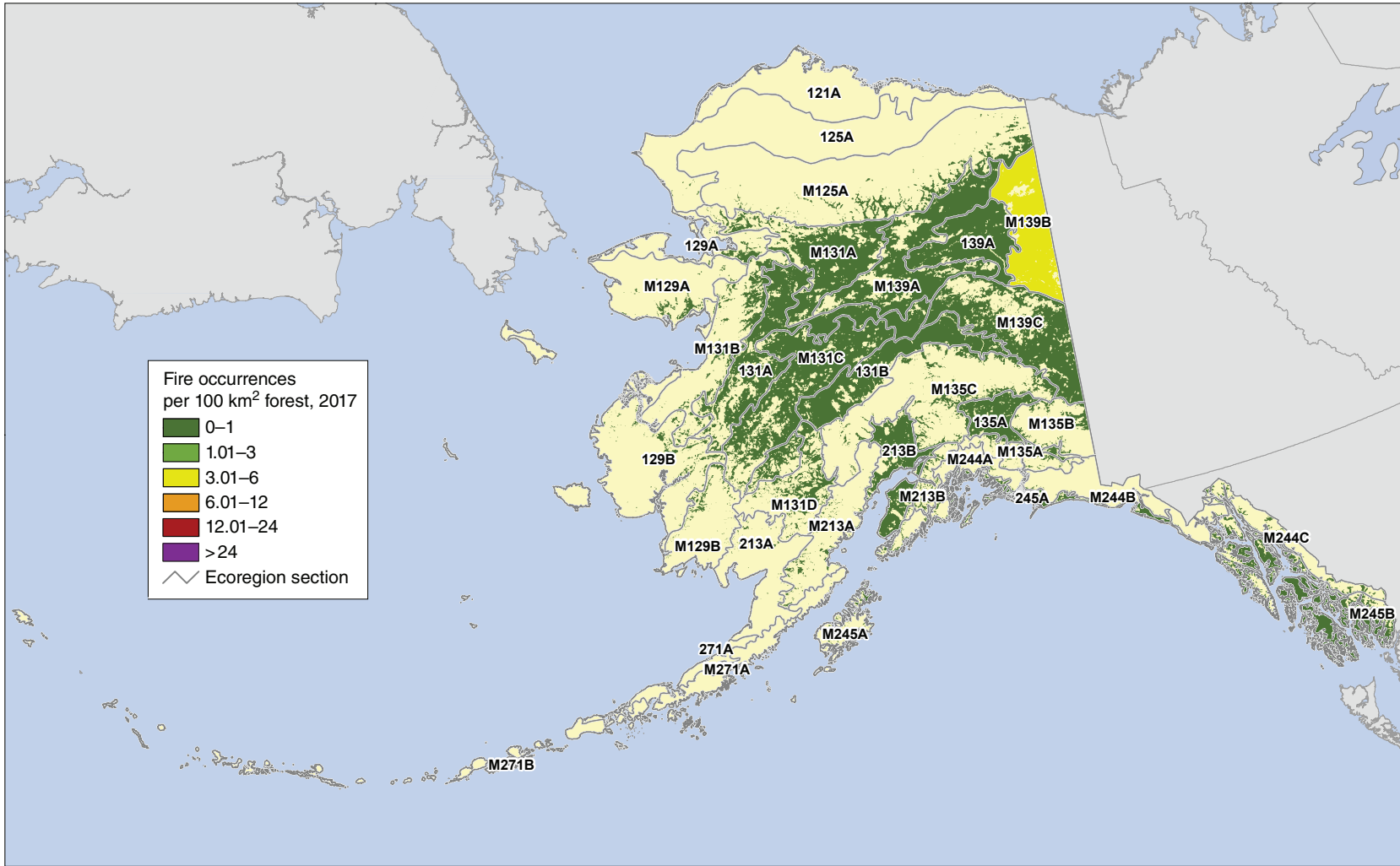


Figure 3.3—The number of forest fire occurrences, per 100 km² (10 000 ha) of forested area, by ecoregion section within Alaska, for 2017. The gray lines delineate ecoregion sections (Nowacki and Brock 1995). Forest cover is derived from MODIS imagery by the Forest Service Remote Sensing Applications Center. (Source of fire data: U.S. Department of Agriculture Forest Service, Remote Sensing Applications Center, in conjunction with the NASA MODIS Rapid Response group)

burned from late June into early October, extending well into the neighboring Yukon Territory of Canada.

In Hawaii, lava flows from the 35-year-long eruption of Pu'u 'Ō'ō, a vent on the flank of the Kīlauea volcano on the Big Island, continued to be the cause of most forest fire occurrences. Fire occurrence density on the Big Island was 2.9/100 km² of forest in 2017 (fig. 3.4), one-tenth of the 29.6 fire occurrences/100 km² of forest recorded in 2016 (Potter 2018). All the other islands in the archipelago experienced <1 fire occurrence/100 km² of forest.

Finally, all of the islands constituting the U.S. Caribbean territories had <1 fire occurrence/100 km² of forest in 2017 (fig. 3.5).

Comparison to Longer Term Trends

The nature of the MODIS Active Fire data makes it possible to contrast, for each ecoregion section and Hawaiian and Caribbean island, short-term (1-year) forest fire occurrence densities with longer term trends encompassing the first 16 full years of data collection (2001–2016). In general, the ecoregion sections with the highest annual fire occurrence means are located in the northern Rocky Mountains, the Southwest, California, Oklahoma, and the Gulf Coastal Plain, while most ecoregion sections

within the Northeastern, Midwestern, Middle Atlantic, and Appalachian regions experienced <1 fire occurrence/100 km² of forest annually during the multiyear period (fig. 3.6A). The forested ecoregion section that experienced the most fire occurrences each year on average was M332A–Idaho Batholith in central Idaho (mean annual fire occurrence density of 13.0) (table 3.2), which also had a high fire occurrence density in 2017. Other ecoregion sections with high mean fire occurrence densities (6.1–12.0 fire occurrences/100 km² of forest) were located along the Gulf Coast in the Southeast; in coastal, northern, and central areas of California; in central Arizona and New Mexico; in the northern Rocky Mountains; and in central Oklahoma (table 3.2). The ecoregion section with the greatest variation in fire occurrence densities from 2001 to 2016 was M332A–Idaho Batholith, with more moderate variation in California, northern Washington, southern and northeastern Oregon, western Montana, central Arizona and west-central New Mexico, and eastern North Carolina (fig. 3.6B). Less variation occurred throughout the central and northern Rocky Mountain States, the Southeast, and central Oregon and Washington. The lowest levels of variation occurred throughout most of the Midwest and Northeast.

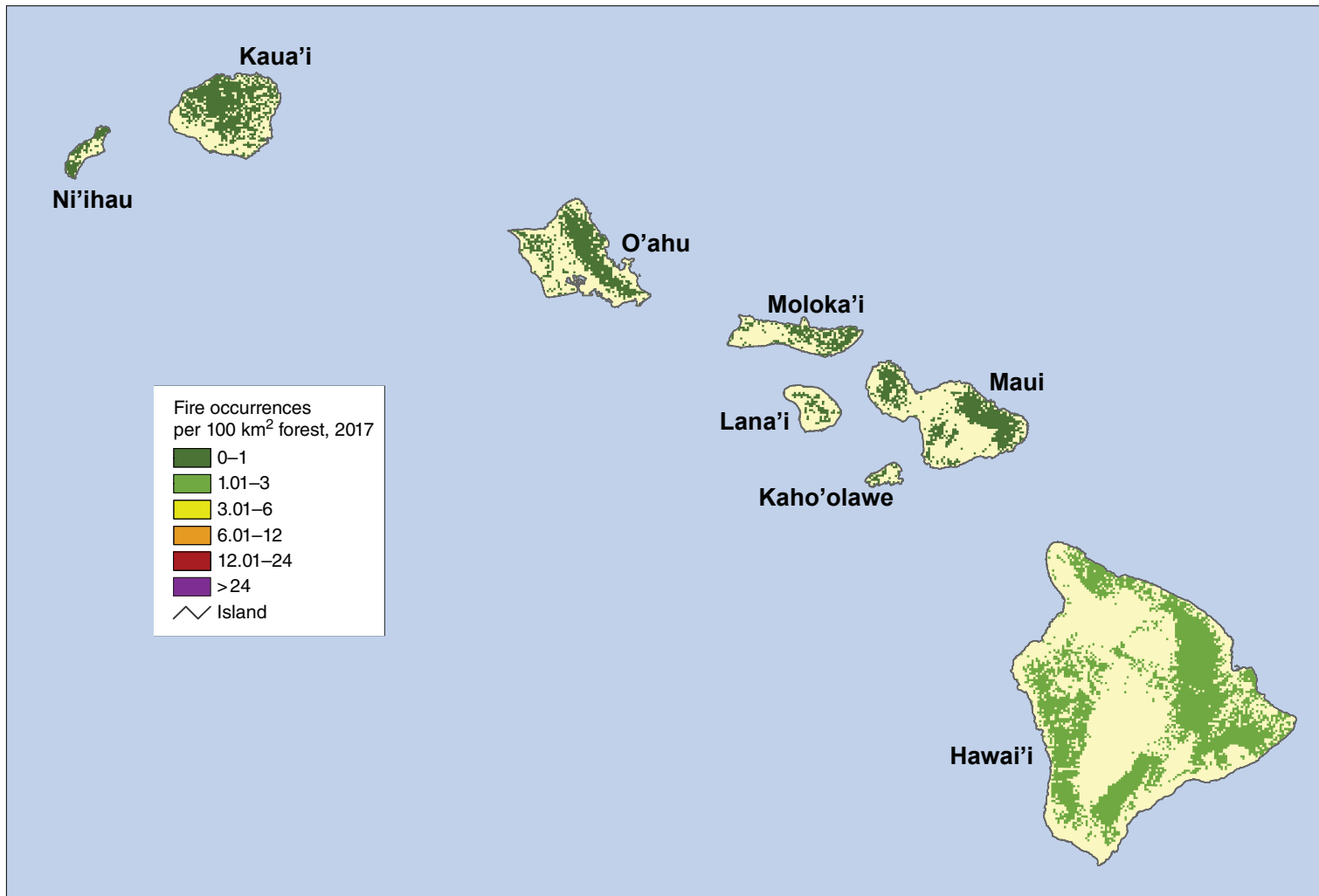


Figure 3.4—The number of forest fire occurrences, per 100 km² (10 000 ha) of forested area, by island in Hawaii, for 2017. Background forest cover is derived from the LANDFIRE program (LANDFIRE 2014). (Source of fire data: U.S. Department of Agriculture Forest Service, Remote Sensing Applications Center, in conjunction with the NASA MODIS Rapid Response group)

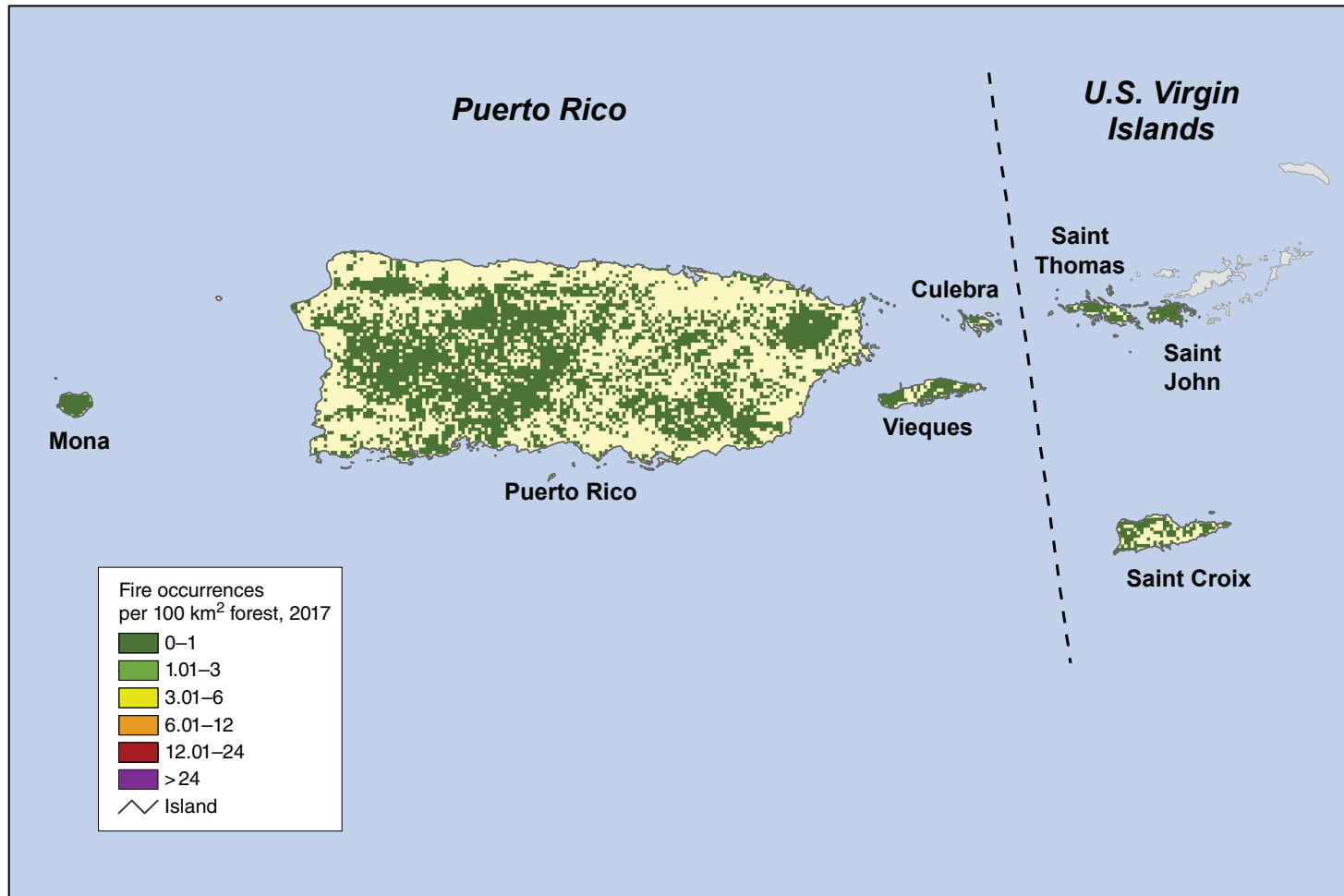


Figure 3.5—The number of forest fire occurrences, per 100 km² (10 000 ha) of forested area, by island in Puerto Rico and the U.S. Virgin Islands, for 2017. Forest cover is from the Forest Service International Institute of Tropical Forestry, derived from a cloud-free Landsat image mosaic developed in cooperation with Forest Service Remote Sensing Applications Center (Kennaway and Helmer 2007, Kennaway and others 2008).

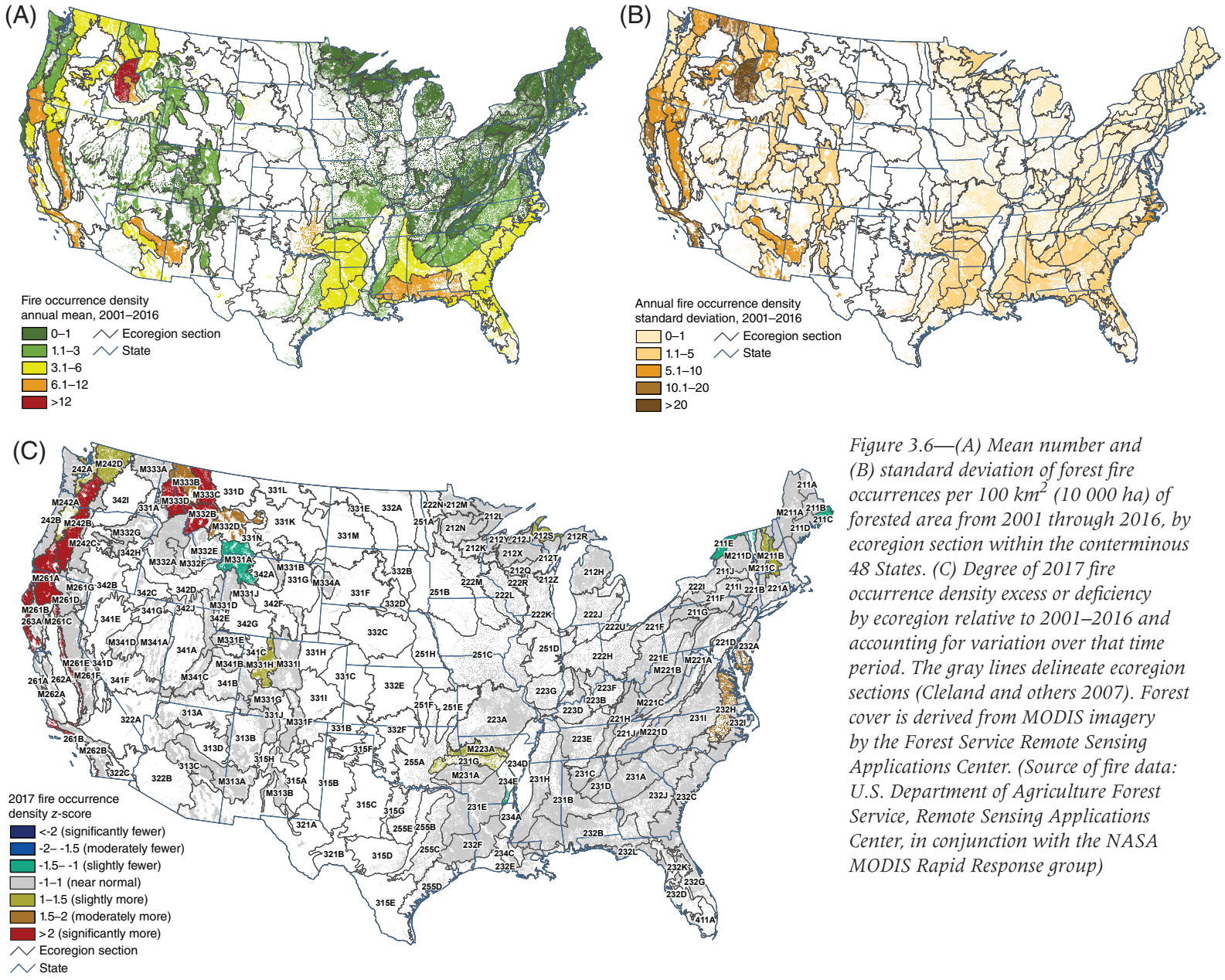


Figure 3.6—(A) Mean number and (B) standard deviation of forest fire occurrences per 100 km² (10 000 ha) of forested area from 2001 through 2016, by ecoregion section within the conterminous 48 States. (C) Degree of 2017 fire occurrence density excess or deficiency by ecoregion relative to 2001–2016 and accounting for variation over that time period. The gray lines delineate ecoregion sections (Cleland and others 2007). Forest cover is derived from MODIS imagery by the Forest Service Remote Sensing Applications Center. (Source of fire data: U.S. Department of Agriculture Forest Service, Remote Sensing Applications Center, in conjunction with the NASA MODIS Rapid Response group)

Table 3.2—The 14 ecoregion sections in the conterminous United States with the highest annual mean fire occurrence densities from 2001 through 2016

Section	Name	Forest area <i>km</i> ²	Mean annual fire occurrence density
332F	South Central and Red Bed Plains	1.5	18.4
M332A	Idaho Batholith	361.0	13.0
331G	Powder River Basin	6.2	10.3
261A	Central California Coast	58.3	9.7
M262B	Southern California Mountain and Valley	155.3	8.6
251F	Flint Hills	0.8	7.8
322C	Colorado Desert	0.4	7.8
M261E	Sierra Nevada	438.1	7.6
M261A	Klamath Mountains	343.1	6.9
331A	Palouse Prairie	28.3	6.6
255A	Cross Timbers and Prairie	79.0	6.4
232B	Gulf Coastal Plains and Flatwoods	732.3	6.3
M313A	White Mountains-San Francisco Peaks-Mogollon Rim	386.7	6.1
M332F	Challis Volcanics	90.0	6.1

As determined by the calculation of standardized fire occurrence z-scores, ecoregion sections in southern, central, and northern California; the Cascade Mountains of Oregon and Washington; and northern Idaho and northwestern Montana experienced significantly greater fire occurrence densities than normal in 2017, compared to the previous 16-year mean and accounting for variability over time (fig. 3.6C). The ecoregion section with the highest fire occurrence density in 2017 (M332B—Northern Rockies and Bitterroot Valley, fig. 3.2) also had a high z-score. Additionally, some

ecoregion sections had moderately or slightly higher fire occurrence density than expected as shown by their z-scores (fig. 3.6C), including 232H—Middle Atlantic Coastal Plains and Flatwoods in eastern North Carolina, Virginia, and the Delmarva Peninsula; M223A—Boston Mountains and 231G—Arkansas Valley in northern Arkansas and eastern Oklahoma; 212S—Northern Upper Peninsula in Michigan; M211B—New England Piedmont in Vermont and New Hampshire; and M331H—North-Central Highlands and Rocky Mountains in central Colorado.

A handful of ecoregion sections across the country had lower fire occurrence densities in 2017 compared to the longer term as indicated by their z-scores: M331A–Yellowstone Highlands in northwestern Wyoming, southwestern Montana, and northeastern Idaho; 234E–Arkansas Alluvial Plains in southeastern Arkansas; 211E–St. Lawrence and Champlain Valley in northern New York and Vermont; and 211C–Fundy Coastal and Interior in southeastern Maine. All had very low fire occurrence densities in 2017, and low or relatively low annual mean fire occurrence density and variation from 2001–2016.

In Alaska, meanwhile, moderate mean fire occurrence density existed in the east-central and central parts of the State centered on the 139A–Yukon Flats ecoregion section and including M139A–Ray Mountains, M139B–Olgivie Mountains, and M139C–Dawson Range (fig. 3.7A). These same areas experienced the greatest degree of variability over the 16-year period preceding 2017 (fig. 3.7B). In 2017, only one ecoregion section, M213B–Kenai Mountains, was outside the range of near-normal fire occurrence density (z -score >2), having many more fire occurrences compared to the mean of the previous 16 years and accounting for variability (fig. 3.7C).

In Hawaii, both mean annual fire occurrence density (fig. 3.8A) and variability (fig. 3.8B) were highest on the Big Island during the

2001–2016 period. The annual mean was <1 fire occurrence/100 km² of forest for all islands except the Big Island (12.7) and Kaho‘olawe (1.7). The annual fire occurrence standard deviation exceeded 1 for only the Big Island (17.7), Kaho‘olawe (5.1), and Lāna‘i (1.2). No Hawaiian island in 2017 was outside the range of near-normal fire occurrence density, controlling for variability over the previous 16 years (z -score between -1 and 1) (fig. 3.7C).

All the islands of the Caribbean territories had annual fire occurrence means and standard deviations <1 (figs. 3.9A and 3.9B). Additionally, each of the islands was within the range of near-normal fire occurrence density (z -score between -1 and 1) (fig. 3.9C).

Geographical Hot Spots of Fire Occurrence Density

Although summarizing fire occurrence data at the ecoregion section scale allows for the quantification of fire occurrence density across the country, a geographical hot spot analysis can offer insights into where, statistically, fire occurrences are more concentrated than expected by chance. In 2017, the SASH method detected three geographical hot spots of very high fire occurrence density ($G_i^* >12$ and ≤ 24) (fig. 3.10). These corresponded with areas of high fire occurrence density (fig. 3.2), including M332B–Northern Rockies and Bitterroot Valley and M261A–Klamath Mountains (see above), as well as M332A–Idaho Batholith.

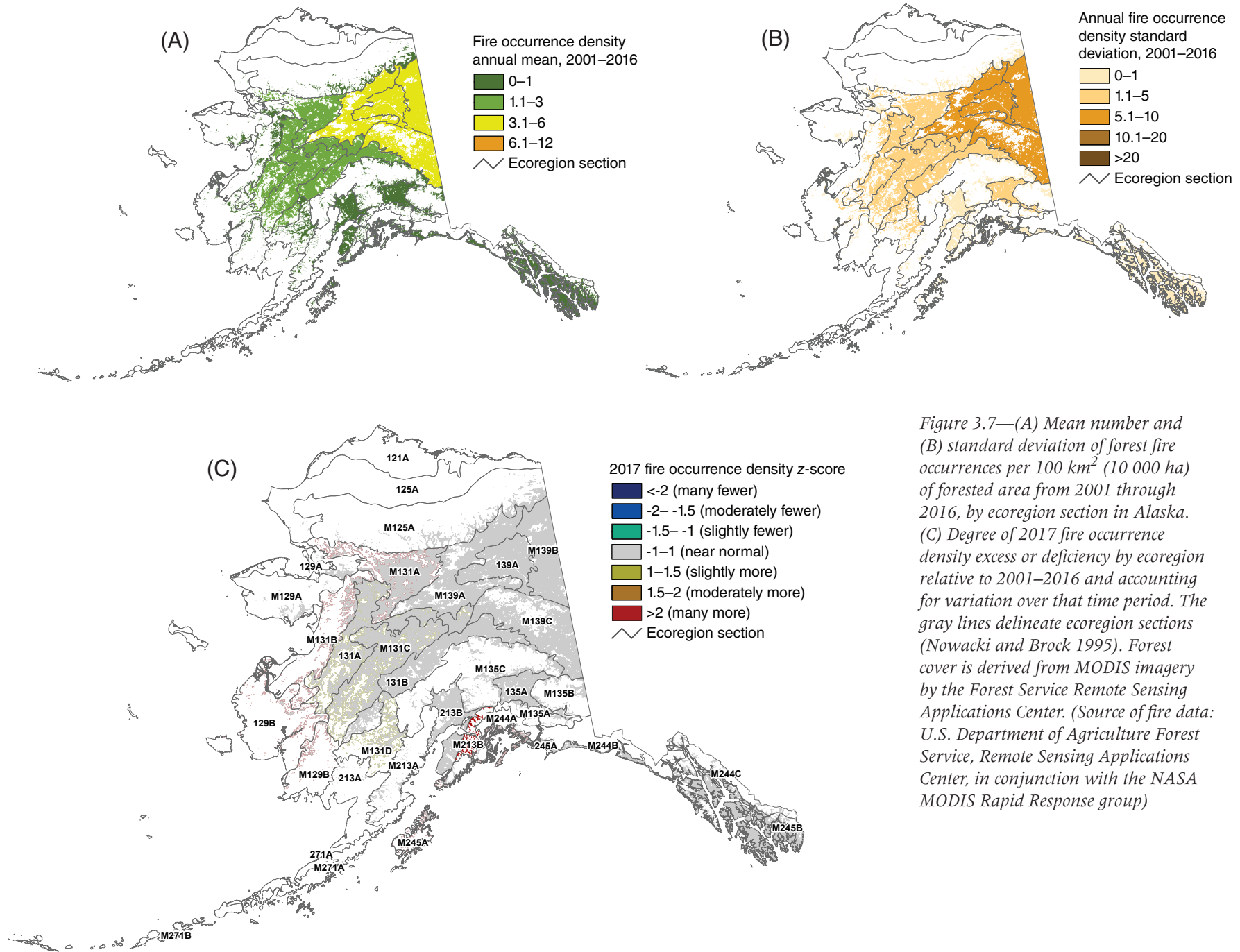


Figure 3.7—(A) Mean number and (B) standard deviation of forest fire occurrences per 100 km² (10 000 ha) of forested area from 2001 through 2016, by ecoregion section in Alaska. (C) Degree of 2017 fire occurrence density excess or deficiency by ecoregion relative to 2001–2016 and accounting for variation over that time period. The gray lines delineate ecoregion sections (Nowacki and Brock 1995). Forest cover is derived from MODIS imagery by the Forest Service Remote Sensing Applications Center. (Source of fire data: U.S. Department of Agriculture Forest Service, Remote Sensing Applications Center, in conjunction with the NASA MODIS Rapid Response group)

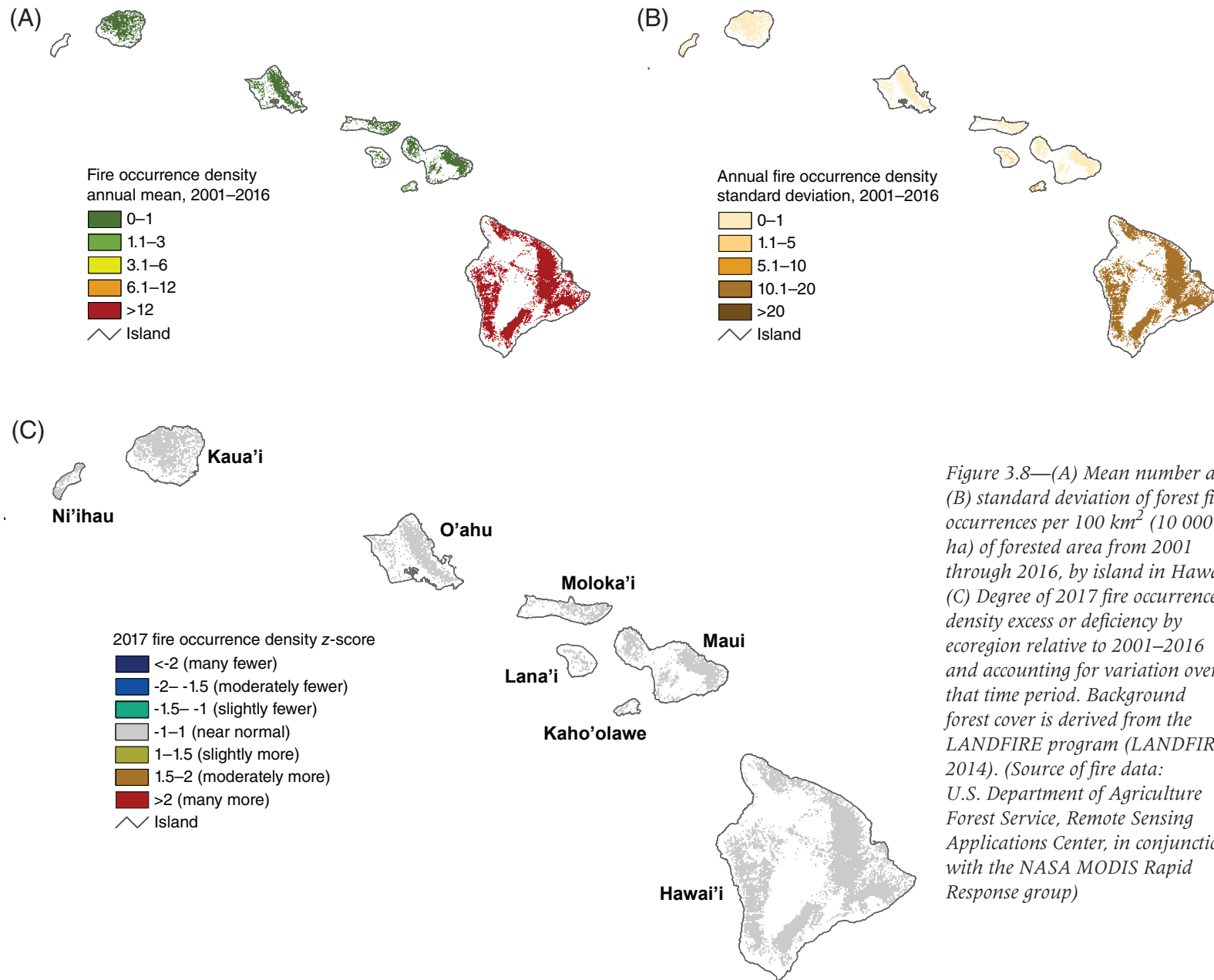


Figure 3.8—(A) Mean number and (B) standard deviation of forest fire occurrences per 100 km² (10 000 ha) of forested area from 2001 through 2016, by island in Hawaii. (C) Degree of 2017 fire occurrence density excess or deficiency by ecoregion relative to 2001–2016 and accounting for variation over that time period. Background forest cover is derived from the LANDFIRE program (LANDFIRE 2014). (Source of fire data: U.S. Department of Agriculture Forest Service, Remote Sensing Applications Center, in conjunction with the NASA MODIS Rapid Response group)

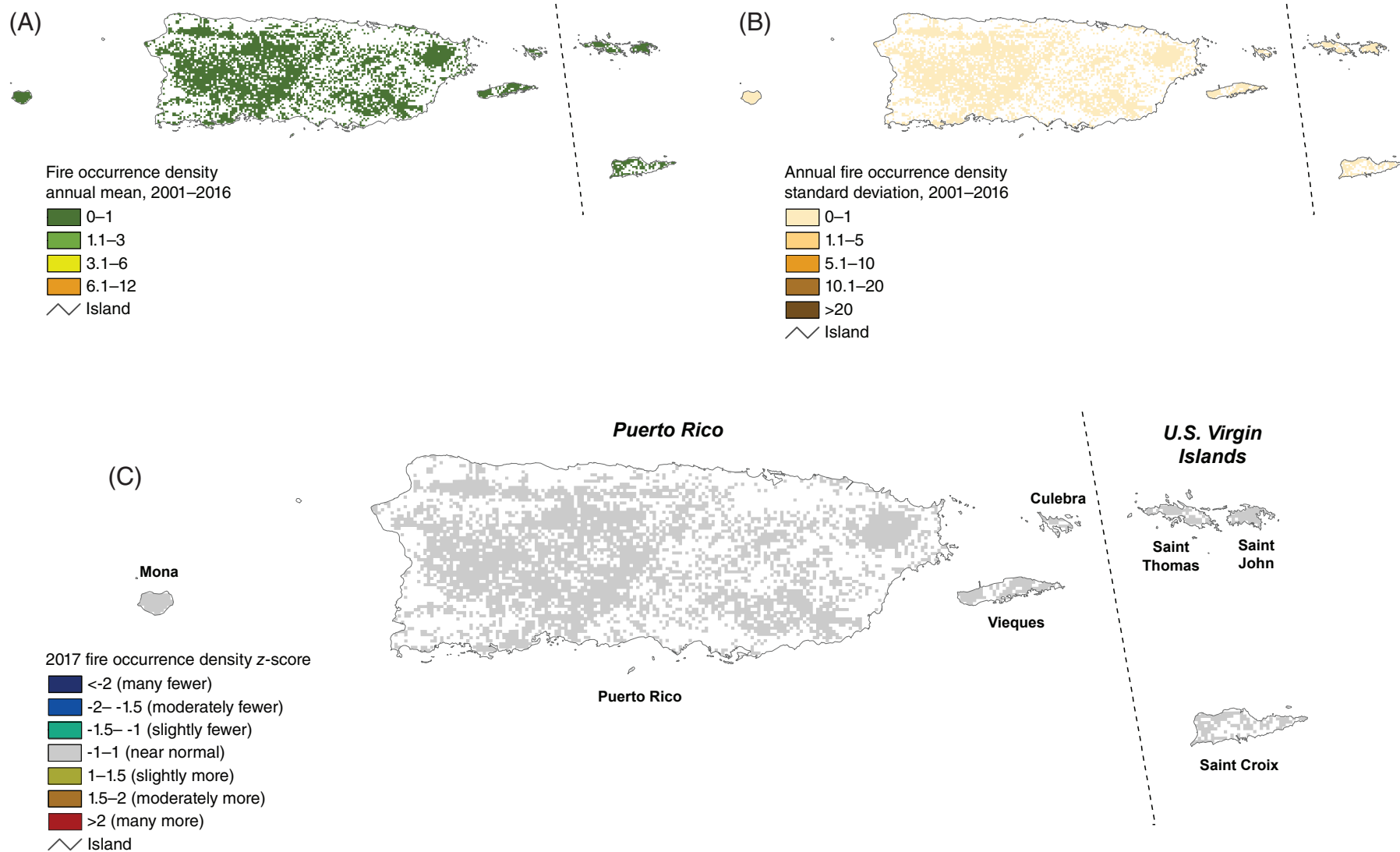


Figure 3.9—(A) Mean number and (B) standard deviation of forest fire occurrences per 100 km² (10 000 ha) of forested area from 2001 through 2016, by island in Puerto Rico and the U.S. Virgin Islands. (C) Degree of 2017 fire occurrence density excess or deficiency by ecoregion relative to 2001–2016 and accounting for variation over that time period. Forest cover is from the Forest Service International Institute of Tropical Forestry (IITF), derived from a cloud-free Landsat image mosaic developed in cooperation with Forest Service Remote Sensing Applications Center (Kennaway and Helmer 2007, Kennaway and others 2008).

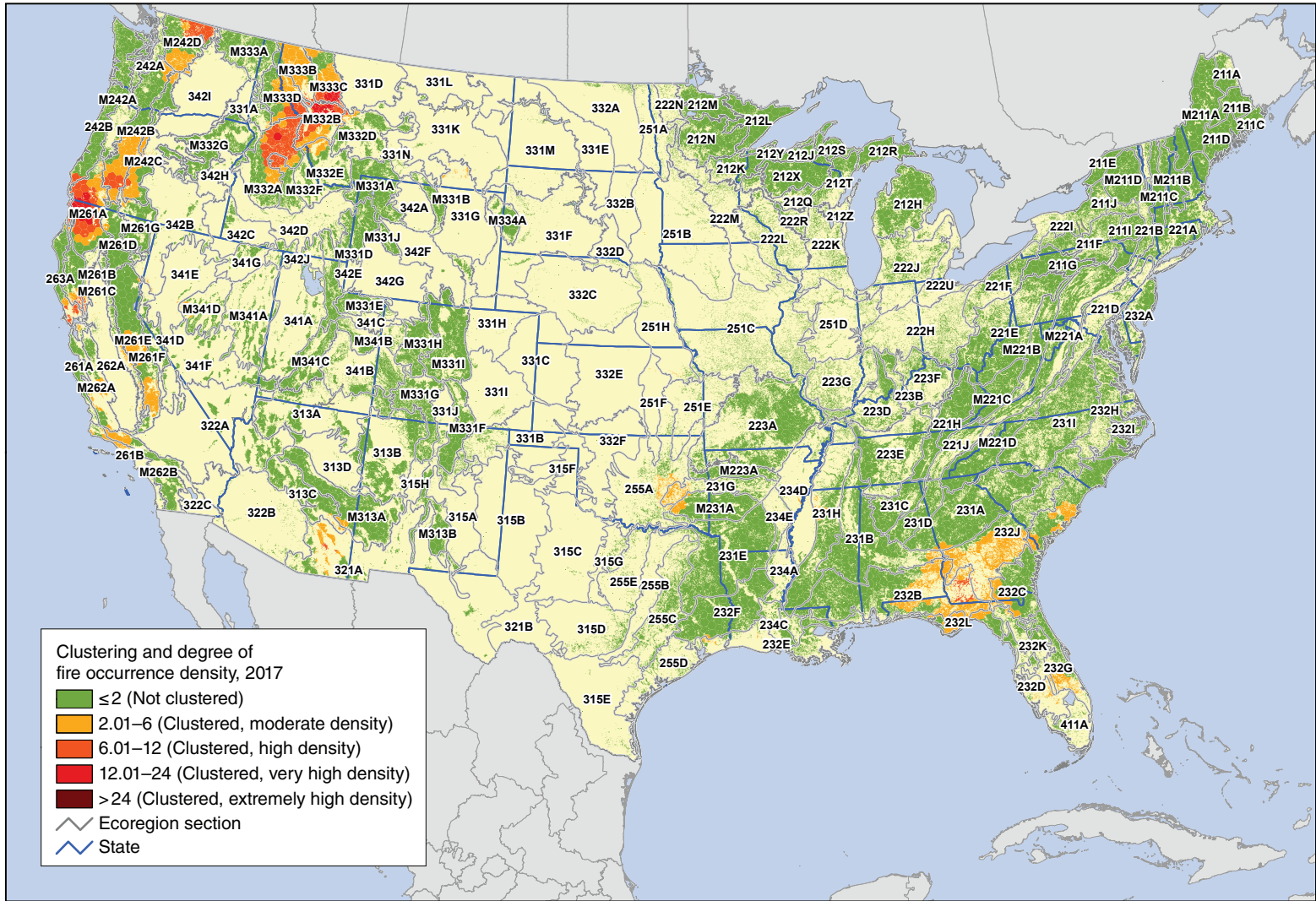


Figure 3.10—Hot spots of fire occurrence across the conterminous United States for 2017. Values are Getis-Ord G_i^* scores, with values >2 representing significant clustering of high fire occurrence densities. (No areas of significant clustering of lower fire occurrence densities, <-2 , were detected.) The gray lines delineate ecoregion sections (Cleland and others 2007). Background forest cover is derived from MODIS imagery by the Forest Service Remote Sensing Applications Center. (Source of fire data: U.S. Department of Agriculture Forest Service, Remote Sensing Applications Center, in conjunction with the NASA MODIS Rapid Response group)

Meanwhile, four hot spots of high fire occurrence density ($G_i^* > 6$ and ≤ 12) were identified in the West, along with one in the East (fig. 3.10). One of these was in coastal California north of San Francisco Bay (in 263A–Northern California Coast, M261B–Northern California Coast Ranges, and M261C–Northern California Interior Coast Ranges), where several wildfires in October burned >99 000 ha, killing 44 and destroying 8,900 structures. It was the costliest wildfire complex in U.S. history, resulting in \$9 billion in insurance claims (Cooper 2017).

The SASH analysis also detected a geographic hot spot (G_i^*) of high fire occurrence density in north-central Washington (M242D–Northern Cascades). This is where the Diamond Creek Fire scorched 51 910 ha between July 23 and October 5, costing \$14.8 million in damages and containment. Other hot spots of similar intensity were located in southern Oregon (M242B–Western Cascades and M242C–Eastern Cascades), southeastern Arizona (321A–Basin and Range), and southwestern Georgia (232B–Gulf Coastal Plains and Flatwoods).

Hot spots of moderate fire density in 2017 ($G_i^* > 2$ and ≤ 6) were scattered elsewhere near the West Coast and in the Southeastern United States (fig. 3.10), including in the following regions:

- Southern California (261B–Southern California Coast, M262B–Southern California Mountain and Valley, and M261E–Sierra Nevada)

- Central California (two in M261E–Sierra Nevada and one in M262A–Central California Coast Ranges)
- Central Nevada (M341D–West Great Basin and Mountains)
- Central Washington (M242D–Northern Cascades, M242B–Western Cascades, and M242C–Eastern Cascades)
- Eastern Oklahoma (255A–Cross Timbers and Prairie, 231G–Arkansas Valley, and M231A–Ouachita Mountains)
- Southeastern Texas (232F–Coastal Plains and Flatwoods–Western Gulf and 232E–Louisiana Coastal Prairie and Marshes)
- Southern Florida (232D–Florida Coastal Lowlands–Gulf and 232G–Florida Coastal Lowlands–Gulf)
- Coastal Plain of South Carolina (232C–Atlantic Coastal Flatwoods)

CONCLUSIONS AND FUTURE WORK

In 2017, the number of MODIS satellite-detected forest fire occurrences recorded for the conterminous States was the fifth most in 17 full years of data collection and the most since 2014. Ecoregion sections in the Pacific Northwest, the northern Rocky Mountains, and California had the highest forest fire occurrence density per 100 km² of forested area. Geographic hot spots of high fire occurrence density were detected in these same areas, as well as in the Southeast and southern Arizona. Ecoregion sections in southern, central, and northern California; the Cascade Mountains of Oregon and Washington; and northern Idaho and northwestern Montana

experienced greater fire occurrence density than normal compared to the previous 16-year mean and accounting for variability over time. Alaska experienced low fire occurrence densities except in one northeastern ecoregion section. The Big Island of Hawai'i experienced a lower fire occurrence density than in recent years as a result of an ongoing volcanic eruption.

The results of these geographic analyses are intended to offer insights into where fire occurrences have been concentrated spatially in a given year and compared to previous years, but are not intended to quantify the severity of a given fire season. Given the limits of MODIS active fire detection using 1-km resolution data, these products also may underrepresent the number of fire occurrences in some ecosystems where small and low-intensity fires are common, and where high cloud frequency can interfere with fire detection. These products can also have commission errors. However, these high temporal fidelity products currently offer the best means for daily monitoring of forest fire occurrences.

Future work related to understanding geographic patterns of forest fire occurrences in the United States could include a comparison of the MODIS detections with those of the VIIRS sensor, an analysis of fire occurrence detections by forest cover types, an evaluation of whether the fire occurrences correspond with mapped burned areas, and an assessment of the relationships between fire occurrence and drought conditions.

Ecological and forest health impacts relating to fire and other abiotic disturbances are scale-dependent properties, which in turn are affected by management objectives (Lundquist and others 2011). Information about the concentration of fire occurrences may help pinpoint areas of concern for aiding management activities and for investigations into the ecological and socioeconomic impacts of forest fire potentially outside the range of historic frequency.

LITERATURE CITED

- Anselin, L. 1992. Spatial data analysis with GIS: an introduction to application in the social sciences. Gen. Tech. Rep. 92-10. Santa Barbara, CA: National Center for Geographic Information and Analysis. 53 p.
- Barbour, M.G.; Burk, J.H.; Pitts, W.D. [and others]. 1999. Terrestrial plant ecology. Menlo Park, CA: Addison Wesley Longman, Inc. 649 p.
- Bond, W.J.; Keeley, J.E. 2005. Fire as a global "herbivore": the ecology and evolution of flammable ecosystems. *Trends in Ecology & Evolution*. 20(7): 387–394.
- Brooks, M.L.; D'Antonio, C.M.; Richardson, D.M. [and others]. 2004. Effects of invasive alien plants on fire regimes. *BioScience*. 54(7): 677–688.
- CAL FIRE. 2018. Top 20 largest California wildfires. Jan. 12, 2018. http://www.fire.ca.gov/communications/downloads/fact_sheets/Top20_Acres.pdf. [Date accessed: May 18, 2018].
- Cleland, D.T.; Freeouf, J.A.; Keys, J.E. [and others]. 2007. Ecological subregions: sections and subsections for the conterminous United States. Gen. Tech. Rep. WO-76D. Washington, DC: U.S. Department of Agriculture Forest Service. Map; Sloan, A.M., cartographer; presentation scale 1:3,500,000; colored. Also on CD-ROM as a GIS coverage in ArcINFO format or at <http://data.fs.usda.gov/geodata/edw/datasets.php>. [Date accessed: July 20, 2015].

- Cooper, J.J. 2017. October's Wine Country fires were the costliest ever. Money. Dec. 7, 2017. <http://time.com/money/5054103/octobers-wine-country-fires-were-the-costliest-ever/>. [Date accessed: May 18, 2018].
- Coulston, J.W.; Ambrose, M.J.; Riitters, K.H.; Conkling, B.L. 2005. Forest Health Monitoring 2004 national technical report. Gen. Tech. Rep. SRS-90. Asheville, NC: U.S. Department of Agriculture Forest Service, Southern Research Station. 81 p.
- Edmonds, R.L.; Agee, J.K.; Gara, R.I. 2011. Forest health and protection. Long Grove, IL: Waveland Press, Inc. 667 p.
- ESRI. 2015. ArcMap® 10.3. Redlands, CA: Environmental Systems Research Institute.
- Getis, A.; Ord, J.K. 1992. The analysis of spatial association by use of distance statistics. *Geographical Analysis*. 24(3): 189–206.
- Gill, A.M.; Stephens, S.L.; Cary, G.J. 2013. The worldwide “wildfire” problem. *Ecological Applications*. 23(2): 438–454.
- Hawbaker, T.J.; Radeloff, V.C.; Syphard, A.D. [and others]. 2008. Detection rates of the MODIS active fire product. *Remote Sensing of Environment*. 112: 2656–2664.
- Justice, C.O.; Giglio, L.; Korontzi, S. [and others]. 2002. The MODIS fire products. *Remote Sensing of Environment*. 83(1–2): 244–262.
- Justice, C.O.; Giglio, L.; Roy, D. [and others]. 2011. MODIS-derived global fire products. In: Ramachandran, B.; Justice, C.O.; Abrams, M.J., eds. Land remote sensing and global environmental change: NASA's earth observing system and the science of ASTER and MODIS. New York: Springer: 661–679.
- Kennaway, T.A., Helmer, E.H. 2007. The forest types and ages cleared for land development in Puerto Rico. *GIScience & Remote Sensing*. 44(4): 356–382.
- Kennaway, T.A., Helmer, E.H., Lefsky, M.A. [and others]. 2008. Mapping land cover and estimating forest structure using satellite imagery and coarse resolution lidar in the Virgin Islands. *Journal of Applied Remote Sensing*. 2(1): 023551. DOI: 10.1117/1.3063939.
- Laffan, S.W. 2006. Assessing regional scale weed distributions, with an Australian example using *Nassella trichotoma*. *Weed Research*. 46(3): 194–206.
- LANDFIRE. 2014. Existing vegetation type layer, LANDFIRE 1.4.0. U.S. Department of the Interior, Geological Survey. <https://www.landfire.gov/evt.php>. [Date accessed: May 2, 2014].
- Lundquist, J.E.; Camp, A.E.; Tyrrell, M.L. [and others]. 2011. Earth, wind and fire: abiotic factors and the impacts of global environmental change on forest health. In: Castello, J.D.; Teale, S.A., eds. Forest health: an integrated perspective. New York: Cambridge University Press: 195–243.
- McKenzie, D.; Peterson, D.L.; Alvarado, E. 1996. Predicting the effect of fire on large-scale vegetation patterns in North America. Res. Pap. PNW-489. Portland, OR: U.S. Department of Agriculture Forest Service, Pacific Northwest Research Station. 38 p.
- National Interagency Coordination Center. 2017. Wildland fire summary and statistics annual report: 2016. http://www.predictiveservices.nifc.gov/intelligence/2016_Statsumm/intro_summary16.pdf. [Date accessed: May 30, 2017].
- National Interagency Coordination Center. 2018. Wildland fire summary and statistics annual report: 2017. https://www.predictiveservices.nifc.gov/intelligence/2017_statsumm/intro_summary17.pdf. [Date accessed: April 30, 2018].
- Nowacki, G.J.; Abrams, M.D. 2008. The demise of fire and “mesophication” of forests in the Eastern United States. *BioScience*. 58(2): 123–138.
- Nowacki, G.; Brock, T. 1995. Ecoregions and subregions of Alaska [EcoMap]. Version 2.0. Juneau, AK: U.S. Department of Agriculture Forest Service, Alaska Region. Map; presentation scale 1:5,000,000; colored.
- Potter, K.M. 2012a. Large-scale patterns of forest fire occurrence in the conterminous United States and Alaska, 2005–07. In: Potter, K.M.; Conkling, B.L., eds. Forest Health Monitoring 2008 national technical report. Gen. Tech. Rep. SRS-158. Asheville, NC: U.S. Department of Agriculture Forest Service, Southern Research Station: 73–83.

- Potter, K.M. 2012b. Large-scale patterns of forest fire occurrence in the conterminous United States and Alaska, 2001–08. In: Potter, K.M.; Conkling, B.L., eds. Forest Health Monitoring 2009 national technical report. Gen. Tech. Rep. SRS-167. Asheville, NC: U.S. Department of Agriculture Forest Service, Southern Research Station: 151–161.
- Potter, K.M. 2013a. Large-scale patterns of forest fire occurrence in the conterminous United States and Alaska, 2009. In: Potter, K.M.; Conkling, B.L., eds. Forest Health Monitoring: national status, trends and analysis, 2010. Gen. Tech. Rep. SRS-176. Asheville, NC: U.S. Department of Agriculture Forest Service, Southern Research Station: 31–39.
- Potter, K.M. 2013b. Large-scale patterns of forest fire occurrence in the conterminous United States and Alaska, 2010. In: Potter, K.M.; Conkling, B.L., eds. Forest Health Monitoring: national status, trends and analysis, 2011. Gen. Tech. Rep. SRS-185. Asheville, NC: U.S. Department of Agriculture Forest Service, Southern Research Station: 29–40.
- Potter, K.M. 2014. Large-scale patterns of forest fire occurrence in the conterminous United States and Alaska, 2011. In: Potter, K.M.; Conkling, B.L., eds. Forest Health Monitoring: national status, trends and analysis, 2012. Gen. Tech. Rep. SRS-198. Asheville, NC: U.S. Department of Agriculture Forest Service, Southern Research Station: 35–48.
- Potter, K.M. 2015a. Large-scale patterns of forest fire occurrence in the conterminous United States and Alaska, 2012. In: Potter, K.M.; Conkling, B.L., eds. Forest Health Monitoring: national status, trends, and analysis 2013. Gen. Tech. Rep. SRS-207. Asheville, NC: U.S. Department of Agriculture Forest Service, Southern Research Station: 37–53.
- Potter, K.M. 2015b. Large-scale patterns of forest fire occurrence in the conterminous United States and Alaska, 2013. In: Potter, K.M.; Conkling, B.L., eds. Forest Health Monitoring: national status, trends, and analysis 2014. Gen. Tech. Rep. SRS-209. Asheville, NC: U.S. Department of Agriculture Forest Service, Southern Research Station: 39–55.
- Potter, K.M. 2016. Large-scale patterns of forest fire occurrence in the conterminous United States, Alaska, and Hawaii, 2014. In: Potter, K.M.; Conkling, B.L., eds. Forest Health Monitoring: national status, trends, and analysis 2015. Gen. Tech. Rep. SRS-213. Asheville, NC: U.S. Department of Agriculture Forest Service, Southern Research Station: 41–60.
- Potter, K.M. 2017. Large-scale patterns of forest fire occurrence in the conterminous United States, Alaska, and Hawaii, 2015. In: Potter, K.M.; Conkling, B.L., eds. Forest Health Monitoring: national status, trends, and analysis 2016. Gen. Tech. Rep. SRS-222. Asheville, NC: U.S. Department of Agriculture Forest Service, Southern Research Station: 43–62.
- Potter, K.M. 2018. Large-scale patterns of forest fire occurrence in the conterminous United States, Alaska, and Hawaii, 2016. In: Potter, K.M.; Conkling, B.L., eds. Forest Health Monitoring: national status, trends, and analysis 2017. Gen. Tech. Rep. SRS-233. Asheville, NC: U.S. Department of Agriculture Forest Service, Southern Research Station: 45–64.
- Potter, K.M.; Koch, F.H.; Oswalt, C.M.; Iannone, B.V. 2016. Data, data everywhere: detecting spatial patterns in fine-scale ecological information collected across a continent. *Landscape Ecology*. 31: 67–84.
- Pyne, S.J. 2010. *America's fires: a historical context for policy and practice*. Durham, NC: Forest History Society. 91 p.
- Reams, G.A.; Smith, W.D.; Hansen, M.H. [and others]. 2005. The Forest Inventory and Analysis sampling frame. In: Bechtold, W.A.; Patterson, P.L., eds. *The enhanced Forest Inventory and Analysis program—national sampling design and estimation procedures*. Asheville, NC: U.S. Department of Agriculture Forest Service, Southern Research Station: 11–26.
- Richardson, L.A.; Champ, P.A.; Loomis, J.B. 2012. The hidden cost of wildfires: economic valuation of health effects of wildfire smoke exposure in southern California. *Journal of Forest Economics*. 18(1): 14–35.
- Schmidt, K.M.; Menakis, J.P.; Hardy, C.C. [and others]. 2002. Development of coarse-scale spatial data for wildland fire and fuel management. Gen. Tech. Rep. RMRS-87. Fort Collins, CO: U.S. Department of Agriculture Forest Service, Rocky Mountain Research Station. 41 p.

- Shima, T.; Sugimoto S.; Okutomi, M. 2010. Comparison of image alignment on hexagonal and square lattices. 2010 IEEE International Conference on Image Processing: 141–144. DOI: 10.1109/icip.2010.5654351.
- Tonini, M.; Tuia, D.; Ratle, F. 2009. Detection of clusters using space-time scan statistics. *International Journal of Wildland Fire*. 18(7): 830–836.
- U.S. Department of Agriculture (USDA) Forest Service. 2008. National forest type data development. http://svinetfc4.fs.fed.us/rastergateway/forest_type/. [Date accessed: May 13, 2008].
- U.S. Department of Agriculture (USDA) Forest Service. 2018. MODIS active fire mapping program: fire detection GIS data. <https://fsapps.nwgc.gov/afm/gisdata.php>. [Date accessed: January 12, 2018].
- Vinton, J.V., ed. 2004. *Wildfires: issues and consequences*. Hauppauge, NY: Nova Science Publishers, Inc. 127 p.
- White, D.; Kimerling, A.J.; Overton, W.S. 1992. Cartographic and geometric components of a global sampling design for environmental monitoring. *Cartography and Geographic Information Systems*. 19(1): 5–22.

INTRODUCTION

Although droughts affect most U.S. forests, there is considerable variation between regions in terms of drought frequency and intensity (Hanson and Weltzin 2000). These differences characterize the regions' prevailing drought regimes. Most forests in the Western United States are subject to annual seasonal droughts. In contrast, forests in the Eastern United States usually experience one of two general drought patterns: random (i.e., occurring at any time of year) occasional droughts, as observed in the Appalachian Mountains and the Northeast, or frequent late-summer droughts, as usually observed in the Southeastern Coastal Plain and the eastern portion of the Great Plains (Hanson and Weltzin 2000).

In forests, moisture scarcity during droughts can result in significant tree stress, particularly when that scarcity is accompanied by high temperatures (L.D.L. Anderegg and others 2013, Peters and others 2015, Williams and others 2013). Trees and other plants respond to this stress by decreasing fundamental growth processes (e.g., cell division and enlargement). Because photosynthesis is less sensitive than these fundamental processes, it decreases slowly at low levels of drought stress, but decreases more quickly as drought stress increases in severity (Kareiva and others 1993, Mattson and Haack 1987). Besides these direct effects, drought stress often makes trees vulnerable to attack by damaging insects and diseases (Clinton and others 1993, Kolb and others 2016, Mattson and Haack 1987, Raffa and others 2008).

Droughts also exacerbate wildland fire risk by limiting breakdown of organic matter and reducing the moisture content of downed woody debris and other potential fire fuels (Clark 1989, Keetch and Byram 1968, Schoennagel and others 2004, Trouet and others 2010).

Generally, forest systems are resistant to short-term droughts, although individual tree species differ in their ability to tolerate drought conditions (Archaux and Wolters 2006, Berdanier and Clark 2016). Because of this resistance, drought duration may be more important for forests than intensity (Archaux and Wolters 2006). For example, forests that experience multiple consecutive years of drought (2–5 years) are much more likely to exhibit high tree mortality than forests that experience a single year of extreme drought (Guarín and Taylor 2005, Millar and others 2007). Therefore, a thorough evaluation of drought impact in forests should include analysis of moisture conditions over multiyear time windows.

In the 2010 Forest Health Monitoring (FHM) National Technical Report, we described a method for mapping drought conditions across the conterminous United States (Koch and others 2013b). Our objective was to generate fine-scale, drought-related spatial datasets that improve upon similar products available from sources such as the National Climatic Data Center (e.g., Vose and others 2014) or the U.S. Drought Monitor program (Svoboda and others 2002). The principal inputs are gridded climate data (i.e., monthly raster maps of precipitation

CHAPTER 4. Drought and Moisture Surplus Patterns in the Conterminous United States: 2017, 2015–2017, and 2013–2017

FRANK H. KOCH

JOHN W. COULSTON

and temperature over a 100-year period) created with the Parameter-elevation Regression on Independent Slopes (PRISM) climate mapping system (Daly and others 2002). The method utilizes a standardized indexing approach that facilitates comparison of a given location's moisture status during different time windows, regardless of their length. The index is easier to calculate than the commonly used Palmer Drought Severity Index, or PDSI (Palmer 1965), and avoids some criticisms of the PDSI (see Alley 1984) regarding its underlying assumptions and limited comparability across space and time. Here, we applied the method outlined in the 2010 FHM Report to the most currently available climate data (i.e., the monthly PRISM data through 2017), thereby providing the ninth installment in an ongoing series of annual drought assessments for the conterminous United States from 2009 forward (Koch and Coulston 2015, 2016, 2017, 2018; Koch and others 2013a, 2013b, 2014, 2015).

This is the fourth year in which we also mapped levels of moisture surplus across the conterminous United States during multiple time windows. While recent refereed literature (e.g., Adams and others 2009, Allen and others 2010, Martínez-Vilalta and others 2012, Peng and others 2011, Williams and others 2013) has focused more often on reports of regional-scale forest decline and mortality due to persistent drought conditions, especially in combination with periods of extremely high temperatures (i.e., heat waves), surplus moisture availability can also be detrimental to forests. Abnormally

high moisture can be a short-term stressor (e.g., an extreme rainfall event with subsequent flooding) or a long-term stressor (e.g., persistent wetness driven by a macroscale climatic pattern such as the El Niño-Southern Oscillation), either of which may lead to tree dieback and mortality (Rozas and García-González 2012, Rozas and Sampedro 2013). Such impacts have been observed in both tropical and temperate forests (Hubbart and others 2016, Laurance and others 2009, Rozas and García-González 2012). While surplus-induced impacts in forests may not be as common as drought-induced impacts, a single index that depicts both moisture surplus and deficit conditions provides a fuller accounting of potential forest health issues.

METHODS

We acquired grids for monthly precipitation and monthly mean temperature for the conterminous United States from the PRISM Climate Group Web site (PRISM Climate Group 2018). At the time of these analyses, gridded datasets were available for all years from 1895 to 2017. However, the grids for December 2017 were only provisional versions (i.e., finalized grids had not yet been released). For analytical purposes, we treated these provisional grids as if they were the final versions. The spatial resolution of the grids was approximately 4 km (cell area = 16 km²). For future applications and to ensure better compatibility with other spatial datasets, all output grids were resampled to a spatial resolution of approximately 2 km (cell area = 4 km²) using a nearest neighbor

approach. The nearest neighbor approach is a computationally simple resampling method that avoids the smoothing of data values observed with methods such as bilinear interpolation or cubic convolution.

Potential Evapotranspiration (PET) Maps

As in our previous drought mapping efforts (Koch and Coulston 2015, 2016, 2017, 2018; Koch and others 2012a, 2012b, 2013a, 2013b, 2014, 2015), we adopted an approach in which a moisture index value is calculated for each location of interest (i.e., each grid cell in a map of the conterminous United States) during a given time period. Moisture indices are intended to reflect the amount of available water in a location (e.g., to support plant growth). In our case, the index is computed using an approach that considers both the amount of precipitation that falls on a location during the period of interest as well as the level of potential evapotranspiration during this period. Potential evapotranspiration measures the loss of soil moisture through plant uptake and transpiration (Akin 1991). It does not measure actual moisture loss, but rather the loss that would occur if there was no possible shortage of moisture for plants to transpire (Akin 1991, Thornthwaite 1948). In simple terms, potential evapotranspiration serves as a measure of moisture demand. By including potential evapotranspiration along with precipitation, our index thus documents the long-term balance between moisture demand and supply for each location of interest.

To complement the available PRISM monthly precipitation grids, we computed corresponding monthly potential evapotranspiration (*PET*) grids using Thornthwaite's formula (Akin 1991, Thornthwaite 1948):

$$PET_m = 1.6L_{lm}\left(10\frac{T_m}{I}\right)^a \quad (1)$$

where

PET_m = the potential evapotranspiration for a given month m in cm

L_{lm} = a correction factor for the mean possible duration of sunlight during month m for all locations (i.e., grid cells) at a particular latitude l [see Table V in Thornthwaite (1948) for a list of L correction factors by month and latitude]

T_m = the mean temperature for month m in degrees C

I = an annual heat index, calculated as

$$I = \sum_{m=1}^{12} \left(\frac{T_m}{5}\right)^{1.514}$$

where

T_m is the mean temperature for each month m of the year

a = an exponent calculated as $a = 6.75 \times 10^{-7}I^3 - 7.71 \times 10^{-5}I^2 + 1.792 \times 10^{-2}I + 0.49239$ [see Appendix I in Thornthwaite (1948) regarding calculation of I and the empirical derivation of a]

Although only a simple approximation, a key advantage of Thornthwaite's formula is that it has modest input data requirements (i.e., mean temperature values) compared to more sophisticated methods of estimating PET such as the Penman-Monteith equation (Monteith 1965), which requires less readily available data on factors such as humidity, radiation, and wind speed. To implement equation (1) spatially, we created a grid of latitude values for determining the L adjustment for any given grid cell (and any given month) in the conterminous United States. We extracted the T_m values for the grid cells from the corresponding PRISM mean monthly temperature grids.

Moisture Index Maps

To estimate baseline conditions, we used the precipitation (P) and PET grids to generate moisture index grids for the past 100 years (i.e., 1918–2017) for the conterminous United States. We used a moisture index described by Willmott and Feddema (1992), which has been applied in a variety of contexts, including global vegetation modeling (Potter and Klooster 1999) and climate change analysis (Grundstein 2009). Willmott and Feddema (1992) devised the index as a refinement of one described earlier

by Thornthwaite (1948) and Thornthwaite and Mather (1955). Their revised index, MI' , has the following form:

$$MI' = \begin{cases} P/PET - 1 & , P < PET \\ 1 - PET/P & , P \geq PET \\ 0 & , P = PET = 0 \end{cases} \quad (2)$$

where

P = precipitation

PET = potential evapotranspiration, as calculated using equation (1)

(P and PET must be in equivalent measurement units, e.g., mm)

This set of equations yields a symmetric, dimensionless index scaled between -1 and 1. A primary advantage of this symmetry is that it enables valid comparisons between any set of locations in terms of their moisture balance (i.e., the balance between moisture demand and supply). MI' can be calculated for any time period, but is commonly calculated on an annual basis using P and PET values summed across the entire year (Willmott and Feddema 1992). An alternative to this summation approach is to

calculate MI' on a monthly basis (i.e., from total measured precipitation and estimated potential evapotranspiration in each month), and then, for a given time window of interest, calculate its moisture index as the mean of the MI' values for all months in the time window. This “mean-of-months” approach limits the ability of short-term peaks in either precipitation or potential evapotranspiration to negate corresponding short-term deficits, as would happen under a summation approach.

For each year in our study period (i.e., 1918–2017), we used the mean-of-months approach to calculate moisture index grids for three different time windows: 1 year (MI_1'), 3 years (MI_3'), and 5 years (MI_5'). Briefly, the MI_1' grids are the mean (i.e., the mean value for each grid cell) of the 12 monthly MI' grids for each year in the study period, the MI_3' grids are the mean of the 36 monthly grids from January of 2 years prior through December of the target year, and the MI_5' grids are the mean of the 60 consecutive monthly MI' grids from January of 4 years prior to December of the target year. Thus, the MI_1' grid for the year 2017 is the mean of the monthly MI' grids from January to December 2017, while the MI_3' grid is the mean of the grids from January 2015 to December 2017, and the MI_5' grid is the mean of the grids from January 2013 to December 2017.

Annual and Multiyear Drought Maps

To determine degree of departure from typical moisture conditions, we first created a normal grid, $MI_{i\ norm}'$, for each of our three time windows, representing the mean (i.e., the mean value for each grid cell) of the 100 corresponding moisture index grids (i.e., the MI_1' , MI_3' , or MI_5' grids, depending on the window; see fig. 4.1). We also created a standard deviation grid, $MI_{i\ SD}'$, for each time window, calculated from the window’s 100 individual moisture index grids as well as its $MI_{i\ norm}'$ grid. We subsequently calculated moisture difference z-scores, MDZ_{ij} , for each time window using these derived datasets:

$$MDZ_{ij} = \frac{MI_i' - MI_{i\ norm}'}{MI_{i\ SD}'} \quad (3)$$

where

i = the analytical time window (i.e., 1, 3, or 5 years)

j = a particular target year in our 100-year study period (i.e., 1918–2017)

MDZ scores may be classified in terms of degree of moisture deficit or surplus (table 4.1). The classification scheme includes categories (e.g., severe drought, extreme drought) like

Table 4.1—Moisture difference z-score (*MDZ*) value ranges for nine wetness and drought categories, along with each category’s approximate theoretical frequency of occurrence

Score	Category	Frequency
$MDZ \leq -2$	Extreme drought	2.3%
$-2 < MDZ \leq -1.5$	Severe drought	4.4%
$-1.5 < MDZ \leq -1$	Moderate drought	9.2%
$-1 < MDZ \leq -0.5$	Mild drought	15%
$-0.5 < MDZ \leq 0.5$	Near normal conditions	38.2%
$0.5 < MDZ \leq 1$	Mild moisture surplus	15%
$1 < MDZ \leq 1.5$	Moderate moisture surplus	9.2%
$1.5 < MDZ \leq 2$	Severe moisture surplus	4.4%
$MDZ > 2$	Extreme moisture surplus	2.3%

those associated with the PDSI. The scheme has also been adopted for other drought indices such as the Standardized Precipitation Index, or SPI (McKee and others 1993). Moreover, the breakpoints between *MDZ* categories resemble those used for the SPI, such that we expect the *MDZ* categories to have theoretical frequencies of occurrence that are similar to their SPI counterparts (e.g., approximately 2.3 percent of the time for extreme drought; see McKee and others 1993, Steinemann 2003). More importantly, because of the standardization in equation (3), the breakpoints between categories remain the same regardless of the size of the time window of interest. For comparative analysis, we generated and classified *MDZ* maps of the conterminous United States, based on all three time windows, for the target year 2017.

RESULTS AND DISCUSSION

The 100-year (1918–2017) mean annual moisture index, or $MI'_{1\text{norm}}$ grid (fig. 4.1) provides an overview of moisture regimes in the conterminous United States. (The 100-year $MI'_{3\text{norm}}$ and $MI'_{5\text{norm}}$ grids were similar to the mean $MI'_{1\text{norm}}$ grid, and so are not shown here.) Wet climates ($MI' > 0$) are typical in the Eastern United States, especially the Northeast. An interesting anomaly is southern Florida, primarily ecoregion sections (Cleland and others 2007) 232D–Florida Coastal Lowlands-Gulf, 232G–Florida Coastal Lowlands-Atlantic, and 411A–Everglades. This region appears to be dry relative to other parts of the East, which is an effect of its tropical climate, which has distinct wet (primarily summer months) and dry (late fall to early spring) seasons. Although southern Florida usually receives a high level of precipitation during the wet season, it can be insufficient to offset the region’s lengthy dry season (Duever and others 1994) or its high level of temperature-driven evapotranspiration, especially during the late spring and summer months, resulting in negative MI' values.

The climatic regime of southern Florida contrasts markedly with the pattern observed in the driest parts of the Western United States, particularly the Southwest (e.g., sections 322A–Mojave Desert, 322B–Sonoran Desert, and 322C–Colorado Desert), where potential evapotranspiration is very high, but precipitation levels are typically very low. In fact, because

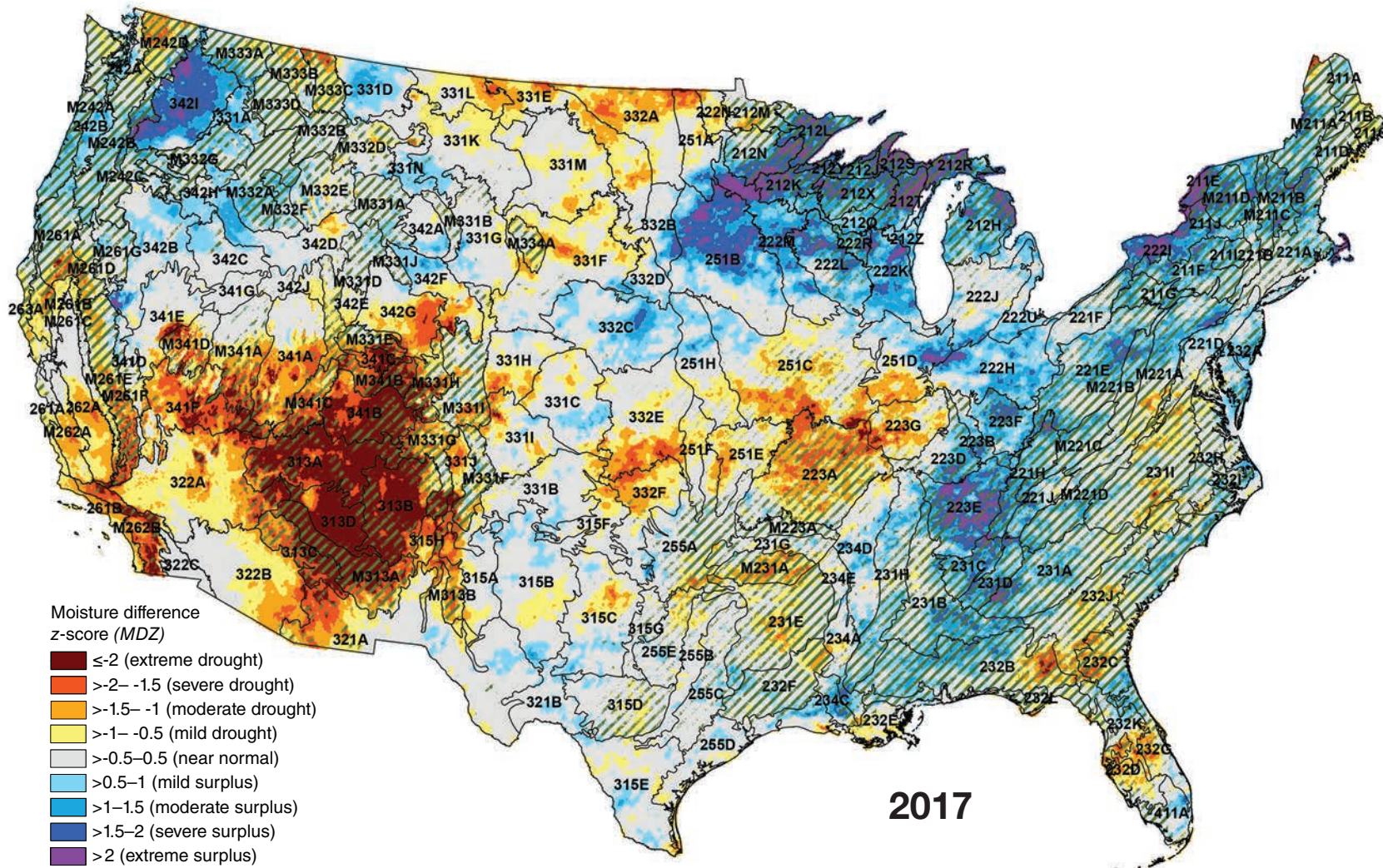
of generally lower precipitation than the East, dry climates ($MI' < 0$) are typical across much of the Western United States. Nevertheless, mountainous areas in the central and northern Rocky Mountains as well as the Pacific Northwest are relatively wet, such as ecoregion sections M242A–Oregon and Washington Coast Ranges, M242B–Western Cascades, M331G–South Central Highlands, and M333C–Northern Rockies. This is driven in part by large amounts of winter snowfall in these regions (Hanson and Weltzin 2000).

Figure 4.2 shows the annual (i.e., 1-year) *MDZ* map for 2017 for the conterminous United States. Although there are areas of mild to extreme drought ($MDZ \leq -0.5$) scattered across the country, the most distinctive feature of the map is a large contiguous zone of extreme drought ($MDZ \leq -2$) in the Southwestern United States. Encompassing virtually the entire “Four Corners” region (southeastern Utah, southwestern Colorado, northwestern New Mexico, and northeastern Arizona), this contiguous zone extended into at least 18 ecoregion sections, including most of 313A–Grand Canyon, 313B–Navajo Canyonlands, 313D–Painted Desert, and M313A–White Mountains-San Francisco Peaks-Mogollon Rim. Although only M313A is predominately forested, all forested areas in 313A, 313B, and 313D experienced extreme drought conditions in 2017, as was similarly the case in 341B–Northern Canyonlands. Other forested ecoregion sections that fell partly in this contiguous zone include 313C–Tonto Transition and M341B–

Tavaputs Plateau. To the south and west of the zone, extreme drought also occurred in the few isolated areas of forest within 321A–Basin and Range, 322A–Mojave Desert, and 341F–Southeastern Great Basin.

Severe to extreme drought conditions ($MDZ \leq -1.5$) affected forests in two ecoregion sections in southern California in 2017: almost all of M262B–Southern California Mountain and Valley as well as the southern portion of M261E–Sierra Nevada. Additionally, a few sizeable contiguous areas of mild to extreme drought occurred in the Midwestern United States. One of these areas affected sections 223G–Central Till Plains-Oak Hickory, 251C–Central Dissected Till Plains, 251D–Central Till Plains and Grand Prairies, as well as the heavily forested 223A–Ozark Highlands. A similar drought area to the west of this fell mostly in sections 332E–South Central Great Plains and 332F–South Central and Red Bed Plains, neither of which contains much forest. A third area along the Canadian border affected portions of 251A–Red River Valley, 331E–Northeastern Glaciated Plains, 331K–North Central Highlands, 331L–Glaciated Northern Highlands, 331M–Missouri Plateau, and 332A (also Northeastern Glaciated Plains); these ecoregion sections contain almost no forest cover.

The 1-year *MDZ* map for 2017 (fig. 4.2) is dramatically different from the 1-year map for 2016 (fig. 4.3). Many of the drought-affected areas that were prominent in the 2016 map saw improved moisture conditions during 2017. Perhaps most notably, the large area of



2017

Figure 4.2—The 2017 annual (i.e., 1-year) moisture difference z-score, or MDZ, for the conterminous United States. Ecoregion section (Cleland and others 2007) boundaries and labels are included for reference. Forest cover data (overlaid green hatching) derived from MODIS imagery by the Forest Service Remote Sensing Applications Center. (Data source: PRISM Climate Group, Oregon State University)

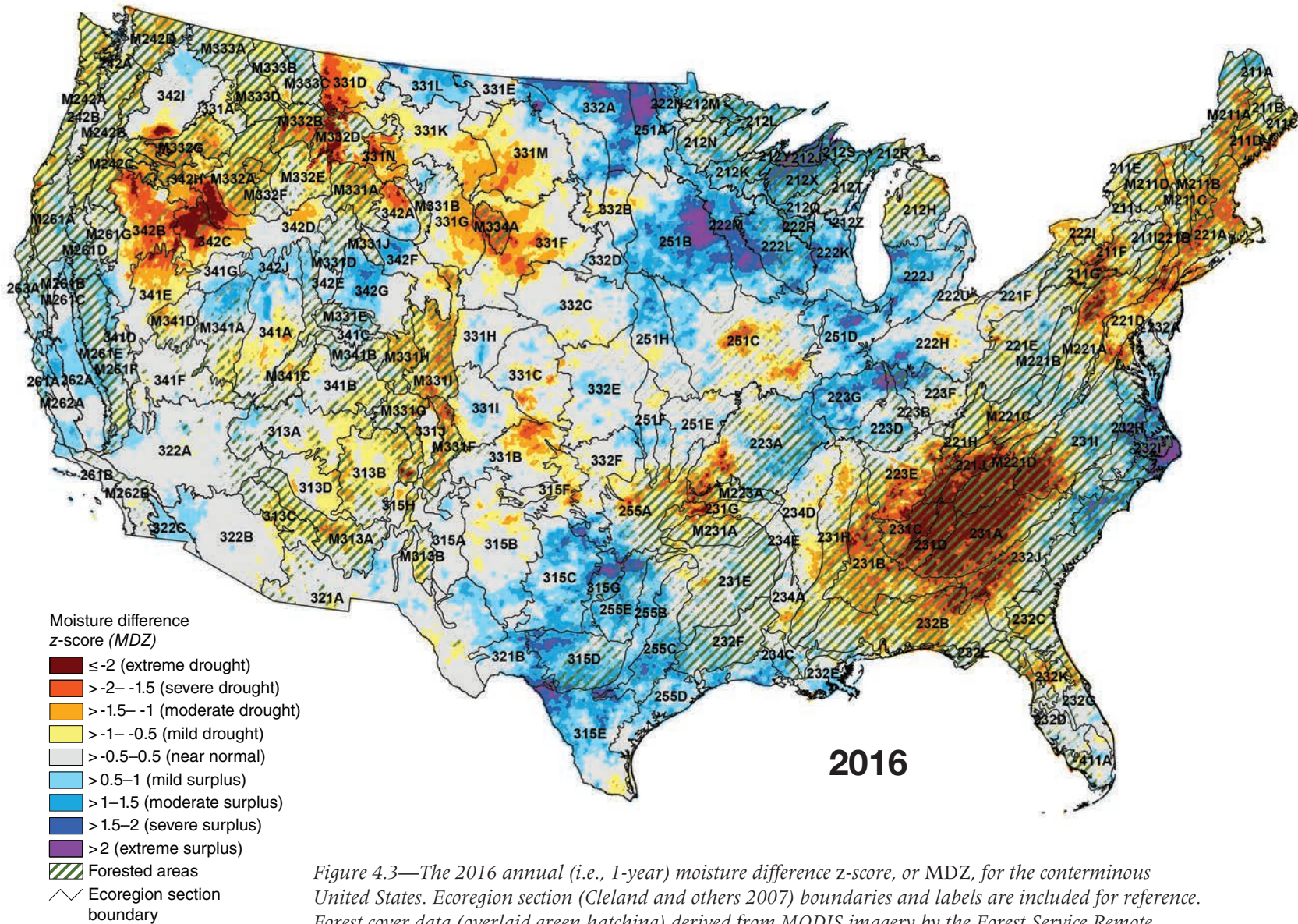


Figure 4.3—The 2016 annual (i.e., 1-year) moisture difference z-score, or MDZ, for the conterminous United States. Ecoregion section (Cleland and others 2007) boundaries and labels are included for reference. Forest cover data (overlaid green hatching) derived from MODIS imagery by the Forest Service Remote Sensing Applications Center. (Data source: PRISM Climate Group, Oregon State University)

severe to extreme drought that covered much of the Southeastern United States in 2016 (including forested sections 221H–Northern Cumberland Plateau, 221J–Central Ridge and Valley, 231A–Southern Appalachian Piedmont, 231C–Southern Cumberland Plateau, and 231D–Southern Ridge and Valley, as well as southern portions of M221D–Blue Ridge Mountains and 231I–Central Appalachian Piedmont) shifted to near normal or surplus conditions in 2017. Likewise, an area of mostly moderate to extreme drought that extended north from the Mid-Atlantic region into New England during 2016 contracted significantly in 2017, with drought conditions persisting only in portions of 211B–Maine-New Brunswick Foothills and Lowlands, 211C–Fundy Coastal and Interior, 211D–Central Maine Coastal and Embayment, and M211A–White Mountains. Unfortunately, most forested areas in California, which experienced near normal to surplus conditions in 2016 after several years of historically exceptional drought, saw drought conditions return in 2017, including the aforementioned severe to extreme drought in sections M262B–Southern California Mountain and Valley and M261E–Sierra Nevada. This return could magnify an already dramatic forest health impact: since 2010, an estimated 129 million trees have died in California due to direct or indirect drought effects (USDA Forest Service Region 5 Forest Health Monitoring program 2018).

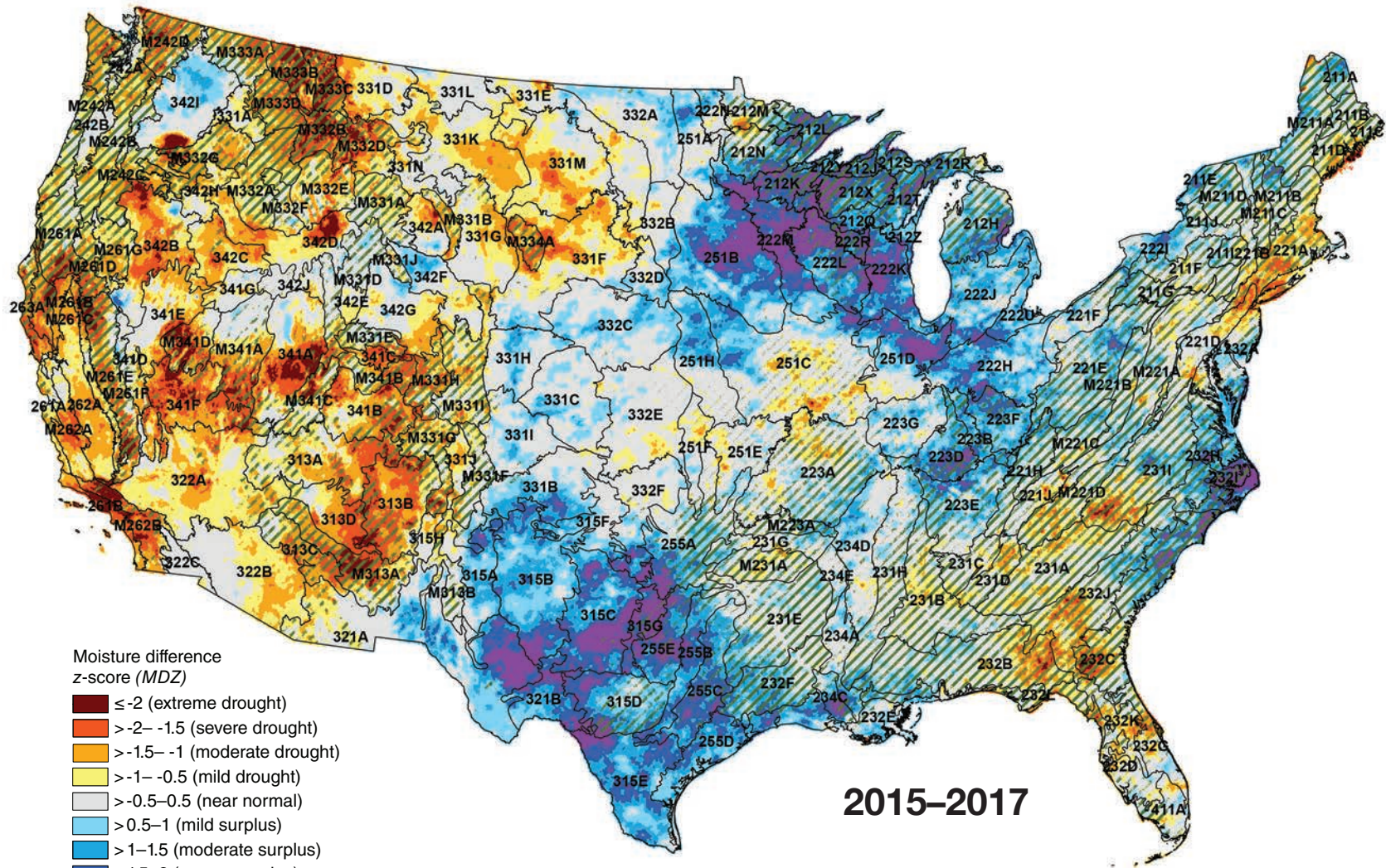
The zone of extreme drought in the Four Corners region in 2017 represented an intensification and geographic expansion of mostly mild drought conditions that were present in 2016. As noted earlier (see fig. 4.1), high temperatures and low precipitation levels are regular features of the climatic regime of the Southwestern United States, so droughts of varying duration and intensity are common throughout the region. In recent years, however, temperatures in the Southwest have trended toward new highs compared to the historical record (i.e., since measurements began in 1895). For example, in Arizona and New Mexico, average temperatures in 2017 and in the corresponding 3-year (2015–2017) and 5-year (2013–2017) time periods were the warmest on record. In Colorado and Utah, 2017 was the third warmest year on record, while 2015–2017 and 2013–2017 were the warmest 3- and 5-year periods to date (National Climatic Data Center 2018b). Notably, none of these States received especially low levels of precipitation during these periods, other than a somewhat anomalous shortage of rainfall in late 2017 (National Climatic Data Center 2018a). Regardless, because climatological data and climate change projections suggest a continued warming trend globally—in terms of both average and extreme temperatures (Gil-Alana 2018, Rahmstorf and others 2017)—it is highly possible, if not likely, that drought impacts will worsen in the Southwest.

The 3-year (2015–2017; fig. 4.4) and 5-year (2013–2017; fig. 4.5) *MDZ* maps reveal other emerging drought patterns in the United States that may be linked to this warming trend. For instance, while droughts have been a persistent concern throughout much of the Western United States for the last several decades (Groisman and Knight 2008, Mueller and others 2005, Woodhouse and others 2010), it is only in the past few years that moderate to extreme drought conditions have been widespread in the Pacific Northwest, as shown in figures 4.4 and 4.5 (in particular, sections M332B–Northern Rockies and Bitterroot Valley, M333B–Flathead Valley, M333C–Northern Rockies, and M333D–Bitterroot Mountains). These conditions did not arise because of a lack of precipitation, but because warm temperatures disrupted the region’s usual water balance; for example, winter precipitation fell as rain rather than snow, substantially reducing snowpack (Marlier and others 2017). Indeed, 2013–2017 was tied with 2012–2016 as the warmest 5-year period on record for the Pacific Northwest in terms of average temperatures (National Climatic Data Center 2018a).

Similarly, but on a smaller scale, the 3-year and 5-year *MDZ* maps show the persistence of drought conditions on New York’s Long Island and in other portions of section 221A–Lower New England. Recently, this area has seen unprecedented outbreaks of the southern pine beetle (*Dendroctonus frontalis*), a native insect that has been associated historically with pine forests of the Southeastern United States.

Although drought stress may be a weaker inciting factor for southern pine beetle activity than it is for other bark beetles (Kolb and others 2016), the emergence of the pest in an apparently novel environment has been linked to warming temperatures (Lesk and others 2017) that intensified drought conditions in the region (Sweet and others 2017). Furthermore, climate change projections suggest the beetle will expand farther into the Northeastern United States in the next few decades (Lesk and others 2017).

Broadly, the 3- and 5-year *MDZ* maps show differences between the Eastern and Western United States that are consistent with their disparate moisture regimes. As illustrated by the 3-year *MDZ* map (fig. 4.4), few forested areas west of the Great Plains experienced near normal or surplus moisture conditions during 2015–2017; indeed, only a handful of ecoregion sections could be characterized as mostly—but not completely—drought-free (e.g., M331D–Overthrust Mountains). By comparison, many forested areas east of the Rocky Mountains were essentially drought-free during this period. Indeed, other than the area in southern New England described previously, these areas of severe to extreme drought were usually restricted to the Southeastern United States (although areas of mild drought were reasonably widespread in the East). Moreover, these severe to extreme drought areas were less prominent in the 5-year *MDZ* map (fig. 4.5) than in the 3-year map (fig. 4.4), which indicates that these conditions developed primarily within



2015–2017

- Moisture difference z-score (MDZ)
- ≤ -2 (extreme drought)
 - > -2– -1.5 (severe drought)
 - > -1.5– -1 (moderate drought)
 - > -1– -0.5 (mild drought)
 - > -0.5– 0.5 (near normal)
 - > 0.5– 1 (mild surplus)
 - > 1– 1.5 (moderate surplus)
 - > 1.5– 2 (severe surplus)
 - > 2 (extreme surplus)
 - ▨ Forested areas
 - Ecoregion section boundary

Figure 4.4—The 2015–2017 (i.e., 3-year) moisture difference z-score (MDZ) for the conterminous United States. Ecoregion section (Cleland and others 2007) boundaries are included for reference. Forest cover data (overlaid green hatching) derived from MODIS imagery by the Forest Service Remote Sensing Applications Center. (Data source: PRISM Climate Group, Oregon State University)

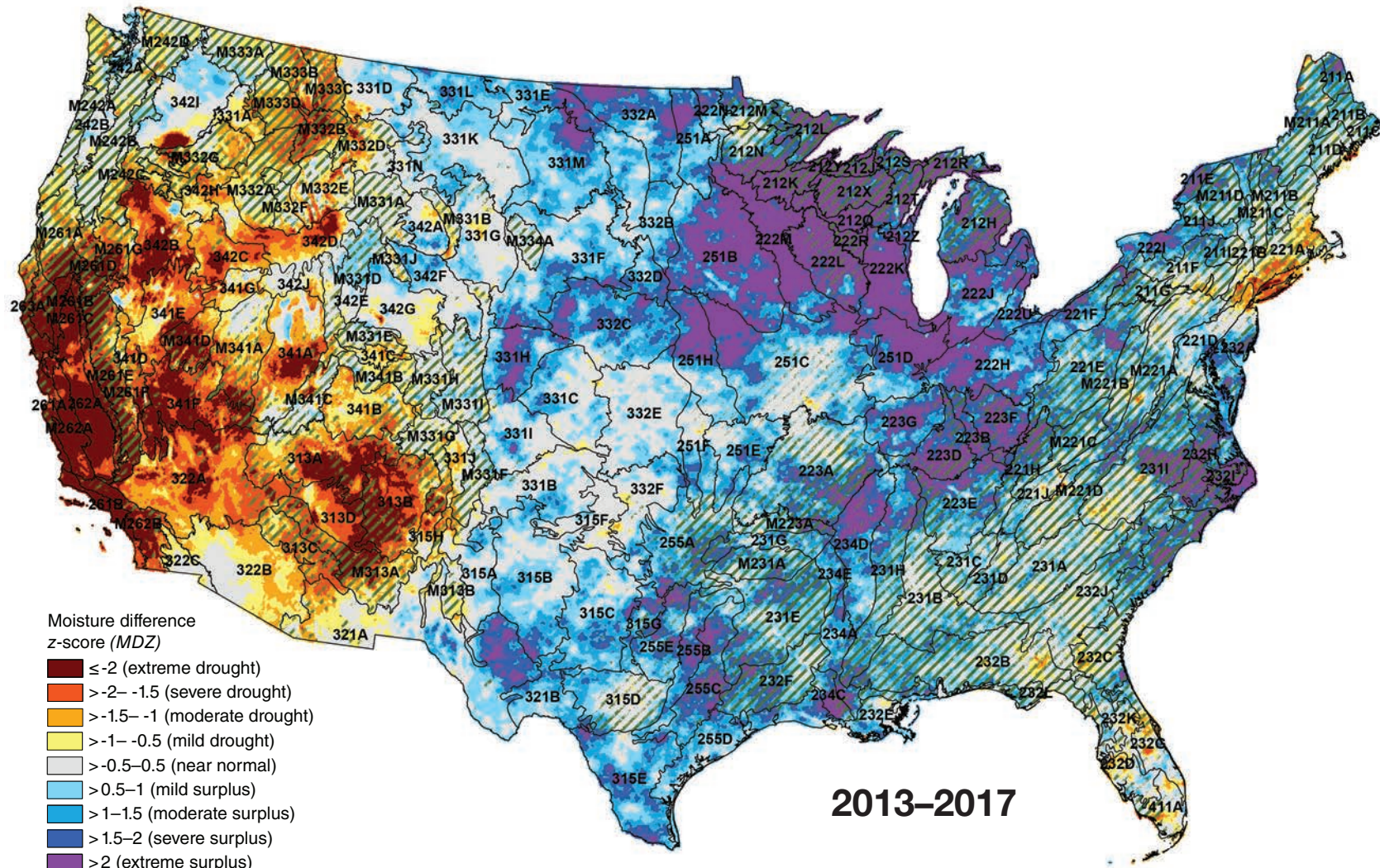


Figure 4.5—The 2013–2017 (i.e., 5-year) moisture difference z-score (MDZ) for the conterminous United States. Ecoregion section (Cleland and others 2007) boundaries are included for reference. Forest cover data (overlaid green hatching) derived from MODIS imagery by the Forest Service Remote Sensing Applications Center. (Data source: PRISM Climate Group, Oregon State University)

the last few years, and likely were preceded by near normal moisture conditions in 2013–2014. For example, one area in section 231I–Central Appalachian Piedmont can mostly be traced to the large contiguous zone of severe to extreme drought that occurred in 2016 (fig. 4.3). Another area in the southern portion of 232C–Atlantic Coastal Flatwoods appears to be linked to conditions that emerged primarily in 2017 (fig. 4.2).

Nevertheless, the contrast between the East and West is perhaps most emphasized by areas of moisture surplus documented in the 3-year and 5-year *MDZ* maps. While areas with severe to extreme surpluses were widespread east of the Rocky Mountains, they were virtually nonexistent west of the range. In particular, a few areas of surplus that appeared in the 5-year *MDZ* map (fig. 4.5) are worth highlighting: in the western Great Lakes region (especially forested sections 212J–Southern Superior Uplands, 212K–Western Superior Uplands, 212Q–North Central Wisconsin Uplands, 212R–Eastern Upper Peninsula, 212X–Northern Highlands, 212Y–Southwest Lake Superior Clay Plain, 222L–North Central U.S. Driftless and Escarpment, and 222R–Wisconsin Central Sands); in Kentucky and southern Indiana (223B–Interior Low Plateau-Transition Hills, 223D–Interior Low Plateau-Shawnee Hills, and 223F–Interior Low Plateau-Bluegrass); and in eastern North Carolina and South Carolina (portions of 231I–Central Appalachian Piedmont, 232C–Atlantic Coastal Flatwoods, 232H–Middle Atlantic Coastal Plains and Flatwoods, and 232I–

Northern Atlantic Coastal Flatwoods). Although no specific forest health impacts have been reported in these areas, recent evidence suggests a link between persistent excess moisture and increased vulnerability of forests to pathogens and other disease-causing agents (Hubbart and others 2016). These agents may be further enabled during times of high climate variability, such as when a period of drought occurs immediately before or after a period of moisture surplus (Hubbart and others 2016). A pertinent geographic example is eastern Texas, which saw multiple areas of moderate to extreme moisture surplus during the 2013–2017 period (in portions of 231E–Mid Coastal Plains-Western, 232F–Coastal Plains and Flatwoods-Western Gulf, 255B–Blackland Prairies, and 255C–Oak Woods and Prairies; see fig. 4.5). Notably, this prolonged period of surplus came shortly after Texas experienced its worst 1-year drought on record in 2011, which resulted in estimated mortality of >6 percent of forest trees statewide, roughly nine times the normal background mortality (Moore and others 2016). Forests in this region should be monitored over the next several years for possible impacts related to this pronounced swing in moisture conditions. Monitoring may also be advisable for the three areas of moisture surplus identified above (i.e., the western Great Lakes region, Kentucky and southern Indiana, and the Carolinas). These areas were less extensive in the 3-year *MDZ* map than in the 5-year map, which may be a preliminary signal of a shift from surplus to drought conditions in some locations.

Future Efforts

We intend to produce 1-year, 3-year, and 5-year *MDZ* maps of the conterminous United States as a regular yearly component of national-scale forest health reporting. To interpret the maps appropriately, it is important to recognize their limitations. Foremost, the *MDZ* approach does not incorporate some factors that may affect a location's moisture supply at a finer spatial scale, such as winter snowpack, surface runoff, or groundwater storage. Furthermore, although the maps use a standardized index scale that applies regardless of the size of the time window, the window size may still merit consideration. For example, an extreme drought that persists for 5 years has substantially different forest health implications than an extreme drought that lasts only a single year. Together, the 1-year, 3-year, and 5-year *MDZ* maps provide a comprehensive short-term overview, but a region's longer term moisture history may also be meaningful with respect to the health of its forests. For instance, in regions where droughts have been frequent historically (e.g., occurring on an annual or nearly annual basis), some tree species may be better drought-adapted than others (McDowell and others 2008). Because of this variability in species' drought resistance, a long period of persistent and severe drought conditions could ultimately lead to changes in regional forest composition (Mueller and others 2005); compositional changes similarly may arise from a long period of persistent moisture surplus (McEwan and others 2011). In turn, such changes are likely

to affect regional responses to future drought or surplus conditions, fire regimes, and the status of ecosystem services such as nutrient cycling and wildlife habitat (W.R.L. Anderegg and others 2013, DeSantis and others 2011). In future work, we hope to provide forest managers and other decisionmakers with better quantitative evidence regarding critical relationships between moisture extremes and significant forest health impacts such as regional-scale tree mortality (e.g., Mitchell and others 2014). We also intend to examine the capacity of moisture extremes to serve as inciting factors for other forest threats such as wildfire or pest outbreaks.

LITERATURE CITED

- Adams, H.D.; Guardiola-Claramonte, M.; Barron-Gafford, G.A. [and others]. 2009. Temperature sensitivity of drought-induced tree mortality portends increased regional die-off under global-change-type drought. *Proceedings of the National Academy of Sciences*. 106(17): 7063–7066.
- Akin, W.E. 1991. *Global patterns: climate, vegetation, and soils*. Norman, OK: University of Oklahoma Press. 370 p.
- Allen, C.D.; Macalady, A.K.; Chenchouni, H. [and others]. 2010. A global overview of drought and heat-induced tree mortality reveals emerging climate change risks for forests. *Forest Ecology and Management*. 259(4): 660–684.
- Alley, W.M. 1984. The Palmer Drought Severity Index: limitations and assumptions. *Journal of Climate and Applied Meteorology*. 23: 1100–1109.
- Anderegg, L.D.L.; Anderegg, W.R.L.; Berry, J.A. 2013. Not all droughts are created equal: translating meteorological drought into woody plant mortality. *Tree Physiology*. 33(7): 672–683.
- Anderegg, W.R.L.; Kane, J.M.; Anderegg, L.D.L. 2013. Consequences of widespread tree mortality triggered by drought and temperature stress. *Nature Climate Change*. 3(1): 30–36.

- Archaux, F.; Wolters, V. 2006. Impact of summer drought on forest biodiversity: what do we know? *Annals of Forest Science*. 63: 645–652.
- Berdanier, A.B.; Clark, J.S. 2016. Multiyear drought-induced morbidity preceding tree death in southeastern U.S. forests. *Ecological Applications*. 26(1): 17–23.
- Clark, J.S. 1989. Effects of long-term water balances on fire regime, north-western Minnesota. *Journal of Ecology*. 77: 989–1004.
- Cleland, D.T.; Freeouf, J.A.; Keys, J.E. [and others]. 2007. Ecological subregions: sections and subsections for the conterminous United States. Gen. Tech. Report WO-76D. Washington, DC: U.S. Department of Agriculture Forest Service. Map; Sloan, A.M., cartographer; presentation scale 1:3,500,000; colored. Also on CD-ROM as a GIS coverage in ArcINFO format or at <http://data.fs.usda.gov/geodata/edw/datasets.php>. [Date accessed: July 20, 2015].
- Clinton, B.D.; Boring, L.R.; Swank, W.T. 1993. Canopy gap characteristics and drought influences in oak forests of the Coweeta Basin. *Ecology*. 74(5): 1551–1558.
- Daly, C.; Gibson, W.P.; Taylor, G.H. [and others]. 2002. A knowledge-based approach to the statistical mapping of climate. *Climate Research*. 22: 99–113.
- DeSantis, R.D.; Hallgren, S.W.; Stahle, D. W. 2011. Drought and fire suppression lead to rapid forest composition change in a forest-prairie ecotone. *Forest Ecology and Management*. 261(11): 1833–1840.
- Duever, M.J.; Meeder, J.F.; Meeder, L.C.; McCollum, J.M. 1994. The climate of south Florida and its role in shaping the Everglades ecosystem. In: Davis, S.M.; Ogden, J.C., eds. *Everglades: the ecosystem and its restoration*. Delray Beach, FL: St. Lucie Press: 225–248.
- Gil-Alana, L.A. 2018. Maximum and minimum temperatures in the United States: time trends and persistence. *Atmospheric Science Letters*. 19(4): e810.
- Groisman, P.Y.; Knight, R.W. 2008. Prolonged dry episodes over the conterminous United States: new tendencies emerging during the last 40 years. *Journal of Climate*. 21: 1850–1862.
- Grundstein, A. 2009. Evaluation of climate change over the continental United States using a moisture index. *Climatic Change*. 93: 103–115.
- Guarín, A.; Taylor, A.H. 2005. Drought triggered tree mortality in mixed conifer forests in Yosemite National Park, California, USA. *Forest Ecology and Management*. 218: 229–244.
- Hanson, P.J.; Weltzin, J.F. 2000. Drought disturbance from climate change: response of United States forests. *Science of the Total Environment*. 262: 205–220.
- Hubbart, J.A.; Guyette, R.; Muzika, R.-M. 2016. More than drought: precipitation variance, excessive wetness, pathogens and the future of the western edge of the Eastern Deciduous Forest. *Science of the Total Environment*. 566–567: 463–467.
- Kareiva, P.M.; Kingsolver, J.G.; Huey, B.B., eds. 1993. *Biotic interactions and global change*. Sunderland, MA: Sinauer Associates, Inc. 559 p.
- Keetch, J.J.; Byram, G.M. 1968. A drought index for forest fire control. Asheville, NC: U.S. Department of Agriculture Forest Service, Southeastern Forest Experiment Station. 33 p.
- Koch, F.H.; Coulston, J.W. 2015. One-year (2013), three-year (2011–2013), and five-year (2009–2013) drought maps for the conterminous United States. In: Potter, K.M.; Conkling, B.L., eds. *Forest Health Monitoring: national status, trends, and analysis 2014*. Gen. Tech. Rep. SRS-209. Asheville, NC: U.S. Department of Agriculture Forest Service, Southern Research Station: 57–71. Chapter 4.
- Koch, F.H.; Coulston, J.W. 2016. 1-year (2014), 3-year (2012–2014), and 5-year (2010–2014) maps of drought and moisture surplus for the conterminous United States. In: Potter, K.M.; Conkling, B.L., eds. *Forest Health Monitoring: national status, trends, and analysis 2015*. Gen. Tech. Rep. SRS-213. Asheville, NC: U.S. Department of Agriculture Forest Service, Southern Research Station: 61–78. Chapter 4.
- Koch, F.H.; Coulston, J.W. 2017. Moisture deficit and surplus in the conterminous United States for three time windows: 2015, 2013–2015, and 2011–2015. In: Potter, K.M.; Conkling, B.L., eds. *Forest Health Monitoring: national status, trends, and analysis 2016*. Gen. Tech. Rep. SRS-222. Asheville, NC: U.S. Department of Agriculture Forest Service, Southern Research Station: 63–80. Chapter 4.

- Koch, F.H.; Coulston, J.W. 2018. Moisture deficit and surplus in the conterminous United States for three time windows: 2016, 2014–2016, and 2012–2016. In: Potter, K.M.; Conkling, B.L., eds. *Forest Health Monitoring: national status, trends, and analysis 2017*. Gen. Tech. Rep. SRS-233. Asheville, NC: U.S. Department of Agriculture Forest Service, Southern Research Station: 65–84. Chapter 4.
- Koch, F.H.; Coulston, J.W.; Smith, W.D. 2012a. High-resolution mapping of drought conditions. In: Potter, K.M.; Conkling, B.L., eds. *Forest Health Monitoring 2008 national technical report*. Gen. Tech. Rep. SRS-158. Asheville, NC: U.S. Department of Agriculture Forest Service, Southern Research Station: 45–62. Chapter 4.
- Koch, F.H.; Coulston, J.W.; Smith, W.D. 2012b. Mapping drought conditions using multi-year windows. In: Potter, K.M.; Conkling, B.L., eds. *Forest Health Monitoring 2009 national technical report*. Gen. Tech. Rep. SRS-167. Asheville, NC: U.S. Department of Agriculture Forest Service, Southern Research Station: 163–179. Chapter 10.
- Koch, F.H.; Smith, W.D.; Coulston, J.W. 2013a. Recent drought conditions in the conterminous United States. In: Potter, K.M.; Conkling, B.L., eds. *Forest Health Monitoring: national status, trends, and analysis 2011*. Gen. Tech. Rep. SRS-185. Asheville, NC: U.S. Department of Agriculture Forest Service, Southern Research Station: 41–58. Chapter 4.
- Koch, F.H.; Smith, W.D.; Coulston, J.W. 2013b. An improved method for standardized mapping of drought conditions. In: Potter, K.M.; Conkling, B.L., eds. *Forest Health Monitoring: national status, trends, and analysis 2010*. Gen. Tech. Rep. SRS-176. Asheville, NC: U.S. Department of Agriculture Forest Service, Southern Research Station: 67–83. Chapter 6.
- Koch, F.H.; Smith, W.D.; Coulston, J.W. 2014. Drought patterns in the conterminous United States and Hawaii. In: Potter, K.M.; Conkling, B.L., eds. *Forest Health Monitoring: national status, trends, and analysis 2012*. Gen. Tech. Rep. SRS-198. Asheville, NC: U.S. Department of Agriculture Forest Service, Southern Research Station: 49–72. Chapter 4.
- Koch, F.H.; Smith, W.D.; Coulston, J.W. 2015. Drought patterns in the conterminous United States, 2012. In: Potter, K.M.; Conkling, B.L., eds. *Forest Health Monitoring: national status, trends, and analysis 2013*. Gen. Tech. Rep. SRS-207. Asheville, NC: U.S. Department of Agriculture Forest Service, Southern Research Station: 55–69. Chapter 4.
- Kolb, T.E.; Fettig, C.J.; Ayres, M.P. [and others]. 2016. Observed and anticipated impacts of drought on forest insects and diseases in the United States. *Forest Ecology and Management*. 380: 321–334.
- Laurance, S.G.W.; Laurance, W.F.; Nascimento, H.E.M. [and others]. 2009. Long-term variation in Amazon forest dynamics. *Journal of Vegetation Science*. 20(2): 323–333.
- Lesk, C.; Coffel, E.; D’Amato, A.W. [and others]. 2017. Threats to North American forests from southern pine beetle with warming winters. *Nature Climate Change*. 7: 713.
- Marlier, M.E.; Xiao, M.; Engel, R. [and others]. 2017. The 2015 drought in Washington State: a harbinger of things to come? *Environmental Research Letters*. 12(11): 114008.
- Martínez-Vilalta, J.; Lloret, F.; Breshears, D.D. 2012. Drought-induced forest decline: causes, scope and implications. *Biology Letters*. 8(5): 689–691.
- Mattson, W.J.; Haack, R.A. 1987. The role of drought in outbreaks of plant-eating insects. *BioScience*. 37(2): 110–118.
- McDowell, N.; Pockman, W.T.; Allen, C.D. [and others]. 2008. Mechanisms of plant survival and mortality during drought: why do some plants survive while others succumb to drought? *New Phytologist*. 178: 719–739.
- McEwan, R.W.; Dyer, J.M.; Pederson, N. 2011. Multiple interacting ecosystem drivers: toward an encompassing hypothesis of oak forest dynamics across eastern North America. *Ecography*. 34: 244–256.
- McKee, T.B.; Doesken, N.J.; Kleist, J. 1993. The relationship of drought frequency and duration to time scales. In: *Eighth conference on applied climatology*. American Meteorological Society: 179–184.

- Millar, C.I.; Westfall, R.D.; Delany, D.L. 2007. Response of high-elevation limber pine (*Pinus flexilis*) to multiyear droughts and 20th-century warming, Sierra Nevada, California, USA. *Canadian Journal of Forest Research*. 37: 2508–2520.
- Mitchell, P.J.; O’Grady, A.P.; Hayes, K.R.; Pinkard, E.A. 2014. Exposure of trees to drought-induced die-off is defined by a common climatic threshold across different vegetation types. *Ecology and Evolution*. 4(7): 1088–1101.
- Monteith, J.L. 1965. Evaporation and environment. *Symposia of the Society for Experimental Biology*. 19: 205–234.
- Moore, G.W.; Edgar, C.B.; Vogel, J.G. [and others]. 2016. Tree mortality from an exceptional drought spanning mesic to semiarid ecoregions. *Ecological Applications*. 26(2): 602–611.
- Mueller, R.C.; Scudder, C.M.; Porter, M.E. [and others]. 2005. Differential tree mortality in response to severe drought: evidence for long-term vegetation shifts. *Journal of Ecology*. 93: 1085–1093.
- National Climatic Data Center. 2018a. Climatological rankings - temperature, precipitation, and drought. <http://www.ncdc.noaa.gov/temp-and-precip/climatological-rankings/index.php>. [Date accessed: September 12, 2018].
- National Climatic Data Center. 2018b. State of the climate - drought - annual report 2017. <https://www.ncdc.noaa.gov/sotc/drought/201713>. [Date accessed: September 10, 2018].
- Palmer, W.C. 1965. *Meteorological drought*. Washington, DC: U.S. Department of Commerce, Weather Bureau. 58 p.
- Peng, C.; Ma, Z.; Lei, X. [and others]. 2011. A drought-induced pervasive increase in tree mortality across Canada’s boreal forests. *Nature Climate Change*. 1(9): 467–471.
- Peters, M.P.; Iverson, L.R.; Matthews, S.N. 2015. Long-term droughtiness and drought tolerance of eastern US forests over five decades. *Forest Ecology and Management*. 345: 56–64.
- Potter, C.S.; Klooster, S.A. 1999. Dynamic global vegetation modelling for prediction of plant functional types and biogenic trace gas fluxes. *Global Ecology and Biogeography*. 8(6): 473–488.
- PRISM Climate Group. 2018. 2.5-arcmin (4 km) gridded monthly climate data. <http://www.prism.oregonstate.edu>. [Date accessed: June 14, 2018].
- Raffa, K.F.; Aukema, B.H.; Bentz, B.J. [and others]. 2008. Cross-scale drivers of natural disturbances prone to anthropogenic amplification: the dynamics of bark beetle eruptions. *BioScience*. 58(6): 501–517.
- Rahmstorf, S.; Foster, G.; Cahill, N. 2017. Global temperature evolution: recent trends and some pitfalls. *Environmental Research Letters*. 12(5): 054001.
- Rozas, V.; García-González, I. 2012. Too wet for oaks? Inter-tree competition and recent persistent wetness predispose oaks to rainfall-induced dieback in Atlantic rainy forest. *Global and Planetary Change*. 94–95: 62–71.
- Rozas, V.; Sampedro, L. 2013. Soil chemical properties and dieback of *Quercus robur* in Atlantic wet forests after a weather extreme. *Plant and Soil*. 373(1–2): 673–685.
- Schoennagel, T.; Veblen, T.T.; Romme, W.H. 2004. The interaction of fire, fuels, and climate across Rocky Mountain forests. *BioScience*. 54(7): 661–676.
- Steinemann, A. 2003. Drought indicators and triggers: a stochastic approach to evaluation. *Journal of the American Water Resources Association*. 39(5): 1217–1233.
- Svoboda, M.; LeComte, D.; Hayes, M. [and others]. 2002. The Drought Monitor. *Bulletin of the American Meteorological Society*. 83(8): 1181–1190.
- Sweet, S.K.; Wolfe, D.W.; DeGaetano, A.; Benner, R. 2017. Anatomy of the 2016 drought in the Northeastern United States: implications for agriculture and water resources in humid climates. *Agricultural and Forest Meteorology*. 247: 571–581.
- Thorntwaite, C.W. 1948. An approach towards a rational classification of climate. *Geographical Review*. 38(1): 55–94.
- Thorntwaite, C.W.; Mather, J.R. 1955. The water balance. *Publications in Climatology*. 8(1): 1–104.
- Trouet, V.; Taylor, A.H.; Wahl, E.R. [and others]. 2010. Fire-climate interactions in the American West since 1400 CE. *Geophysical Research Letters*. 37(4): L04702.

- USDA Forest Service Region 5 Forest Health Monitoring program. 2018. 2017 aerial survey results: California. Press Rel. R5-PR-034. Davis, CA: U.S. Department of Agriculture Forest Service, Pacific Southwest Region. 18 p.
- Vose, R.S.; Applequist, S.; Squires, M. [and others]. 2014. Improved historical temperature and precipitation time series for U.S. climate divisions. *Journal of Applied Meteorology and Climatology*. 53(5): 1232–1251.
- Williams, A.P.; Allen, C.D.; Macalady, A.K. [and others]. 2013. Temperature as a potent driver of regional forest drought stress and tree mortality. *Nature Climate Change*. 3(3): 292–297.
- Willmott, C.J.; Feddema, J.J. 1992. A more rational climatic moisture index. *Professional Geographer*. 44(1): 84–87.
- Woodhouse, C.A.; Meko, D.M.; MacDonald, G.M. [and others]. 2010. A 1,200-year perspective of 21st century drought in southwestern North America. *Proceedings of the National Academy of Sciences*. 107(50): 21283–21288.

INTRODUCTION

Tree mortality is a natural process in all forest ecosystems. High mortality can be an indicator of forest health problems. On a regional scale, high mortality levels may indicate widespread insect or disease impacts. High mortality may also occur if a large proportion of the forest in a particular region is made up of older, senescent stands. The approach presented here seeks to detect mortality patterns that might reflect changes to ecosystem processes at large scales. In many cases, the proximate cause of mortality may be discernable. Understanding proximate causes of mortality *may* provide insight into whether the mortality is within the range of natural variation or reflects more fundamental changes to ecological processes.

DATA

Forest Inventory and Analysis (FIA) Phase 2 (P2) data were the basis of the mortality analysis. The FIA P2 data are collected across forested land throughout the United States, with approximately one plot per 6,000 acres of forest, using a rotating panel sample design (Bechtold and Patterson 2005). Field plots are divided into spatially balanced panels, with one panel being measured each year. A single cycle of measurements consists of measuring all panels. This “annualized” method of inventory was adopted, State by State, beginning in 1999. The cycle length (i.e., number of years required to measure all plot panels) ranges from 5 to 10 years.

An analysis of mortality requires data collected at a minimum of two points in time. Therefore, mortality analysis was possible for areas where data from repeated plot measurements using consistent sampling protocols were available (i.e., where one cycle of measurements had been completed and at least one panel of the next cycle had been measured, and where there had been no changes to the protocols affecting measurements of trees or saplings). In this report, as in recent years, the repeated P2 data were available for all of the Central and Eastern States. The most recent cycle of remeasurements for each State was used in this analysis.

In addition, mortality data have become available from parts of the Western United States. In the West, plots are remeasured on a 10-year cycle. Thus, estimates of growth and mortality from the West are based on less than a complete cycle of remeasurement. Remeasurement data were available for all Western States in the conterminous United States except Wyoming. However, for several States, the proportion of plots that have been remeasured is small, making the effective sampling intensity for growth and mortality estimates significantly lower than FIA’s standard of one plot: 6,000 acres (table 5.1). Therefore, the percent sampling error on growth and mortality estimates tends to be large. Results are not presented for ecoregion sections where <50 plots had been remeasured or where the percent error was unacceptably high. Nevertheless, results presented for the West should be viewed

CHAPTER 5.

Tree Mortality

MARK J. AMBROSE

Table 5.1—Western States from which repeated Forest Inventory and Analysis Phase 2 measurements were available, the time period spanned by the data, and the effective sample intensity (on the proportion of plots that had been remeasured) in the available datasets

State	Time period	Effective sample intensity
Arizona	2001–2016	one plot: 10,000 acres
California	2001–2016	one plot: 10,000 acres
Colorado	2002–2016	one plot: 12,000 acres
Idaho	2004–2016	one plot: 20,000 acres
Montana	2003–2016	one plot: 15,000 acres
Nevada	2004–2016	one plot: 20,000 acres
New Mexico	2005–2016	one plot: 30,000 acres
Oregon	2001–2016	one plot: 8,571 acres
Utah	2000–2016	one plot: 8,571 acres
Washington	2002–2016	one plot: 12,000 acres

as preliminary. Because of this, results from the West are discussed separately from those from the Eastern and Central United States. The division of Eastern/Central versus Western States, as well as the forest cover within those States, is shown in figure 5.1.

METHODS

Forest Inventory and Analysis calculates the growth, mortality, and removal volume on each plot over the interval between repeated measurements. These values are stored in the FIA database (version 7.0.1) (Burrill and others

2017; USDA Forest Service, Forest Inventory and Analysis program 2017). Forest Inventory and Analysis' EVALIDator (ver. 1.7.0.01) is an online tool for querying the FIA database and generating area-based reports on forest characteristics (Miles 2015). EVALIDator was used to obtain net growth rates and mortality rates over the most recent measurement cycle for each of 97 ecoregion sections (Cleland and others 2007, McNab and others 2007) covering the Eastern and Central United States and 23 ecoregion sections in the Western¹ United States. For most States, the most recent cycle of available data ran through 2016 (e.g., data collected 2011 through 2016).

To compare mortality across forest types and climate zones, the ratio of annual mortality volume to gross annual volume growth (MRATIO) was used as a standardized mortality indicator (Coulston and others 2005). The MRATIO has proven to be a useful indicator of forest health, but it can be a problematic indicator, especially when growth rates are very low. The MRATIO can also be difficult to interpret when there is high uncertainty to growth estimates. Both of these are the case with the data currently available from the West.

¹ At the time that this analysis was being completed, updates being made to EVALIDator and the FIA database made it impossible to generate growth estimates for the Interior West, so MRATIOS were only calculated for the West Coast States.

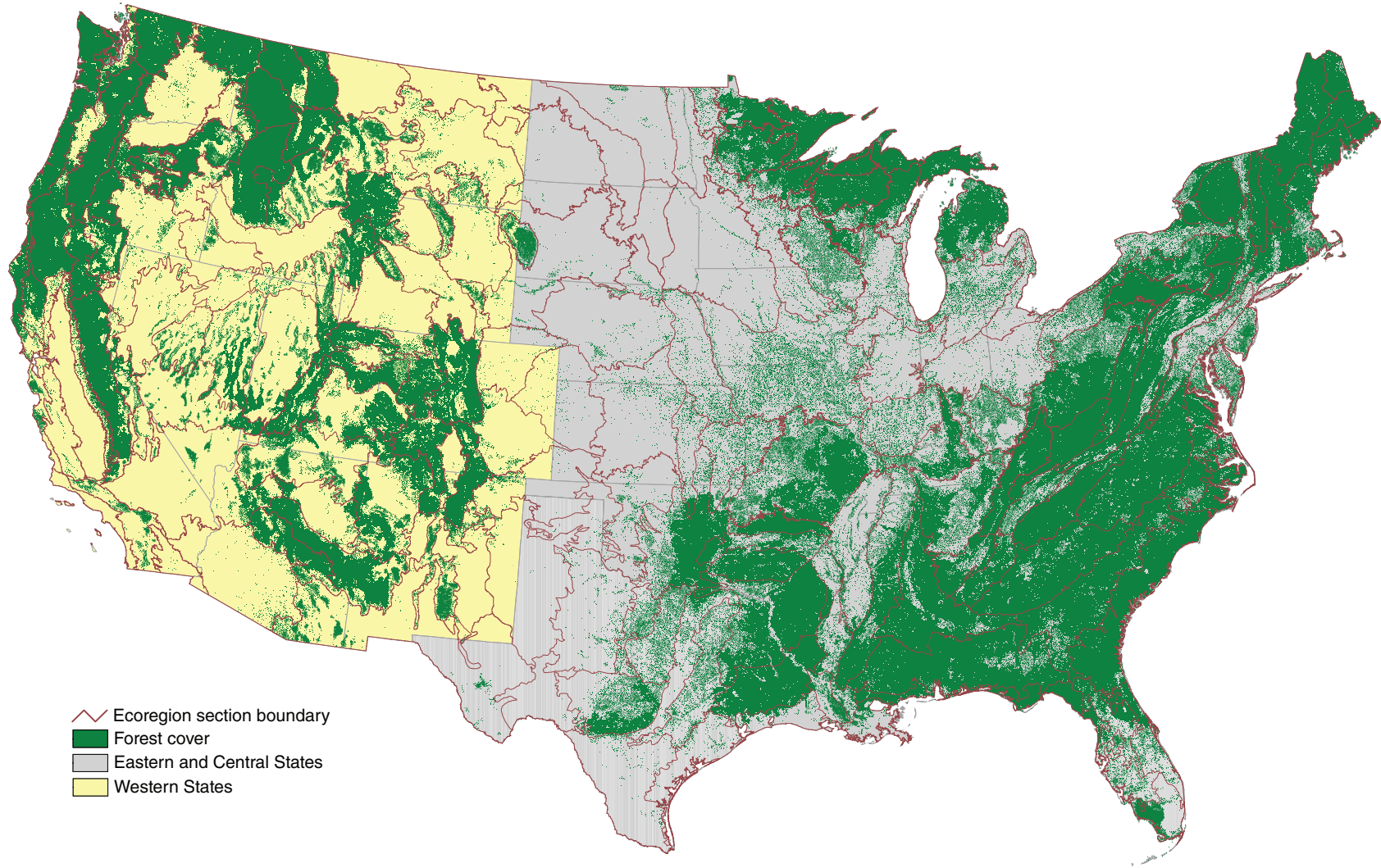


Figure 5.1—Forest cover in the States where mortality was analyzed by ecoregion section (Cleland and others 2007). Mortality in Eastern and Central States was analyzed using a complete remeasurement cycle; in Western States, mortality was analyzed using a partial cycle of remeasurements, and results there should be considered preliminary. Forest cover was derived from MODIS satellite imagery (USDA Forest Service 2008).

Therefore, mortality as a percentage of live growing stock also was calculated:

$$\text{Mortality percent} = m / v_l * 100$$

where

m = annual mortality (cubic feet per year)

v_l = total live tree volume (cubic feet)

When both this mortality percentage and the MRATIO are high, it suggests a possibly serious forest health concern.

In addition, mortality rates were derived for each forest type group (USDA Forest Service 2008) for each ecoregion section. Identifying the forest types experiencing high mortality in an ecoregion section is a first step in identifying what forest health issue may be affecting the forests. Although determining particular causal agents associated with all observed mortality is beyond the scope of this report, often there are well-known insects and pathogens that are “likely suspects” once the affected forest types are identified.

To identify possible causal agents for the observed mortality, EVALIDator was also used to report the cause of death that was recorded for trees that died. Causes of death are reported as general categories (e.g., insects, fire, weather). Care must be used in interpreting these causes because tree mortality may actually be caused by a combination of factors such as drought and insects. Further information about the cause of mortality is provided by the aerial survey of insects and disease (see ch. 2 in this report). It

is difficult to directly match aerial survey data to mortality observed on FIA plots. However, I incorporate the results of this survey into the discussion by consulting State Forest Health Highlights, which reflect in large part the results of aerial surveys.

RESULTS AND DISCUSSION

The MRATIO values are shown in figure 5.2. The MRATIO can be large if an over-mature forest is senescing and losing a cohort of older trees. If forests are not naturally senescing, a high MRATIO (>0.6) may indicate high mortality due to some acute cause (insects or pathogens) or due to generally deteriorating forest health conditions. The 10 ecoregion sections with the highest MRATIOS are labeled on the map. In the discussion that follows, I focus on the ecoregion sections having MRATIOS >0.5 (i.e., where mortality was greater than half of gross growth).

Eastern and Central States

The highest MRATIOS occurred in ecoregion sections 332D–North-Central Great Plains (MRATIO = 1.05) in South Dakota and Nebraska and M334A–Black Hills (MRATIO = 1.01). Other areas of high mortality relative to growth on the Great Plains were ecoregion sections 331F–Western Great Plains (MRATIO= 0.83) in South Dakota and Nebraska, 331M–Missouri Plateau (MRATIO = 0.75) in North and South Dakota, and 332A–Northeastern Glaciated Plains (MRATIO = 0.72) in North Dakota. In these Great Plains ecoregion sections where mortality is high relative to growth, the predominant

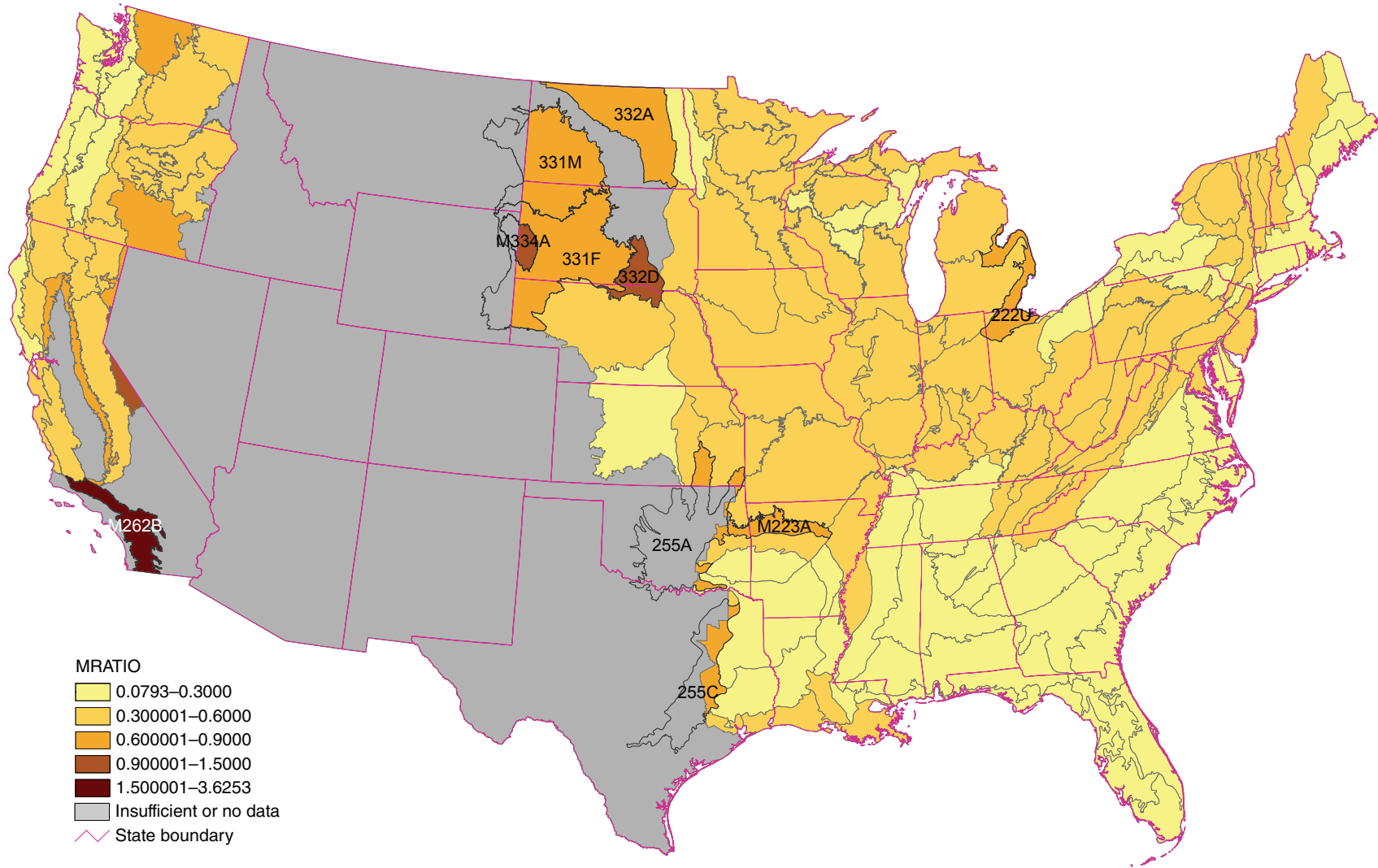


Figure 5.2—Tree mortality expressed as the ratio of annual mortality volume to gross annual volume growth (MRATIO) by ecoregion section (Cleland and others 2007). (Data source: U.S. Department of Agriculture Forest Service, Forest Inventory and Analysis program)

vegetation is grassland. Although the ecoregion sections are quite large, there was relatively little forest land to measure (e.g., 112 plots in section 331F and 86 plots in section 331M). In the Plains, tree growth is generally slow because of naturally dry conditions. Where the number of sample plots is small and tree growth is naturally slow, care must be taken in interpreting mortality relative to growth.

In 332D–North-Central Great Plains (MRATIO = 1.05), 46 percent of mortality was weather-related (table 5.2). Adverse weather conditions, including both droughts and excessively wet conditions, occurred multiple times during the remeasurement cycle. These included a drought that affected almost all of Nebraska in 2012 and 2013 and a major drought in South Dakota in 2017 (Ball and others 2017; Nebraska Forest Service 2012,

2013; South Dakota Department of Agriculture 2012). Most of the mortality occurred in the elm-ash-cottonwood (48 percent) and oak-hickory (17 percent) forest type groups. A number of agents may have contributed to the mortality, including oak decline, which has been reported in northern and eastern Nebraska (Nebraska Forest Service 2017), bur oak blight (*Tubakia iowensis*), and Dutch elm disease (*Ophiostoma novo-ulmi*) (Ball and others 2017).

In ecoregion section M334A–Black Hills (MRATIO = 1.01), the vast majority (76 percent) of mortality occurred in the ponderosa pine forest type group; 62 percent of mortality was caused by insects, while 23 percent was caused by fire (table 5.2). Mortality in this ecoregion section is most likely related to mountain pine beetle (*Dendroctonus ponderosae*) as there had been an ongoing pine beetle outbreak in the

Table 5.2—Ecoregion sections in the Eastern and Central United States having the highest mortality relative to growth (MRATIO), annual growth and mortality rates, and associated causes of mortality

Ecoregion section	Average annual gross growth	Average annual mortality	MRATIO	Major causes of mortality
	----- cubic feet per year -----			
332D–North-Central Great Plains	12,118,379	12,751,261	1.05	Weather-related (46%)
M334A–Black Hills	41,386,310	41,794,634	1.01	Insects (62%), fire (23%)
331F–Western Great Plains	13,823,354	11,454,079	0.83	Fire (40%), weather-related (22%)
255C–Oak Woods and Prairies	131,511,673	103,745,282	0.79	Weather-related (67%), disease (14%)
222U–Lake Whittlesey Glaciolacustrine Plain	63,480,976	50,049,630	0.79	Insects (73%)
331M–Missouri Plateau	9,373,439	7,010,951	0.75	Weather-related (63%), insects (11%), disease (10%)
332A–Northeastern Glaciated Plains	10,579,158	7,659,833	0.72	Weather-related (43%), animals (12%), disease (11%)
255A–Cross Timbers and Prairie	26,192,558	18,069,016	0.69	Disease (45%), weather-related (27%), fire (14%)
M223A–Boston Mountains	138,005,580	84,964,283	0.62	Disease (42%), weather-related (39%), insects (14%)

Black Hills region (Ball and others 2015, 2016; South Dakota Department of Agriculture 2011, 2012, 2013, 2014). Pine beetle activity has declined dramatically in the region since 2015 (Ball and others 2017, Wyoming State Forestry Division 2017), and the pine beetle outbreak has now ended, but reported mortality remains high because results reported, based on the most recent cycles of FIA data, reflect mortality over the period that includes the peak of the outbreak in 2015.

Both ecoregion sections 331F–Western Great Plains and 331M–Missouri Plateau have had high mortality relative to growth in recent years (Ambrose 2013, 2014, 2015a, 2015b, 2016, 2017), so the observed mortality is not a new phenomenon. Tree growth rates in these regions (especially in 331M–Missouri Plateau) are quite low, so the high MRATIOS are due to a combination of low growth and high mortality. Much of the forest in these sections is riparian, and most of the species experiencing greatest mortality are commonly found in riparian areas. The major exception was high ponderosa pine (*Pinus ponderosa*) mortality in ecoregion section 331F–Western Great Plains. Ponderosa pine is not a riparian tree species, but like the riparian species, it only occurs in a relatively small area of the ecoregion section, on discontinuous mountains, plateaus, canyons, and breaks in the plains (Burns and Honkala 1990).

In ecoregion section 331F–Western Great Plains, fire caused 40 percent of mortality; another 22 percent of mortality was weather-related (table 5.2). As mentioned previously, much of the mortality in this ecoregion section (about 36 percent) occurred in the ponderosa pine forest type group; most of the rest of the mortality occurred in various hardwood forest type groups. However, the pine mortality represented a relatively small proportion of the growing stock in the ponderosa pine forest type (0.47 percent) in the region. The pine mortality in this ecoregion section is very likely related to mountain pine beetle due to an ongoing pine beetle outbreak in the adjacent Black Hills region (Ball and others 2015, 2016; South Dakota Department of Agriculture 2011, 2012, 2013, 2014). Mountain pine beetle-related mortality also was reported in western Nebraska (Nebraska Forest Service 2011, 2012), with an outbreak that began in 2009, though pine beetle-related mortality there has fallen significantly recently (Ball and others 2017; Nebraska Forest Service 2014, 2015, 2016, 2017). The pine beetle outbreak has ended, but reported mortality remains high because the results shown, based on the most recent cycles of FIA data, reflect mortality over the period that includes the peak of the outbreak.

More recently, several other agents have been reported as affecting ponderosa pine in western Nebraska, including Ips beetles and

Diplodia blight (Nebraska Forest Service 2015, 2016, 2017). Drought in 2012 and 2013, affecting much of South Dakota and Nebraska (Nebraska Forest Service 2012, 2013; South Dakota Department of Agriculture 2012), may also have contributed to pine mortality, as well as that of other species, in ecoregion section 331F–Western Great Plains.

In ecoregion section 331M–Missouri Plateau, about 63 percent of the mortality (by volume) occurred in the elm-ash-cottonwood forest type group, and about 15 percent of mortality occurred in the oak-hickory forest type group. About 63 percent of mortality was identified as weather-related (table 5.2). Adverse weather conditions, including both drought and excessively wet conditions, occurred during the remeasurement cycle (Ball and others 2017; Johnson 2017; North Dakota Forest Service 2012, 2013; South Dakota Department of Agriculture 2012). Multiple tree-damaging storm events, including both hail storms and tornadoes, also occurred over that period (Johnson 2017, North Dakota Forest Service 2016). About 11 percent of mortality was caused by insects and 10 percent caused by disease (table 5.2). Prior analyses identified three species as suffering high mortality in this region: eastern cottonwood (*Populus deltoides*), bur oak (*Quercus macrocarpa*), and green ash (*Fraxinus pennsylvanica*) (Ambrose 2015a). Green ash has been affected by ash/lilac borer (*Podosesia syringae*), as well as other native ash borers, in both North and South Dakota (Ball and others 2015, 2016; North Dakota Forest Service 2012;

South Dakota Department of Agriculture 2012). Cottonwood canker fungi have been identified as a problem throughout North Dakota (North Dakota Forest Service 2014, 2015); these fungi may be contributing to the observed cottonwood mortality.

The majority of the mortality in ecoregion section 332A–Northeastern Glaciated Plains of North Dakota was split between the elm-ash-cottonwood (15 percent), aspen-birch (28 percent), and oak-hickory (19 percent) forest type groups. This ecoregion section includes the Turtle Mountains, where thousands of acres of forest tent caterpillar and large aspen tortrix defoliation have occurred in recent years (North Dakota Forest Service 2014). Overmaturity of aspen (*Populus tremuloides*) stands in North Dakota has led to increasing insect and disease issues (North Dakota Forest Service 2015). In addition, 4,000 acres of aspen decline, also related to over-mature stands, have been identified in this ecoregion section (North Dakota Forest Service 2014). The defoliation together with the aspen decline may be the cause of most of the mortality in the aspen-birch forest type. Cottonwood canker fungi have been a problem throughout North Dakota (North Dakota Forest Service 2014, 2015) and may be a cause of the mortality in the elm-ash-cottonwood forest type. About 43 percent of the mortality was related to adverse weather (table 5.2). North Dakota experienced numerous storm events over the past several years, including 435 hail events and 66 tornadoes during the 2015 and 2016 growing seasons.

Damage due to hail storms can make trees susceptible to a number of fungal diseases (North Dakota Forest Service 2015, 2016).

Mortality relative to growth was also rather high (MRATIO = 0.79) in ecoregion section 222U–Lake Whittlesey Glaciolacustrine Plain. There the majority of the mortality was split between the oak-hickory (45 percent) and elm-ash-cottonwood (36 percent) forest type groups. About 73 percent of the mortality in that ecoregion section was caused by insects (table 5.2). Much of the mortality in the elm-ash-cottonwood group is likely due to emerald ash borer (*Agrilus planipennis*), which has produced extremely high ash mortality throughout Ohio and Michigan (Michigan Department of Natural Resources 2014, 2015, 2016, 2017; Ohio Department of Natural Resources, Division of Forestry 2014, 2015), and, in fact, has caused the death of the “vast majority” of native ash in northwestern Ohio (Ohio Department of Natural Resources, Division of Forestry 2016). The cause of mortality in the oak-hickory forest type group is less clear. Several oak (*Quercus* spp.) pests were reported in Ohio as well as “leaf-curl syndrome” of unknown origin (Ohio Department of Natural Resources, Division of Forestry 2015, 2016). In Michigan, oak wilt (caused by the pathogen *Ceratocystis fagacearum*) has been confirmed in at least part of the ecoregion section (Michigan Department of Natural Resources 2015, 2016, 2017).

Ecoregion section 255C–Oak Woods and Prairies in Texas also had relatively high mortality (MRATIO = 0.79). About 52 percent of the mortality occurred in the oak-hickory forest type group, 12 percent occurred in the oak-gum-cypress forest type group, and another 12 percent occurred in the oak-pine forest type group. About 11 percent of mortality occurred in the loblolly-shortleaf pine type group. The vast majority (67 percent) of mortality in this ecoregion section was identified as weather-related. A record-setting drought in 2011 that affected Oklahoma and Texas was reported as weakening both pines and hardwoods in Texas, making them susceptible to a variety of pests and pathogens (Smith 2013, 2014). Disease was the reported cause of another 14 percent of mortality (table 5.2). Oak wilt has been a major problem in oak woodlands in central Texas (Smith 2014; Texas A & M Forest Service 2015, 2016) and probably contributed to the mortality in the oak-hickory and oak-gum-cypress forest types. Pine engraver beetle (*Ips* spp.) has been a problem in Texas’ pine forests and may have contributed to mortality in the loblolly-shortleaf pine forests (Smith 2014; Texas A & M Forest Service 2015, 2016, 2017).

Ecoregion section 255A–Cross Timbers and Prairie experienced relatively high mortality (MRATIO = 0.69). However, the majority of the ecoregion section is located in central Oklahoma, where annualized mortality data are not yet available. Therefore, the results shown

are based on data collected in the relatively small portion of the ecoregion section located in eastern Oklahoma and southeastern Kansas. About 75 percent of the mortality (in terms of tree volume) occurred in the oak-hickory forest type group; another 18 percent of the mortality occurred in the elm-ash-cottonwood forest type group. Disease was the reported cause of 45 percent of mortality, 27 percent of mortality was weather-related, and 14 percent of mortality was due to fire. As mentioned above, a record drought in 2011 and 2012 affected Oklahoma and Texas, stressing trees. Officials in Oklahoma and Texas have been working together to monitor the impacts of drought on forest health in both States (Oklahoma Forestry Services 2014, 2015, 2016). Oaks have been especially strongly affected by the drought (Oklahoma Forestry Services 2017). Following the drought, hypoxylon canker has become a problem on the drought-stressed trees (Oklahoma Forestry Services 2017).

In ecoregion section M223A–Boston Mountains (MRATIO = 0.62) in Oklahoma and Arkansas, 87 percent of mortality occurred in the oak-hickory forest type group. Most of the mortality was due to disease (42 percent) or weather (39 percent). As in the adjacent ecoregion section 255A–Cross Timbers and Prairie, a record drought in 2011 and 2012 severely stressed trees, and drought stress was often followed by hypoxylon canker (Barton 2014, Oklahoma Forestry Services 2017). In addition, widespread oak mortality has been

observed throughout Arkansas. This “oak decline” is due to a number of factors that are not all well-understood (Barton 2015).

Western States

As mentioned above, in much of the West, only a relatively small proportion of plots have been remeasured. Thus, the mortality results presented here should be considered preliminary. Also, one must be aware that, because of the longer 10-year measurement cycle in the West, results shown represent mortality that may have occurred any time during the period spanned by the data (see table 5.1), which may have been as long as 16 years.

For large portions of the West, no MRATIO was calculated. At the time this chapter was being written, due to changes being made to the FIA database, growth estimates were not available for the Interior West FIA region. Thus, no MRATIOS were calculated for ecoregion sections in those States. MRATIOS were also not calculated for some ecoregion sections in West Coast States. This was because either (1) <50 plots had been remeasured in an ecoregion section, or (2) the percent sampling error for the growth estimate was too high (>100 percent). One expects that as the first cycle of plot remeasurements is completed in future years, it will be possible to estimate an MRATIO for most of the West. In the ecoregion sections of the West Coast States where the MRATIO could be calculated, ecoregion section M262B–Southern

California Mountain and Valley (MRATIO = 2.50) stands out. This is the highest MRATIO found anywhere in the United States.

Annual mortality as a percentage of total live tree volume is shown in figure 5.3. Besides a sliver of ecoregion section 331F–Western Great Plains (discussed in Eastern and Central States results above) in southeast Montana, there are only two ecoregion sections in which annual mortality exceeded 2 percent of live volume. These are ecoregion sections M262B–Southern California Mountain and Valley and M331E–Uinta Mountains of Utah.

In southern California, tree mortality is most likely related to a combination of prolonged drought (2011–2015), bark beetles, and fire (California Forest Pest Council 2015, 2016). A variety of pests, including mountain pine beetle, fir engraver beetle (*Scolytus ventralis*), and spruce beetle (*D. rufipennis*) have been affecting ecoregion section M331E–Uinta Mountains (USDA Forest Service, Uinta-Wasatch-Cache National Forest [N.d]; Utah Department of Natural Resources, Forestry, Fire, & State Lands 2016).

SUMMARY

This analysis shows that in most of the Eastern and Central United States, mortality is low relative to tree growth. The areas of highest mortality occur in the mostly riparian forests of Great Plains ecoregion sections. A common characteristic of most of these ecoregion sections

having high mortality is that they are on the margins of land suitable for forest growth, being very dry. Thus, they tend to be extremely vulnerable to changes in weather patterns that might produce prolonged and/or extreme drought. Drought, combined with a variety of other biotic and/or abiotic stressors, is likely responsible for much of the mortality observed.

The preliminary analysis of the Western United States shows that, in several parts of the West, mortality is very high as a percent of live volume. These areas correspond to regions where insect outbreaks (see ch. 2) as well as fire (ch. 3) and/or severe drought (ch. 4) have occurred.

It is also important to realize that the analyses presented in this chapter alone cannot tell the complete story regarding tree mortality. Mortality that is concentrated in highly fragmented forest or nonforest areas adjacent to human development may not be detected because the available FIA data do not cover most urban areas or other places not defined as forest by FIA. Also, these analyses are unlikely to detect a pest or pathogen attacking a particular tree species in a mixed-species forest where other species are growing vigorously. This is especially true of species that make up a relatively small proportion of many eastern forests (e.g., ash). For example, it is known that emerald ash borer has been causing very high ash mortality in many Eastern and Central States in recent years (Ohio Department of

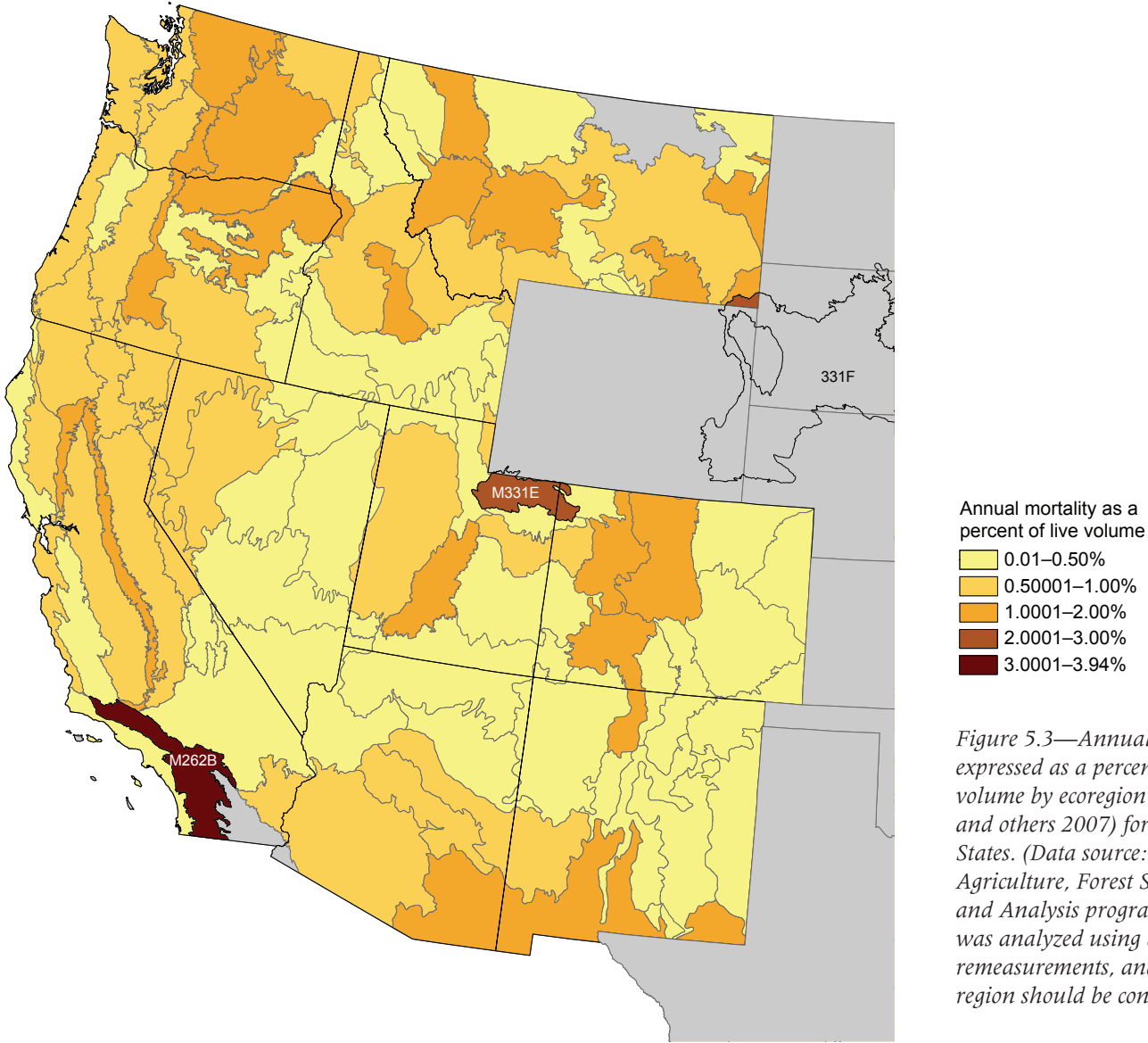


Figure 5.3—Annual tree mortality expressed as a percentage of live tree volume by ecoregion section (Cleland and others 2007) for the Western United States. (Data source: U.S. Department of Agriculture, Forest Service Forest Inventory and Analysis program). Mortality was analyzed using a partial cycle of remeasurements, and results from the region should be considered preliminary.

Natural Resources, Division of Forestry 2016; USDA Animal and Plant Health Inspection Service 2018). Yet, this mortality stands out only in ecoregion section 222U–Lake Whittlesey Glaciolacustrine Plain. Elsewhere in the East, though ash mortality is known to be extremely high, the mortality is masked because ash is a relatively minor component of the forest.

To gain a more complete understanding of mortality, one should consider the results of this analysis together with other indicators of forest health. Forest Inventory and Analysis tree damage data (USDA Forest Service, Forest Inventory and Analysis program 2017), as well as Evaluation Monitoring projects that focus on particular mortality-causing agents (ch. 8–10), can provide insight into smaller scale or species-specific mortality issues. Large-scale analyses of forest-damaging events, including insect and disease activity (ch. 2) and fire (ch. 3), are also important for understanding mortality patterns. This can be especially important in the West, where mortality data are limited.

LITERATURE CITED

- Ambrose, M.J. 2013. Mortality. In: Potter, K.M.; Conkling, B.L., eds. Forest Health Monitoring: national status, trends, and analysis 2011. Gen. Tech. Rep. SRS-185. Asheville, NC: U.S. Department of Agriculture Forest Service, Southern Research Station. 149 p. Chapter 5.
- Ambrose, M.J. 2014. Mortality. In: Potter, K.M.; Conkling, B.L., eds. Forest Health Monitoring: national status, trends, and analysis 2012. Gen. Tech. Rep. SRS-198. Asheville, NC: U.S. Department of Agriculture Forest Service, Southern Research Station. 192 p. Chapter 5.
- Ambrose, M.J. 2015a. Mortality. In: Potter, K.M.; Conkling, B.L., eds. Forest Health Monitoring: national status, trends, and analysis 2014. Gen. Tech. Rep. SRS-209. Asheville, NC: U.S. Department of Agriculture Forest Service, Southern Research Station. 190 p. Chapter 5.
- Ambrose, M.J. 2015b. Mortality. In: Potter, K.M.; Conkling, B.L., eds. Forest Health Monitoring: national status, trends, and analysis 2013. Gen. Tech. Rep. SRS-207. Asheville, NC: U.S. Department of Agriculture Forest Service, Southern Research Station. 199 p. Chapter 5.
- Ambrose, M.J. 2016. Mortality. In: Potter, K.M.; Conkling, B.L., eds. Forest Health Monitoring: national status, trends, and analysis 2015. Gen. Tech. Rep. SRS-213. Asheville, NC: U.S. Department of Agriculture Forest Service, Southern Research Station. 199 p. Chapter 5.
- Ambrose, M.J. 2017. Mortality. In: Potter, K.M.; Conkling, B.L., eds. Forest Health Monitoring: national status, trends, and analysis 2016. Gen. Tech. Rep. SRS-222. Asheville, NC: U.S. Department of Agriculture Forest Service, Southern Research Station. 195 p. Chapter 5.
- Ball, J.; Pyser, N.; Warnke, M. 2016. Forest health highlights in South Dakota 2016. Pierre, SD: South Dakota Department of Agriculture, Division of Resource Conservation and Forestry. 6 p. <https://www.fs.fed.us/foresthealth/protecting-forest/forest-health-monitoring/monitoring-forest-highlights.shtml>. [Date accessed: May 9, 2018].
- Ball, J.; Seidl, A.; Warnke, M. 2017. State of South Dakota forest health highlights 2017. Pierre, SD: South Dakota Department of Agriculture, Division of Resource Conservation and Forestry. 8 p. https://sdda.sd.gov/conservation-forestry/forest-health/SDHighlights_2017-2.pdf. [Date accessed: March 15, 2019].
- Ball, J.; Warnke, M.; Garbisch, B. 2015. Forest health highlights in South Dakota 2015. Pierre, SD: South Dakota Department of Agriculture, Division of Resource Conservation and Forestry. 9 p. <https://www.fs.fed.us/foresthealth/protecting-forest/forest-health-monitoring/monitoring-forest-highlights.shtml>. [Date accessed: May 9, 2018].
- Barton, C. 2014. Arkansas forest health highlights 2015. Little Rock, AR: Arkansas Forestry Commission. 4 p. https://www.fs.fed.us/foresthealth/docs/fhh/AR_FHH_2014.pdf. [Date accessed: May 9, 2018].

- Barton, C. 2015. Arkansas forest health highlights 2014. Little Rock, AR: Arkansas Forestry Commission. 4 p. https://www.fs.fed.us/foresthealth/docs/fhh/AR_FHH_2015.pdf. [Date accessed: May 9, 2018].
- Bechtold, W.A.; Patterson, P.L., eds. 2005. The enhanced Forest Inventory and Analysis program—national sampling design and estimation procedures. Gen. Tech. Rep. SRS-80. Asheville, NC: U.S. Department of Agriculture Forest Service, Southern Research Station. 85 p.
- Burns, R.M.; Honkala, B.H. 1990. Silvics of North America, volume 1: conifers. Agriculture Handbook 654. Washington, DC: U.S. Department of Agriculture Forest Service. 675 p.
- Burrill, E.A.; Wilson, A.M.; Turner, J.A. [and others]. 2017. The Forest Inventory and Analysis database: database description and users manual for Phase 2 (version 7.0.1). Washington, DC: U.S. Department of Agriculture Forest Service. <http://fia.fs.fed.us/library/database-documentation/>. [Date accessed: May 16, 2018].
- California Forest Pest Council. 2015. 2015 California forest health highlights. 21 p. <https://www.fs.fed.us/foresthealth/protecting-forest/forest-health-monitoring/monitoring-forest-highlights.shtml>. [Date accessed May 9, 2018].
- California Forest Pest Council. 2016. 2016 California forest health highlights. 31 p. <https://www.fs.fed.us/foresthealth/protecting-forest/forest-health-monitoring/monitoring-forest-highlights.shtml>. [Date accessed: May 9, 2018].
- Cleland, D.T.; Freeouf, J.A.; Keys, J.E. [and others]. 2007. Ecological subregions: sections and subsections for the conterminous United States. Gen. Tech. Report WO-76D. Washington, DC: U.S. Department of Agriculture Forest Service. Map; Sloan, A.M., cartographer; presentation scale 1:3,500,000; colored. Also on CD-ROM as a GIS coverage in ArcINFO format or at <http://data.fs.usda.gov/geodata/edw/datasets.php>. [Date accessed: July 20, 2015].
- Coulston, J.W.; Ambrose, M.J.; Stolte, K.S. [and others]. 2005. Criterion 3 – health and vitality. In: Conkling, B.L.; Coulston, J.W.; Ambrose, M.J., eds. Forest Health Monitoring 2001 national technical report. Gen. Tech. Rep. SRS-81. Asheville, NC: U.S. Department of Agriculture Forest Service, Southern Research Station. 204 p.
- Johnson, L. 2017. Forest health highlights: North Dakota 2017. 12 p. <https://www.ag.ndsu.edu/ndfs/documents/north-dakota-forest-health-highlights-2017.pdf>. [Date accessed: March 15, 2019].
- McNab, W.H.; Cleland, D.T.; Freeouf, J.A. [and others], comps. 2007. Description of ecological subregions: sections of the conterminous United States [CD-ROM]. Gen. Tech. Report WO-76B. Washington, DC: U.S. Department of Agriculture Forest Service. 80 p.
- Michigan Department of Natural Resources. 2014. 2014 forest health highlights. 51 p. <https://www.fs.fed.us/foresthealth/protecting-forest/forest-health-monitoring/monitoring-forest-highlights.shtml>. [Date accessed: April 27, 2018].
- Michigan Department of Natural Resources. 2015. 2015 forest health highlights. 50 p. <https://www.fs.fed.us/foresthealth/protecting-forest/forest-health-monitoring/monitoring-forest-highlights.shtml>. [Date accessed: April 8, 2018].
- Michigan Department of Natural Resources. 2016. 2016 forest health highlights. 51 p. <https://www.fs.fed.us/foresthealth/protecting-forest/forest-health-monitoring/monitoring-forest-highlights.shtml>. [Date accessed: April 8, 2018].
- Michigan Department of Natural Resources. 2017. 2017 forest health highlights. 31 p. https://www.michigan.gov/documents/dnr/frsthlthghlghts_513144_7.pdf. [Date accessed: May 8, 2018].
- Miles, P.D. 2015. Forest Inventory EVALIDator web-application version 1.7.0.01. St. Paul, MN: U.S. Department of Agriculture Forest Service, Northern Research Station. <http://apps.fs.fed.us/Evalidator/evalidator.jsp>. [Date accessed: May 13, 2018].
- Nebraska Forest Service. 2011. Nebraska forest health highlights 2011. 5 p. <https://www.fs.fed.us/foresthealth/protecting-forest/forest-health-monitoring/monitoring-forest-highlights.shtml>. [Date accessed: May 1, 2018].
- Nebraska Forest Service. 2012. Nebraska forest health highlights 2012. 5 p. <https://www.fs.fed.us/foresthealth/protecting-forest/forest-health-monitoring/monitoring-forest-highlights.shtml>. [Date accessed: May 1, 2018].

- Nebraska Forest Service. 2013. Nebraska forest health highlights 2013. 4 p. <https://www.fs.fed.us/foresthealth/protecting-forest/forest-health-monitoring/monitoring-forest-highlights.shtml>. [Date accessed: June 2, 2018].
- Nebraska Forest Service. 2014. Nebraska forest health highlights 2014. 4 p. <https://www.fs.fed.us/foresthealth/protecting-forest/forest-health-monitoring/monitoring-forest-highlights.shtml>. [Date accessed: June 2, 2018].
- Nebraska Forest Service. 2015. Nebraska forest health highlights 2015. 6 p. <https://www.fs.fed.us/foresthealth/protecting-forest/forest-health-monitoring/monitoring-forest-highlights.shtml>. [Date accessed: May 10, 2018].
- Nebraska Forest Service. 2016. Nebraska forest health highlights 2016. 6 p. <https://www.fs.fed.us/foresthealth/protecting-forest/forest-health-monitoring/monitoring-forest-highlights.shtml>. [Date accessed: May 10, 2018].
- Nebraska Forest Service. 2017. Nebraska forest health highlights 2017. 6 p. https://www.fs.fed.us/foresthealth/docs/fhh/NE_FHH_2017.pdf. [Date accessed: August 25, 2018].
- North Dakota Forest Service. 2012. North Dakota forest health highlights 2012. 12 p. <https://www.fs.fed.us/foresthealth/protecting-forest/forest-health-monitoring/monitoring-forest-highlights.shtml>. [Date accessed: May 15, 2018].
- North Dakota Forest Service. 2013. North Dakota forest health highlights 2013. 12 p. <https://www.fs.fed.us/foresthealth/protecting-forest/forest-health-monitoring/monitoring-forest-highlights.shtml>. [Date accessed: April 26, 2018].
- North Dakota Forest Service. 2014. North Dakota forest health highlights 2014. 24 p. <https://www.fs.fed.us/foresthealth/protecting-forest/forest-health-monitoring/monitoring-forest-highlights.shtml>. [Date accessed: April 12, 2018].
- North Dakota Forest Service. 2015. North Dakota forest health highlights 2015. 24 p. <https://www.fs.fed.us/foresthealth/protecting-forest/forest-health-monitoring/monitoring-forest-highlights.shtml>. [Date accessed: April 12, 2018].
- North Dakota Forest Service. 2016. North Dakota forest health highlights 2016. 4 p. <https://www.ag.ndsu.edu/ndfs/documents/north-dakota-forest-health-highlights-2016.pdf>. [Date accessed: August 25, 2018].
- Ohio Department of Natural Resources, Division of Forestry. 2014. 2014 Ohio forest health highlights. 7 p. Columbus, OH: Ohio Department of Natural Resources, Division of Forestry. <https://www.fs.fed.us/foresthealth/protecting-forest/forest-health-monitoring/monitoring-forest-highlights.shtml>. [Date accessed: April 27, 2018].
- Ohio Department of Natural Resources, Division of Forestry. 2015. 2015 Ohio forest health highlights. 8 p. Columbus, OH: Ohio Department of Natural Resources, Division of Forestry. <https://www.fs.fed.us/foresthealth/protecting-forest/forest-health-monitoring/monitoring-forest-highlights.shtml>. [Date accessed: April 17, 2018].
- Ohio Department of Natural Resources, Division of Forestry. 2016. 2016 Ohio forest health highlights. 8 p. Columbus, OH: Ohio Department of Natural Resources, Division of Forestry. <https://www.fs.fed.us/foresthealth/protecting-forest/forest-health-monitoring/monitoring-forest-highlights.shtml>. [Date accessed: April 17, 2018].
- Oklahoma Forestry Services. 2014. Oklahoma forest health highlights 2014. 5 p. <https://www.fs.fed.us/foresthealth/protecting-forest/forest-health-monitoring/monitoring-forest-highlights.shtml>. [Date accessed: April 2, 2018].
- Oklahoma Forestry Services. 2015. Oklahoma forest health highlights 2015. 6 p. <https://www.fs.fed.us/foresthealth/protecting-forest/forest-health-monitoring/monitoring-forest-highlights.shtml>. [Date accessed: April 3, 2018].
- Oklahoma Forestry Services. 2016. Oklahoma forest health highlights 2016. 6 p. <https://www.fs.fed.us/foresthealth/protecting-forest/forest-health-monitoring/monitoring-forest-highlights.shtml>. [Date accessed: April 2, 2018].
- Oklahoma Forestry Services. 2017. Oklahoma forest health highlights 2017. 7 p. https://www.fs.fed.us/foresthealth/docs/fhh/OK_FHH_2017.pdf. [Date accessed: August 25, 2018].
- Smith, L.A. 2013. Forest health insects and diseases conditions Texas 2013. Longview, TX: Texas A & M Forest Service. 5 p. <https://www.fs.fed.us/foresthealth/protecting-forest/forest-health-monitoring/monitoring-forest-highlights.shtml>. [Date accessed: April 27, 2018].

- Smith, L.A. 2014. Forest health highlights in Texas 2014. Longview, TX: Texas A & M Forest Service. 1 p. <https://www.fs.fed.us/foresthealth/protecting-forest/forest-health-monitoring/monitoring-forest-highlights.shtml>. [Date accessed: April 27, 2018].
- South Dakota Department of Agriculture. 2011. South Dakota forest health highlights 2011. Pierre, SD: South Dakota Department of Agriculture, Division of Resource Conservation and Forestry. 4 p. <https://www.fs.fed.us/foresthealth/protecting-forest/forest-health-monitoring/monitoring-forest-highlights.shtml>. [Date accessed: May 1, 2018].
- South Dakota Department of Agriculture. 2012. South Dakota 2012 forest health highlights. Pierre, SD: South Dakota Department of Agriculture, Division of Resource Conservation and Forestry. 5 p. <https://www.fs.fed.us/foresthealth/protecting-forest/forest-health-monitoring/monitoring-forest-highlights.shtml>. [Date accessed: March 15, 2018].
- South Dakota Department of Agriculture. 2013. South Dakota 2013 forest health highlights. Pierre, SD: South Dakota Department of Agriculture, Division of Resource Conservation and Forestry. 5 p. <https://www.fs.fed.us/foresthealth/protecting-forest/forest-health-monitoring/monitoring-forest-highlights.shtml>. [Date accessed: March 15, 2018].
- South Dakota Department of Agriculture. 2014. South Dakota 2014 forest health highlights. Pierre, SD: South Dakota Department of Agriculture, Division of Resource Conservation and Forestry. 7 p. <https://www.fs.fed.us/foresthealth/protecting-forest/forest-health-monitoring/monitoring-forest-highlights.shtml>. [Date accessed: March 15, 2018].
- Texas A & M Forest Service. 2015. Forest health highlights in Texas 2015. Longview, TX: Texas A & M Forest Service. 1 p. <https://www.fs.fed.us/foresthealth/protecting-forest/forest-health-monitoring/monitoring-forest-highlights.shtml>. [Date accessed: April 20, 2018].
- Texas A & M Forest Service. 2016. Forest health highlights in Texas 2016. Longview, TX: Texas A & M Forest Service. 1 p. <https://www.fs.fed.us/foresthealth/protecting-forest/forest-health-monitoring/monitoring-forest-highlights.shtml>. [Date accessed: April 20, 2018].
- Texas A & M Forest Service. 2017. Forest health highlights 2017. Longview, TX: Texas A & M Forest Service. 2 p. <https://www.fs.fed.us/foresthealth/protecting-forest/forest-health-monitoring/monitoring-forest-highlights.shtml>. [Date accessed: May 21, 2018].
- U.S. Department of Agriculture (USDA) Animal and Plant Health Inspection Service. 2018. Emerald ash borer. <https://www.aphis.usda.gov/aphis/resources/pests-diseases/hungry-pests/the-threat/emerald-ash-borer/emerald-ash-borer-beetle>. [Date accessed: August 31, 2018].
- U.S. Department of Agriculture (USDA) Forest Service. 2008. National forest type dataset. http://data.fs.usda.gov/geodata/rastergateway/forest_type/index.php. [Date accessed: September 13, 2016].
- U.S. Department of Agriculture (USDA) Forest Service, Forest Inventory and Analysis program. 2017. Forest Inventory and Analysis Database, St. Paul, MN: U.S. Department of Agriculture Forest Service, Northern Research Station. <https://apps.fs.usda.gov/fia/datamart/datamart.html>. [Date accessed: March 1, 2019].
- U.S. Department of Agriculture (USDA) Forest Service, Uinta-Wasatch-Cache National Forest. [N.d.]. Beetle activity on the Uinta-Wasatch-Cache National Forest. <http://www.fs.usda.gov/detail/uwcnf/home/?cid=STELPRDB5145143>. [Date accessed: July 25, 2017].
- Utah Department of Natural Resources, Forestry, Fire, & State Lands. 2016. Utah forest health highlights 2016. 3 p. <https://www.fs.fed.us/foresthealth/protecting-forest/forest-health-monitoring/monitoring-forest-highlights.shtml>. [Date accessed: April 24, 2018].
- Wyoming State Forestry Division. 2017. 2017 Wyoming forest health highlights. 17 p. https://www.fs.fed.us/foresthealth/docs/fhh/WY_FHH_2017.pdf. [Date accessed: August 25, 2018].

Section 2.

Analyses of
Long-Term Forest
Health Trends and
Presentations of
New Techniques

INTRODUCTION

Invasive species can cause a variety of undesirable changes in forest health simply by altering forest species composition (Fei and others 2014, Kettenring and Adams 2011, Mack and others 2000). In the Eastern United States, forest inventory data suggest that a large proportion of the rural forest area already contains harmful invasive species (Oswalt and Oswalt 2015, Oswalt and others 2015). To further inform forest managers about the relative risks of adverse impacts in different situations, the objectives of this study were (1) to compare forest types in the Eastern United States with respect to the likelihood that they contain invasive forest plants, and (2) to evaluate the relative roles of public versus private forest ownership for conserving the uninvaded forest area. Our goal was to identify forest types with relatively high or low probabilities of current invasion, and to highlight the forest types for which either public or private forest management could be focused on the conservation of the uninvaded area. The study area (fig. 6.1) included the 13 ecological provinces (Bailey 1995, Cleland and others 2007) that contain most of the temperate and boreal forest in the Eastern United States. Almost all of the forest in the region has been modified by humans, and approximately 40 percent of the original forest area has been

converted to other land uses (Smith and others 2009). Approximately three-fourths of the forest area is privately owned (Oswalt and others 2014). Observations made on Forest Inventory and Analysis (FIA) plots have found 71 harmful invasive plant species (as defined by Ries and others 2004) (Iannone 2018¹) on approximately one-half of the plots surveyed in the study area (Oswalt and Oswalt 2015, Oswalt and others 2015).

METHODS

The plot data alone do not provide a statistical basis for regional comparisons of invasions among forest types or owners because invasive plant observations have not been made at all FIA plots in the study area. Instead, to accomplish our objectives we integrated a plot-level model of forest plant invasions with a statistically representative sample of FIA plots. Invasibility (the probability that a forest plot has been invaded) was estimated from plot and landscape (neighborhood) attributes. Invadedness (the absolute areas of invaded and uninvaded forest) was estimated by using the statistical design of the forest inventory to scale up the plot-level invasibility estimates to all forest area. Comparisons of forest types and ownerships were then conducted by post-stratifying the estimates of invasibility and invadedness by forest type and land ownership.

¹ Personal communication. 2018. B. Iannone III, Assistant Professor, Residential Landscape Ecology, University of Florida, P.O. Box 110940, Gainesville, FL 32611-0940.

CHAPTER 6.

The Invasibility and Invadedness of Eastern U.S. Forest Types

KURT H. RIITERS

KEVIN M. POTTER

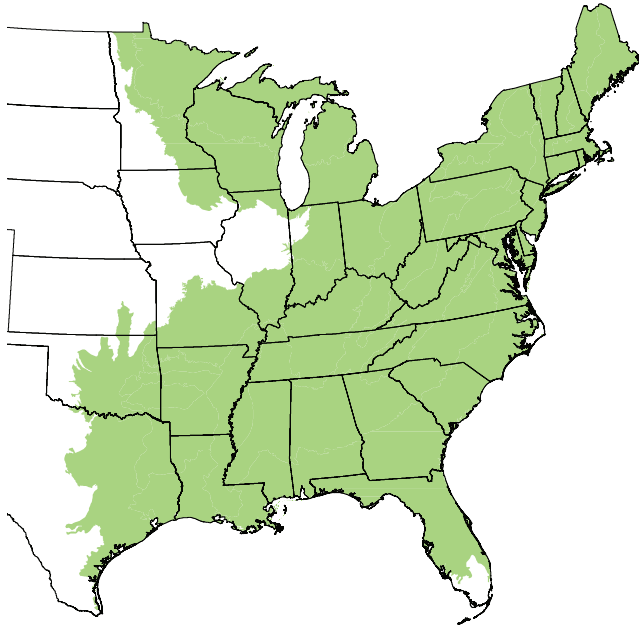


Figure 6.1—The study area encompassed most of the temperate and boreal forest in the Eastern United States. (Data source: Cleland and others 2007)

The plot-level invasibility model (similar to the model described by Riitters and others 2017) was developed using 23,039 FIA plots that had been surveyed for invasive plants between 2001 and 2011. To predict invasibility, the model employed logistic regression with independent variables measuring ecological province, site productivity, distance to a road, land use (590-ha neighborhood), and forest

fragmentation (15-ha neighborhood). The model was applied to a representative sample of 82,506 FIA plots from the FIA database (O’Connell and others 2015) that constituted a statistical basis for forest area estimation circa 2006. Each plot record had an expansion factor that indicated the forest area represented by a given condition (defined by, among other attributes, site productivity, forest type, and ownership) (Bechtold and Patterson 2005). The expansion factors accounted for within-plot variability of forest type and ownership.

We applied the approach described by Riitters and others (2011) to extrapolate and stratify the plot-level estimates of invasibility. In the same way that a regional estimate of the area of a given forest type is the sum of the expansion factors for the plot records of that type, a regional estimate of a given level of invasibility was the sum of the expansion factors over all plots with that invasibility. Furthermore, since the product of invasibility and expansion factor estimates the area invaded, a regional estimate of invadedness (total area invaded) was the sum of those estimates over all plots. Finally, stratification was performed by defining subsets of plots according to forest type and/or ownership, and summing the area within each subset. There were 74 forest types (O’Connell and others 2015) after excluding those that were not included in the development

of the plot-level invasibility model.² The 17 FIA ownership categories (O’Connell and others 2015) were combined into four classes—Federal (government), State and local (government), private corporate, and private non-corporate.

For simplicity, we report area estimates without confidence intervals. The model correctly classified randomly drawn pairs of invaded and uninvaded plots 76 percent of the time, a reasonably good rate that was significantly ($X^2 = 232$; $p < 0.001$) better than chance. At a broader spatial scale, the regional pattern of predicted, per-plot invasibility was similar to the pattern of observed per-county invasion rates (Oswalt and Oswalt 2015). The FIA sample design has a target precision of ± 3 percent for forest area estimates in the Eastern United States (Bechtold and Patterson 2005).

RESULTS AND DISCUSSON

We estimated that invasive forest plants occur on 51 percent of the 152 million ha of forest land considered in this study (table 6.1). Estimated invadedness ranged from 20 to 61 percent of total area of each of the 10 forest type groups recognized by FIA. Over half of the

² The following forest type groups were excluded because they were not included in the development of the invasibility model: other eastern softwoods; pinyon-juniper; exotic softwoods; other hardwoods; woodland hardwoods; tropical hardwoods; and exotic hardwoods. Also excluded were the Fraser fir forest type (because of small sample size), and data records lacking forest type information (including non-stocked plots).

Table 6.1—Total area and invadedness of 10 FIA forest type groups in the Eastern United States, by percent area invaded

Forest type group	Total area ^a		Invadedness (area invaded) ^a
	<i>thousand ha</i>	<i>percent</i>	<i>thousand ha</i>
Loblolly-shortleaf pine	23 225	61	14 096
Elm-ash-cottonwood	8 442	59	5 004
Oak-pine	11 319	58	6 564
Oak-hickory	57 732	58	33 480
Oak-gum-cypress	9 639	49	4 702
Longleaf-slash pine	5 256	43	2 268
White-red-jack pine	3 584	40	1 420
Maple-beech-birch	18 936	34	6 446
Aspen-birch	6 925	32	2 186
Spruce-fir	6 124	20	1 199
All forest type groups	151 180	51	77 365

^a Sums may have rounding error.

invaded area was contained in two forest type groups (loblolly-shortleaf pine, oak-hickory), in part because those two types were the most common types in the region.³ The statistics in table 6.1 suggested broad geographical patterns resulting from the overall geographical distinctness of different forest types. For example, the spruce-fir, maple-beech-birch, and aspen-birch type groups tend to occur in the relatively remote portions of the study area, where invasion pressures are probably lower than elsewhere (Iannone and others 2015).

³ See O’Connell and others (2015) for scientific names of species, and fuller descriptions of forest types and forest type groups.

At the same time, invadedness varied substantially among forest types within forest type groups (table 6.2). For example, the loblolly-shortleaf pine type group had the highest percent invadedness (61 percent; table 6.1), but included two forest types that exhibited relatively low percent invadedness—pond pine (28 percent) and Table Mountain pine (21 percent). Conversely, within the spruce-fir type group that had the lowest percent invadedness (20 percent; table 6.1), invadedness ranged from 10 percent (red spruce-balsam fir type) to 36 percent (white spruce type). Invadedness also varied substantially among ownerships (table 6.3). Approximately one-third of public forest land was invaded, compared to 46 percent of private corporate forest and 59 percent of private non-corporate forest. The overall percent of forest invaded (51 percent) reflected the higher percentages in private ownerships that together comprised 81 percent of total forest area.

Since forest types are not distributed uniformly across ownerships (results not shown), the large variation of invadedness among both forest types and ownerships implies that conservation of uninvaded forest (or remediation of invaded forest) could potentially be focused on either public or private forest management depending on the forest type to be conserved (or remediated). To allow detailed examination of those possibilities, the invaded and uninvaded forest type areas by ownership are shown in figure 6.2. In figure 6.2, each row represents a single forest type. Along the

Table 6.2—Invadedness and area by forest type

Forest type group ^a	Forest type	Invadedness	Area
		percent	thousand ha
Loblolly-shortleaf pine	Virginia pine	70	836
	Loblolly pine	62	20 207
	Shortleaf pine	53	1329
	Spruce pine	48	18
	Pitch pine	34	305
	Sand pine	32	249
	Pond pine	28	264
	Table Mountain pine	21	18
Elm-ash-cottonwood	Silver maple-American elm	75	328
	Cottonwood	69	252
	Cottonwood-willow	69	145
	River birch-sycamore	68	759
	Sugarberry-hackberry-elm-green ash	63	3217
	Sycamore-pecan-American elm	62	1210
	Willow	53	445
	Red maple (lowland)	51	871
	Black ash-American elm-red maple	42	1217
Oak-pine	Virginia pine-southern red oak	67	867
	Eastern redcedar-hardwood	65	1053
	Loblolly pine-hardwood	63	5075
	Shortleaf pine-oak	59	1192
	Eastern white pine-northern red oak	48	1328
	Longleaf pine-oak	44	395
	Slash pine-hardwood	44	606
	Other pine-hardwood	38	803

continued

Table 6.2 (continued)—Invadedness and area by forest type

Forest type group ^a	Forest type	Invadedness	Area
		percent	thousand ha
Oak-hickory	Black walnut	75	259
	Sweetgum-yellow-poplar	71	3080
	Bur oak	69	265
	Cherry-white ash-yellow-poplar	66	2226
	Black locust	65	353
	Elm-ash-black locust	64	2280
	Yellow-poplar	63	1242
	Mixed upland hardwoods	62	8556
	Sassafras-persimmon	61	968
	White oak-red oak-hickory	60	17 967
	White oak	60	2833
	Yellow-poplar-white oak-northern red oak	57	3027
	Red maple-oak	57	1344
	Post oak-blackjack oak	55	4461
	Scarlet oak	52	419
	Chestnut oak-black oak-scarlet oak	44	3754
	Northern red oak	43	1862
Chestnut oak	37	2122	
Southern scrub oak	37	713	
Oak-gum-cypress	Swamp chestnut oak-cherrybark oak	60	559
	Sweetgum-Nuttall oak-willow oak	55	3866
	Overcup oak-water hickory	47	557
	Sweetbay-swamp tupelo-red maple	44	3288
	Baldcypress-water tupelo	41	968
	Baldcypress-pondcypress	34	371
	Atlantic white-cedar	27	32

continued

Forest type group ^a	Forest type	Invadedness	Area
		percent	thousand ha
Longleaf-slash pine	Slash pine	43	3942
	Longleaf pine	42	1313
White-red-jack pine	Eastern white pine	47	1377
	Eastern white pine-eastern hemlock	40	203
	Red pine	38	923
	Eastern hemlock	33	511
	Jack pine	31	570
Maple-beech-birch	Black cherry	57	554
	Hard maple-basswood	47	3760
	Red maple (upland)	32	1843
	Sugar maple-beech-yellow birch	29	12 778
Aspen-birch	Gray birch	42	131
	Aspen	34	4941
	Balsam poplar	34	358
	Pin cherry	26	122
	Paper birch	22	1373
Spruce-fir	White spruce	36	241
	Tamarack	24	733
	Northern white-cedar	23	1417
	Balsam fir	18	1509
	Black spruce	18	1212
	Red spruce	13	503
	Red spruce-balsam fir	10	508

^a Forest type group is shown for reference.

Table 6.3—Area and invadedness by ownership

Ownership	Total area ^a		Invadedness (area invaded) ^a	
	thousand ha	percent	thousand ha	
Federal	13 641	35	4 762	
State and local	15 597	33	5 173	
Private corporate	35 124	46	16 052	
Private non-corporate	86 818	59	51 378	
All ownerships	151 180	51	77 365	

^aSums may have rounding error.

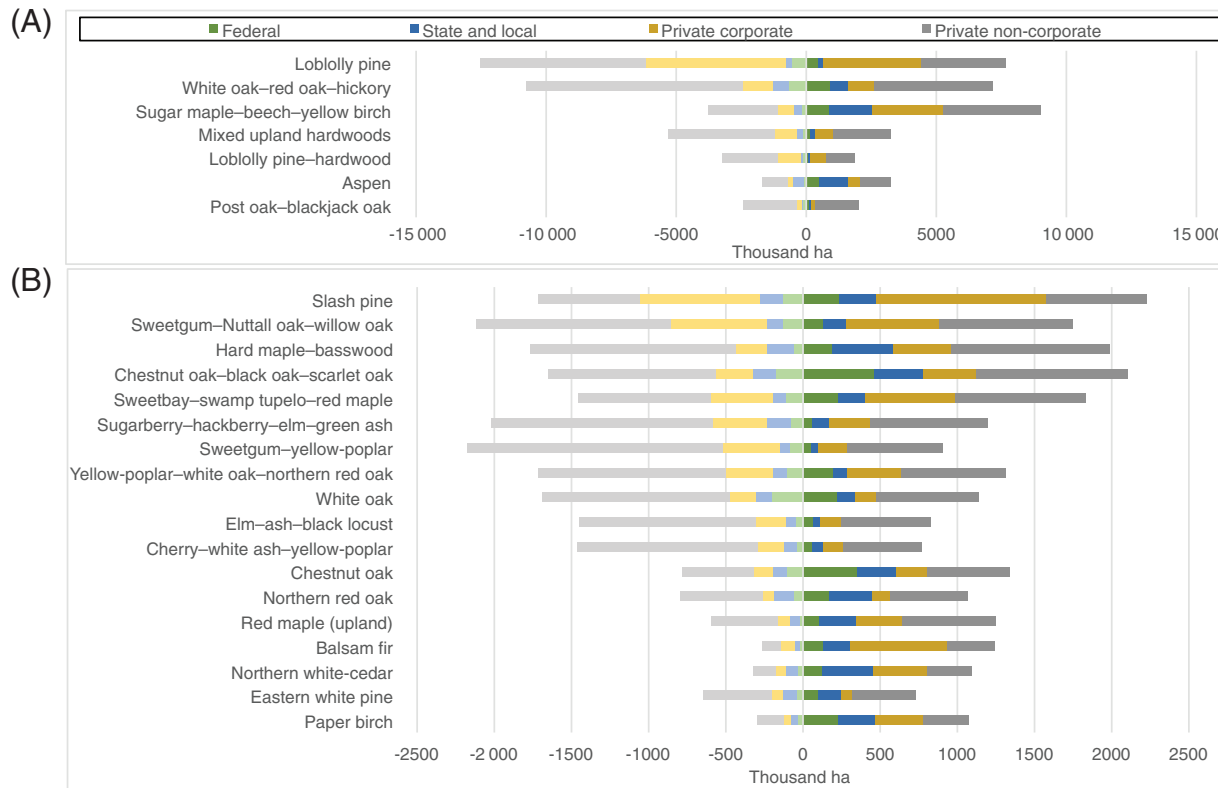


Figure 6.2—Summary of invaded and uninvaded forest area by forest type and ownership. The four panels (A, B, C, D) group forest types with similar total area; note the change in the horizontal axis scale between panels. Within each panel, forest types are sorted by decreasing total area. The invaded area is indicated by negative numbers (left of zero); the uninvaded area is indicated by positive numbers (right of zero). Colors indicate ownership, with lighter shades used for the invaded area. (Data sources: Forest Service Forest Inventory and Analysis; Riitters and others 2017) (continued to next page)

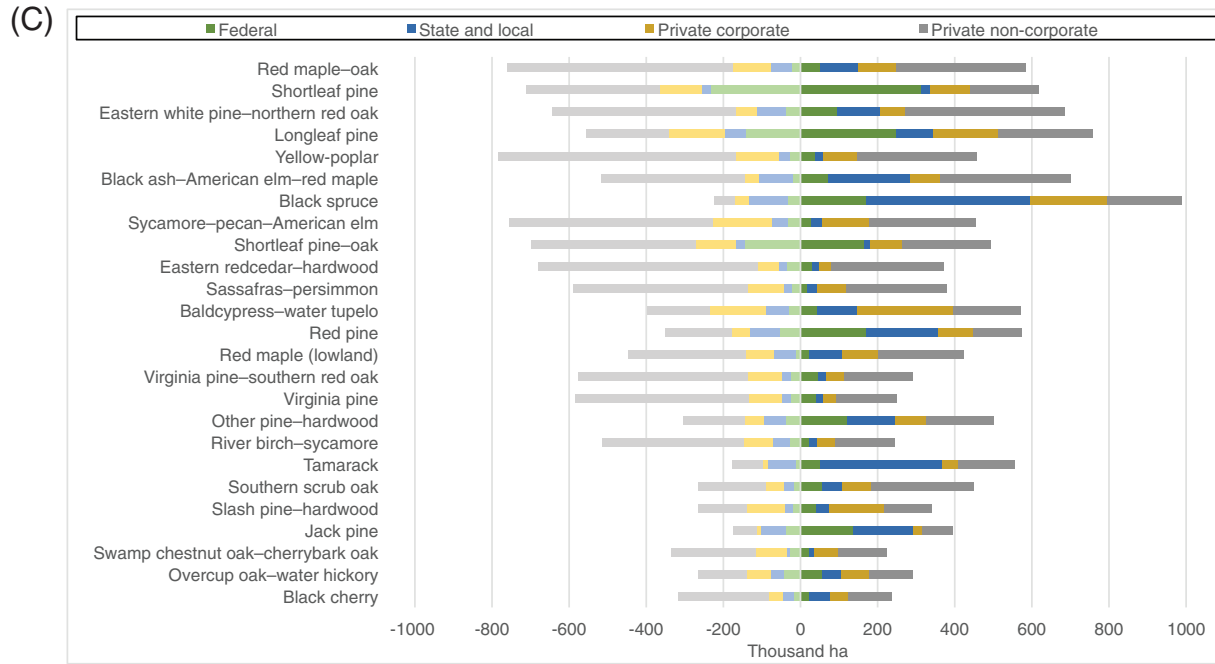
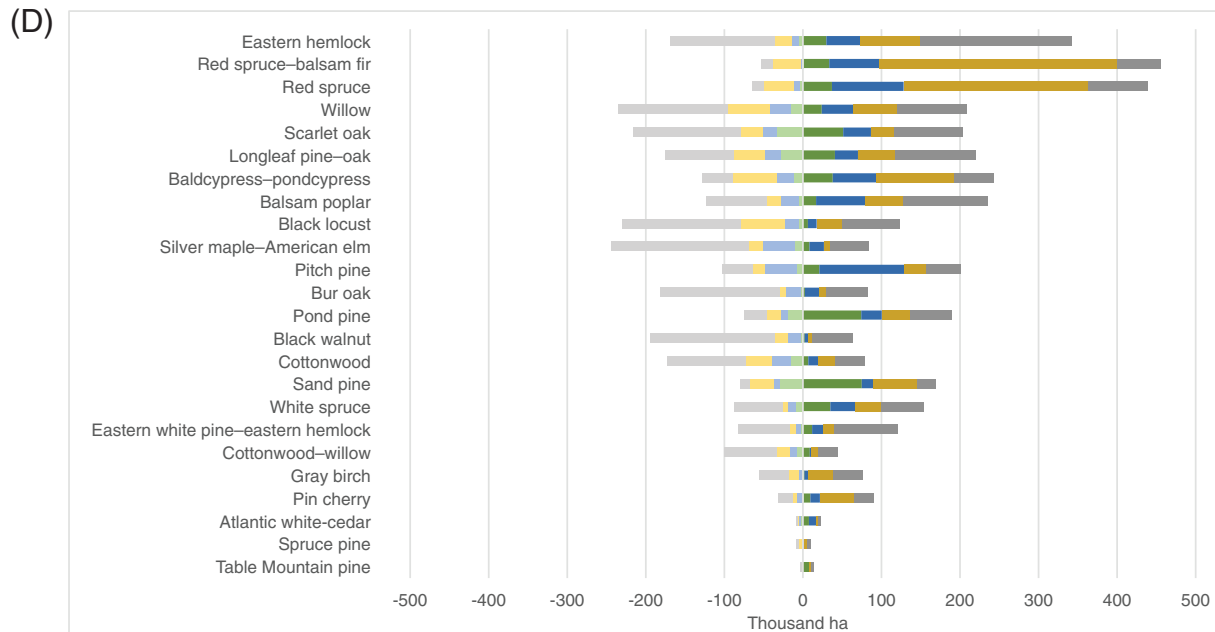


Figure 6.2 (continued)— Summary of invaded and uninvaded forest area by forest type and ownership. The four panels (A, B, C, D) group forest types with similar total area; note the change in the horizontal axis scale between panels. Within each panel, forest types are sorted by decreasing total area. The invaded area is indicated by negative numbers (left of zero); the uninvaded area is indicated by positive numbers (right of zero). Colors indicate ownership, with lighter shades used for the invaded area. (Data sources: Forest Service Forest Inventory and Analysis; Riitters and others 2017)



horizontal axis, the negative numbers indicate the estimated invaded area, and the positive numbers indicate the estimated uninverted area. The four primary colors on each bar represent the four types of ownership, with lighter shades of those colors used for the uninverted area. The scale of the horizontal axis changes between the panels of figure 6.2 to make it easier to see results for the less-common forest types. Using the loblolly pine type as an example (see first row of fig. 6.2A), and reading left to right, the invaded area includes 6.4 million ha of private non-corporate forest (light gray), 5.4 million ha of private corporate forest (light gold), 0.2 million ha of State and local forest (light blue), and 0.6 million ha of Federal forest (light green). The uninverted loblolly pine type includes 0.5 million ha of Federal forest (green), 0.2 million ha of State and local forest (blue), 3.8 million ha of private corporate forest (gold), and 3.2 million ha of private non-corporate forest (gray).

To simplify the information and to address our immediate objective, that information was condensed to show the percent share of forest type area in public ownership (Federal, State, local) in relation to the percent of forest type area that was invaded (fig. 6.3). From the chart it is apparent that any strategy to mitigate or remediate conditions in highly-invaded (e.g., $>2/3$ of total area) forest types could be focused on private ownerships, because the public ownership share of the area of those forest types is typically <20 percent. At the other extreme, the conservation of relatively less invaded (e.g., $<1/3$ of total area) forest types could be

focused on either public ownerships or private ownerships depending on the specific forest type. For example, conservation on public lands could focus on Atlantic white-cedar, jack pine, tamarack, and black spruce, while conservation on private lands could focus on red spruce, balsam fir, pin cherry, and red maple (upland).

CONCLUSIONS

We combined the statistical power of the FIA forest inventory system with the predictive power of a plot-level plant invasion model to compare forest types in the Eastern United States with respect to the likelihood that they contain invasive forest plants, and to evaluate the relative roles of public versus private forest ownership for conserving the uninverted forest area. We estimated that approximately half of the total area of 74 forest types was invaded, and that invasions were almost twice as likely on privately owned land than on publicly owned land. Individual forest types varied widely in terms of historical invasions, but ownership alone was the deciding factor for the most-invaded forest types. There were no forest types for which a remediation focus on public land would be efficient, i.e., consideration of privately owned lands is probably necessary for controlling invasive plants. For the least-invaded forest types, there were several instances for which the efficiency of a conservation focus on either public or private land would depend on the forest type. While a regional analysis can suggest forest management strategies such as these, actual implementation necessarily depends on local conditions.

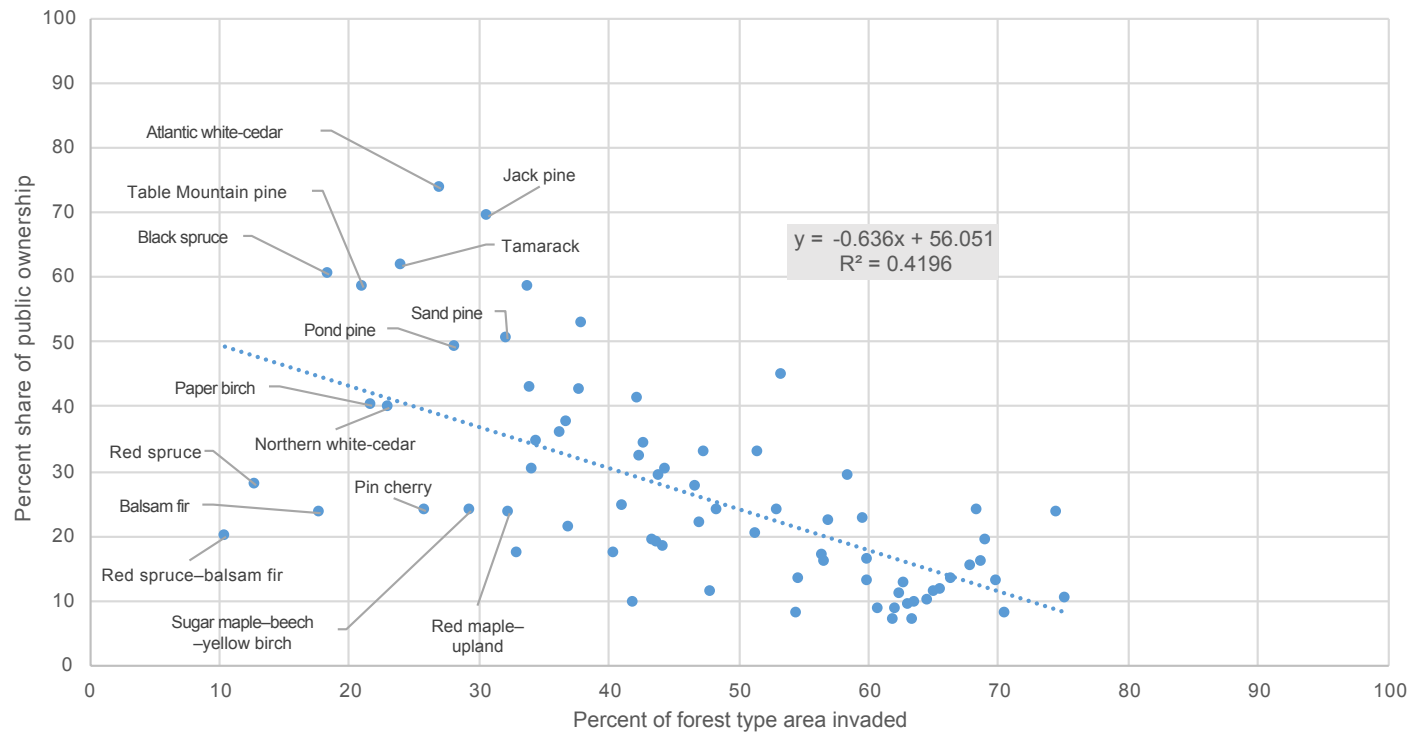


Figure 6.3—Share of public ownership in relation to percent of area invaded for 74 forest types. The forest types with less than one-third of total area invaded are labeled. Public ownership includes Federal, State, and local government ownership. The estimated linear regression line is shown for information only.

ACKNOWLEDGMENTS

Thanks are due the many U.S. Department of Agriculture Forest Service FIA staff who collected all of the data used in this study. Basil Iannone III (University of Florida) and Christopher Oswalt (U.S. Department of Agriculture Forest Service) provided FIA plot summaries of invasive forest plant data. John

Coulston (U.S. Department of Agriculture Forest Service) identified the representative set of FIA plots and provided plot summaries of statistical weights, forest types, and ownerships. This research was supported in part by U.S. Department of Agriculture Forest Service Agreement 13-JV-113301-046 with North Carolina State University.

LITERATURE CITED

- Bailey, R.G. 1995. Descriptions of the ecoregions of the United States. 2d ed. Misc. Publ. 1391. Washington, DC: U.S. Department of Agriculture Forest Service. 108 p.
- Bechtold, W.A.; Patterson, P.L., eds. 2005. The enhanced Forest Inventory and Analysis program – national sampling design and estimation procedures. Gen. Tech. Rep. SRS-80. Asheville, NC: U.S. Department of Agriculture Forest Service, Southern Research Station. 85 p.
- Cleland, D.T.; Freeouf, J.A.; Keys, J.E. [and others]. 2007. Ecological subregions: sections and subsections for the conterminous United States. Gen. Tech. Rep. WO-76D. Washington, DC: U.S. Department of Agriculture Forest Service. Map; Sloan, A.M., cartographer; presentation scale 1:3,500,000; colored. Also on CD-ROM as a GIS coverage in ArcINFO format or at <http://data.fs.usda.gov/geodata/edw/datasets.php>. [Date accessed: July 20, 2015].
- Fei, S.; Phillips, J.; Shouse, M. 2014. Biogeomorphic impacts of invasive species. *Annual Review of Ecology, Evolution, and Systematics*. 45: 69–87.
- Iannone, B.V.; Oswalt, C.M.; Liebhold, A.M. [and others]. 2015. Region-specific patterns and drivers of macroscale forest plant invasions. *Diversity and Distributions*. 21: 1181–1192.
- Kettenring, K.M.; Adams, C.R. 2011. Lessons learned from invasive plant control experiments: a systematic review and meta-analysis. *Journal of Applied Ecology*. 48: 970–979.
- Mack, R.N.; Simberloff, D.; Lonsdale, W.M. [and others]. 2000. Biotic invasions: causes, epidemiology, global consequences, and control. *Ecological Applications*. 10: 689–710.
- O’Connell, B.M.; LaPoint, E.B.; Turner, J.A. [and others]. 2015. The Forest Inventory and Analysis database: database description and user guide version 6.0.2 for Phase 2. U.S. Department of Agriculture Forest Service. 748 p. <http://www.fia.fs.fed.us/library/database-documentation/index.php>. [Date accessed: October 25, 2017].
- Oswalt, C.; Fei, S.; Guo, Q. [and others]. 2015. A subcontinental view of forest plant invasions using national inventory data. *NeoBiota*. 24: 49–54.
- Oswalt, C.M.; Oswalt, S.N. 2015. Invasive plants on forest land in the United States. In: Potter, K.M.; Conkling, B.L., eds. *Forest health monitoring: national status, trends, and analysis 2013*. Gen. Tech. Rep. SRS-207. Asheville, NC: U.S. Department of Agriculture Forest Service, Southern Research Station: 123–134.
- Oswalt, S.N.; Smith, W.B.; Miles, P.D.; Pugh, S.A. 2014. Forest resources of the United States, 2012: a technical document supporting the Forest Service 2015 update of the RPA Assessment. Gen. Tech. Rep. WO-91. Washington, DC: U.S. Department of Agriculture Forest Service, Washington Office. 218 p.
- Ries, P.; Dix, M.E.; Lelmini, M.; Thomas, D. 2004. National strategy and implementation plan for invasive species management. FS-805. Washington, DC: U.S. Department of Agriculture Forest Service. 17 p.
- Riitters, K.; Coulston, J.; Wickham, J. 2011. Fragmentation of forest communities in the Eastern United States. *Forest Ecology and Management*. 263: 85–93.
- Riitters, K.; Potter, K.; Iannone, B.V. [and others]. 2017. Landscape correlates of forest plant invasions: a high-resolution analysis across the Eastern United States. *Diversity and Distributions*. 6(3): 274–284. DOI: 10.1111/ddi.12680.
- Smith, W.B.; Miles, P.D.; Perry, C.H.; Pugh, S.A. 2009. Forest resources of the United States, 2007. Gen. Tech. Rep. WO-78. Washington, DC: U.S. Department of Agriculture, Forest Service. 336 p.

INTRODUCTION

Among other responsibilities, the Forest Health Assessment and Applied Sciences Team (FHAAST) of the U.S. Department of Agriculture Forest Service Forest Health Protection (FHP) program has spent the past several years developing the Digital Mobile Sketch Mapper (DMSM) for its aerial survey program. This is intended to replace the Digital Aerial Sketch Mapper (DASM) as the primary way that aerial survey data are collected, stored, accessed, and processed. The Insect and Disease Survey (IDS) program is currently transitioning from DASM to DMSM. The IDS database (DB) contains mostly DASM data, but some regions started using DMSM in 2015. By 2018, all regions were using DMSM, and DASM will soon be completely phased out. With DMSM comes a fully synchronized IDS DB, which will continue to represent the most updated, comprehensive, and authoritative dataset of forest health conditions in the United States. This dataset is essential for providing multiscale spatiotemporal summaries of forest pest outbreaks and informing the estimated impacts on forest resources. Insect and Disease Survey data have a wide variety of Forest Service users, including FHAAST and regional and forest entomologists, as well as academic researchers and State, industrial, and private landowners outside of the Forest Service. The end goals of each user likely vary, so it is important to make data accessible and meaningful for use by all parties as much as possible. While it is not the goal of FHAAST to conduct research, by encouraging research

use of IDS we benefit by possibly adopting what the research community learns. This chapter helps address the goal of FHAAST's Quantitative Analysis program to support the development of DMSM and help users better interpret and use the new IDS data that are being collected with DMSM.

With the reconceptualization of aerial survey methods and the resulting DMSM, one goal was to better allow for accurate reporting of total damage across multiple regions and nationally, despite the variability in canopy density across and even within regions. For example, one might argue that, for a national report on bark beetle mortality, an area containing bark beetle mortality in dense lodgepole pine (*Pinus contorta*) forest results in more tree mortality than the same acreage of bark beetle mortality in sparse ponderosa pine (*P. ponderosa*) woodlands. This concept of “acres of,” rather than “acres with,” can be helpful when comparing damage summaries across different regions, hosts, or agents. Among some of the key changes in DMSM are the introduction of grid cells as a new data collection feature type in addition to polygons and points; replacing “trees per acre” and “number of trees” measures of mortality with a five-class rating system based on percent of trees affected; and replacing defoliation “severity” and “pattern” with three severity classes. In addition to streamlining and standardizing aerial survey reports, these changes will help FHAAST better integrate aerial survey data with remote sensing and ground survey data (FHAAST 2017).

CHAPTER 7. Using Tree Canopy Cover Data to Help Estimate Acres of Damage

ERIN BERRYMAN

ANDREW McMAHAN

In DMSM, damage is recorded based on the visual assessment of the percent of live and standing dead trees that are affected; therefore, tree cover, as defined by all standing live and dead trees detectable at a 30-m resolution as viewed from directly above, is inherently assessed during flights along with damage type, agent, host, and severity (FHAAS 2017). A key issue with obtaining accurate estimates of damage occurs when damage polygons include untreed area, such as meadows or farms, or when the forest is very sparse, resulting in significant gaps between trees. Often in cases of complex damage patterns on the landscape, surveyors have no choice but to draw large, general polygons or grid cells to indicate damage, yet these areas inevitably contain untreed area in all but the most densely stocked forests. Because of this reason, IDS polygons and grid cells are treated by FHAAS as representing more general “acres with” damage due to the nature of their collection. What are needed for data summaries, however, are “acres of” damage that take into account both percent of trees affected and overall treed versus untreed area. While this is still not a true representation of reality, it represents an improvement in accounting of damage that allows a more fair comparison of damage among different regions and damage-causing agents. Updated, accurate geospatial information about tree cover can serve as a critical data input to adjusting IDS polygons for more accurate estimates of acres of damage. For our purposes and continued use with DMSM, there are several key considerations when choosing a treed cover layer:

- Wall-to-wall national coverage;
- Updated at least once every 5 years to reflect an accurate depiction of conditions during the most recent aerial surveys;
- Appropriate spatial resolution to correspond with DMSM data (30 m to 240 m); and
- Consistent methods across product updates, or a measure of error introduced by using different methods.

The National Land Cover Database (NLCD) Tree Canopy Cover (TCC) product (Yang and others 2018) is a 30-m resolution, satellite-derived canopy cover layer. Some important considerations for the use of this layer for adjusting IDS data to “acres of” damage are:

- It relates ground-measured tree cover to satellite-measured spectral reflectance (i.e., greenness) from Landsat to identify signatures that delineate forested cover from nonforested cover.
- Burned areas with standing dead trees may register as tree canopy cover, albeit at lower canopy cover than surrounding unburned forest.
- To obtain the highest-quality data and imagery, data may be used from a range of years leading up to the product release. For example, the 2011 TCC product uses imagery from 2009–2011.
- Products from different years are difficult to directly compare to each other because they use slightly different methodology.

- The data layer reports percent canopy cover that can either be used raw or be converted to a binary treed/untreed layer by selecting a canopy cover threshold.

This chapter describes analyses for determining the potential of this data source to help adjust IDS polygons to better represent “acres of” damage rather than “acres with” damage. First, NLCD TCC was directly compared to FHAASST’s in-house forested/nonforested layer that was developed in 2002 and last refined in 2012 using various thresholds for delineating forested versus nonforested. Next, the proportion of treed area inside actual IDS polygons was examined using the in-house forested/nonforested layer, and we then analyzed the sensitivity of IDS-derived acres of damage using different thresholds of NLCD TCC for use as a forested/nonforested layer. Finally, aerial surveyor assessments of treed area inside IDS polygons was compared to NLCD TCC-derived estimates of treed area, also at different NLCD TCC thresholds.

METHODS

NLCD Comparison with FNF

An analysis was conducted to compare FHAASST’s forested-nonforested layer (FNF) (Ellenwood and others 2015) to the TCC layer derived from NLCD. The FNF layer was developed at 30-m resolution using a similar approach as NLCD TCC: relating ground tree [≥ 1 -inch diameter at breast height (d.b.h.)] survey measurements to spatial data on greenness, topography, and other environmental

variables. The modeled product is a raster of live forested basal area (BA) at 30-m resolution which is then classified as forest or nonforest based on a threshold of 1.7 square feet of BA per 30-m pixel. This layer uses data collected around 2002, an important consideration when comparing it to TCC from 2011. Because analyses were done at 240-m resolution, the 240-m version of FNF was used. This layer contains values from 0–64, indicating how many of the component sixty-four 30 m-pixels are “treed” (i.e., have a modelled BA ≥ 1.7 square feet). This was reclassified into two classes: treed (1–64 treed 30-m pixels per 240 m) or untreed (0 treed 30-m pixels per each 240-m pixel). This 240-m treed/untreed layer was then compared to a similar layer produced using data from NLCD.

A treed/non-treed classification layer was established from NLCD TCC using a number of different thresholds of treed canopy cover to delineate treed pixels: 10, 20, 25, 30, 35, and 50 percent. It was first reclassified into a binary raster using these NLCD TCC thresholds, and then the 30-m cells were summed into 240-m resolution with values 0–64, similar to the FNF layer. These were reclassified into the same treed/untreed classes as the FNF 240-m layer.

Confusion matrices were created at both the national scale and for each Environmental Protection Agency (EPA) Level 3 Ecoregion. Kappa statistics were calculated from the confusion matrices as a measure of agreement between the FNF layer and the NLCD TCC layers at each threshold (Congalton and Green 2008).

Kappa was examined for trends by NLCD TCC threshold and ecoregion. It was hypothesized that classification based on NLCD TCC threshold would probably vary according to forest type and structure, such as what would be delineated by general aridity of the ecoregion. To assess this, we grouped ecoregions into six classes according to annual precipitation, obtained from spatially averaging [using “Zonal Statistics” in ArcGIS (ESRI 2011)] the 30-year mean of annual precipitation from the PRISM dataset (4-km resolution; PRISM Climate Group, Oregon State University 2017). Then, in each group, kappa was plotted against NLCD TCC threshold to determine which TCC threshold resulted in the greatest agreement between FNF and NLCD TCC for each precipitation class. The results of this analysis will help determine what range of NLCD TCC threshold to further examine for use as a treed layer.

To examine the variability in FNF treed cover in actual IDS polygons, treed cover was calculated for each IDS polygon >50 acres for 2 years: 2008 and 2015. Zonal Statistics in ArcGIS was used to calculate FNF treed cover as a proportion of each polygon. Histograms of proportion of treed area were generated for each year.

Sensitivity of IDS Polygons to Threshold

Our objective was to determine how selection of a particular NLCD TCC threshold would impact summary statistics computed in DMSM. We calculated treed area using different methods on a new subset of IDS polygons (grid cells were not yet being used in 2015) selected according to the following criteria:

1. Collected in 2008 and 2015 (to include both DASM and DMSM)
2. >100 acres (i.e., more likely to contain nonforested area)
3. General shape rather than specific (i.e., round; low circumference-to-area ratio)

This resulted in a total of 7,795 polygons in 2008 and 6,928 polygons in 2015. To limit the influence of polygon size on the results (i.e., tradeoff between specificity and size), we selected the same size area within each polygon within which to calculate statistics. We centered a 480-m “superpixel” within each selected IDS polygon and calculated treed area (using Zonal Statistics in ArcGIS) from different treed area products: FNF, three different NLCD TCC thresholds (10, 20, and 30 percent), and the raw NLCD TCC product (i.e., mean TCC within the superpixel). These treed area values were then averaged for each EPA Level 1 Ecoregion to detect general trends among FNF, different NLCD TCC thresholds, and raw NLCD TCC.

Consistency of Treed Layers with Aerial Survey Assessment

In addition, we randomly selected 60 of the above superpixels (30 from 2008 and 30 from 2015) for a manual exercise to compare NLCD TCC-derived treed area with aerial surveyor assessments. An equal number of images was selected from each year to avoid bias associated with switching from DASM to DMSM. Average treed cover for the superpixel was calculated using the three different NLCD TCC thresholds, raw NLCD TCC, and FNF. To assess which GIS layers of treed cover were most consistent with aerial surveyor assessment of treed cover during flights, high-resolution aerial imagery from NAIP (National Agriculture Imagery Program) was examined for each of the 60 superpixels by two experts in aerial survey techniques. Experts were asked to quickly visually estimate treed cover within each 480-m superpixel with the mindset of an aerial surveyor (i.e., what areas would they consider when making a damage severity assessment from a plane?). We calculated the degree of agreement between each NLCD TCC threshold layer and the observers' assessments using root mean squared error (RMSE):

$$RMSE = \sqrt{\frac{1}{n} \sum_{i=1}^n (C_i - \hat{C}_i)^2}$$

where

C_i = for each superpixel i , the observed value (expert assessment of treed cover)

\hat{C}_i = for each superpixel i , the predicted value (cover from treed layer)

n = the number of observations (60 for observer 1's assessment, 54 for observer 2's assessment)

Root mean squared error was calculated for each of three NLCD TCC thresholds (10, 20, and 30 percent) separately for polygons in the Western United States (west of the Mississippi River) and Eastern United States and for all polygons combined. Root mean squared error was also calculated for the same three TCC thresholds but aggregated to 60-m (four pixels) and 90-m (nine pixels) resolution to see if agreement depended on spatial resolution of the treed layer. All analyses are summarized in table 7.1.

Table 7.1—Summaries of analyses for this report

Data layers	Spatial resolution	Subset	Analysis performed
NLCD TCC, FNF	240 m	All pixels from conterminous United States	Compared treed versus untreed classification accuracy and how accuracy varied by ecoregion and precipitation regime
IDS, FNF	30 m	>50 acres, 2008 and 2015 only	Calculated proportion of treed area in each polygon and examined distribution using histograms
IDS, NLCD TCC, NLCD10, NLCD20, NLCD30, FNF	30 m	>100 acres, 2008 and 2015, round polygons	Calculated proportion of treed area using each of five different treed or forest canopy cover layers inside a 480-m superpixel centered inside each polygon
Same as above	30 m	Same criteria as above; 30 randomly selected in 2008, 30 randomly selected in 2015	Added expert assessment of treed area within a 480-m superpixel centered inside each polygon; RMSE determined between each expert assessment and GIS treed area calculation

NLCD TCC: National Land Cover Database Tree Canopy Cover; FNF: forested-nonforested; IDS: Insect and Disease Survey; NLCD10: 10-percent NLCD TCC threshold; NLCD20: 20-percent NLCD TCC threshold; NLCD30: 30-percent NLCD TCC threshold.

RESULTS

NLCD Comparison with FNF

Applying a threshold of 10-percent TCC to delineate a pixel as “treed” results in roughly 20 percent more area of the contiguous United States being construed as “treed” relative to FNF. The distribution of canopy cover classes varies geographically, with more western and arid regions having most treed pixels classed into lower canopy cover classes; pixels are classed conversely in the wetter, eastern areas.

The kappa statistic, which reflects the overall classification accuracy of NLCD TCC-derived treed area compared to FNF, varied depending on both ecoregion and TCC threshold. In the Western United States, kappa was highest at canopy cover threshold of 10 to 20 percent

(fig. 7.1). In eastern ecoregions, kappa was highest when 30- to 35-percent canopy cover threshold was used. In general, regardless of TCC threshold, agreement between TCC-derived treed area and FNF was highest for eastern, wetter ecoregions than for western, drier ecoregions (fig. 7.2). Based on these results, we chose to further examine the performance of 10-, 20-, and 30-percent NLCD TCC threshold layers with IDS data—these are denoted as NLCD10, NLCD20, and NLCD30 from here forward.

Sensitivity of IDS Polygons to Threshold

Within IDS polygons >50 acres, 70 percent of them were >90 percent treed in 2008, with 74 percent of them >90 percent treed in 2015 (fig. 7.3), according to the FNF treed layer.

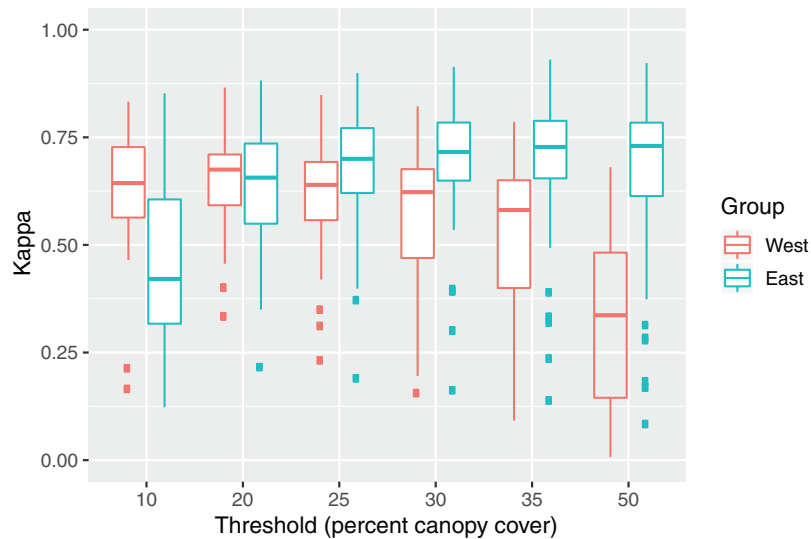


Figure 7.1—Kappa statistic (TCC versus FNF) for each Level 3 Ecoregion plotted against the canopy cover threshold, grouped into western U.S. ecoregions and eastern U.S. ecoregions. Boxplots approximate the distribution of the kappa values within each category, showing the median kappa as the horizontal line, bracketed by the first and third quantiles as the extent of the boxes. Outliers are outside 1.5 times the range indicated by the box height. This illustrates that (1) the best performing TCC threshold is higher for eastern ecoregions compared to western ecoregions; and (2) western ecoregions overall show a poorer fit of TCC with FNF.

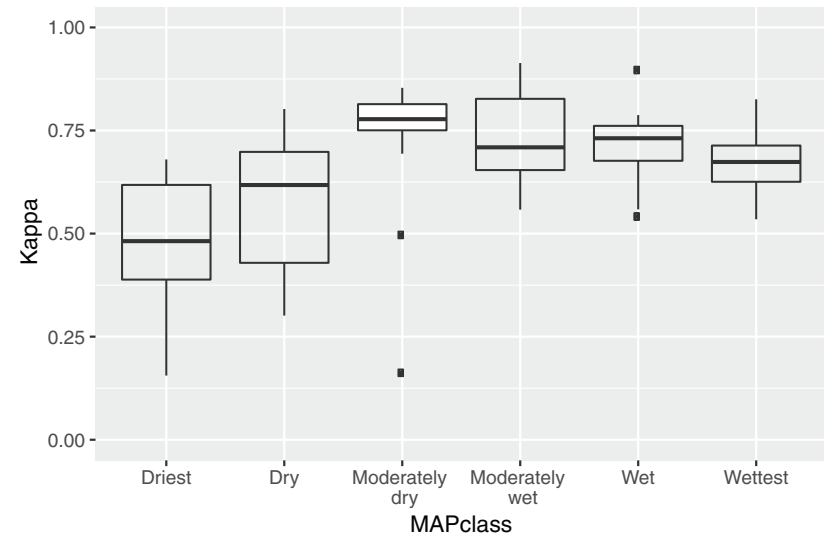


Figure 7.2—Kappa statistic (TCC at 30-percent threshold versus FNF) for each Level 3 Ecoregion plotted against the mean annual precipitation class (MAPclass) of the ecoregion. Boxplots approximate the distribution of the kappa values within each category, showing the median kappa as the horizontal line, bracketed by the first and third quantiles as the extent of the boxes. Outliers are outside 1.5 times the range indicated by the box height. This illustrates TCC forested cover compares better to FNF forested cover in wetter ecoregions than in drier ecoregions. Therefore, caution should be used when using TCC to delineate forested cover in dry forests.

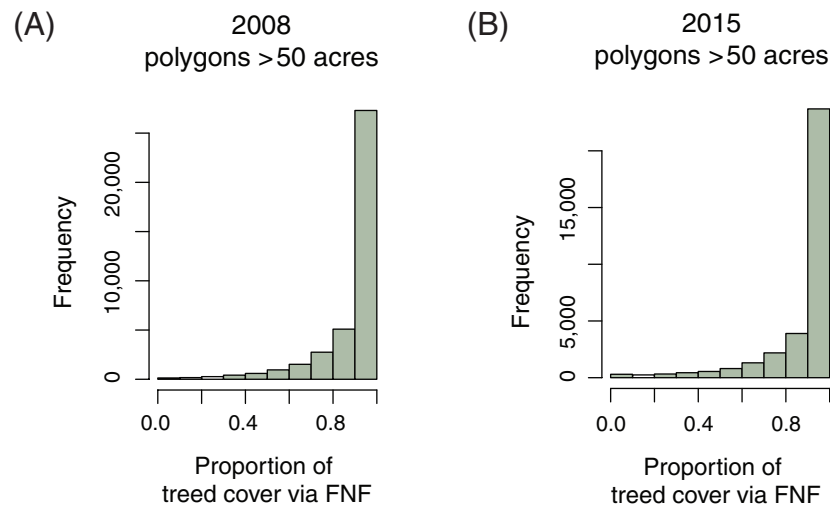


Figure 7.3—Histogram of (A) 2008 and (B) 2015 IDS polygon tree proportion (according to FNF) only including polygons >50 acres.

Within 480-m superpixels inside IDS polygons, the largest discrepancies in tree area between different layers occurred in drier Level 1 Ecoregions, i.e., Great Plains, Mediterranean California, North American Deserts, and Temperate Sierras (fig. 7.4). Averaged across Level 1 Ecoregions, NLCD TCC was always the lowest out of all measures. NLCD10 consistently resulted in the highest mean tree cover in the IDS superpixels, although in many ecoregions it was similar to measures from NLCD20 and NLCD30.

In 2015, about 2 percent of the total area contained within IDS polygons was (arbitrarily)

considered highly sensitive to the placement of the NLCD TCC threshold; that is, there was a >30-percent difference between tree cover estimates within IDS polygons moving from NLCD10 to NLCD30. In other words, in 98 percent of the area covered by damage polygons in 2015, the calculated tree acres did not vary much depending on what TCC threshold was used: 10, 20, or 30 percent. The remaining polygons that were sensitive to TCC threshold tended to be concentrated in the Western United States (Intermountain West and Inland Northwest) (fig. 7.5).

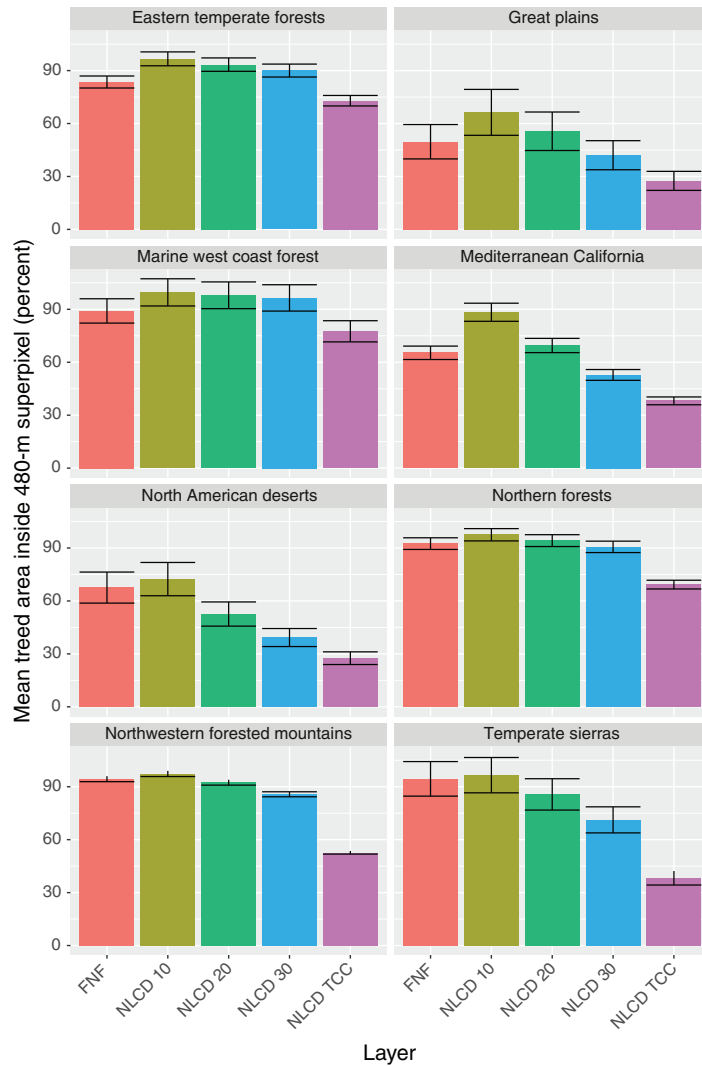


Figure 7.4—Mean treed area by Level 1 Ecoregion within 480-m superpixels centered inside large, round 2015 IDS polygons using five different treed cover or canopy cover layers: FNF (FHAASST native); NLCD 2011 with a 10-, 20-, and 30-percent canopy cover threshold; and NLCD TCC. Error bars represent +/- standard error.

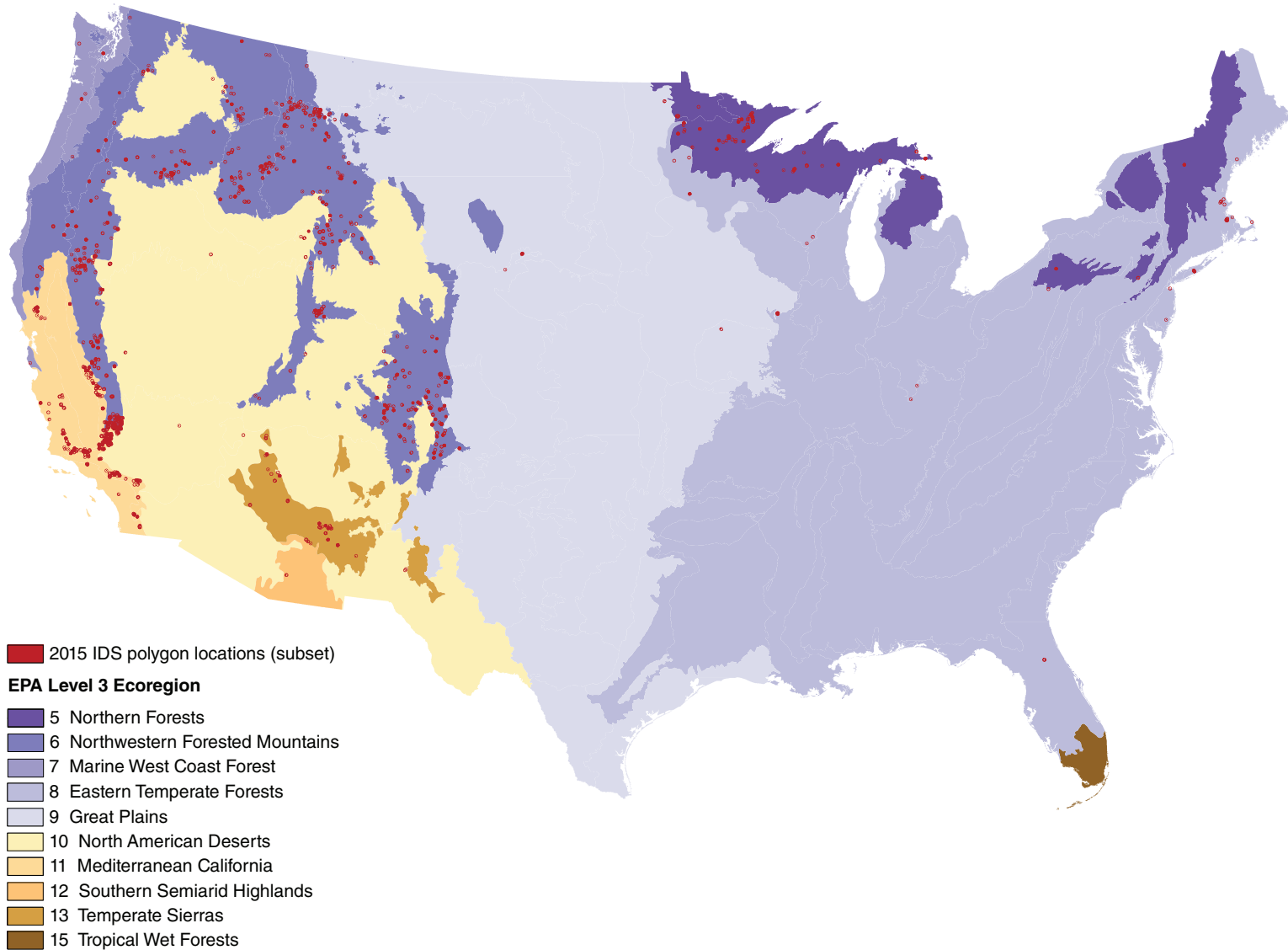


Figure 7.5—2015 IDS polygons where there was at least a 30-percent difference in treed area between using a 10-percent TCC threshold for NLCD and a 30-percent threshold for NLCD. This represents 2 percent of the total damage acreage mapped via polygons in 2015. Note that, because not all land was surveyed in 2015, this figure only indicates presence of damage and not absence of damage and may include false negatives.

Consistency of Treed Area with Aerial Survey Assessment

Aerial survey experts noted a few challenges with assessing treed cover. First, observer 2 noted that determining a percent treed cover is not consciously done when conducting an aerial survey. Both of the observers noted that the assessment of severity is done very quickly concurrently with other assessments of host, agent, and size of area.

Aerial surveyors' assessment of treed area in NAIP imagery was overall closest to the NLCD30 threshold versus NLCD10 or NLCD20 (table 7.2). Agreement was similar among 30-, 60-, and 90-m resolution, with slightly worse agreement at larger spatial resolution; only the NLCD10 aggregated to 60-m resolution had lower RMSE than its 30-m counterpart (19.4 percent and 21.1 percent for observer 1's and observer 2's assessments, respectively). Error was higher for

polygons in the Western United States compared to the Eastern United States (table 7.2). The two different experts had similar RMSE with each other, suggesting consistency among aerial surveyors from different regions, although it is difficult to conclude this based on only two surveyors. The exercise revealed two key issues with determining canopy cover using NLCD (fig. 7.6). First, aerial surveyors are trained to read areas containing standing dead trees as "treed," whereas NLCD would classify them as low canopy cover due to its reliance on spectral data and lack of live canopy in those areas. Second, in NLCD, sparse forests and woodlands may register as low canopy cover, making these places particularly sensitive to the placement of the canopy cover threshold for NLCD data. Expert assessment revealed that there may be large differences between different surveyors' treatment of a sparse woodland as treed or untreed when making a damage rating.

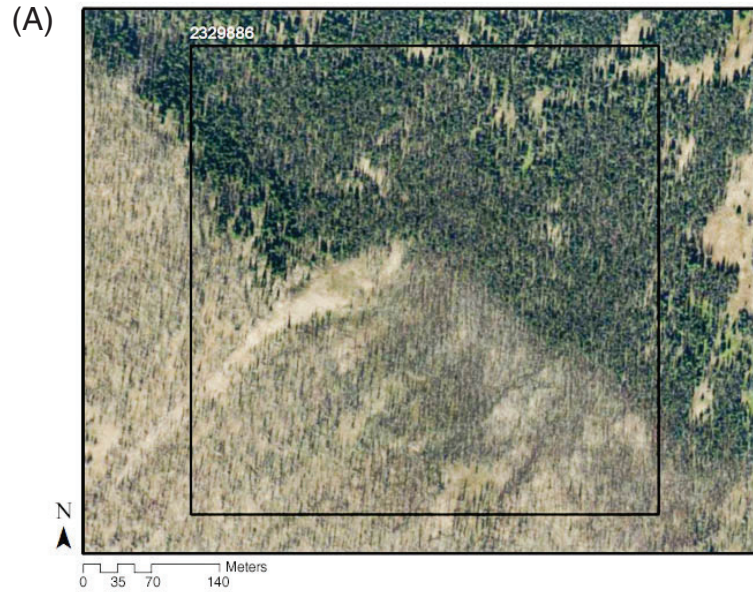
Table 7.2—Root mean squared error (RMSE) between treed cover estimates from expert assessment and from canopy cover layers derived from NLCD for 480-m superpixels randomly selected from large, round polygons located west of the Great Plains ("West") and east of the Great Plains ("East") in 2008 and 2015

Expert	NLCD10 ^a			NLCD20 ^b			NLCD30 ^c		
	West	East	All	West	East	All	West	East	All
----- percent treed cover -----									
Observer 1	21.6	13.9	19.7	20.6	9.3	18.1	17.8	9.1	15.8
Observer 2	22.4	18.5	21.6	20.5	7.5	18.9	17.1	4.9	15.4

^a NLCD TCC-derived treed area using a 10-percent TCC threshold.

^b NLCD TCC-derived treed area using a 20-percent TCC threshold.

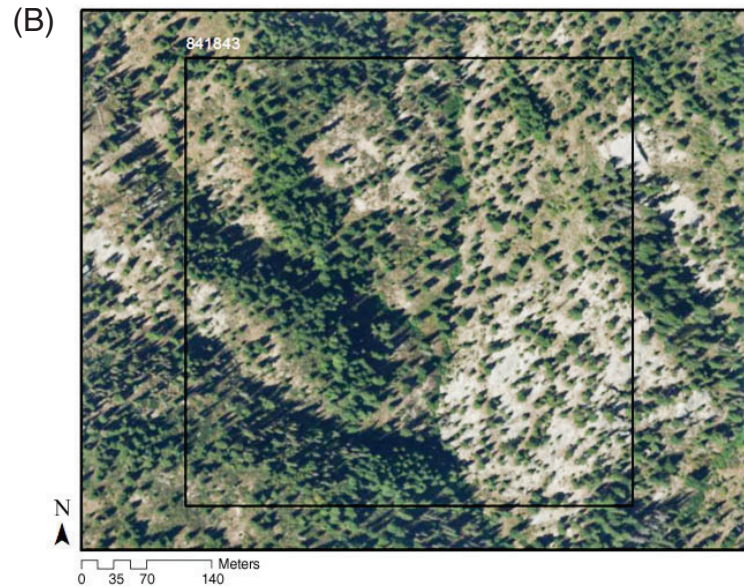
^c NLCD TCC-derived treed area using a 30-percent TCC threshold.



NLCD10: 78%
NLCD20: 50%
NLCD30: 45%

FNF: 98%

O1: 95%
 O2: 95%



NLCD10: 71%
NLCD20: 41%
NLCD30: 30%

FNF: 80%

O1: 65%
 O2: 40%

Figure 7.6—NAIP imagery from selected 480-m superpixels randomly sampled from large, round IDS polygons in 2008 and 2015 and different estimates of the percentage of treed area within the superpixel. (A) An area containing standing dead trees from a wildfire, which are read as “untreed” by NLCD. (B) An area where complex terrain results in spatial heterogeneity of forest density and widely varying assessments of treed cover depending on canopy cover threshold and expert. The red text indicates the layer that came closest to the expert assessment of treed cover. NLCD10 = treed cover from NLCD using a 10-percent canopy cover threshold; NLCD20 = treed cover from NLCD using a 20-percent canopy cover threshold; NLCD30 = treed cover from NLCD using a 30-percent canopy cover threshold; FNF = FHAAST native treed layer (Ellenwood and others 2015); O1 = observer 1’s visual assessment from NAIP imagery; O2 = observer 2’s visual assessment from NAIP imagery.

DISCUSSION

A key calculation needed for inclusion in the DMSM Desktop and Reporting Tools is adjustment for untreed area included in polygons or grid cells reported by surveyors. To accomplish this in a GIS setting, a raster denoting treed versus untreed area could be used in post-survey processing. For example, the user could view the intersection of IDS feature classes (polygons or grid cells) with treed cover and perhaps aerial imagery, such as NAIP, giving the surveyor the option to calculate treed acres for each feature. An important requirement for the continued use of a treed layer by FHAAST is that the layer is updated frequently to remain representative of conditions during the survey. Since 2002, FHAAST has developed the FNF treed cover layer at 30-m and 240-m resolutions. However, the latest vintage of the FNF layer represents 2011 conditions, considered outdated during the writing of this report. Thus, there is a need for a new, updated treed cover layer available for use with IDS data. Our analysis found that the NLCD TCC can be a feasible option to use for adjusting IDS polygons to represent only treed area for use in IDS summaries, but with caveats. Due to overall lower percent canopy cover in arid, western forests compared to eastern forests, using the unadjusted raw NLCD TCC product to determine canopy cover may underestimate western U.S. forest damage compared to the Eastern United States. Instead, NLCD TCC should be converted

to a binary treed/untreed layer based on a canopy cover threshold, similar to FHAAST's ca. 2011 FNF layer.

The results from this analysis could be useful to inform decisionmaking that uses NLCD TCC thresholds to define a treed/untreed mask for the area of interest (AOI). Considering variability in forest cover across the AOI may aid in selecting a NLCD TCC threshold for delineating treed area. For example, if one decides to use NLCD30 to define "treed area," then it is important to recognize that such a threshold will cut off a larger proportion of the tails of the distributions in more arid ecosystems than in others. Our results suggest that there can be greater inaccuracies in assigning treed cover to IDS data in the Western United States than in the Eastern United States, where sparser forests and woodlands may cloud the distinction between calling something "treed" versus "untreed." At the national scale, when errors in these large polygons are considered in the context of all IDS data for a given year, the overall error is low. This is because most polygons drawn in any given year are small and specific enough to contain mostly treed area, and the problem is largely restricted to certain regions, like arid, sparse forests. Ultimately, the decision of what NLCD TCC threshold to use might be a choice between under- or over-estimation of acres of damage in western forests compared to eastern forests. Differences in survey intensity and accuracy between

western and eastern regions may play a factor in this decision; for example, it is arguably more challenging to accurately map tree damage in many eastern areas compared to western, so it may make sense to err on the side of an eastern-appropriate threshold than western.

To decide what TCC threshold to use for delineating forested area within the polygons, one consideration could be that whatever threshold is used should have results that are consistent with how the aerial surveyor assesses forested area when deciding what the mortality severity is. According to the experts we contacted, this is difficult to quantify, because aerial surveyors work quickly and subconsciously when making a judgment about how much of the forest is impacted. What is deemed “untreed” may differ by surveyor and region. Despite this, the two aerial surveyors with whom we worked on this analysis had assessments of treed area from aerial imagery that were very similar to each other, with the exception of areas that were very sparsely wooded. The NLCD TCC threshold that compared best to aerial surveyors’ assessments was 30 percent, although the accuracy did not decrease very much for 20- or 10-percent TCC thresholds. Accuracy was noticeably higher for polygons located in the Eastern United States compared to the Western United States (table 7.2).

In this work, we only considered the use of NLCD TCC layer to distinguish treed cover. It may be worthwhile to seek out and test other products given some other key limitations

of TCC. For example, NLCD uses different methodologies for its 2006, 2011, 2016, and planned 2021 products. This would make it difficult to compare measured “acres of” damage across consecutive years that overlap with these transitions from one product to the next. Another major issue with using NLCD as a treed layer for our purposes is that any spectral-derived layer of forested cover will have large errors in burned areas. Aerial surveyors consider standing dead trees as “treed,” whereas the lack of vegetation would result in a reflectance-derived layer (like TCC) to call burned areas “untreed.” This could be overcome by using a burned area layer to correct for these areas, such as Monitoring Trends in Burn Severity (MTBS), the newer U.S. Geological Survey Burned Area product (Hawbaker and others 2017), or the forest cover layer updated annually by Hansen and others (2013).

In cases where forests are fairly continuous or where damage is concentrated and easily contained within a general polygon shape or grid cell, use of a treed layer may not provide much advantage. However, many regions, especially those in the Eastern United States, are characterized by non-continuous forest due to farms, meadows, and urban infrastructure on the landscape. With the change in how mortality severity is recorded in DMSM compared to DASM, it is important to consider how uncertainty inherent in using mortality classes (rather than trees per acre) compares to uncertainty added by the use of a treed layer that may under- or over-estimate treed area in

a given feature class. As an example, consider an aerial surveyor who makes an assessment of a 1920-m grid cell in an urban area as having Light (4–10 percent) mortality severity due to emerald ash borer (*Agilus planipennis*) (fig. 7.7, grid cell A). To adjust the grid cell acreage to “acres of” damage, one approach would be to multiply the midpoint of the mortality range (7 percent) by the size of the grid cell (911 acres) = 64 acres of damage. However, the

grid cell includes farmland and roads and thus only 80 percent of the cell is treed. Applying this treed area adjustment would result in 64 acres x 0.80 = 51 acres of damage. This is the same “acres of” damage value as we would get with NO treed area correction and estimating 6 percent mortality instead of 7 percent mortality, still falling within the Light mortality severity category. In contrast, grid cell B in figure 7.7 is only 25 percent treed and was also assessed



Figure 7.7—IDS data from 2015 showing 1920-m grid cells used to map emerald ash borer mortality in Michigan. Grid cell A has higher tree cover than grid cell B, and both cells were mapped at the same mortality severity (Light).

as having Light (4–10 percent) emerald ash borer mortality severity. Again, multiplying the mortality midpoint times the grid cell acreage results in 64 acres of mortality. Further adjusting this to only consider treed area results in 16 acres of damage. This same acreage of damage is equivalent to about 2 percent mortality if we do not account for untreed area, which would be considered Very Light mortality severity. Therefore, considering treed versus untreed area can make a difference in damage assessments when treed area is relatively low. This demonstrates the utility of using grid cells along with treed area for improving estimates of “acres of” damage, especially in areas with farms and urban development mixed in with forest which may not be feasible to distinguish by drawing polygons.

In our analysis, we found that NLCD30 agreed more often than NLCD10 or NLCD20 with aerial surveyors’ assessments of treed cover contained within large, round IDS polygons. However, the uncertainty (RMSE) was not very different across the thresholds (a range of 15- to 22-percent error). Based on our analyses, national-scale IDS summaries on widespread pests may be largely insensitive to differences in treed cover layers

that may be used to adjust polygons or grid cells for “acres of” damage. However, for analyses at scales smaller than the continental United States and for restricted-range pests and diseases, this error could be substantial depending on the region and pest of interest. The error associated with using one canopy cover threshold over another for a treed layer will often be smaller than the uncertainty inherent in the damage severity classes, although lower damage severity classes, with narrower ranges of error than moderate or high severity, could be most affected by error in tree canopy cover threshold. A bigger concern might be the possibility for large errors in treed cover in burned areas where standing dead trees remain, because NLCD will have much lower treed area than aerial surveyors would consider when assigning a mortality severity class. In such cases, using data derived locally that are more accurate than national products such as NLCD TCC would be desirable. Ultimately, the need for adjusting IDS polygons for treed area to improve “acres of” damage estimates must be decided on a case-by-case basis, depending on the region of interest, the goals of the summary, and the damage severity categories that have been mapped.

Overall conclusions:

- The use of severity classes in DMSM allows for an initial estimate of “acres of” damage by multiplying polygon or grid “acres with” damage by the midpoint of the assigned mortality class.
- Further adjustments for treed cover will have a lesser impact on “acres of” damage but may be necessary for large, general polygons and grid cells. A binary treed cover layer derived from the NLCD TCC product can feasibly delineate treed area inside IDS polygons and grid cells with a threshold of 20- or 30-percent TCC. Key uncertainties lie with delineating treed area in western, arid forests and where wildfires recently burned, and with using NLCD from different years (e.g., 2006 and 2011) due to changing methodologies.
- Crosswalking legacy measures of damage severity with DMSM will be challenging. Further analysis and testing are recommended to determine the appropriate methodology for representing cumulative “acre of” damage in an outbreak that spans both DASM and DMSM.

ACKNOWLEDGMENTS

The authors would like to thank Dan Ryerson [U.S. Department of Agriculture Forest Service (New Mexico)] and Scott Lint (Michigan Department of Natural Resources) for their vital contributions to this work.

LITERATURE CITED

- Congalton, R.G.; Green, K. 2008. Assessing the accuracy of remotely sensed data: principles and practices. Boca Raton, FL: CRC Press. 177 p.
- Ellenwood, J.R.; Krist, F.J., Jr.; Romero, S.A. 2015. National individual tree species atlas. FHTET-15-01. Fort Collins, CO: U.S. Department of Agriculture Forest Service, Forest Health Technology Enterprise Team. 320 p.
- ESRI. 2011. ArcGIS desktop: release 10. Redlands, CA: Environmental Systems Research Institute.
- Forest Health Assessment and Applied Sciences Team (FHAAS). 2017. Digital Mobile Sketch Mapping (DMSM) updates to forest health survey with DMSM. Ft. Collins, CO: U.S. Department of Agriculture Forest Service.
- Hansen, M.C.; Potapov, P.V.; Moore, R. [and others]. 2013. High-resolution global maps of 21st-century forest cover change. *Science*. 342(6160): 850–853.
- Hawbaker, T.J.; Vanderhoof, M.K.; Beal, Y.-J. [and others]. 2017. Mapping burned areas using dense time-series of Landsat data. *Remote Sensing of Environment*. 198: 504–522.
- PRISM Climate Group, Oregon State University. 2017. Descriptions of PRISM spatial climate datasets for the conterminous United States. http://www.prism.oregonstate.edu/documents/PRISM_datasets.pdf. [Date accessed: March 17, 2019].
- Yang, L.; Jin, S.; Danielson, P. [and others]. 2018. A new generation of the United States National Land Cover Database: requirements, research priorities, design, and implementation strategies. *ISPRS Journal of Photogrammetry and Remote Sensing*. 146: 108–123.

Each year the Forest Health Monitoring (FHM) program funds a variety of Evaluation Monitoring (EM) projects, which are “designed to determine the extent, severity, and causes of undesirable changes in forest health identified through Detection Monitoring (DM) and other means” (FHM 2015). In addition, EM projects can produce information about forest health improvements. Evaluation Monitoring projects are submitted, reviewed, and selected through an established process. More detailed information about how EM projects are selected, the most recent call letter, lists of EM projects awarded by year, and EM project poster presentations can all be found on the FHM Web site: www.fs.fed.us/foresthealth/fhm.

Beginning in 2008, each FHM national report contains summaries of recently completed EM projects. Each summary provides an overview of the project and results, citations for products and other relevant information, and a contact for questions or further information. The summaries provide an introduction to the kinds of monitoring projects supported by FHM and include enough information for readers to pursue specific interests. Three project summaries are included in this report.

LITERATURE CITED

Forest Health Monitoring (FHM). 2015. Evaluation monitoring. <https://www.fs.fed.us/foresthealth/fhm/em/index.shtml>. [Date accessed: August 22, 2018].

SECTION 3. Evaluation Monitoring Project Summaries

INTRODUCTION

This project seeks to understand the causes of a dramatic decline of bishop pine (*Pinus muricata*) stands on the northern California coast in Mendocino and Sonoma Counties. The northern bishop pine forest is designated by the State of California as a sensitive vegetation type with a global rank of G2 (endangered) and a State rank of S2.2 (threatened) (Sawyer and others 2009). Stand decline and high mortality levels have been reported, especially in mid- to northern Mendocino County, since the early to mid-2000s; a drive along U.S. Highway 1 through these two counties or even a cursory examination of Google Earth imagery confirms the severity of the problem. Coupled with reported declines of bishop pine in the southern part of its California range, this northern decline may imperil the future not only of the species, but also of the unusual forest ecosystems it supports and the people who depend on them.¹ However, this decline is not yet represented in the scientific literature, nor does it show up in aerial survey records or Forest Inventory and Analysis (FIA) plots because of its coastal position. Our project proposed to remedy this need by collecting a

¹ For example, in 2010, tourism—much of which is focused along the coast where bishop pine grows—accounted for 38.8 percent of total local taxes generated in Mendocino County as well as >\$300 million in total local spending and >\$6 million in transient occupancy taxes (County of Mendocino 2010); additionally, the Kashia Band of Pomo Indians attach enormous cultural importance to forest lands, including bishop pine stands, along the coast (Moore 2017).

set of systematic observations throughout the range of the decline. We investigated the decline using a twofold approach: (1) the application of dendroecological methods to a subset of trees in several stands to determine stand age structure, growth, and regeneration trends within the past century; and (2) an inventory of pest (pathogen and insect) problems present in these stands to gauge their prevalence and identify any that appear to be primary causes of the decline.

METHODS

Locations containing both healthy and declining stands were selected in 2015. Locations (fig. 8.1) included a northern cluster of sites near the towns of Fort Bragg and Mendocino (MCK, RG, HQ, and WS) and a southern cluster south of the town of Gualala (SR, FMC, SALT, and SPP). WS and SPP were pygmy/oligotrophic forest sites, while the others comprised stands with full-sized, mature bishop pines as dominants or codominants. Some soils were also collected from a limited number of sites with 100 percent bishop pine mortality. At each site with living pines remaining, one to three 0.1-ha plots were established. In each plot, each standing stem of any species >5 cm diameter was inventoried. Heights of selected living bishop pines were recorded using a laser rangefinder. Percent crown density (relative to 100 percent density, in which all visible space within the crown is occupied by living foliage) and percent branch dieback within the crown were recorded for each bishop pine. All observable insect pests and pathogens were recorded on plot bishop pines, and dwarf mistletoe and western gall

CHAPTER 8.

Investigating Causes of Bishop Pine Decline on California's North Coast (Project WC-B-16-02)

CHRISTOPHER A. LEE

STEVE VOELKER

PETER A. ANGWIN

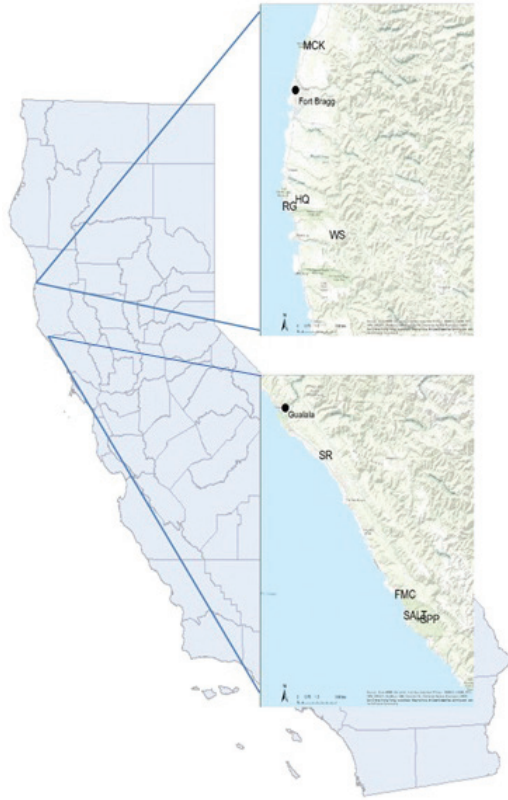


Figure 8.1—Study site locations.

rust incidence within the crown were recorded on a 0 (no infection) to 6 (greatest infection) scale, following the rating system presented in Hawksworth (1977). Some pest identifications required sampling of infected tree tissues followed by surface sterilization in 10-percent sodium hypochlorite (NaOCl) solution and plating on half-strength potato dextrose agar amended with 1 mL/L 85-percent lactic acid solution (Wick 2013); resulting cultures were

sent to the California Department of Food and Agriculture (CDFA), Sacramento, CA, for DNA extraction, polymerase chain reaction (PCR)-based genomic amplification, sequencing of the amplicon, and identification based on homology of the amplicon to ones curated on the general biological database GenBank or the *Phytophthora*-specific databases *Phytophthora*-ID (<http://phytophthora-id.org>) and *Phytophthora* Database (<http://phytophthoradb.org>) (Martin and others 2012). On each plot, 8–12 living and dead bishop pines were cored (two orthogonal cores taken for each pine). Cores were dried and sanded to reveal growth ring fine features and the rings measured at Utah State University. Soils were characterized at each site by digging soil pits to 100-cm depth, collecting samples from each clearly discernible horizon, and recording a complete suite of physical characteristics for each horizon, including but not limited to pH, texture, coarse and fine root presence, color, and presence of redox features. Mineral soil was collected from the upper 10 cm of the profile at least twice from each plot in fall and spring to bait for oomycete pathogens. The baiting procedure involved flooding approximately 300 g of soil with distilled water, adding whole pears to the top of the flooded soil as well as floating Port Orford-cedar leaflets on the water, and plating the leaflets or lesioned portions of the pears on PARPNH-V8 agar, a growth medium selective for *Phytophthora* species (Bernhardt and Swiecki 2015, Schmitthenner and Bhat 1994). Resulting cultures of oomycetes were sent to the CDFA lab for PCR, sequencing, and identification.

RESULTS

Tree Statistics

Patterns of dieback varied from dramatic mortality of entire patches to more diffuse and gradual crown dieback within stands (fig. 8.2). Mean diameter at breast height (d.b.h.) for all trees on plots ranged from 19.7–56.7 cm, whereas mean d.b.h. for bishop pines alone was generally larger (range: 21.8–76.6 cm). Stem densities for all trees varied from 210 stems/ha (at WS10) to 890 stems/ha (at MCK); stem densities for bishop pines alone varied from 120 stems/ha (at RG5) to 510 stems/ha (at SALT2). Basal area of all trees ranged from 8 m²/ha (at WS10) to 113 m²/ha (at HQ); basal area of bishop pines alone ranged from 5.2 m²/ha (at WS9) to 90.1 m²/ha (at HQ). Although mean crown density for bishop pines varied little among sites, it was relatively low at all sites, with most sites averaging 55- to 75-percent density (fig. 8.3). Bishop pine branch dieback within the crown was significantly lower at sites with some of the greatest mean crown density (HQ and RG) than at other sites (fig. 8.3). Basal area increment (BAI) began to decline across all sites beginning mid-1990s according to our bishop pine tree core data (fig. 8.4; minimum mean BAI 8 cm²/year; maximum mean BAI 23 cm²/year). Of the trees cored, 20 percent established between 1850–1930, 66 percent established between 1935–1960, and 14 percent established since 1960 (fig. 8.5).

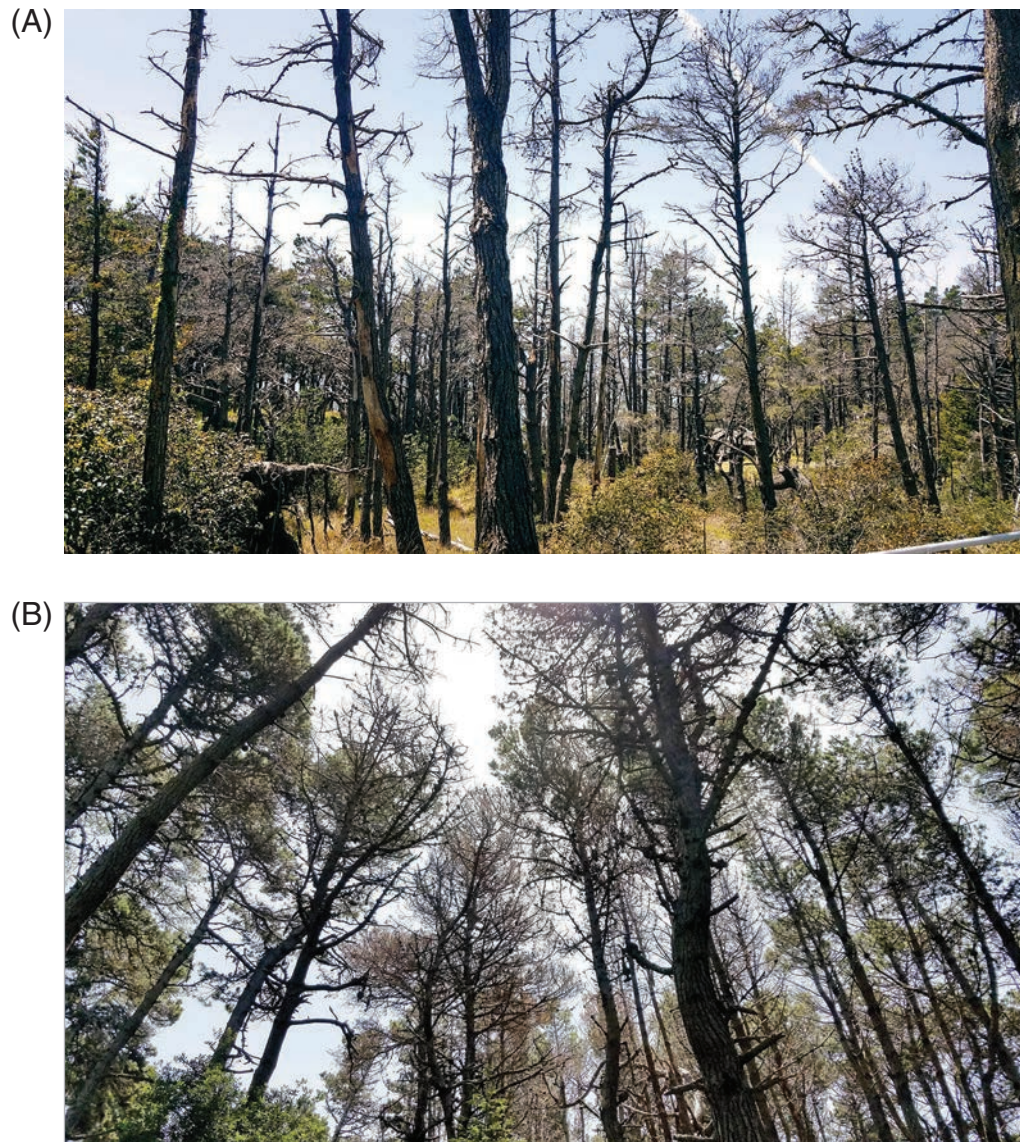


Figure 8.2—Bishop pine decline in northern Sonoma County. (A) Wide-scale, synchronous mortality; (B) gradual decline in crown conditions. (Photos by Christopher Lee, California Department of Forestry and Fire Protection)

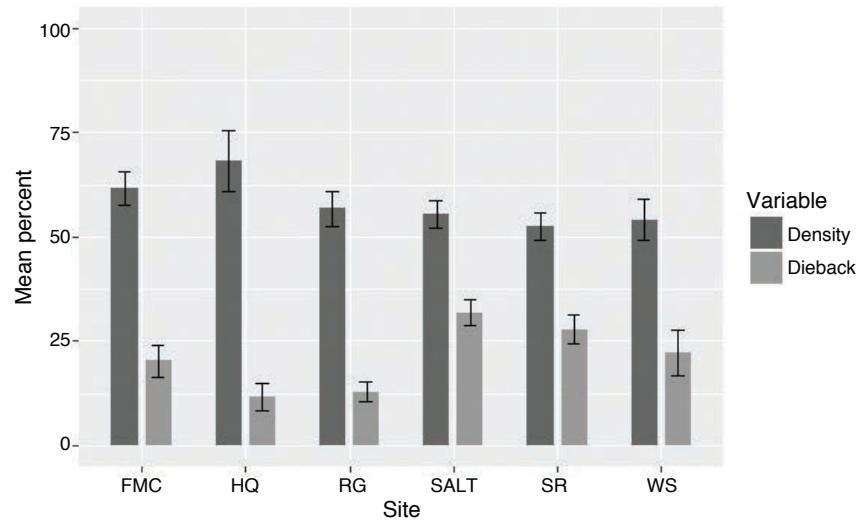


Figure 8.3—Bishop pine crown health metrics (mean percent crown density and mean percent crown dieback) across study sites with multiple plots containing Bishop pine.

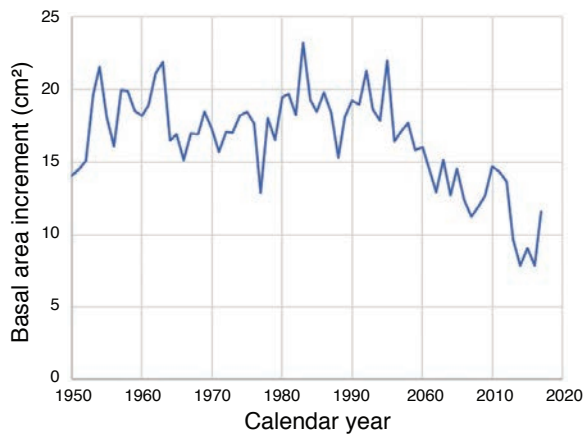


Figure 8.4—Basal area increment (BAI) averaged across all cored bishop pines at all study sites.

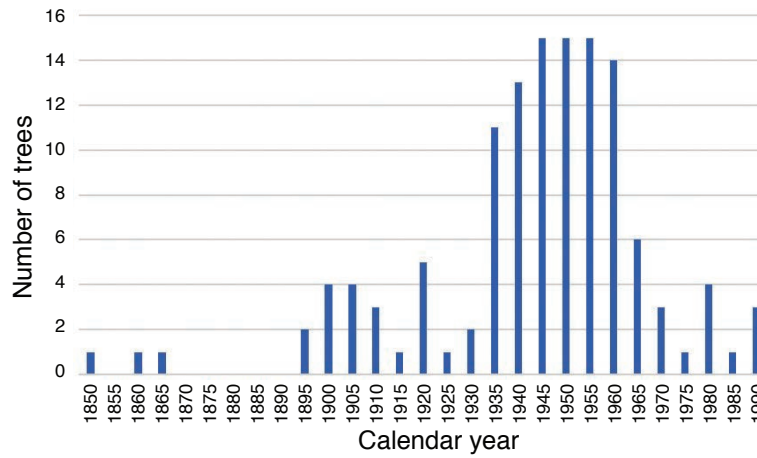


Figure 8.5—Dates of bishop pine establishment across study sites.

Pest Incidence

A large number of pests were observed on study pines; a list is given in table 8.1. Western gall rust incidence was locally heavy but averaged 1.2 on a 0–6 scale over all sites. Coastal dwarf mistletoe (*Arceuthobium littorum*) was severe only at the WS (pygmy forest) site (mean score 4.29 on a 0–6 scale), although it was present at several other sites (mean score <1). Some pests were observed at only one or a few locations (e.g., *P. cambivora*, the bark beetles); others were much more widespread (e.g., western gall rust, schweinitzii and tomentosus root rots, and stem decays). In

general, widespread fungal activity was observed in this moist coastal ecosystem, both within woody substrates and in the prevalence of pathogenic fungi that disperse as spores in the air (e.g., *Diplodia scrobiculata*, *Fusarium circinatum*). At the southern sites, branch infections caused by *F. circinatum* have increased in number and prominence every year for the past few years, and symptomatic trees appear farther north along the roadside every year. Both *D. scrobiculata* and another *Fusarium* species (one closely related to *F. avenaceum*) have also been isolated from dead and dying seedling- and sapling-sized Monterey pines (*P. radiata*) in Sonoma, Mendocino, and Humboldt Counties.

Table 8.1—Pests observed on bishop pine, arranged by plant part affected

Pest (scientific name)	Disease caused (common name)	Plant part affected	Relative damage and extent
<i>Armillaria</i> spp.	Armillaria root disease	Large (structural) roots	Moderately severe/wide extent
<i>Phaeolus schweinitzii</i>	Schweinitzii root disease	Large (structural) roots	Moderately severe/wide extent
<i>Onnia</i> sp.	Tomentosus root disease	Large (structural) roots	Moderately severe/wide extent
<i>Phytophthora cinnamomi</i>	Phytophthora dieback	Fine roots	Severe/restricted extent
<i>Elongisporangium</i> (= <i>Pythium</i>) <i>undulatum</i>	None	Fine roots	Severe/restricted extent
<i>Pythium</i> spp.	None	Fine roots	Mild/wide extent
<i>Phytophthora cambivora</i>	Phytophthora dieback	Fine roots and root crown	Moderately severe/restricted extent
<i>Fusarium circinatum</i>	Pine pitch canker	Branches and stem	Severe/restricted but increasing extent
<i>Phomopsis/Diaporthe</i> spp.	Phomopsis canker	Branches and stem	Mild (tree), severe (seedling)/wide extent
<i>Diplodia scrobiculata</i>	Diplodia blight	Branches and stem	Mild (tree), severe (seedling)/wide extent
<i>Arceuthobium littorum</i>	Coastal dwarf mistletoe	Branches and stem	Severe/restricted extent (mostly pygmy forest)
<i>Endocronartium harknessii</i>	Western gall rust	Branches and stem	Severe/wide extent
<i>Dendroctonus valens</i>	Red turpentine beetle	Lower stem	Mild/restricted extent
<i>Ips plastographus</i>	Coastal pine engraver	Stem	Moderately severe/restricted extent
<i>Pseudips mexicanus</i>	Monterey pine Ips	Stem	Moderately severe/restricted extent
<i>Hylastes</i> spp.	Bark beetle	Stem	Moderately severe/restricted extent
<i>Porodaedalia</i> (= <i>Phellinus</i>) <i>pini</i>	White pocket/heart rot	Stem	Moderately severe/wide extent

Soils

Soils data are still under analysis, but field observations revealed large variations in soil physical characteristics from site to site, even in similar physiographic situations located within short distances from each other. Observations made so far have comprised gleyed soils, largely undeveloped sands, well-developed alfisols, and highly weathered, acidic spodosols. Water tables at several locations (e.g., MCK, FMC) are located high in the soil profile, and at FMC a blowdown event occurred at the edge of one plot in winter 2017–2018 involving large numbers of mature pines and revealing extensive *Armillaria* occurrence on the root systems.

DISCUSSION AND CONCLUSIONS

Our investigation confirms an ongoing, pervasive tree species decline in this part of the range of bishop pine. The decline fits a classic pattern involving many potential causal factors and varying rates and manifestations of decline at various sites. What distinguishes this decline from many others and gives it added urgency, however, is the already restricted range of the affected species. Although common patterns are hard to discern in the data from this project at this stage, the plots established and information gathered so far provide a solid foundation for further observation and the development of more focused research questions concerning specific mechanisms of decline. The literature of tree declines around the world shows the formidable range of possible causes of decline, but several of the most common can be ruled out

in this isolated and relatively undisturbed part of the California coast, including air pollution (e.g., LeFohn and others 1997), overbrowsing (e.g., Diaci and others 2011), and excessively acidic soils (e.g., Park and others 2008). Increased mortality of this species in the southern part of its range (the Channel Islands) has been well documented (Baguskas and others 2014), with investigations of the cause centering on water stress, possibly caused by reductions in winter rainfall, summer fog delivery, or both; the importance of summer fog to tree maintenance and growth has been extensively covered by these research projects (e.g., Carbone and others 2013, Fischer and others 2016, Williams and others 2008). Johnstone and Dawson (2010) documented a moderate decrease in summer fog along the California coast during the last half of the 20th century, and Abatzoglou and others (2014) tracked a trend of warming winter temperatures throughout the Pacific Northwest. Both trends could potentially increase tree stress, directly decrease tree growth, and contribute to increased forest pest growth and activity.

In the northern part of bishop pine's range, the most common anecdotal explanation for the decline proposes the following chain of causes: (1) this pine has a short lifespan; (2) the pine depends on wildfire for successful regeneration, and wildfires have been absent along this part of the coast for many decades because of successful fire suppression efforts; (3) thus, the currently observed decline consists of an inevitable descent down a demographic curve coupled with no population replenishment (Giusti 2011).

However, our data, along with emerging understanding of plant aging, complicate this explanation in several ways:

1. No clear pattern of decline emerges from the data at this point in time. At some locations, bishop pine mortality is total or nearly so (e.g., the single plot at MCK, not included in fig. 8.3) or occurs in large patches or “centers,” while at other locations the decline manifests primarily as a more uniform and more progressive loss of crown vitality (e.g., FMC). We initially expected stands at the southern end of our study region to constitute healthy “reference” stands. However, while we saw less mortality of entire patches of trees in the south, we observed levels of crown decline comparable to those of still-living trees in the north. Patterns in the pygmy forest/oligotrophic soils locations differ from more mature coastal stands, with the former sites displaying far more pest-related issues, especially very obvious coastal dwarf mistletoe infestations; paradoxically, however, pygmy forest sites have more regeneration than sites with large-stature pines.
2. Our systematic survey revealed that, in several locations, pine decline involves not only bishop pine, but Monterey pine and shore pine (*P. contorta* ssp. *contorta*) as well.
3. There is an emerging understanding within the field of plant physiological ecology that most perennial plants, and among

them especially trees, have no genetically programmed lifespans. Rather, aging in most of these perennial plants depends on some interplay between environmental stresses and plant physiological/metabolic processes and rates, although this interplay may produce relatively predictable demographic senescence curves for individual plant species (Lee and Muzika 2014).

Although lack of regeneration is clearly a major problem for bishop pine management throughout the range of this decline, unambiguous evidence that this is an age-related decline (i.e., cohort senescence *sensu* Mueller-Dombois 1987) is so far lacking. Within our dataset, some sites with very large, presumably old pines (e.g., HQ) displayed some of the densest crowns and least branch dieback, while conversely, other nearby sites (e.g., RG) also had large, old trees but much higher levels of crown transparency and branch dieback, and much greater mortality levels. Only two-thirds of the trees could be considered even-aged, having established within a 25-year time frame in the mid-20th century, whereas growth decline beginning in the 1990s was apparent across the dataset as a whole (fig. 8.4).

Our dataset so far supports the hypothesis that various stress factors are converging on bishop pine stands at unequal rates and with unequal effects throughout the range of the decline. Future work could concentrate on isolating some of these stress factors, which likely include the following:

1. Western gall rust and stem decay pathogens (and, at the pygmy forest sites, coastal dwarf mistletoes) that progressively break down tree crowns and that, in the absence of fire, rain down inoculum upon any regeneration that does exist beneath the forest canopy, leading to premature death. These pathogens likely thrive in the extended coastal wet climate, and periodic fire previously produced more heterogeneous stand structure and reduced pathogen inoculum within the stands.
2. A diverse set of exotic pathogens that are encroaching on bishop pine stands from various directions: *P. cinnamomi* and *F. circinatum* (pine pitch canker) in the south, *P. cambivora* in the north, and several of unclear provenance as well as unclear pathogenicity. We know little about the pathogenicity or spread of such pathogens as *Elongisporangium undulatum* and *D. scrobiculata* (Diplodia blight). Bark beetles may also be vectoring exotic vascular wilts such as *Leptographium wingfieldii* (blue stain fungus), which has been observed on bishop pine in Humboldt County (along with other, as-yet unidentified Ophiostomatoid wilt fungi).
3. Increased tree susceptibility to both native and nonnative pathogens and insects incited by underlying shifts in water availability and seasonal timing, solar radiation, nutrient cycling, and/or fog-delivered water to surface soils. Several residents have reported fewer summertime foggy days than in previous decades.

Future work has already commenced and includes the following: (1) further analysis and tabulation of study site soil physical characteristics; (2) detailed mapping and quantification of bishop pine decline throughout coastal Sonoma and Mendocino Counties using GIS techniques such as unsupervised and supervised image classification; (3) continued growth analysis using tree cores already collected and some to be collected in the future; and (4) addition of more plots to supply deficiencies in the existing dataset, particularly the addition of more healthy reference plots. Following this work, individual research projects can begin to investigate the roles of specific decline factors in more detail, especially underlying shifts in components of the coastal climate. Future management projects proposed by California State Parks (focused particularly on regenerating young pines), provided they include an adaptive management-oriented monitoring program, should also shed more light on how to promote healthier stands in the future.

For more information, contact: Chris Lee, California Department of Forestry and Fire Protection, christopher.lee@fire.ca.gov.

LITERATURE CITED

- Abatzoglou, J.T.; Rupp, D.E.; Mote, P.W. 2014. Seasonal climate variability and change in the Pacific Northwest of the United States. *Journal of Climate*. 27: 2125–2142.
- Baguskas, S.A.; Peterson, S.H.; Bookhagen, B.; Still, C.J. 2014. Evaluating spatial patterns of drought-induced tree mortality in a coastal California pine forest. *Forest Ecology and Management*. 315: 43–53.

- Bernhardt, E.; Swiecki, T. 2015. Using green pears to bait for *Phytophthora*. Phytosphere Research. <http://phytosphere.com/soilphytophthora/pearbaitingPhytophthora.htm>. [Date accessed: May 23, 2018].
- Carbone, M.S.; Williams, A.P.; Ambrose, A.R. [and others]. 2013. Cloud shading and fog drip influence the metabolism of a coastal pine ecosystem. *Global Change Biology*. 19: 484–297.
- County of Mendocino. 2010. 2010 Comprehensive Economic Development Strategy (CEDS). <http://edfc.org/wp-content/uploads/2014/09/Mendocino-County-CEDS-2010-full.pdf>. [Date accessed: May 23, 2018].
- Diaci, J.; Rozenbergar, D.; Anic, I. [and others]. 2011. Structural dynamics and synchronous silver fir decline in mixed old-growth mountain forests in eastern and southeastern Europe. *Forestry*. 84(5): 479–491.
- Fischer, D.T.; Still, C.J.; Ebert, C.M. [and others]. 2016. Fog drip maintains dry season ecological function in a California coastal pine forest. *Ecosphere*. 7(6): 1–21.
- Giusti, G. 2011. Watching the demise of a coastal forest type—bishop pine. University of California, Cooperative Extension. <http://cemendocino.ucanr.edu/files/199447.pdf>. [Date accessed: April 22, 2018].
- Hawksworth, F.G. 1977. The 6-class dwarf mistletoe rating system. Gen. Tech. Rep. RMRS-48. Fort Collins, CO: U.S. Department of Agriculture Forest Service, Rocky Mountain Forest and Range Experiment Station. 7 p.
- Johnstone, J.A.; Dawson, T.E. 2010. Climatic context and ecological implications of summer fog decline in the coast redwood region. *Proceedings of the National Academy of Sciences of the USA*. 107(10): 4533–4538.
- Lee, C.A.; Muzika, R.-M. 2014. Plant senescence for ecologists: precision in scale, concept, and terminology. *Plant Ecology*. 215(12): 1417–1422.
- Lefohn A.S.; Jackson, W.; Shadwick, D.S.; Knudsen, H.P. 1997. Effect of surface ozone exposures on vegetation grown in the southern Appalachian Mountains: identification of possible areas of concern. *Atmospheric Environment*. 31(11): 1695–1708.
- Martin, F.N.; Abad, Z.G.; Balci, Y.; Ivors, K. 2012. Identification and detection of *Phytophthora*: reviewing our progress, identifying our needs. *Plant Disease*. 96(8): 1080–1103.
- Moore, D. 2017. Sonoma Coast's Stewarts Point becomes part of historic agreement for coastal ranch. Santa Rosa Press-Democrat. Feb 23, 2017. <http://www.pressdemocrat.com/news/6700683-181/sonoma-coasts-stewarts-point-becomes?sba=AAS>. [Date accessed: May 23, 2018].
- Mueller-Dombois, D. 1987. Natural dieback in forests. *BioScience*. 37(8): 575–583.
- Park, B.B.; Yanai, R.D.; Fahey, T.J. [and others]. 2008. Fine root dynamics and forest production across a calcium gradient in northern hardwood and conifer ecosystems. *Ecosystems*. 11: 325–341.
- Sawyer, J.; Keeler-Wolf, T.; Evans, J. 2009. A manual of California vegetation. Sacramento: California Native Plant Society Press. 1300 p.
- Schmitthenner, A.F.; Bhat, R.G. 1994. Useful methods for studying *Phytophthora* in the laboratory. Wooster, OH: The Ohio State University. https://kb.osu.edu/dspace/bitstream/handle/1811/71884/1/OARDC_special_circular_n143.pdf. [Date accessed: May 22, 2018].
- Wick, R.L. 2013. Culture media for plant pathogenic fungi and bacteria. Amherst, MA: University of Massachusetts. https://wiki.bugwood.org/UMass_diagnostic_manual. [Date accessed: May 23, 2018].
- Williams, A.P.; Still, C.J.; Fischer, D.T.; Leavitt, S.W. 2008. The influence of summertime fog and overcast clouds on the growth of a coastal Californian pine: a tree-ring study. *Oecologia*. 156: 601–611.

INTRODUCTION

Myoporum thrips, (*Klambothrips myopori*) was detected in California in 2005, where it has caused high levels of mortality in ornamental *Myoporum* species used for landscaping residential and freeway margins (Sullivan 2014). Before its detection in California, this was an unknown species to science and was subsequently formally described by Mound and Morris (2007). It is now known that this species is native to Tasmania.

Myoporum thrips feeds on terminal growth of plants in the genus *Myoporum*. Feeding causes gall-like symptoms in young leaves. Infested new leaves normally harbor multiple life stages. High infestations can cause terminal dieback that can eventually lead to plant mortality (Bethke and Shaw 2008). It was first detected in Hawaii in March of 2009 attacking the native *Myoporum sandwicense*, locally known as naio (Conant and others 2009).

Locally known as naio thrips, the distribution of myoporum thrips in Hawaii is currently restricted to the Big Island (Hawai'i Island). The high mortality rates seen in California provide cause for alarm for forest managers and landscapers in Hawaii, where naio is an appreciated native species that is often used in ornamental plantings, holds cultural significance to native Hawaiians, and is an integral component of native Hawaiian ecosystems. While naio is most dominant in dry forests, lowlands, and upland shrublands,

the species also populates mesic and wet forest habitats. Naio is distributed across all of the main Hawaiian Islands and is present from sea level to 3000 m (Wagner and others 1990). The loss of this species would be both a significant loss of native biodiversity and a structural loss to native forest habitats.

In September of 2010, the Hawaii Department of Land and Natural Resources (DLNR) Division of Forestry and Wildlife (DOFAW) and the University of Hawai'i initiated efforts to determine spatial distribution, infestation rates, and overall tree health of naio populations on the Big Island. This report summarizes information of a 4-year monitoring period at nine sites. The main objective of the project was to document myoporum thrips infestation and dieback rates on the native *M. sandwicense* at these selected sites.

METHODS

Monitoring Sites on Hawai'i Island

Nine monitoring sites were established on the Big Island in November of 2010 (fig. 9.1). All these sites were protected natural habitats.

Sites spanned an elevational gradient and included an array of habitats: Kaloko-Honokōhau (2 m), Oweowe (589 m), Pelekane (792 m), Koai'a Sanctuary (975 m), Pu'u Wa'awa'a Low (975 m), Pu'u Wa'awa'a Mid (1289 m), Pu'u Wa'awa'a High (1603 m), Kaohe Low (1778 m), and Kaohe High (2128 m).

CHAPTER 9.

Monitoring *Myoporum thrips*, *Klambothrips myopori* (Thysanoptera: Phlaeothripidae), in Hawaii (Project WC-EM-B-10-02)

LEYLA V. KAUFMAN
ELLIOTT PARSONS
DOMINIQUE ZARDERS
CYNTHIA KING
ROBERT HAUFF

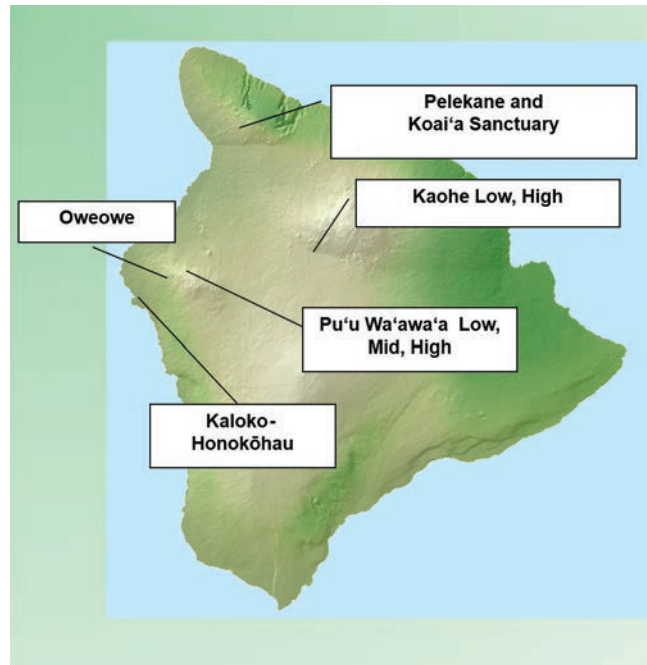


Figure 9.1—Monitoring sites on Hawai'i Island.

Monitoring Infestation and Dieback Levels

Selected sites were visited at monthly intervals for a 3-year period. During the fourth year, sites were monitored every 3–4 months. At each visit, 20 young shoots per plant were randomly chosen and inspected to determine infestation and dieback levels. A total of 10 plants were inspected per site, whenever possible. A four-point scale (0–3) was used to assess the levels of infestation (fig. 9.2) and levels of dieback (fig. 9.3).

RESULTS

Results show that myoporum thrips has spread and colonized natural habitats on the leeward side of Hawai'i Island. Infestation rates increased considerably at all sites over the duration of the sampling period. Trees experiencing high infestation levels also showed branch dieback. Sites that showed no to low infestation levels at the start of the monitoring,

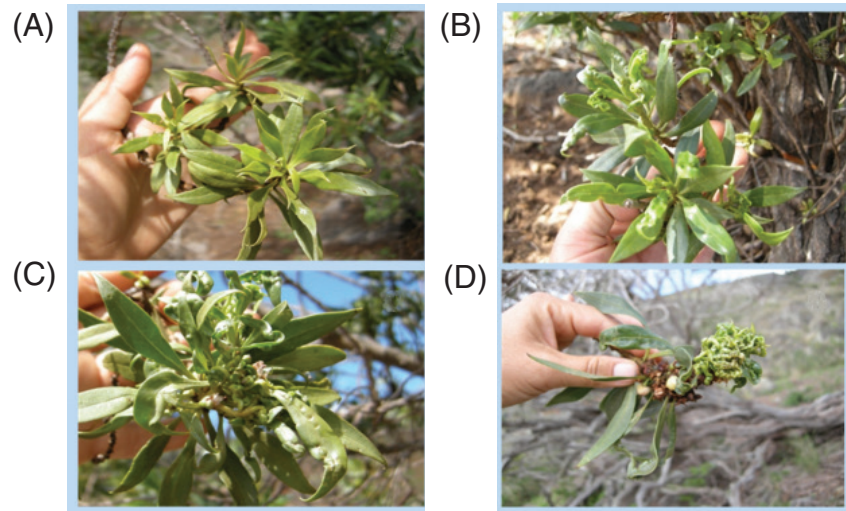


Figure 9.2—Infestation scale: (A) 0 = no galls; (B) 1 = <33 percent tissue galled; (C) 2 = 33–66 percent of tissue galled; (D) 3 = >66 percent of tissue galled. (Photos by Leyla Kaufman, The Pacific Cooperative Studies Unit (PCSU), University of Hawai‘i)

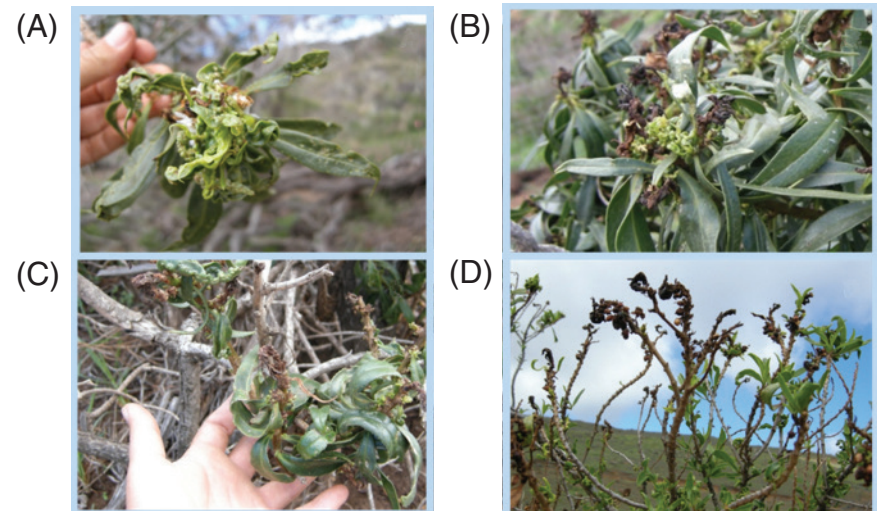


Figure 9.3—Dieback scale: (A) 0 = no dieback; (B) 1 = <33 percent tissue with dieback; (C) 2 = 33–66 percent of tissue with dieback; (D) 3 = >66 percent of tissue with dieback. (Photos by Leyla Kaufman, The Pacific Cooperative Studies Unit (PCSU), University of Hawai‘i)

such as Kaohe Low, suffered visibly high infestation levels by the end of the monitoring period (fig. 9.4).

Medium-elevation sites (between 500–999 m) Oweowe and Koai‘a had the highest infestation and dieback levels (figs. 9.4 and 9.5). Over 70 percent of the shoots inspected at medium-elevation sites had the highest infestation and dieback scores. At the medium-elevation Koai‘a and Pelekane sites, over 70 percent of the monitoring trees have died due to myoporum thrips damage (fig. 9.6).

DISCUSSION

It was expected that trees that had high levels of infestation and dieback would tend to have reduced reproductive capacity; nevertheless, highly infested trees may sometimes flower and fruit vigorously. Probably this happens as a stress response, to make sure seeds are produced and left in the soil seed bank. Even though flowers and fruits were still seen at all sites, little to no plant recruitment was observed at these sites.

The invasive myoporum thrips is still confined to the Big Island and has not yet been detected on neighboring islands. It is expected that

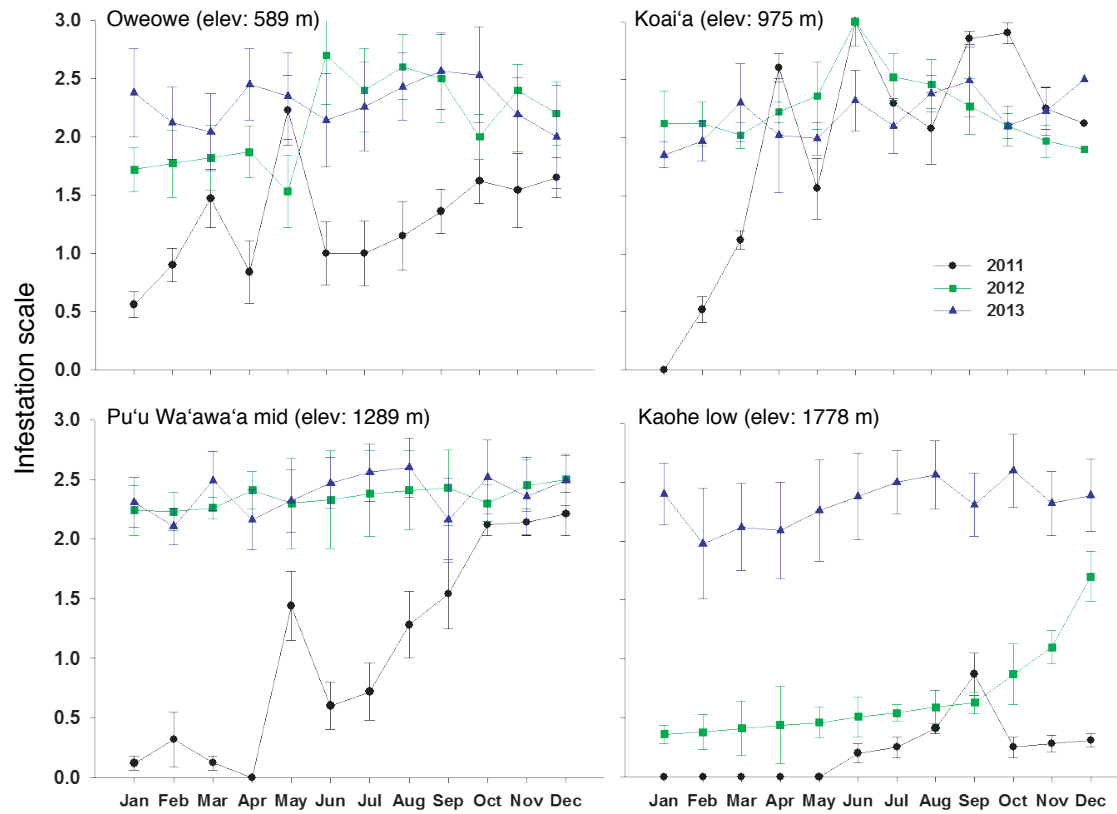


Figure 9.4—Naio thrips infestation levels by year (selected sites), on a 0–3 scale as described under Methods.

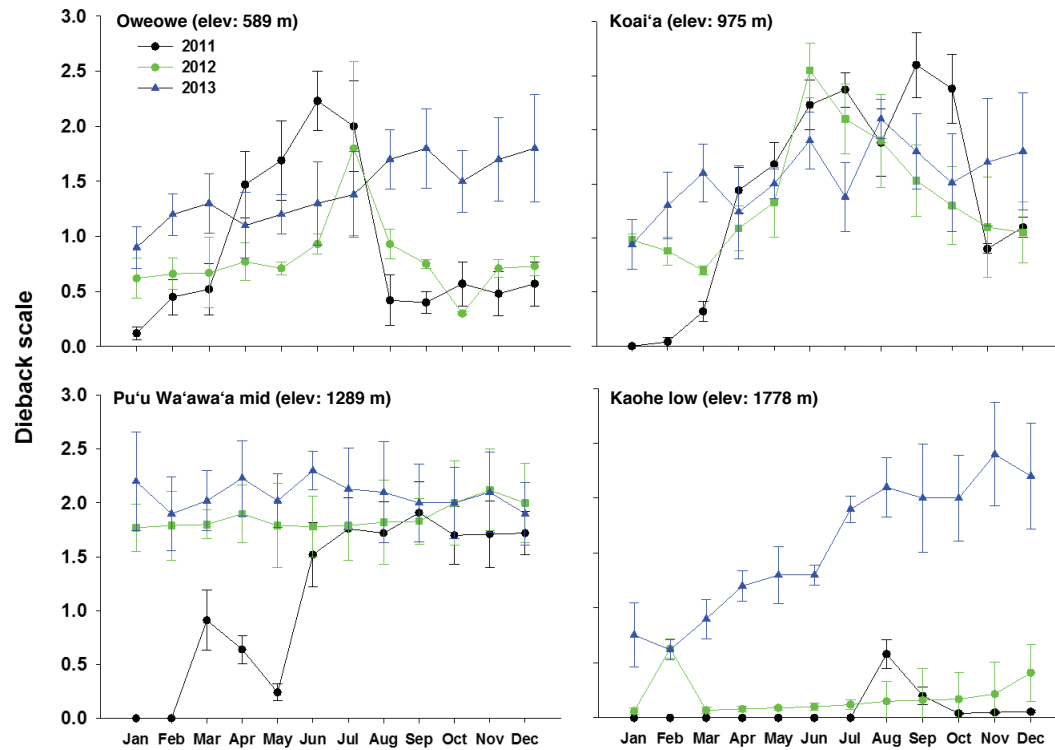


Figure 9.5—Plant dieback levels by year (selected sites), attributed to *naio* thrips.

Myoporum populations on neighboring islands will be as susceptible to myoporum thrips as the Big Island populations. During the monitoring period, no potential biocontrol agents were detected; this likely explains the successful establishment and population increases of this invasive species in Hawaii. It is possible that the highest infestation and dieback levels observed at medium-elevation sites might be due to early colonization of thrips at those sites; however, this has not been confirmed.

CONCLUSIONS

Myoporum thrips continues to threaten the native *Myoporum* populations on Hawai'i Island, where levels of infestation and dieback levels increased considerably throughout the monitoring period. Tree mortality due to thrips has been observed in medium-elevation sites. Early detection and rapid response (e.g., pesticide applications) are currently the only tools available for neighboring islands to prevent colonization and establishment.

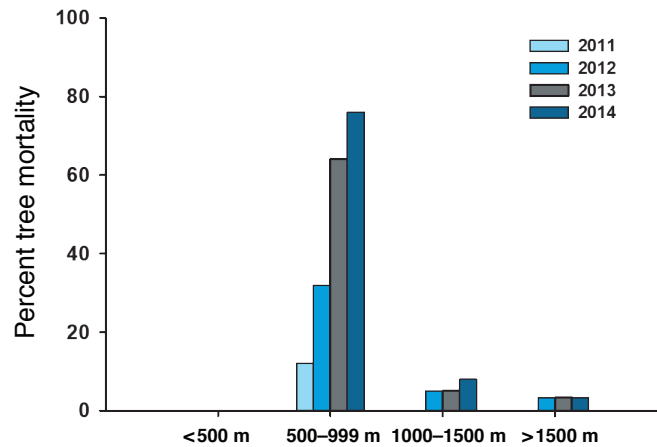


Figure 9.6—Naio mortality by elevation attributable to naio thrips damage.

ACKNOWLEDGMENTS

The following agencies and people have provided invaluable assistance: Pat Conant (Hawaii Department of Agriculture), U.S. Army Pōhakuloa Training Area, Big Island Invasive Species Committee, Kohala Watershed Partnership, Three Mountain Alliance, and Kamehameha Schools. This research was funded by a grant from the U.S. Department of Agriculture Forest Service Forest Health Monitoring program (Project WC-EM-B-10-02).

For more information, contact: Leyla Kaufman, leyla@hawaii.edu.

LITERATURE CITED

- Bethke, J.A.; Shaw, D.A. 2008. *Myoporum thrips* control. San Diego County, CA: University of California Cooperative Extension. http://www.smgrowers.com/info/Myoporum_Thrips.asp. [Date accessed: June 27, 2018].
- Conant, P.; Kirayama, C.Y.; Lee, M.I. [and others]. 2009. Naio thrips. New Pest Advisory. Honolulu No. 09-02. Honolulu, HI: State of Hawaii, Department of Agriculture.
- Mound, L.A.; Morris, D.C. 2007. A new thrips pest of *Myoporum* cultivars in California, in a new genus of leaf-galling Australian Phlaeothripidae (Thysanoptera). *Zootaxa*. 1495: 35–45.
- Sullivan, J.J. 2014. Inadvertent biological control: an Australian thrips killing an invasive New Zealand tree in California. *Biological Invasions*. 16: 445–453.
- Wagner, W.L.; Darrel, R.H.; Sohmer, S.H. 1990. Manual of flowering plants of Hawaii, volume 1. Bishop Museum Special Publications. Honolulu, HI: University of Hawai'i Press and Bishop Museum Press.

INTRODUCTION

Great Basin bristlecone pine, *Pinus longaeva* (GBBP), is one of the longest-lived, non-clonal organisms on Earth and is also one of the most highly fragmented high-elevation conifer species. Great basin bristlecone pine ecosystems contain many biodiversity “hot spots” with a high degree of species endemism. Throughout the Great Basin, GBBP communities are being threatened by changing disturbance regimes, invasive species, and climate change. The loss of GBBP can detrimentally impact biodiversity and valuable resources including wildlife habitat, watershed and soil protection, aesthetics, and recreation (Gibson and others 2008).

The impact of climate change may be especially acute in sky islands of the Great Basin as warming temperatures drive montane and alpine ecosystems upslope and result in overstory tree mortality at the lower margins of tree distributions (Bower and others 2011). Overstory tree mortality directly related to warming may induce changes to the fire regime of GBBP communities; however, little is known about their fuel characteristics and fire dynamics.

In this study, we compared the relationship between forest structure and environmental gradients to predict changes in surface and canopy fuels of GBBP communities with increasing temperatures. The results of this study were published in Gray and Jenkins (2017).

Land managers can use this information to help plan for transitions to new conditions expected within future climatic gradients and altered fire regimes (Millar and others 2007).

METHODS

Data Collection

In the Great Basin of Nevada and western Utah, mountains and basins create steep environmental gradients which greatly influence the composition and structure of vegetative communities (Peet 2000). We used U.S. Department of Agriculture Forest Service Forest Inventory and Analysis (FIA) program plots (O’Connell and others 2015) that contained GBBP tree species to obtain tree height, diameter at breast height (d.b.h.), canopy base height (c.b.h.), coarse woody debris counts (c.w.d.; >7.6 cm diameter), fine woody debris counts (f.w.d.; 0–7.6 cm diameter), and canopy fuels measurements from stands that were distributed at elevation bands below 3000 m, between 3000 and 3300 m, and above 3300 m. Temperature regimes within these elevational bands reflect those of predicted climatic gradients.

Due to the small number of suitable FIA plots, we also quantified fuel loading of the four major surface fuel components (litter, duff, f.w.d., and c.w.d.) on a total of 76 plots located within additional study sites. We collected these data using Brown’s method (also called the line-intersect or planar-intersect method) (Brown 1974).

CHAPTER 10.

Monitoring the Impact of Climate Change on the Frequency and Severity of Fires and Distribution of Great Basin Bristlecone Pine Sky Island Ecosystems

MICHAEL J. JENKINS

CURTIS A. GRAY

To quantify the unique patchy and discontinuous distribution of surface and aerial fuels at high-elevation sites, we used tree-specific fuels sampling following methods described in Jenkins (2011). In brief, fuels are measured within the fuel zone (fuels lying within the drip line of a tree) of select trees along the planar transects extending from the tree bole in the four cardinal directions (N, S, E, and W) and within the non-pine fuel matrix (the area between adjacent trees). We only collected litter and duff data from under trees near treeline after initial sampling indicated that these classes comprised the majority of fuels.

We next assessed the relative degree of fuels continuity by utilizing Landsat satellite images. The August 24, 2012 Landsat 7 Enhanced Thematic Mapper Plus (ETM+) image was chosen because it was the cloud-free image closest to the dates of field sampling. The spectral indices Normalized Difference Vegetation Index (NDVI), Brightness, and Greenness estimate both fuels cover and continuity.

To assess live foliar moisture content (f.m.c.), we collected needles from four randomly selected GBBP trees at three different elevations (low = 2640 m, mid = 2910 m, high = 3160 m) during the first week of July, August, and September ($n = 36$). Approximately 20 g of live needles from each sample were weighed to the nearest 0.01 g and then oven-dried at 105 °C for 48 hours and reweighed to obtain a dry weight (Matthews 2010). Samples were kept

frozen until processed. Foliar moisture content was computed as the percentage of the oven-dry weight to dry foliage weight.

Data Analyses

For comparing forest floor c.w.d. and f.w.d. within elevational bands, transect counts were converted to weight of fuel per unit area (kg/m^2) following Brown and others (1982). Litter and duff weight per unit area (kg/m^2) was estimated from depth measurements by using the equation developed for foxtail pine (*P. balfouriana*), a close relative to GBBP (van Wagtenonk and others 1998). Regression coefficients via generalized linear models (GLM) were developed relating forest floor mass to elevation. To characterize surface fuels dissimilarity along environmental gradients, a non-metric multidimensional scaling (NMDS) ordination based on a matrix of Euclidean dissimilarities was calculated on f.w.d., c.w.d., litter, and duff amounts. Non-metric multidimensional scaling collapses information from multiple dimensions to fewer dimensions, so that data can be visualized and interpreted (McCune and others 2002). Stand densities in trees/ha were calculated for each plot using the tree expansion factors (coefficient used to scale each tree on a plot to a per-area basis) in the FIA user manual (O'Connell and others 2015). Regression coefficients were also calculated for stand density (trees/ha) and height to live crown for the same elevational gradients. Post hoc mean comparisons using Tukey-Kramer tests were used when a significant difference among elevation class was identified in canopy fuels.

A GLM with a negative binomial link was fit to the litter and duff measurements made in the four cardinal directions under the sampled individual trees. Generalized linear models are mathematical extensions of linear models that do not force data into unnatural scales, and thereby allow for nonlinearity and non-constant variance structures in the data (Hastie and Tibshirani 1990). We used the negative binomial distribution because data with many zero values cause over-dispersion, or greater variability than would be expected. The negative binomial distribution generates realistic heterogeneity representative of spatial clustering of individuals and other small-scale processes (Bolker 2008). All statistics were completed using R statistical software (R Development Core Team 2015).

RESULTS AND DISCUSSION

Linear regression showed that all classes of f.w.d. decreased with increasing elevation, and only 1,000-hour fuels remained constant across elevational transects. The NMDS ordination supported the results of linear regression analysis with all measurements of fuels except c.w.d. being highly correlated with elevation and slope. All crown fuels metrics varied by elevation. Tree height, c.b.h., and crown length decreased with increasing elevation, while available crown fuel load and canopy bulk density increased with elevation. Canopy base height declined significantly with increasing elevation ($p < 0.001$, $R^2 = 0.74$). Foliar moisture content was significantly less at the upper elevation site (ANOVA with $p < 0.001$), while

f.m.c. at the mid and low sites did not differ. Foliar moisture content varied significantly by month. September had the highest f.m.c. and July the lowest with values likely influenced by monsoonal precipitation events (Scalzitti and others 2016).

The results from the Landsat indices of vegetation cover reiterate the findings from c.w.d. and f.w.d. sampling. As elevation increased, NDVI and Greenness decreased, indicating less vegetation and fuels available to carry a surface fire. Conversely, Brightness (a measure of exposed soil) increased with increasing elevation indicating larger gaps between trees, or a decrease in GBBP stand density (trees/ha) and less continuous fuel cover.

Measurements of litter and duff in the four cardinal directions directly beneath GBBP trees showed higher litter and duff fuel loads near the bole of the tree. While there might not be sufficient fuels between individual trees to carry a surface fire, nearly each individual tree had a pocket of litter and duff directly beneath it.

Forest tree distribution data suggest an upward movement of lower elevation species with temperatures of 2–4 °C warmer than historical averages (Scalzitti and others 2016). We expect the structure, composition, and fuel condition of future GBBP stands to more closely approximate those that currently exist in vegetation communities at mid and low elevations. The accumulation of fuels in lower elevation vegetation communities has proven to

amplify the effects of fire in the high-elevation/low fire return interval systems. More important than fuel load is a reduction in the size of fuel gaps that typically limit fire propagation. Our research indicates that if climate warming changes fuel conditions, then the frequency of fire in GBBP systems at low and mid elevations could increase where stands are denser and surface fuel is greatest. Two of the recent large fires in GBBP forests resulted from ignitions at low elevations that spread up into pure GBBP stands. Fire spread from ignitions at upper elevations is unlikely to result in crown fires since surface fuels are low and GBBP intercrown distance is large. However, as elevation increased, the branches of GBBP were closer to the ground, which could facilitate the transition of fire into the crown of the trees.

CONCLUSIONS

As climate change continues to impact high-elevation forests, treeline species like GBBP may be extremely important in maintaining forest ecosystems. We characterized fuels within elevational and latitudinal ranges of GBBP communities and showed how alterations in fuels and associated changes in fire behavior may threaten high-elevation GBBP stands in the future, particularly when coupled with climate change and with very low GBBP regeneration in the post-fire environment. Land managers can use this information for planning and improving practices used to sustain high-elevation GBBP forests.

LITERATURE CITED

- Bolker, B.M. 2008. Ecological models and data in R. Princeton, NJ: Princeton University Press. 396 p.
- Bower, A.D.; McLane, S.C.; Eckert, A. [and others]. 2011. Conservation genetics of high elevation five-needle white pines. In: Keane, R.E.; Tomback, D.F.; Murray, M.P.; Smith, C.M., eds. The future of high-elevation, five-needle white pines in Western North America: proceedings of the high five symposium. 28-30 June 2010; Missoula, MT. Proceedings RMRS-P-63. Fort Collins, CO: U.S. Department of Agriculture Forest Service, Rocky Mountain Research Station: 98–117.
- Brown, J.K. 1974. Handbook for inventorying downed woody material. Gen. Tech. Rep. INT-16. Ogden, UT: U.S. Department of Agriculture Forest Service, Intermountain Forest and Range Experiment Station. 24 p.
- Brown, J.K.; Oberheu, R.D.; Johnston, C.M. 1982. Handbook for inventorying surface fuels and biomass in the interior west. Gen. Tech. Rep. INT-129. Ogden, UT: U.S. Department of Agriculture Forest Service, Intermountain Forest and Range Experiment Station. 48 p.
- Gibson, K.E.; Skov, K.; Kegley, S. [and others]. 2008. Mountain pine beetle impacts in high-elevation five-needle pines: current trends and challenges. R1-08-020. Washington, DC: U.S. Department of Agriculture Forest Service, Forest Health Protection. 32 p.
- Gray, C.A.; Jenkins, M.J. 2017. Climate warming alters fuels across elevational gradients in Great Basin bristlecone pine-dominated sky island forests. *Forest Ecology and Management*. 392: 125–136.
- Hastie, T.J.; Tibshirani, R.J. 1990. Generalized additive models. Monographs on statistics and applied probability 43. [Location of publisher unknown]: Chapman and Hall/CRC Press. 352 p.
- Jenkins, M.J. 2011. Fuel and fire behavior in high-elevation five-needle pines affected by mountain pine beetle. In: Keane, R.E.; Tomback, D.F.; Murray, M.P.; Smith, C.M., eds. The future of high-elevation, five-needle white pines in Western North America: proceedings of the high five symposium. 28-30 June 2010; Missoula, MT. Proceedings RMRS-P-63. Fort Collins, CO: U.S. Department of Agriculture Forest Service, Rocky Mountain Research Station: 198–205.

- Matthews, S. 2010. Effect of drying temperature on fuel moisture content measurements. *International Journal of Wildland Fire*. 19: 800–802.
- McCune, B.; Grace, J.B.; Urban, D.L. 2002. *Analysis of ecological communities*. Glenden Beach, OR: MjM Software Design. 300 p.
- Millar, C.I.; Stephenson, N.L.; Stephens, S.L. 2007. Climate change and forests of the future: managing in the face of uncertainty. *Ecological Applications*. 17: 2145–2151.
- O’Connell, B.M.; LaPoint, E.B.; Turner, J.A. [and others]. 2015. *The Forest Inventory and Analysis database: database description and user guide version 6.0.2 for Phase 2*. U.S. Department of Agriculture Forest Service. 748 p.
- Peet, R.K. 2000. Forests and meadows of the Rocky Mountains. *North American Terrestrial Vegetation*. 2: 75–122.
- R Development Core Team. 2015. *R: A language and environment for statistical computing*. R Foundation for Statistical Computing. DOI: ISBN 3-900051-07-0.
- Scalzitti, J.; Strong, C.; Kochanski, A. 2016. Climate change impact on the roles of temperature and precipitation in western snowpack variability. *Geophysical Research Letters*. 43: 5361–5369.
- van Wagtenonk, J.W.; Benedict, J.M.; Sydorik, W.M. 1998. Fuel bed characteristics of Sierra Nevada conifers. *Western Journal of Applied Forestry*. 13(3): 73–84.

ACKNOWLEDGMENTS

This research presented in this report was supported in part through the project “Forest Health Monitoring, Assessment, and Analysis” of Cost Share Agreement 17-CS-11330110-025 (March 30, 2017 through April 30, 2019) and the project “Forest Health Monitoring and Assessment” of Cost Share Agreement 18-CS-11330110-026 (June 15, 2018 through October 31, 2019) between North Carolina State University (this institution is an equal opportunity provider) and the U.S. Department of Agriculture Forest Service, Southern Research Station, Asheville, NC. This

research was supported by funds provided by the U.S. Department of Agriculture Forest Service, Southern Research Station, Asheville, NC.

The editors and authors of this report thank the following for their reviews and constructive comments: Chris Asaro, Susan Frankel, Tom Hall, Zack Heath, Elizabeth Hebertson, Basil Iannone, Danielle Malesky, Roshan Manandhar, Jeff Moore, Chris Oswalt, Jeanine Paschke, Margaret Pettygrove, Karen Ripley, Beth Schulz, David Shaw, Sheri Smith, Joseph Spruce, Jim Steinman, Mark Wright, Denys Yemshanov, Stan Zarnoch, and Mark Zweifler.

Sections 1 and 2, Forest Health Monitoring Research

MARK J. AMBROSE, Research Assistant, North Carolina State University, Department of Forestry and Environmental Resources, Raleigh, NC 27695.

ERIN BERRYMAN, Quantitative Ecologist, Cherokee Nation Technologies, Fort Collins, CO 80526.

JOHN W. COULSTON, Supervisory Research Forester, U.S. Department of Agriculture Forest Service, Southern Research Station, Blacksburg, VA 24060.

FRANK H. KOCH, Research Ecologist, U.S. Department of Agriculture Forest Service, Southern Research Station, Eastern Forest Environmental Threat Assessment Center, Research Triangle Park, NC 27709.

ANDREW McMAHAN, Quantitative Ecologist (retired), Cherokee Nation Technologies, Fort Collins, CO 80526.

JEANINE L. PASCHKE, Geographic Information Systems Analyst, Cherokee Nation Technologies, Fort Collins, CO 80526.

KEVIN M. POTTER, Research Associate Professor, North Carolina State University, Department of Forestry and Environmental Resources, Raleigh, NC 27695.

KURT H. RITTERS, Research Ecologist, U.S. Department of Agriculture Forest Service, Southern Research Station, Eastern Forest Environmental Threat Assessment Center, Research Triangle Park, NC 27709.

MARK O. ZWEIFLER, Technology Knowledge Transfer Specialist, Cherokee Nation Technologies, Fort Collins, CO 80526.

AUTHOR INFORMATION

Author Information, cont.

Section 3, Evaluation Monitoring Project Summaries

PETER A. ANGWIN, Plant Pathologist, U.S. Department of Agriculture Forest Service, Forest Health Protection, Northern California Shared Service Area, Redding, CA 96002.

CURTIS A. GRAY, Research Assistant, Department of Wildland Resources, Utah State University, Logan, UT 84322-5230.

ROBERT HAUFF, Department of Land and Natural Resources, Division of Forestry and Wildlife, Honolulu, HI 96813.

MICHAEL J. JENKINS, Associate Professor, Department of Wildland Resources, Utah State University, Logan, UT 84322-5230.

LEYLA V. KAUFMAN, The Pacific Cooperative Studies Unit (PCSU), University of Hawai'i, Honolulu HI 96822.

CYNTHIA KING, Department of Land and Natural Resources, Division of Forestry and Wildlife, Honolulu, HI 96813.

CHRISTOPHER A. LEE, Forest Health Specialist, California Department of Forestry and Fire Protection, Fortuna, CA 95521.

ELLIOTT PARSONS, Department of Land and Natural Resources, Division of Forestry and Wildlife, Hilo, HI 96720.

STEVE VOELKER, Assistant Professor, Utah State University, Logan, UT 84322.

DOMINIQUE ZARDERS, University of Hawai'i at Hilo, Hilo, HI 96720.

Potter, Kevin M.; Conkling, Barbara L., eds. 2019. Forest health monitoring: national status, trends, and analysis 2018. Gen. Tech. Rep. SRS-239. Asheville, NC: U.S. Department of Agriculture, Forest Service, Southern Research Station. 168 p.

The annual national report of the Forest Health Monitoring (FHM) program of the Forest Service, U.S. Department of Agriculture, presents forest health status and trends from a national or multi-State regional perspective using a variety of sources, introduces new techniques for analyzing forest health data, and summarizes results of recently completed Evaluation Monitoring projects funded through the FHM national program. In this 18th edition in a series of annual reports, national survey data are used to identify geographic patterns of insect and disease activity. Satellite data are employed to detect geographic patterns of forest fire occurrence. Recent drought and moisture surplus conditions are compared across the conterminous United States. Data collected by the Forest Inventory and Analysis (FIA) program are employed to detect regional differences in tree mortality. Forest Inventory and Analysis data also were used to identify forest types in the Eastern United States with relatively high or low rates of invasion by invasive plants. Methods are explored for more accurately reporting insect and disease damage across multiple regions and nationally using the new Digital Mobile Sketch Mapper (DMSM) platform. National Land Cover Database (NLCD) tree canopy cover data are applied to adjust Forest Health Protection (FHP) Insect and Disease Survey data to better represent acres of forest damage. Three recently completed Evaluation Monitoring projects are summarized, addressing forest health concerns at smaller scales.

Keywords—Change detection, drought, fire, forest health, forest insects and disease, invasive species, tree canopy, tree mortality.

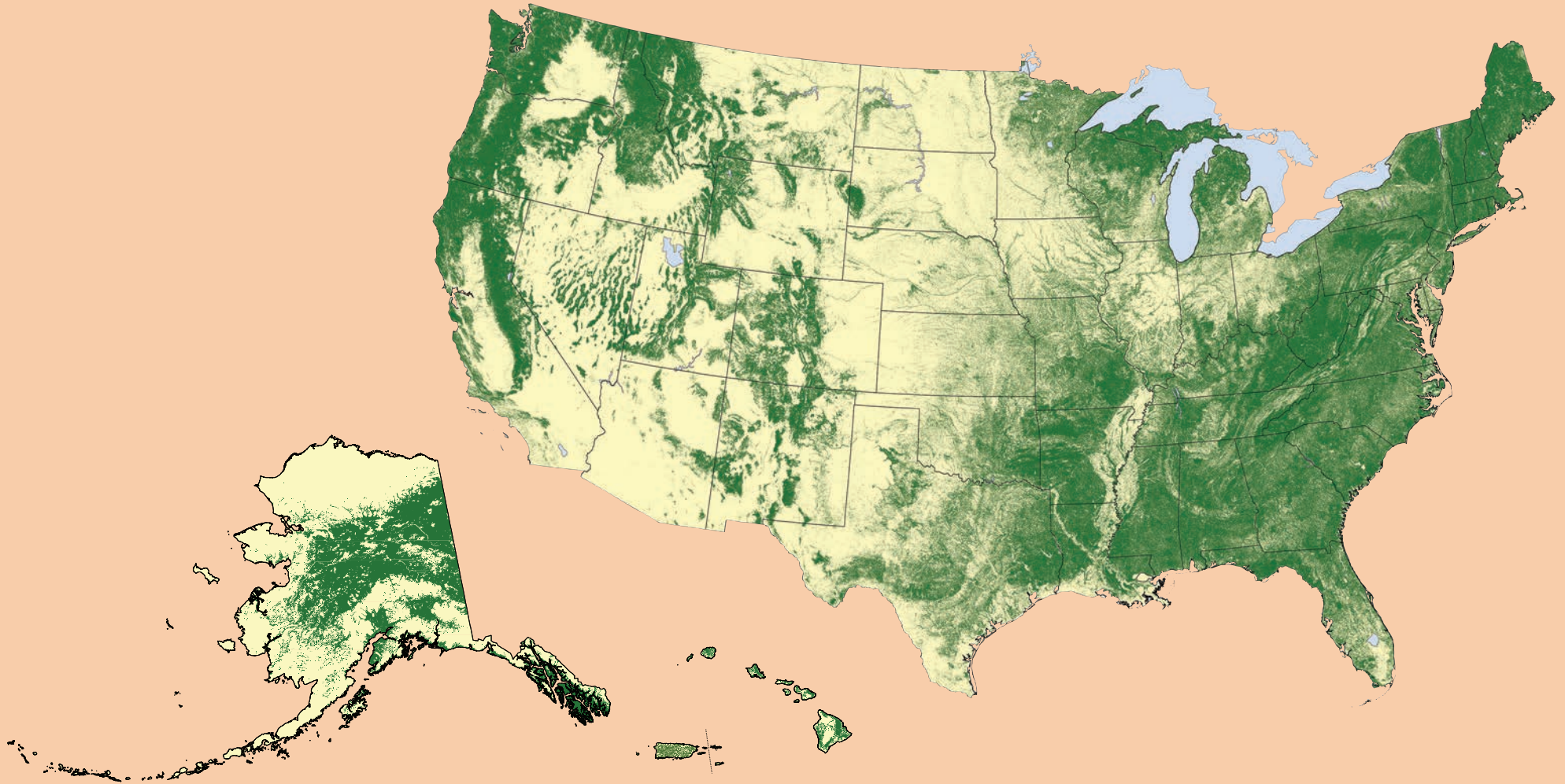


Scan this code to submit your feedback,
or go to www.srs.fs.usda.gov/pubeval.



A copy of this report is available for
download at www.srs.fs.usda.gov/pubs/.

Please direct inquiries about the availability of hard copies to pubrequest@fs.fed.us.
Number of copies is limited to two per person.



In accordance with Federal civil rights law and U.S. Department of Agriculture (USDA) civil rights regulations and policies, the USDA, its Agencies, offices, and employees, and institutions participating in or administering USDA programs are prohibited from discriminating based on race, color, national origin, religion, sex, gender identity (including gender expression), sexual orientation, disability, age, marital status, family/parental status, income derived from a public assistance program, political beliefs, or reprisal or retaliation for prior civil rights activity, in any program or activity conducted or funded by USDA (not all bases apply to all programs).

Remedies and complaint filing deadlines vary by program or incident. Persons with disabilities who require alternative means of communication for program information (e.g., Braille, large print, audiotape, American Sign Language, etc.) should contact the responsible Agency or USDA's TARGET Center at (202) 720-2600 (voice and TTY) or contact USDA through the Federal Relay Service at (800) 877-8339. Additionally, program information may be made available in languages other than English.

To file a program discrimination complaint, complete the USDA Program Discrimination Complaint Form, AD-3027, found online at <http://www.aphis.usda.gov>

www.ascr.usda.gov/complaint_filing_cust.html and at any USDA office or write a letter addressed to USDA and provide in the letter all of the information requested in the form. To request a copy of the complaint form, call (866) 632-9992. Submit your completed form or letter to USDA by: (1) mail: U.S. Department of Agriculture, Office of the Assistant Secretary for Civil Rights, 1400 Independence Avenue, SW, Washington, D.C. 20250-9410; (2) fax: (202) 690-7442; or (3) email: program.intake@usda.gov.

USDA is an equal opportunity provider, employer, and lender.

